

Exploring the therapeutic potential of recombinant AAV vectors in
stem cell and transplantation model systems
for the treatment of heart diseases

Inaugural-Dissertation

zur

Erlangung des Doktorgrades

der Mathematisch-Naturwissenschaftlichen Fakultät

der Universität zu Köln

vorgelegt von

Natascha Schuhmann

aus Weinheim

Köln

2008

Berichtersteller/in: Prof. Dr. Jens Brüning

Prof. Dr. Herbert Pfister

PD Dr. Hildegard Büning

Tag der mündlichen Prüfung: 24.6.2008

Die vorliegende Arbeit wurde in der Zeit von April 2004 bis April 2008 unter der Anleitung von PD Dr. Hildegard Büning in der Medizinischen Klinik I des Universitätsklinikums zu Köln angefertigt.

Im Verlauf dieser Arbeit entstanden folgende Publikationen:

Hacker, U. T., Wingenfeld, L., Kofler, D. M., **Schuhmann, N. K.**, Lutz, S., Herold, T., King, S. B., Gerner, F. M., Perabo, L., Rabinowitz, J., McCarty, D. M., Samulski, R. J., Hallek, M., and Buning, H. (2005). Adeno-associated virus serotypes 1 to 5 mediated tumor cell directed gene transfer and improvement of transduction efficiency. *J Gene Med* **7**(11), 1429-38.

Schuhmann, N.*, Burdorf, L.* , Postrach, J., Thein, E., Hallek, M., Reichart, B. Buning, H.⁺, and Schmoeckel, M.⁺ (2007). AAV-mediated gene transfer to cardiac cells in a heterotopic rat heart transplantation model. *Transplant Proc* **39**(2), 567-8. (* + equal contribution)

Zuber, C.* , Mitteregger, G.* , **Schuhmann, N.**, Rey, C., Knackmuss, S., Rupprecht, W., Reusch, U., Pace, C., Little, M., Kretzschmar, H. A., Hallek, M., Buning, H., and Weiss, S. (2008). Delivery of single-chain antibodies scFvs directed against the 37 kDa/67 kDa laminin receptor into mice via recombinant Adeno-associated viral vectors for prion disease gene therapy. *J Gen Virol*, in press (* equal contribution)

Für meine Eltern

Table of contents

| | | |
|-----------|---|----|
| 1 | Zusammenfassung | 1 |
| 2 | Abstract | 4 |
| 3 | Introduction | 7 |
| 3.1 | Adeno-associated virus | 7 |
| 3.1.1 | Classification of adeno-associated virus | 7 |
| 3.1.2 | Genome organization | 9 |
| 3.1.3 | Infection biology of AAV | 11 |
| 3.1.3.1 | <i>Virus-cell interaction</i> | 13 |
| 3.1.3.2 | <i>Receptor-mediated endocytosis</i> | 14 |
| 3.1.3.3 | <i>Endosomal processing and escape</i> | 14 |
| 3.1.3.4 | <i>Nuclear translocation</i> | 15 |
| 3.1.3.5 | <i>Latent and lytic life cycle of AAV</i> | 16 |
| 3.1.4 | Adenovirus-free AAV production and recombinant AAV vectors (rAAV) | 17 |
| 3.1.5 | AAV as vector in gene therapy | 19 |
| 3.1.5.1 | <i>Gene therapy of ischemic cardiovascular diseases</i> | 21 |
| 3.2 | Stem cells | 25 |
| 3.2.1 | Hematopoietic stem cells and endothelial progenitor cells | 26 |
| 3.2.2 | Bone marrow stem cell niche, mobilization and homing | 29 |
| 3.2.3 | Therapeutic potentials of EPC transplantation and gene therapy | 32 |
| 3.2.4 | Aim of the study | 35 |
| 4 | Results | 37 |
| 4.1 | rAAV transfer into heart | 37 |
| 4.1.1 | rAAV transfer into rodent heart | 37 |
| 4.1.1.1 | <i>Heterogenic rat heart transplantation</i> | 37 |
| 4.1.1.1.1 | Delivery of vector genomes into transplanted hearts | 39 |
| 4.1.1.1.2 | Transgene mRNA expression cannot be detected in | 43 |
| 4.1.1.1.3 | Beta-Galactosidase activity is not detectable in tissue sections | 45 |
| 4.1.1.2 | <i>In vitro analyses of rAAV-mediated rat cell transduction</i> | 48 |
| 4.1.1.2.1 | AAV2 capsids are detectable in the cytoplasm and perinuclear | 49 |
| 4.1.1.2.2 | CMV promoter induces transgene expression after transfection | 50 |
| 4.1.1.2.3 | RAECs are poorly transduceable with AAV serotypes 1 to 5, | 51 |
| 4.1.1.2.4 | Neonatal rat cardiomyocytes show highest transgene | 54 |
| 4.1.2 | rAAV-mediated gene transfer into porcine heart | 56 |
| 4.1.2.1 | <i>Identification of the most suited serotype using PAECs as in vitro model</i> | 56 |
| 4.1.2.1.1 | PAECs are efficiently transduceable with rAAV2 | 57 |
| 4.1.2.1.2 | Visualization of rAAV2 capsids in the cytoplasm of PAECs | 59 |
| 4.1.2.2 | <i>Heterogenic pig heart transplantation</i> | 60 |
| 4.1.2.2.1 | Successful vector delivery, but no transgene expression from | 63 |
| 4.1.2.2.2 | Successful vector delivery and transgene expression from | 67 |
| 4.2 | Establishment of rAAV-mediated gene transfer into CD34 ⁺ cells | 74 |
| 4.2.1 | Second-strand synthesis is a limiting step in CD34 ⁺ cell transduction | 74 |
| 4.2.2 | Loss of transgene expression during prolonged cultivation times | 78 |

| | | |
|---------|---|-----|
| 4.2.3 | Heparin inhibits transduction with rAAV2 approving HSPG as primary receptor | 79 |
| 4.2.4 | Transduction efficiency correlated with the availability of $\alpha_5\beta_1$ integrins | 81 |
| 4.2.5 | Enhancement of transgene expression using retinoic acid and Trichostatin A | 84 |
| 4.2.6 | CD34 ⁺ cells are able to take up Dil-AcLDL after endothelial differentiation assay | 87 |
| 4.3 | Further applications of serotypes | 90 |
| 4.3.1 | Serotype 2 is superior in transduction of primary melanoma cells | 90 |
| 4.3.2 | Serotype 2 is superior in transduction of primary porcine fibroblasts and HeLa cells | 91 |
| 4.4 | Vector genomes are detected in spleen following intracerebral injection of rAAV2 | 94 |
| 5 | Discussion | 96 |
| 5.1 | Heterotopic heart transplantations | 96 |
| 5.1.1 | Approaches for endothelial transduction in rat model | 96 |
| 5.1.2 | <i>In vitro</i> studies of RAECs | 99 |
| 5.1.2.1 | <i>Superiority of rAAV1 in rat cardiac endothelial and cardiomyocyte transduction</i> | 99 |
| 5.1.2.2 | <i>Barriers in endothelial cells impair rAAV-mediated transgene expression</i> | 100 |
| 5.1.3 | Porcine endothelial cells are highly permissive for AAV | 103 |
| 5.1.4 | AAV vector mediated transgene expression in porcine hearts | 103 |
| 5.1.5 | Distribution of transgene DNA and product in the two animals | 105 |
| 5.1.6 | Potential of rAAV2 for animal cloning | 107 |
| 5.2 | Investigations on CD34 ⁺ cells | 108 |
| 5.2.1 | Most efficient serotype rAAV2 is limited by second-strand synthesis .. | 108 |
| 5.2.2 | Transduction procedure does not interfere with endothelial differentiation | 110 |
| 5.2.3 | Receptor and coreceptor studies | 111 |
| 5.2.4 | Effects of the transcriptionally active drugs TSA and RA | 113 |
| 5.2.5 | Outlook | 115 |
| 6 | Materials | 117 |
| 6.1 | Chemicals and Solutions | 117 |
| 6.2 | Enzymes and Kits | 118 |
| 6.3 | Plasmids | 118 |
| 6.4 | Primers | 120 |
| 6.5 | Antibodies | 121 |
| 6.6 | Bacteria Strains | 121 |
| 6.7 | Eukaryotic Cells | 121 |
| 6.7.1 | Immortalized Cell Lines | 121 |
| 6.7.2 | Primary cells | 122 |
| 6.8 | Culture Media and Supplements | 123 |
| 6.9 | Laboratory Equipment and Disposables | 125 |
| 6.10 | Data Treating Software | 126 |
| 7 | Methods | 127 |
| 7.1 | Bacteria Culture | 127 |
| 7.1.1 | Cultivation of Bacteria | 127 |
| 7.1.2 | Preparation of Competent Bacteria | 127 |
| 7.1.3 | Transformation of Bacteria | 128 |
| 7.2 | Working with nucleic acids | 128 |
| 7.2.1 | Plasmid amplification and extraction | 128 |

| | | |
|---------|---|------------|
| 7.2.2 | DNA and RNA Quantification..... | 129 |
| 7.2.3 | Restriction Enzyme Digest..... | 129 |
| 7.2.4 | Agarose Gel Electrophoresis | 129 |
| 7.2.5 | Tissue DNA extraction | 130 |
| 7.2.6 | Tissue RNA extraction | 130 |
| 7.2.7 | DNase I digest and cDNA synthesis | 131 |
| 7.2.8 | Quantitative Polymerase-Chain-Reaction..... | 132 |
| 7.3 | Eukaryotic cell culture | 135 |
| 7.3.1 | Cultivation of Cells..... | 135 |
| 7.3.2 | Trypsinization..... | 135 |
| 7.3.3 | Counting | 135 |
| 7.3.4 | Seeding / Passaging..... | 135 |
| 7.3.5 | Freezing and Thawing Cells | 136 |
| 7.3.6 | Vector production and purification | 136 |
| 7.3.6.1 | <i>AAV-Vector Packaging.....</i> | <i>136</i> |
| 7.3.6.2 | <i>Iodixanol Gradient Purification.....</i> | <i>137</i> |
| 7.3.6.3 | <i>Heparin Affinity Chromatography</i> | <i>137</i> |
| 7.3.6.4 | <i>Vector titration.....</i> | <i>138</i> |
| 7.3.7 | Working with CD34 ⁺ cells | 138 |
| 7.3.7.1 | <i>Isolation and culturing of CD34⁺ cells.....</i> | <i>138</i> |
| 7.3.7.2 | <i>Thawing of CD34⁺ cells.....</i> | <i>139</i> |
| 7.3.7.3 | <i>Transduction of CD34⁺ cells with AAV.....</i> | <i>139</i> |
| 7.3.7.4 | <i>Analysis of transduced CD34⁺ cells by FACS.....</i> | <i>139</i> |
| 7.3.8 | Dil-AcLDL uptake..... | 140 |
| 7.4 | Determination of protein..... | 140 |
| 7.4.1 | Detection of beta-Galactosidase activity in tissue sections..... | 140 |
| 7.4.2 | Staining for beta-Galactosidase activity in cells..... | 141 |
| 7.4.3 | Bradford Assay | 141 |
| 7.4.4 | Luciferase Assay | 142 |
| 7.5 | Heterotopic heart transplantation | 142 |
| 7.5.1 | Rat heart transplantation | 142 |
| 7.5.2 | Pig heart transplantation..... | 143 |
| 8 | Abbreviations..... | 146 |
| 9 | References | 148 |

1 Zusammenfassung

Herzerkrankungen sind weltweit die Hauptursache für einen vorzeitigen Tod. Sowohl Gentransfer als auch zelluläre Therapien werden derzeit als neue Behandlungsmöglichkeiten für diese Erkrankungen entwickelt.

Im ersten Teil dieser Arbeit sollte der AAV-vermittelte Gentransfer von Transgenen ins Herzgewebe von Donororganen, die anschließend transplantiert wurden, etabliert werden. Als Tiermodelle für die heterotopen Herztransplantationen wurden Sprague Dawley Ratten und Deutsche Landrasseschweine gewählt. rAAV Serotype 2, welcher für diesen Zweck als geeignet beschrieben wurde, wurde intracoronar entweder in das normotherme (n=3) oder hypotherme (n=3) Herz appliziert, welches anschließend in eine Empfängerratte transplantiert wurde. Der Gentransfer erfolgte mit einer besseren Effizienz in normotherme Herzen verglichen mit hypothermen Herzen. Trotz des erfolgreichen Transfers und der Nachweisbarkeit von Vektor-DNA in Gewebeprobe 28 Tage nach Transplantation konnte jedoch weder Transgen-spezifische mRNA noch Proteinexpression detektiert werden. Zur Bestimmung potentieller Barrieren, welche die rAAV2-vermittelte Transgenexpression in unserem Rattenmodell beeinträchtigen, wurden *in vitro* Analysen in Rattenaortenendothelzellen (RAECs) durchgeführt. Wir konnten Zelleintritt und intrazelluläres trafficking der viralen Partikel ebenso als inhibierende Faktoren ausschließen wie die Expression vom gewählten CMV Promotor. Die Applikation des Proteasomeninhibitors MG132 erhöhte die Transgenexpression jedoch signifikant für die Serotypen 1 und 2 (6-fach und 7.3-fach). Ersterer war in unseren *in vitro* Experimenten der effizienteste Serotyp der analysierten 5 Serotypen (rAAV1 bis rAAV5). Da MG132 die Funktion der Proteasomen inhibiert, könnte eine blockierte Vektordegradation die beobachteten Ergebnisse erklären. Darüberhinaus sind auch indirekte Effekte wie eine erhöhte Ubiquitinierung des Vektorkapsids denkbar, von der man annimmt, dass sie das sogenannte *vector uncoating* oder die Translokation in den Nucleus erleichtert (Duan et al., 2000; Yan et al., 2002). Des Weiteren konnte eine geringfügig eingeschränkte Fähigkeit zur Zweitstrangsynthese beobachtet werden. Diese wird benötigt, um das einzelsträngige DNA-Genom herkömmlich verwendeter AAV-Vektoren in einen transkribierbaren Doppelstrang zu verwandeln. Zusammenfassend muss man feststellen, dass sich die analysierten rAAV Serotypen als ungeeignete Gentransfervektoren für Rattenendothelzellen

erwiesen haben. Im Gegensatz dazu wurde in primären Rattencardiomyocyten *in vitro* eine deutlich höhere Transduktionseffizienz erzielt. Dies veranlasste uns, die vasoaktive Substanz Histamin in unserem heterotopen porcinen Transplantationsmodell anzuwenden, um *in vivo* sowohl Endothelzellen als auch Cardiomyocyten zu transduzieren. Interessanterweise zeigten *in vitro* Analysen porciner Aortenendothelzellen – im Gegensatz zu unseren erfolglosen Versuchen in RAECs – Transduktionseffizienzen von ca. 90 % mit rAAV2. Daher wurde dieser Serotyp zusammen mit Histamin in normotherme Herzen appliziert unter Verwendung des neuentwickelten *in situ* Langendorff Reperfusionssystems, welches eine verlängerte Rezirkulation des Vektors im Herzen erlaubte. In beiden Tieren konnte der Nachweis eines erfolgreichen Gentransfers anhand deutlich messbarer Transgen-DNA-Mengen erbracht werden. In einem der beiden Tiere wurde zudem funktionales Protein nachgewiesen. Dieses Schwein hatte zehnmal höhere Vektormengen erhalten. Dieser Vektor kodierte zudem für das Transgen Luciferase und wies eine *self-complementary* (Pseudo-Doppelstrang) Vektorgenom-Konformation auf. Im Gegensatz dazu wurde das Schwein, das keine Expression zeigte, mit einem Vektor behandelt, der für beta-Galaktosidase in einer Einzelstrang-Vektorgenom-Konformation kodierte. Obwohl weitere Experimente zur Bestimmung des Einflusses der drei Parameter (Vektormenge, Vektorgenom-Konformation und Wahl des Transgens), einzeln oder in Kombination, benötigt werden, konnten wir zeigen, dass ein rAAV2-vermittelter Gentransfer in porcines Herzgewebe im Rahmen eines (Xeno-) Transplantationsansatzes im Prinzip möglich ist.

Im zweiten Teil meiner Arbeit wurde ein Protokoll zur effizienten Transduktion humaner CD34⁺ Zellen aus Nabelschnurblut etabliert. Derartige Protokolle ermöglichen eine Kombination von Zell- und Gentherapie, welche für ein breites Spektrum an Anwendungen vorteilhaft ist. Vergleiche der Serotypen 2, 3 und 5 ermittelten rAAV2 als den effizientesten Serotyp in Zelleintritt und Transgenexpression. Der Zelleintritt von rAAV2 in CD34⁺ Zellen war abhängig von Heparansulfatproteoglycan, wie mithilfe von Konkurrenzexperimenten bestimmt wurde, und von $\alpha_5\beta_1$ Integrin, was wir mittels einer Mutante für die Bindung des Rezeptors ermittelten. Interessanterweise waren nur auf vorexpanzierten Zellen $\alpha_5\beta_1$ Integrine nachweisbar. Dies erlaubt den Schluss, dass zumindest einige der kontroversen Berichte zur rAAV-vermittelten Transduktion von CD34⁺ Zellen auf

die verwendeten Kulturbedingungen zurückzuführen sind. Darüberhinaus ist die Synthese des Zweitstrangs in CD34⁺ Zellen beeinträchtigt, da nur die Zugabe von Vektoren mit Genomen in der *self-complementary* Konformation in erfolgreichen Transduktionen resultierte. Die ohnehin schon sehr effiziente Transduktion (61 %), die mit rAAV2 Vektoren mit *self-complementary* Genomen in vorexpanzierten Zellen erzielt wurde, konnte signifikant (auf 86 %) durch die Zugabe von all-trans Retinsäure und dem Histon-Deacetylase-Inhibitor Trichostatin A erhöht werden. Darüberhinaus weisen unsere Ergebnisse darauf hin, dass Transduktionen mit rAAV nicht mit der Fähigkeit der CD34⁺ Zellen zur endothelialen Differenzierung interferieren. Zusammenfassend kann festgestellt werden, dass unter Verwendung des hier etablierten Protokolls CD34⁺ Zellen effizient mit rAAV2 transduziert werden können und sich rAAV2 somit als ein geeignetes Vektorsystem zur transienten Modifikation dieser Zellen anbietet.

2 Abstract

Heart diseases are the main cause of premature death in the population worldwide. Gene transfer as well as cell-based therapies are currently developed as new treatment options.

In the first part of this thesis, AAV-mediated gene transfer to deliver transgenes into heart tissue before transplantation ought to be established. As model system, the Sprague Dawley heterotopic rat model and the German Landrace pig model were chosen. rAAV serotype 2, described to be suited for this purpose, was intracoronarily delivered either in the normothermic (n=3) or hypothermic (n=3) hearts which were subsequently transplanted into a recipient rat. Gene transfer into normothermic hearts occurred with a better efficiency compared to hypothermic hearts. However, despite successful delivery and detection of vector DNA in tissue samples 28 d post transplantation, neither transgene-specific mRNA nor protein expression could be detected. To identify potential barriers that impair rAAV2-mediated transgene expression in our rat model, *in vitro* analyses in rat aortic endothelial cells (RAECs) were performed. We could exclude cell entry, intracellular trafficking of viral particles as well as expression from the chosen CMV promoter as inhibiting factors. However, application of the proteasome inhibitor MG132 significantly enhanced rAAV1- and rAAV2-mediated transgene expression (6-fold and 7.3-fold, respectively). The latter was in our hand the most efficient serotype in RAEC transduction among the serotypes rAAV1 to rAAV5. Since MG132 is a proteasome inhibitor blocking of vector degradation could be an explanation for the observed effect. Moreover, also indirect effects can be imagined like enhanced ubiquitination of the vector capsid, which is believed to facilitate vector uncoating or nuclear translocation of vector genomes (Duan et al., 2000; Yan et al., 2002). Furthermore, we observed a certain, albeit rather minor, limitation in second-strand synthesis. This step is necessary for the generation of a double-stranded DNA as template for transcription of the commonly used single-stranded DNA genome. In summary, the analyzed rAAV serotypes have been revealed as inappropriate gene transfer vectors in targeting of rat endothelial cells. In contrast, in primary rat cardiomyocytes *in vitro* a higher transduction efficiency was observed. Therefore, we decided to administer the vasoactive substance histamine in our heterotopic pig heart transplantation model in order to target cardiomyocytes in addition to endothelial cells. Interestingly, *in vitro* analyses of

porcine aortic endothelial cells revealed – in contrast to the unsuccessful attempts on RAECs – transduction efficiencies of about 90 % using rAAV2. Thus, this serotype was applied together with histamine into normothermic hearts using the newly developed *in situ* Langendorff reperfusion system which permitted prolonged recirculation of the vector in the heart. Transgene DNA detected in the graft of two transplanted animals displayed successful gene transfer. In one of the two animals functional protein was detected. This pig had received tenfold higher amounts of the vector which displayed a self-complementary vector genome conformation and encoded for the transgene luciferase. In contrast, the animal showing no expression was treated with a vector coding for beta-galactosidase in the single-stranded vector genome conformation. Although further experiments are needed to determine the influence of the three parameters (vector amount, vector genome conformation and choice of transgene) alone or in combination we could show that rAAV2-mediated gene delivery into the porcine heart tissue in a (xeno-) transplantation setting is in principle possible.

In the second part of my thesis, a protocol for efficient transduction of human cord blood-derived CD34⁺ cells was established. Such protocols enable a combination of cell and gene therapy which is advantageous for a wide range of applications. Among the serotypes 2, 3 and 5, rAAV2 was identified as the most efficient serotype in cell entry and in transgene expression. Cell entry of rAAV2 into CD34⁺ cells was dependent on heparin sulfate proteoglycan as determined by competition experiments, and on $\alpha_5\beta_1$ integrin as assessed by a receptor binding mutant. Interestingly, only pre-expanded cells displayed $\alpha_5\beta_1$ integrin allowing to conclude that at least some of the contradictory reports on rAAV-mediated transduction of CD34⁺ cells are due to the applied cultivation conditions. Furthermore, CD34⁺ cells are impaired in second-strand synthesis as only administration of vectors encoding the transgene in a self-complementary vector conformation resulted in successful transductions. The already high transduction level (61 %) achieved with rAAV2 using self-complementary vector genomes and pre-expanded cells could be significantly enhanced up to 86 % by addition of all-trans retinoic acid and the histone deacetylase inhibitor Trichostatin A. Furthermore, our results provide strong evidence that transductions by rAAV2 vectors do not interfere with endothelial differentiation potential of CD34⁺ cells. Thus, an efficient protocol for rAAV2-mediated transduction of CD34⁺ cells was

established revealing that rAAV2 is an appropriate vector system for transient modification of this cell type.

3 Introduction

3.1 Adeno-associated virus

3.1.1 Classification of adeno-associated virus

Adeno-associated viruses are classed into the *Parvoviridae* family. The *Parvoviridae* belong to the smallest known viruses (lat. parvus = small) consisting

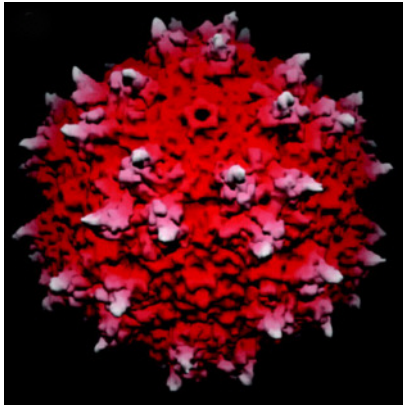


Figure 1: Atomic structure of AAV serotype 2 determined by X-ray crystallography. (Xie et al., 2003)

of a non-enveloped icosahedral capsid with a diameter of 18 to 26 nm and a linear single-stranded DNA genome (Figure 1). The *Parvoviridae* comprises two subfamilies: the vertebrate-infecting *Parvovirinae* and the *Densovirinae* which infect insects. The subfamily of *Parvovirinae* is further divided into the three genera *Parvo-*, *Erythro-* and *Dependovirus*. AAV belongs to the latter genus. *Erythrovirinae* infect erythroid precursor cells, whereas Parvovirus B19 is the only human pathogenic parvovirus and causes fifth disease (Erythema infectiosum) and complications during pregnancy (anemia, hydrops fetalis, abortions). Viruses belonging to the genus of *Parvovirus* are pathogenic for animals, examples are feline, canine and porcine parvovirus as well as minute virus of mice or aleutian mink disease virus. While erythro- and parvoviruses are autonomous viruses, dependoviruses require the presence of a helper virus like adenovirus (Ad), herpes simplex virus (HSV), vaccinia virus, human cytomegalovirus (HCMV) or papilloma virus (HPV) to undergo a productive life cycle (Atchison, Casto, and Hammon, 1965; McPherson, Rosenthal, and Rose, 1985; Richardson and Westphal, 1981; Schlehofer, Ehrbar, and zur Hausen, 1986). On the other hand, AAV seems to inhibit replication of helper viruses and also to interfere with malignant transformation induced by adenovirus, human or bovine papilloma virus (Heilbronn et al., 1990; Hermonat, 1992; Timpe, Verrill, and Trempe, 2006; You et al., 2006). Moreover, it was described that replication might be induced upon cellular genotoxic stress (Schlehofer, Ehrbar, and zur Hausen, 1986; Yakobson et al., 1989; Yakobson, Koch, and Winocour, 1987; Yalkinoglu et al., 1988).

Until now, 12 serotypes have been described. In the 1960's, AAV was discovered as contaminant of simian Adenovirus 15 preparations by several groups (Atchison, Casto, and Hammon, 1965; Mayor et al., 1965; Melnick et al., 1965). AAV serotype 2 has been isolated out of simian Adenovirus type 12 and AAV3 out of Adenovirus type 7 preparations (Hoggan, Blacklow, and Rowe, 1966). AAV4 has been found in African green monkeys infected with simian adenovirus 15 (Parks et al., 1967). In contrast, AAV5 was isolated out of a human clinical sample, a penile condylomatous lesion (Bantel-Schaal and zur Hausen, 1984). This virus is less related to the other serotypes considering sequence homology and serology (Chiorini et al., 1999). AAV6 has originally been identified as contaminant of an Adenovirus 5 stock. Its close relatedness to AAV1 with a variation of only 6 amino acids in the capsid sequence points either to a natural variant of serotype 1 or to a recombination between AAV1 and AAV2 as origin of AAV6 (Rutledge, Halbert, and Russell, 1998; Xiao et al., 1999). Wilson's group discovered the serotypes AAV7 and AAV8 by PCR scanning for AAV sequence homologies in rhesus monkey tissues (Gao et al., 2002). The same group screened human tissues from various sources to detect latent AAV genomes and identified thereby a serologically different serotype, called AAV9 (Gao et al., 2004). Mori and colleagues isolated two new AAV variants out of cynomolgus monkey tissue designated AAV10 and AAV11 (Mori et al., 2004). Despite their isolation out of non-human primate tissues, these serotypes are also suited for transduction of human tissues (Gao et al., 2004). Recently, AAV serotype 12 has been identified in simian Adenovirus 18 contaminated vervet monkey cells from ATCC stocks (Schmidt et al., 2006). Considering seroepidemiologic analyses, the serotypes AAV2, 3 and 5 are suggested to be endemic in humans (Gao et al., 2002). So far, AAV9 has only been found in human tissue. In contrast, monkeys are suggested to be the natural host for the serotypes 1, 4, 7 and 8 (Chiorini et al., 1997; Grimm and Kay, 2003; Xiao et al., 1999). AAV serotypes differ in their tropism. For example, AAV1 is appropriate for transduction of skeletal muscle or retina, whereas AAV5 is better suited for applications in the central nervous system or the lung as determined in mouse models (Auricchio et al., 2001; Davidson et al., 2000; Xiao et al., 1999; Zabner et al., 2000).

Moreover, AAV variants have also been isolated out of species other than primates including cow, bird, sheep, snake, lizard and goat (Bossis and Chiorini,

2003; Clarke et al., 1979; Farkas et al., 2004; Jacobson et al., 1996; Olson et al., 2004; Schmidt et al., 2004). So far, the best investigated AAV is the human serotype 2.

3.1.2 Genome organization

Wild type AAV contains a single-stranded DNA genome within an icosahedral capsid of 25 nm diameter. AAV serotype 2, the first serotype available as vector, has a genome size of 4680 nt with two open reading frames (ORFs) (Srivastava, Lusby, and Berns, 1983). These ORFs, encoding for the structural (*cap*; capsid) and non-structural proteins (*rep*; replication), are flanked by the inverted terminal repeats (ITRs) (Carter and Samulski, 2000) (Figure 2). This organization is conserved in all serotypes. The AAV2 genome contains three promoters (p5, p19, p40, describing their map position), but all transcripts share a common polyadenylation signal.

The 145 nt (for AAV2) long ITRs form the 3'- and 5'-end of the genome and hybridize to hairpin-like structures. Within the ITR region a Rep binding site (RBS) and a terminal resolution site (TRS) important for nicking of duplex DNA by the large Rep proteins are located (Im and Muzyczka, 1990; McCarty et al., 1994). In addition, this region is crucial for site-specific integration events, rescue of the provirus and serves as origin of replication (Berns, 1990; Feng et al., 2006; Hauswirth and Berns, 1977; Labow and Berns, 1988; McLaughlin et al., 1988). Moreover, the ITRs are required for packaging of the viral genomes into the preformed capsid.

The 5'-ORF encodes for four multifunctional, non-structural proteins named Rep78, Rep68, Rep52 and Rep40, according to their size (Lusby and Berns, 1982). While the p5 promoter controls the expression of the larger transcripts (Rep78 and Rep68) the expression of the smaller proteins Rep52 and Rep40 is under the control of the p19 promoter. Rep68 and Rep40 are splice variants of their larger counterparts (Figure 2). The Rep proteins have numerous functions. The two larger Rep proteins which possess a nuclear localization signal at their C-terminus are essential for replication, transcription and site-specific integration (Cassell and Weitzman, 2004). The smaller Rep proteins mediate accumulation and packaging of the viral genome into the preformed capsid in a helicase-dependent manner (Dubielzig et al., 1999; King et al., 2001). While the Rep

proteins can act as transactivator of transcription of the three viral promoters in presence of helper virus, they can also repress transcription of the p5 and p19 promoters in absence of helper virus (Kyostio et al., 1994; Pereira, McCarty, and Muzyczka, 1997). Moreover, the large Rep proteins can regulate the processing of the *cap* transcripts (Qiu and Pintel, 2002).

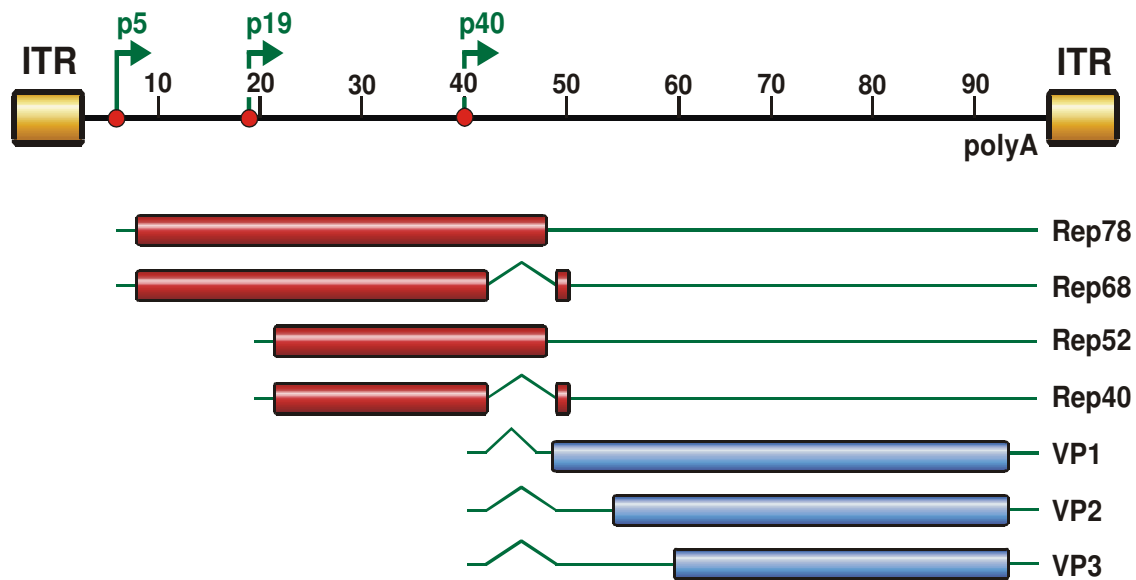


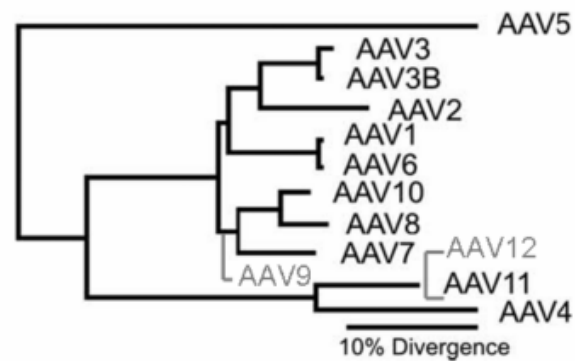
Figure 2: Genome organization of AAV2. The AAV2 genome, flanked by the ITRs, spans 4680 nt divided into units of 100 nt. Shown are the three promoters p5, p19 and p40 at map position 5, 19 and 40 and the polyadenylation signal (polyA) at position 96. The open reading frames are indicated by rectangles, translated regions in red or blue, untranslated regions by thin solid lines while introns are marked as nicks. The p5 promoter controls expression of the large Rep proteins (Rep78, Rep68), while the p19 promoter is responsible for the expression of the small Rep proteins (Rep52, Rep40). Rep68 and Rep40 are spliced variants of Rep78 and Rep52, respectively. The gene encoding for the capsid proteins VP1, VP2 and VP3 is controlled by the p40 promoter. (Figure kindly provided by N. Huttner)

The three structural proteins VP1, VP2 and VP3 are situated in the 3'-ORF *cap* controlled by the p40 promoter. These three proteins form the 60 subunits of the viral capsid at a ratio of 1:1:8 (Kronenberg, Kleinschmidt, and Bottcher, 2001; Rose et al., 1971). All capsid proteins share a common C-terminus, but differ in their N-terminus. The efficiency of translation for VP1 is regulated by alternative splicing while translation of VP2 is initiated from an unusual initiation codon (ACG) (Becerra et al., 1988; Becerra et al., 1985). This is the reason for the 10-fold lower translation efficiency of VP2 compared to VP3 which is regulated by an AUG

initiation codon (Becerra et al., 1985). The molecular weight of the three capsid proteins is 90 kDa (VP1), 72 kDa (VP2) and 60 kDa (VP3). Considering the functions of the capsid proteins, VP1 seems to be essential for infectivity whereas VP3 is sufficient for capsid formation (Warrington et al., 2004). VP2 is proposed to be neither necessary for capsid formation nor for production of infectious particles (Lux et al., 2005; Warrington et al., 2004).

Regarding phylogenetic relations between AAV2 and the other serotypes, a homology of 80 to 90 % was

observed for AAV1, 3, 6 to 8 and 10 in the amino acid sequence of VP1 (Gao et al., 2002; Mori et al., 2004) (Figure 3). AAV4 and AAV11 showed a 60 % and 65 % homology to AAV2 VP1, respectively (Gao et al., 2004; Mori et al., 2004).



AAV12's closest relatives within the AAV family are AAV11 (84 %) and AAV4 (78 %) (Schmidt

Figure 3: Phylogenetic analysis of the amino acid sequences of the capsid protein VP1. Modified scheme (grey) (Mori et al., 2004).

et al., 2007). AAV5 is the most divergent serotype with only 58 % similarity compared to AAV2 VP1 (Bantel-Schaal et al., 1999). Additionally to the divergence of the capsid protein to the other serotypes, AAV5 contains an extra polyadenylation signal located within the intron thus producing mainly the unspliced Rep proteins Rep78 and Rep52 (Qiu et al., 2002). In general, homologies in the VP1 proteins are comparable to the phylogenetic results obtained by the nucleotide sequence (Grimm and Kay, 2003). About the recently described serotypes AAV9 to 12 only little is known so far.

3.1.3 Infection biology of AAV

A successful infection of cells by AAV is a multistep process including attachment, uptake, intracellular trafficking, nuclear translocation and replication of the virus (Figure 4). Its understanding is crucial to identify potential barriers in AAV infection that have to be overcome for its use as gene therapy vector. The current knowledge of AAV2 infection is described in detail in the following chapters.

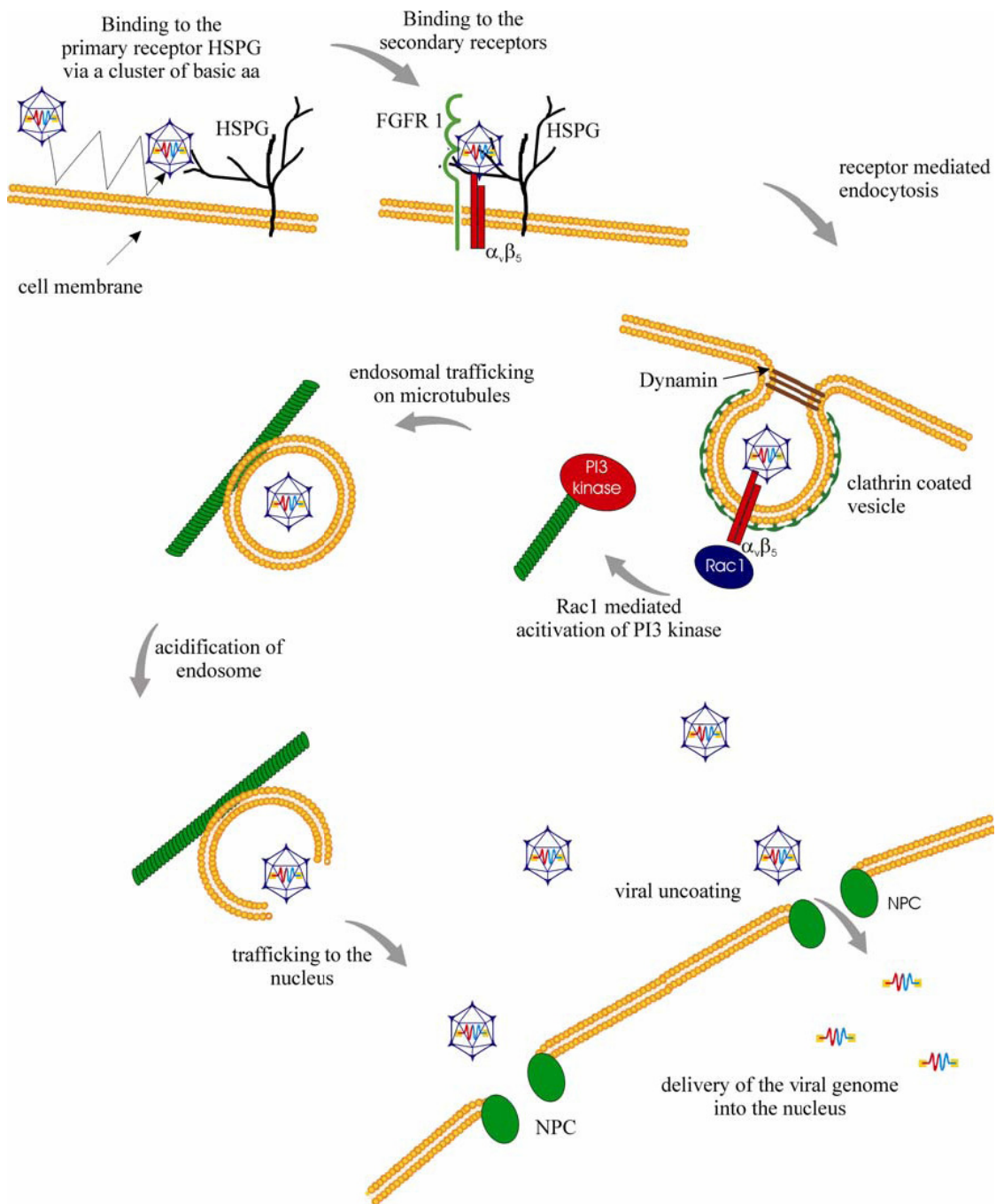


Figure 4: Infection pathway of AAV2 in HeLa cells. AAV2 touches the host cell several times and attaches to its primary receptor heparan sulfate proteoglycan (HSPG) and to the coreceptors fibroblast growth factor receptor 1 (FGFR-1) and the integrin $\alpha_v\beta_5$. The virus is internalized by receptor-mediated endocytosis into clathrin-coated vesicles in a dynamin-dependent way. The GTP-binding protein Rac1 is believed to be activated by integrin-binding and rearranges the cytoskeleton thus facilitating endosomal trafficking. Acidification of the endosomes leads to an escape of the AAV particles, maybe due to conformational changes. Viral uncoating takes place before or during nuclear entry. Also the exact mechanism of viral DNA import into the nucleus is yet unknown.(aa, amino acid)(Buning et al., 2003a)

3.1.3.1 Virus-cell interaction

As Single Virus Tracing studies revealed, AAV2 contacts the cell membrane several times before it enters the cell (Seisenberger et al., 2001). For AAV2, the widely expressed cell surface receptor heparan sulfate proteoglycan (HSPG) has been identified as primary receptor (Summerford and Samulski, 1998). This contact is mediated by surface structures on the AAV capsid, namely the residues R484, R487, K532, R585 and R588 in the common VP3 region (Kern et al., 2003; Wu et al., 2000). Attachment to HSPG seems to induce a reversible structural change thus facilitating coreceptor binding and cell entry (Asokan et al., 2006). Surprisingly, some cell lines have been shown to take up virions even in the absence of HSPG (Duan et al., 1998b; Duan et al., 2000). Also AAV3 is suggested to use HSPG as primary receptor whereas the serotypes 1, 4, 5 and 6 bind to sialic acid (Rabinowitz et al., 2002). In 2006, Wu identified α 2,3 and α 2,6 sialic acids present on N-linked glycoproteins as primary receptors for AAV1 and AAV6 (Wu et al., 2006). AAV4 and AAV5 both bind to α 2,3 sialic acid, but differ in their linkage specificity. While AAV4 requires O-linked, AAV5 prefers N-linked α 2,3 sialic acids (Kaludov et al., 2001; Walters et al., 2001). Recently, the 37/67 kDa laminin receptor was proposed as a receptor for AAV8 (Akache et al., 2006). Interestingly, overexpression of this receptor rendered cells also more susceptible for transduction with AAV2, 3 and 9 proposing a role for laminin receptor for cell infection of these serotypes. For AAV12, recently published data point towards a HSPG and sialic acid independent entry mechanism (Schmidt et al., 2007). The primary receptors for AAV7 and 9 to 12 have yet to be determined.

For efficient internalization, the additional binding to coreceptors is required. For AAV2, five secondary receptors have been proposed so far. Human fibroblast growth factor receptor 1 (FGFR-1), hepatocyte growth factor receptor (HGFR or c-met) and laminin receptor seem to support virus:cell interaction (Akache et al., 2006; Kashiwakura et al., 2005; Qing et al., 1999). On the other hand, the integrins $\alpha_v\beta_5$ and $\alpha_5\beta_1$ are proposed as further coreceptors (Asokan et al., 2006; Sanlioglu et al., 2000; Summerford, Bartlett, and Samulski, 1999).

For AAV3, FGFR-1 has been described as potential coreceptor (Blackburn, Steadman, and Johnson, 2006). Concerning AAV5, the platelet-derived growth factor receptor (PDGFR) was identified as secondary receptor (Di Pasquale et al., 2003). It is conceivable that PDGFR might act alone as AAV5 receptor as it is a

sialo-proteoglycan containing oligosaccharides chains with sialic acids (Daniel et al., 1987; Hosang, 1988).

3.1.3.2 Receptor-mediated endocytosis

Following receptor binding and structural rearrangement, the virion enters the cell predominantly by receptor-mediated endocytosis in a dynamin-dependent manner (Bartlett, Wilcher, and Samulski, 2000; Duan et al., 1999; Hinshaw and Schmid, 1995). Single Virus Tracing studies revealed that the uptake of virions occurs within 100 ms (Seisenberger et al., 2001). Clustering of $\alpha_v\beta_5$ integrins seems to facilitate localization of the virion into clathrin-coated pits (Bartlett, Wilcher, and Samulski, 2000). Also for AAV5, localization in clathrin-coated pits has been claimed despite usage of alternate receptors (sialic acid and/or PDGFR) (Bantel-Schaal, Hub, and Kartenbeck, 2002). In addition, integrins interact with intracellular signalling molecules, e.g. Rac1, which support the internalization processes (Sanlioglu et al., 2000). Moreover, the activation of this small GTP-binding molecule leads to a subsequent activation of the phosphatidylinositol-3 kinase (PI3K) pathway which is involved in vesicular trafficking and rearrangement of microtubules and microfilaments (Kapeller and Cantley, 1994; Sanlioglu et al., 2000). Interestingly, Rac1 and PI3K pathways are also crucial for internalization of adenovirus, a helper virus of AAV which is also located in clathrin-coated vesicles shortly after cell entry (Li et al., 1998).

3.1.3.3 Endosomal processing and escape

Even though details about the endosomal pathway used by AAV remain to be elucidated, it seems to be assured that trafficking of the virion-containing endosomes along the microtubules and microfilaments towards the nuclear area is essential for successful transduction (Bartlett, Wilcher, and Samulski, 2000; Douar et al., 2001). As Sanlioglu and colleagues described, application of nocodazole to depolymerize microtubules reduces perinuclear accumulation of AAV2 (Sanlioglu et al., 2000). Moreover, investigations on certain non-transduceable cell types revealed inefficient endosomal processing and nuclear trafficking as critical steps (Duan et al., 2000; Hansen, Qing, and Srivastava, 2001a). However, publications about intracellular processes remain controversial. While some groups postulate an escape from the early endosome, others observe a trafficking into the late endosomal compartment (Bartlett, Wilcher, and Samulski, 2000; Douar et al.,

2001; Hansen, Qing, and Srivastava, 2001a; Xiao et al., 2002). For AAV2 and AAV5, also an accumulation in the Golgi compartment was stated (Bantel-Schaal, Hub, and Kartenbeck, 2002; Pajusola et al., 2002).

To escape from the endosomes for trafficking to the nucleus, AAV requires endosomal acidification. This assumption is based on the observation that inhibition of acidification by bafilomycin A or ammonium chloride blocks transduction (Bartlett, Wilcher, and Samulski, 2000). It has been postulated that the progressively decreasing pH inside the endosomes induces a conformational change in the capsid leading to the exposure of a phospholipase A₂ (PLA₂) homology domain within the N-terminus of VP1 (Kronenberg et al., 2005; Sonntag et al., 2006). This domain is conserved among parvoviruses and required for infectivity (Girod et al., 2002). It is discussed to be involved in nuclear entry or, most likely, in endosomal escape (Girod et al., 2002; Sonntag et al., 2006). The importance of endosomal acidification is also known for other viruses, e.g. for rhabdovirus which exposes domains to facilitate membrane fusion or for adenovirus to disrupt the endosome (Marsh and Helenius, 1989).

When released from the endosomes, as shown for AAV2 and AAV5, the capsids are a target for ubiquitination which usually serves as a signal for proteasomal degradation (Yan et al., 2002). Ubiquitin, however, also mediates proteasome-independent functions (Mukhopadhyay and Riezman, 2007). Interestingly, addition of proteasome inhibitors, e.g. MG132, resulted in an enhancement of transgene expression in some cell lines transduced by the serotypes 1 to 5 and by AAV2 in mouse lungs *in vivo* (Douar et al., 2001; Duan et al., 2000; Hacker et al., 2005; Jennings et al., 2005; Yan et al., 2004). Though the mechanisms remain unclear, it has been suggested that proteasome inhibitors block capsid degradation, facilitate vector uncoating, lead to an increased perinuclear accumulation or translocation into the nucleus (Duan et al., 2000; Yan et al., 2002).

3.1.3.4 Nuclear translocation

Viral particles start to accumulate in the perinuclear area between 15 and 30 min post infection (p.i.) (Bartlett, Wilcher, and Samulski, 2000; Seisenberger et al., 2001). Moreover, viral capsids can be detected in nuclear invaginations (Lux et al., 2005; Seisenberger et al., 2001). In comparison to entry and intracellular trafficking, translocation of the virus into the nucleus is a comparably slow and

inefficient step (Lux et al., 2005). However, reports on intact viral particles within the nucleus have been published (Sanlioglu et al., 2000).

If viral uncoating occurs before or after entering the nucleus is still a controversially discussed question. Lux and colleagues reported that uncoating occurs before or during entry into the nucleus independently of the helper virus since at viral-to-cell ratios at which viral genomes could be detected within the nucleus. Signals for intact viral capsid were exclusively detected outside the nucleus in the perinuclear area or in nuclear invaginations (Lux et al., 2005). In presence of helper virus, however, the rare event of intranuclear localization of intact virals capsids is increased (Xiao et al., 2002).

Moreover, it is still discussed whether AAV and/or AAV genomes enter the nucleus through the nuclear pore complex (NPC) or in a NPC-independent way (Hansen, Qing, and Srivastava, 2001b). However, several agents have been shown to enhance nuclear accumulation and gene expression of AAV including adenovirus as well as hydroxyurea and the previously mentioned proteasome inhibitors (Hansen, Qing, and Srivastava, 2001a; Jennings et al., 2005; Xiao et al., 2002).

3.1.3.5 Latent and lytic life cycle of AAV

The presence or absence of helper virus determines if AAV enters a lytic or latent life cycle. Lacking the helper viral functions, the virus latently infects cells by integrating into the genome. Integration occurs in dividing and, to a lesser extent, in non-dividing cells (Podsakoff, Wong, and Chatterjee, 1994; Russell, Miller, and Alexander, 1994). First, second-strand synthesis of the single-stranded virus genome and a basal expression of the Rep proteins are activated (Brister and Muzyczka, 2000; Redemann, Mendelson, and Carter, 1989). In presence of the large Rep proteins (Rep68, Rep78) and intact ITRs, integration occurs, although not exclusively, at the so-called AAVS1 site on the human chromosome 19 (19q13.3-qter) (Kotin, Linden, and Berns, 1992; Kotin et al., 1990). The AAVS1 locus resides a Rep binding element (RBS) and a terminal resolution site (TRS) equivalent to the AAV genome (Linden et al., 1996; Linden, Winocour, and Berns, 1996; Weitzman et al., 1994). Usually, proviral sequences are integrated as viral concatemers in a head-to-tail conformation (Linden et al., 1996). The ability to integrate site-specifically into the human genome is unique among eukaryotic viruses and explains the attractivity of AAV as vector for gene therapy. Helper viral

superinfection can rescue the integrated provirus initiating a lytic, productive life cycle (Berns and Giraud, 1996).

During virus replication, the 3'-OH end of the hairpin-like ITR may serve as primer for second-strand synthesis (Berns, 1990). The large Rep proteins unwind the ITR by their helicase activity which leads to exposure of the TRS which is nicked by the Rep endonuclease and enables complete synthesis of the second-strand by switching templates (Brister and Muzyczka, 2000; Im and Muzyczka, 1990; Ni et al., 1994). The single-stranded DNA is then converted into a parental duplex replicative form and production of viral progeny can proceed.

3.1.4 Adenovirus-free AAV production and recombinant AAV vectors (rAAV)

For the production of recombinant AAV (rAAV), the only viral elements required *in cis* are the ITRs while the two ORFs *rep* and *cap* are sufficient when provided *in trans* (helper plasmid) (Collaco, Cao, and Trempe, 1999). The deleted *rep/cap* sequences of the parental virus can then be replaced by marker or therapeutic genes resulting in the production of vectors which are unable to replicate even in presence of helper virus (Collaco, Cao, and Trempe, 1999). The flanking ITRs are necessary for packaging into the newly formed capsids. In general, rAAV is produced in a helper virus-free manner to avoid helper virus contaminations of vector preparations. The essential adenoviral genes *VA*, *E2A* and *E4* have been cloned into an adenoviral helper plasmid and are provided *in trans* (Collaco, Cao, and Trempe, 1999; Grimm and Kleinschmidt, 1999; Xiao, Li, and Samulski, 1998). HEK293 cells which are commonly used for the production of viral particles are transgenic for the adenoviral genes *E1a* and *E1b*.

The helper, vector and adenoviral plasmids are brought in HEK293 cells by triple transfection (Figure 5). 48h later, viral progeny can be isolated out of the cell lysates and purified by either CsCl or Iodixanol gradient ultracentrifugation (Hermens et al., 1999; Zolotukhin et al., 1999). AAV2 is appropriate for purification directly from crude lysates or from gradient purified fractions by heparin affinity chromatography (Zolotukhin et al., 1999).

All serotypes can be produced as recombinant vectors as described above. Therefore, only the *cap* sequence of AAV2 has to be replaced by the serotype-

specific *cap*. The ITRs as well as the *rep* ORF are typically derived from AAV2. This method is called pseudotyping or cross-packaging (Rabinowitz et al., 2002).

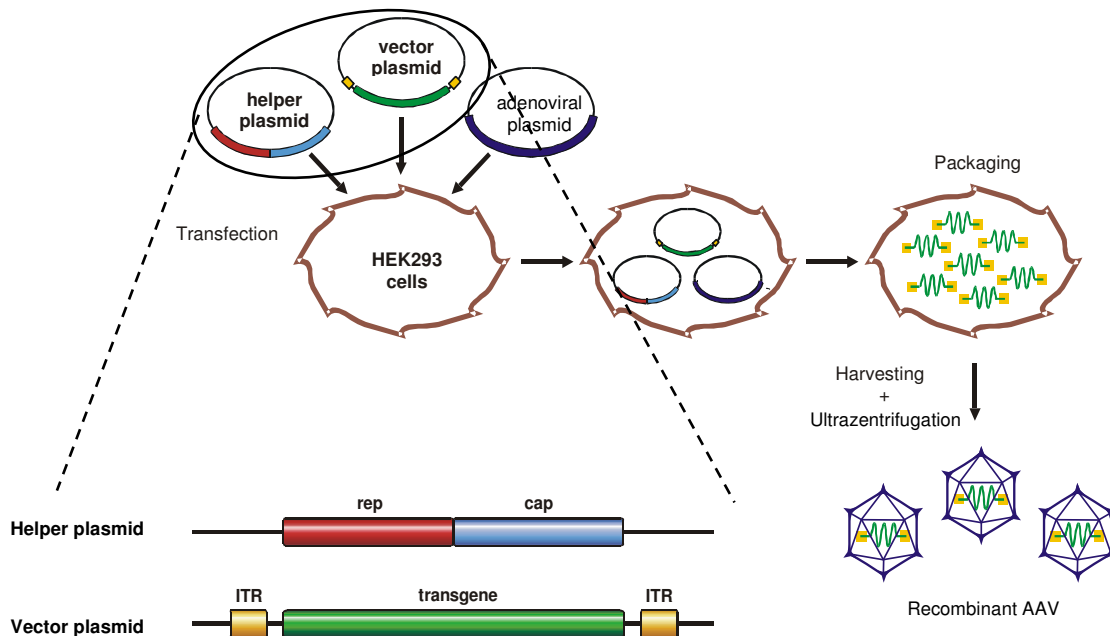


Figure 5: Packaging of recombinant AAV vectors. HEK293 cells are transfected by 3 plasmids: A helper plasmid encoding for the *rep* and *cap* ORFs, a vector plasmid carrying the desired transgene flanked by the packaging sequences (ITRs) and an adenoviral helper plasmid to provide helper virus functions. After vector assembly, the cells are lysed and rAAV is purified, e.g. by ultracentrifugation. (Figure was kindly provided by H. Büning)

Transduction efficiency in numerous cell lines has been reported to be limited by insufficient second-strand synthesis of the single-stranded (ss) DNA genome (Ferrari et al., 1996; Fisher et al., 1996). This step is necessary to obtain a double-stranded DNA template for initiation of gene expression. Hence, McCarty and colleagues developed a pseudo double-stranded, self-complementary (sc) genome in order to overcome this limitation (McCarty, Monahan, and Samulski, 2001). Their construct contains an extra copy of the palindromic terminal repeat thus enabling the DNA to re-fold and form a duplex DNA (Figure 6). Thereby, the requirement for host cell-mediated second-strand DNA synthesis can be circumvented and high transduction efficiencies are obtained *in vitro* and *in vivo* (Hacker et al., 2005; McCarty et al., 2003; Wang et al., 2003). Due to the duplex structure of the self-complementary genome conformation, its packaging capacity is limited to half of the single-stranded construct that is about 2.3 kb compared to

4.6 kb including ITRs. Therefore, self-complementary vectors are not suitable for larger transgenes.

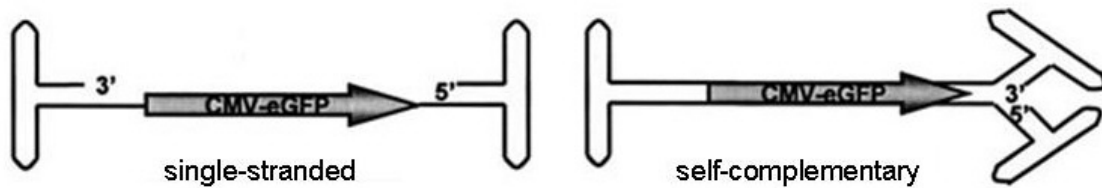


Figure 6: Single-stranded and self-complementary vector genome conformation. On the left side, the natural, single-stranded conformation of AAV is shown. On the right side, the same transgene cassette consisting of a CMV promoter-driven eGFP gene is depicted as a self-complementary DNA. An additional terminal repeat allows folding into a duplex DNA. (McCarty, Monahan, and Samulski, 2001)

3.1.5 AAV as vector in gene therapy

Gene therapy bases on the idea of introducing genetic material into an organism in order to cure or improve the status of a disease. In general, two different systems are applied, the viral and non-viral vectors. Whereas the viral systems include adeno-, retro-, vaccinia-, pox-, herpes simplex- and adeno-associated-viral vectors, the non-viral vector strategy uses naked DNA and lipid- or polyethylenglycol- (PEG) covered DNA (Gould and Favorov, 2003; Minato et al., 2003; Omori et al., 2003).

Ideally, gene therapeutical vectors should combine efficiency and safety. Unique for AAV is that no disease could be related to this virus despite its broad tissue tropism (Berns and Linden, 1995). The transduceability of various cell types including dividing as well as post-mitotic or quiescent cells and differentiated tissues such as brain, muscle, lung and liver, qualifies AAV for a wide range of applications (Alexander et al., 1996; Fisher et al., 1997; Flotte et al., 1993; Kaplitt et al., 1994; Kaplitt et al., 1996; Manno et al., 2006; Podsakoff, Wong, and Chatterjee, 1994). Moreover, AAV has also been shown to mediate long-term expression, e.g. in a muscle-directed trial where transgene expression sustained for more than four years in a canine hemophilia B model (Fisher et al., 1997; Herzog et al., 1999). As another important aspect, AAV does not need to integrate into the host genome in contrast to lenti- or retroviral vectors. Actually, vector genomes seem more likely to exist as episomes (Duan et al., 1998a; Nakai et al.,

2001). Moreover, in presence of the large Rep proteins, AAV is able to integrate site-specifically into the human chromosome 19 thus minimizing the risk of insertional mutagenesis (Huttner et al., 2003; Kotin et al., 1990). By the development of high titer-reaching helpervirus-free production methods as well as improvements in purification this vector system has become even more attractive. As recombinant AAV vectors are gutless vectors, they are unable to replicate even in presence of helper virus (Samulski, Chang, and Shenk, 1987).

In general, immunologic reactions to AAV are low. The importance of that aspect becomes evident when AAV is compared to adenovirus which elicits high immune responses (Raper et al., 2003; Zaiss et al., 2002). Apparently, AAV has only a minimal inflammatory potential and seems not to engage pattern recognition receptors like toll-like receptors (TLRs) mediating innate immune responses (Hensley and Amalfitano, 2007; Zaiss et al., 2002). The prevalence of antibodies against AAV2 due to natural infections is as high as 50 to 96 % in the human population. The amount of neutralizing antibodies varies from 18 to 68 % depending on age and ethnic group (Chirmule et al., 1999; Erles, Sebokova, and Schlehofer, 1999; Moskalenko et al., 2000). Animal experiments have confirmed that neutralizing antibodies have strong negative implications on transduction efficiency if the same serotype is reapplied (Scallan et al., 2006). Although human data are limited, at least for one patient in a clinical hemophilia B trial, neutralizing antibodies seem to account for the absence of transgene expression (Manno et al., 2006). Additionally, an anti-capsid response was observed.

Disadvantages of the AAV vector system are its small genome size limiting the coding capacity for transgenes including ITRs to a maximum of 4.1 to 4.9 kb and its broad tissue tropism interfering with a cell-specific *in vivo* gene transfer (Dong, Fan, and Frizzell, 1996).

For overcoming pre-existing immune reactions and off-target gene expression, several options are available. The use of serotypes other than AAV2 which show different tropisms and immune responses can be considered and technology, respectively, are likely to cope with these limitations (Buning et al., 2003b; Grimm and Kay, 2003; Limberis and Wilson, 2006; Wu, Asokan, and Samulski, 2006). Furthermore, several strategies have been developed to overcome the size

limitation (Duan et al., 2001). Overall, AAV is a promising vector for gene therapy as assessed in clinical trials.

Since the first gene therapy clinical trial in 1989, 1308 more studies have been initiated worldwide (<http://www.wiley.co.uk/genmed/clinical/>). The main focus for gene therapeutical applications is the treatment of cancer with 66.5 % clinical trials followed by cardiovascular (9.1 %) and monogenic (8.3 %) diseases. In most cases, adeno- (24.7 %) or retroviral (22.8 %) vectors find application, while AAV vectors are used only in 3.5 % of the approaches. In complete, 32 clinical trials involving AAV vectors are still open, whereas 14 are already closed. Currently, evaluation of safety of AAV as a vector system is of main interest in clinical trials. First published data dealt with the monogenic diseases cystic fibrosis and hemophilia B in gene therapy trials. Administration of the cystic fibrosis transmembrane conductance regulator (CFTR) as transgene on the nasal sinus and bronchial epithelium resulted in an improvement of pulmonary function and partial correction of hyperinflammatory responses and electrophysiological defects (Moss et al., 2004; Wagner et al., 1999; Wagner et al., 1998). AAV was approved to be safe in these clinical settings as well as in the treatment of hemophilia B by intramuscular or intrahepatic vector administration (Kay et al., 2000; Manno et al., 2003; Manno et al., 2006). Evidences for transduction were found in all patients of the muscle-directed study and long-term expression of the therapeutic gene, coagulation factor IX (FIX), could be detected albeit at low levels. Highest vector amount administered into the hepatic artery resulted in therapeutic, but transient (<8 weeks) transgene expression levels.

3.1.5.1 Gene therapy of ischemic cardiovascular diseases

As mentioned above, cardiovascular diseases are a main target for human gene therapy. Despite considerable advances in conventional treatment strategies, heart diseases remain the prevalent cause of disability and premature death in the human population (17 million deaths per year) world-wide (World Health Organization 2008). Since organ regeneration, pharmacotherapy and invasive interventions are limited, alternative therapies are urgently needed. Currently, xenotransplantation, gene- and cell-based therapies are the focus of intense investigations. Most efforts in the latter two fields are made on the development of strategies to induce angiogenesis (vessel formation from pre-existing ones) and vasculogenesis (*de novo* vessel formation) (Khan, Sellke, and Laham, 2003; Melo

et al., 2004). Such therapies could be administered either for protection of myocardium at risk or for rescue after infarction (Khan, Sellke, and Laham, 2003).

Investigations on the molecular and cellular basis of cardiac diseases have identified potential therapeutic genes. The promising therapeutic potential of angiogenic factors such as vascular endothelial growth factor (VEGF), fibroblast growth factor (FGF) or hepatocyte growth factor (HGF) has already been successfully demonstrated in clinical trials (Baumgartner et al., 1998; Grines et al., 2003; Losordo et al., 2002; Morishita et al., 2004). Overexpression of cytoprotective genes like antioxidant genes (e.g. heme oxygenase 1 (HO-1)), survival genes (e.g. Bcl-2, HGF), genes encoding for heat shock proteins and anti-inflammatory cytokines (e.g. IL-4, IL-10, IL-13, TGF- β) as well as inhibition of proapoptotic genes (e.g. Bad) might be useful in myocardial protection as described in various publications and reviewed by Melo and colleagues (Melo et al., 2005).

Generally, gene transfer vectors are administered into the heart tissue by either of the two routes, intracoronary or intramyocardial. Injection into the myocardium resulted in local transgene expression in a patchy pattern (French et al., 1994). In order to reach homogenous vector distribution, vector can be applied intracoronary. However, this procedure is limited by the short exposure time of the vector to the endothelium and fast systemic distribution. If transduction of the myocardium is desired, the vector has to overcome the endothelial barrier. Therefore, novel techniques have been developed to increase endothelial permeability and to prolong exposure time. Capillary-modulating substances like histamine, serotonin or VEGF as well as high intravascular pressure or ultrasound have been described to permeabilize the endothelial barrier (Beerli et al., 2002; Bekeredjian et al., 2003; Donahue et al., 1998; Logeart et al., 2001). As demonstrated in a rat model, simultaneous clamping of the pulmonary artery and the aorta allowed the adenoviral vector to recirculate in the coronaries over a short period of time and resulted in successful transgene expression (Hajjar et al., 1998). Prolongation can also be reached by hypothermia or cardiac arrest (Ding et al., 2004; Iwanaga et al., 2004).

On the other hand, direct targeting of the endothelium might be favourable in endothelial dysfunction which plays a pivotal role in atherosclerosis, coronary

artery disease and hypercholesterolemia. Under physiological conditions, the endothelium retains numerous prominent roles in maintaining vessel wall homeostasis such as regulation of angiogenesis, thrombolysis, leukocyte adhesion, platelet adhesion and aggregation (Cooke, 2000). Therefore, anti-thrombotic, anti-adhesion (e.g. inhibition of intercellular adhesion molecule 1 (ICAM-1)) or anti-inflammatory genes are considered as therapeutic targets in endothelial dysfunction and should preferentially be expressed by endothelial cells (Vassalli et al., 2003). In diseases associated with high oxidative stress, the overexpression of enzymes that act as anti-oxidants could be beneficial as shown in a rat postmyocardial infarction model using rAAV to deliver heme oxygenase 1 (HO-1) delivery (Liu et al., 2006).

AAV2 was reported to transduce endothelial cells *in vitro* and *in vivo* with low efficiency (Nicklin et al., 2001a; Pajusola et al., 2002). Besides AAV, also adeno-, retro- and lentiviruses have been used as gene therapy vectors for cardiac diseases. Additionally to the disadvantages discussed above, the potential of retroviruses is limited as they require dividing cells for efficient transduction, whereas lentiviruses are appropriate vectors for endothelial transduction (Byun et al., 2000; Sakoda et al., 2007). Adenovirus might provoke myocarditis in response to immune reactions and shows only short-term transgene expression (Calabrese and Thiene, 2003; Guzman et al., 1993). In targeting of the myocardium, comparative analyses of the AAV serotypes in mouse and non-human primate models revealed the recently discovered AAV9 as the most efficient serotype (Pacak et al., 2006; Palomeque et al., 2007).

Recently, the identification of stem cells capable of contributing to tissue regeneration has ignited significant interest in the possibility that cell therapy might be used therapeutically for repair of damaged myocardium. Thereby, the combination of cell- and gene-based therapies could result in even higher beneficial effects. This interesting field is discussed separately in chapter 3.2.3.

Transplantations as potential therapy are limited primarily by donor organ shortage and the need for optimal tissue matching to minimize the risk of organ rejection. Nevertheless, organ recipients require life-long immunosuppression. Currently, researchers are determining the potential and limiting factors of porcine grafts which are functionally and physically closely related to human hearts. In

xenotransplantation and transplantation, gene therapy could allow the production of immunomodulatory proteins locally within the donor graft or the induction of donor-specific tolerance and other mechanisms preventing graft rejection (Chen, Sung, and Bromberg, 2002). Moreover, the identification of beneficial effectors could account for the generation of transgenic animals for xenotransplantation. Both, innate and adaptive immune reactions are responsible for organ rejection. The hyperacute rejection occurring within minutes is due to complement-dependent reactions of pre-existing alloantibodies to blood group or major histocompatibility complex (MHC) antigens. As complement-regulatory molecules are working less efficient across species-barriers and recognize directly certain porcine oligosaccharides (e.g. α Gal), this step is very problematic for xenografts. Nevertheless, the main mediators for acute organ rejection are T-cells. They can be either activated directly by donor antigen-presenting cells (APC) or indirectly by the recipient's APCs which present phagozytosed non-self molecules to T-cells. Additionally, T-cells play an important role in chronic rejection processes caused by inflammatory vascular injury. Briefly, alloreactive T-cells infiltrate the graft and recruit inflammatory cells by cytokine release and stimulation of endothelial adhesion molecules. Gene therapeutical approaches encompass the inhibition of anti-graft responses and induction of graft protective mechanisms (Chen, Sung, and Bromberg, 2002). As already discussed above, delivery of genes encoding for anti-adhesive, anti-apoptotic, anti-inflammatory and antioxidant proteins might be useful in this regard as well. Moreover, blockage of specific functions of the adaptive immune system showed promising effects. For example, inhibition of the costimulatory signal (CD28-CD80/86) between APC and T-cell by expression of CTLA-4Ig prolongs cardiac graft survival using AAV as vector system (Chen et al., 2003). Expression of immunomodulatory cytokines such as IL-4, IL-10, IL-13 and TGF- β resulted in prolonged allograft survival in various models (Chan et al., 2000; David et al., 2000; Ke et al., 2000; Ke et al., 2002). Another example is viral IL-10 (vIL-10) which is encoded by the Epstein-Barr virus. It has the same properties like IL-10, but lacks T-cell immunostimulatory functions and has been shown to prolong heart survival time in an adenovirus-mediated vIL-10 rat transplantation model (Zuo et al., 2001).

3.2 Stem cells

By definition, stem cells (SC) are undifferentiated cells able to generate new stem cells of identical differentiation potency or to produce cells that differentiate along a lineage pathway. The first of these two activities of stem cells is described as symmetric, the second as asymmetric division. Both types of cell divisions contribute to the homeostasis of the stem cell population within the stem cell niche, whereas asymmetric divisions are responsible for renewal of the respective, differentiated tissue. In the adult tissue, quiescent stem or progenitor cells are normally mobilized upon stimuli for physiological and pathological tissue regeneration.

Stem cells can be divided into three different types depending on their developmental potential. Embryonic totipotent stem cells are able to differentiate into all embryonic and extra-embryonic cell types (e.g. placenta, umbilical cord) while pluripotent – the so-called embryonic stem cells – possess the ability to generate all tissues of an adult organism. Pluripotent cells give rise to the three types of germ layer stem cells for ecto-, endo- and mesoderm (Figure 7). As development proceeds the differentiation properties get more restricted. The multipotent stem cell gives rise to only a limited number of cell types of fully developed organs maintaining a steady-state homeostasis in the tissue. If only one terminally differentiated cell type can be generated, the cell is referred to as unipotent.

Multipotent and unipotent cells are designated as somatic or adult stem cells and are present in tissues where terminally differentiated cells do not divide or have only a short life span. Indeed, long time it was believed that organs responding poorly to regenerative pressure (e.g. heart, brain) would not reside any stem cells. Then it turned out that even organs considered as post-mitotic were able to regenerate although at lower levels. Anyway, multipotent stem cells are more abundant in tissues with a high cell turnover rate such as epithelia, vasculature or blood and to a lesser extent in organs or tissues undergoing little self-renewal like the central nervous system or the myocard (Beltrami et al., 2003; Lemoli, 2005; Lois and Alvarez-Buylla, 1993; Oh et al., 2003). The best characterized multipotent cells are hematopoietic stem cells (HSC) which give rise to the entire blood lineages.

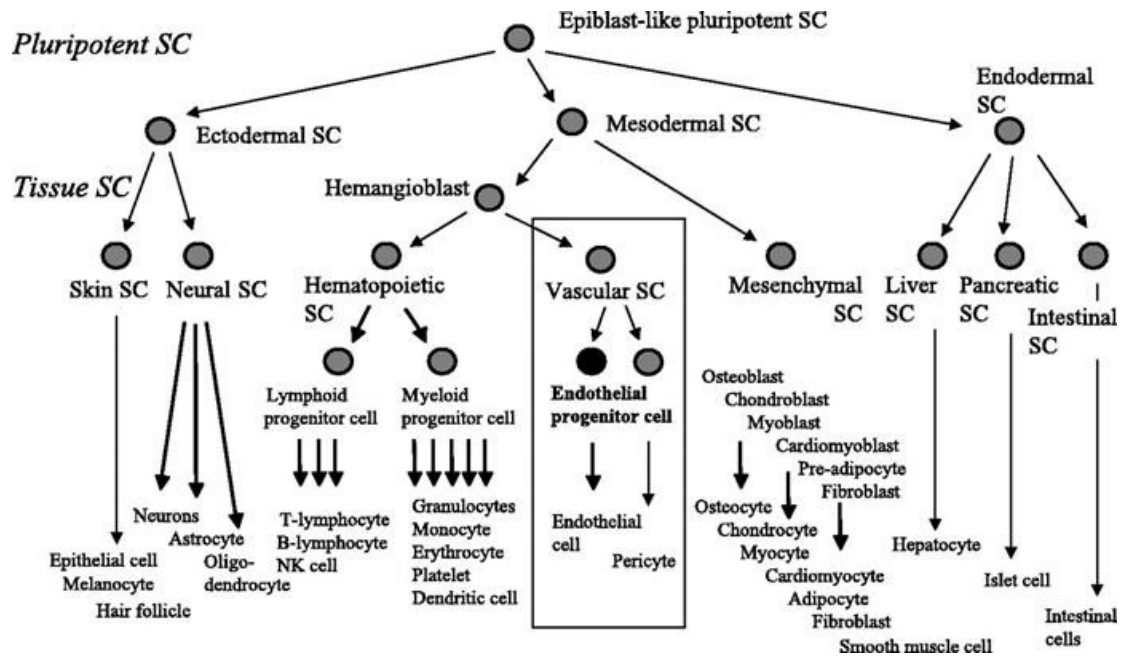


Figure 7: Postnatal stem and progenitor cells. SC, stem cell. (Asahara and Kawamoto, 2004)

3.2.1 Hematopoietic stem cells and endothelial progenitor cells

Since blood cells have only a limited life span and essential functions like gas transport, immunity and other vital functions have to be maintained, a continuous production of new cells is needed. The hematopoietic stem cell (HSC) provides all the blood lineage cells and is well described. In the 1960's first evidence for the existence of clonogenic cells able to generate myeloerythroid cells after bone marrow transplantation in lethally irradiated mice was given (Becker, Mc, and Till, 1963; Wu et al., 1968).

Regarding embryonic development hematopoietic and endothelial progenitor cells share a common mesodermal precursor called hemangioblast. These cells can be found in the extra embryonic yolk sac where they are accumulating in the so-called blood islands. In the inner part of these aggregates cells possess hematopoietic properties whereas the outer cells begin to form endothelial cells (EC) (Asahara and Kawamoto, 2004). These first developing vessels are marking the onset of vasculogenesis. Long time it was believed that this process only takes place during embryogenesis in contrast to angiogenesis, meaning the sprouting of new vessels out of pre-existing ones. Then, in 1997, Asahara and colleagues published the intriguing observation that $CD34^+$ hematopoietic progenitor cells purified from

adults were able to differentiate *ex vivo* into the endothelial lineage (Asahara et al., 1997). They were expressing a number of endothelial markers like Flk-1, Tie-2 and CD34 and were shown to incorporate into neovessels at ischemic sites. This subgroup of hematopoietic progenitor cells was named “endothelial progenitor cells” (EPC). In the following year, Rafii’s group showed that CD34⁺ cells cultured in presence of basic fibroblast growth factor, insulin-like growth factor-1 and vascular endothelial growth factor (VEGF) differentiated into endothelial cells as staining for von Willebrand Factor (vWF) and the incorporation of acetylated low-density lipoprotein (Ac-LDL) proved (Shi et al., 1998). Even more interesting was the fact that after bone marrow transplantation in a canine animal model, donor “circulating bone marrow-derived endothelial cells” colonized a Dacron graft. This indicates that a CD34⁺ subpopulation can be mobilized to the circulation and populates prostheses.

EPCs were described as positive for CD34 and for the endothelial marker vascular endothelial growth factor receptor 2 (VEGFR2) (Peichev et al., 2000). HSCs and postnatal EPCs share certain epitopes including Flk-1, Tie-2, CD133, Sca-1, c-Kit and CD34 which can also be found on mature endothelial cells (Hatzopoulos et al., 1998). Further analysis revealed CD133 (also called AC133 or prominin), an orphan receptor, as a marker for more immature hematopoietic stem cells, because of its absence on mature endothelial cells and monocytic cells (Figure 8) (Peichev et al., 2000). Therefore it can be expected that CD133⁺VEGFR2⁺ cells may represent more likely the population of immature progenitor cells. Nevertheless, the ability to differentiate into the endothelial lineage and not preliminary the surface marker profile is defining the population of EPCs. Thus, the group of “EPCs” might range from stages of hemangioblast to fully differentiated ECs and also its putative precursors and stages of lineage differentiation remain to be investigated (Figure 8).

Moreover, there are consolidating evidences also for myeloid cells as origin of EPCs. Hebbel and colleagues observed first that morphologically and functionally distinct endothelial cell subpopulations can be generated out of peripheral blood (Lin et al., 2000). CD14⁺/CD34⁻ myeloid cells showed coexpression of endothelial markers and the ability to form tube-like structures in cell culture (Schmeisser et al., 2001). Even stronger evidence demonstrated *in vivo* experiments where *ex vivo* expanded CD14⁺ mononuclear cells were able to incorporate as endothelial

cells into newly formed vessels in a mouse hind limb model (Urbich et al., 2003). Thus, it can be concluded from these data that myeloid cells can differentiate (or transdifferentiate) into the endothelial lineage (Figure 8).

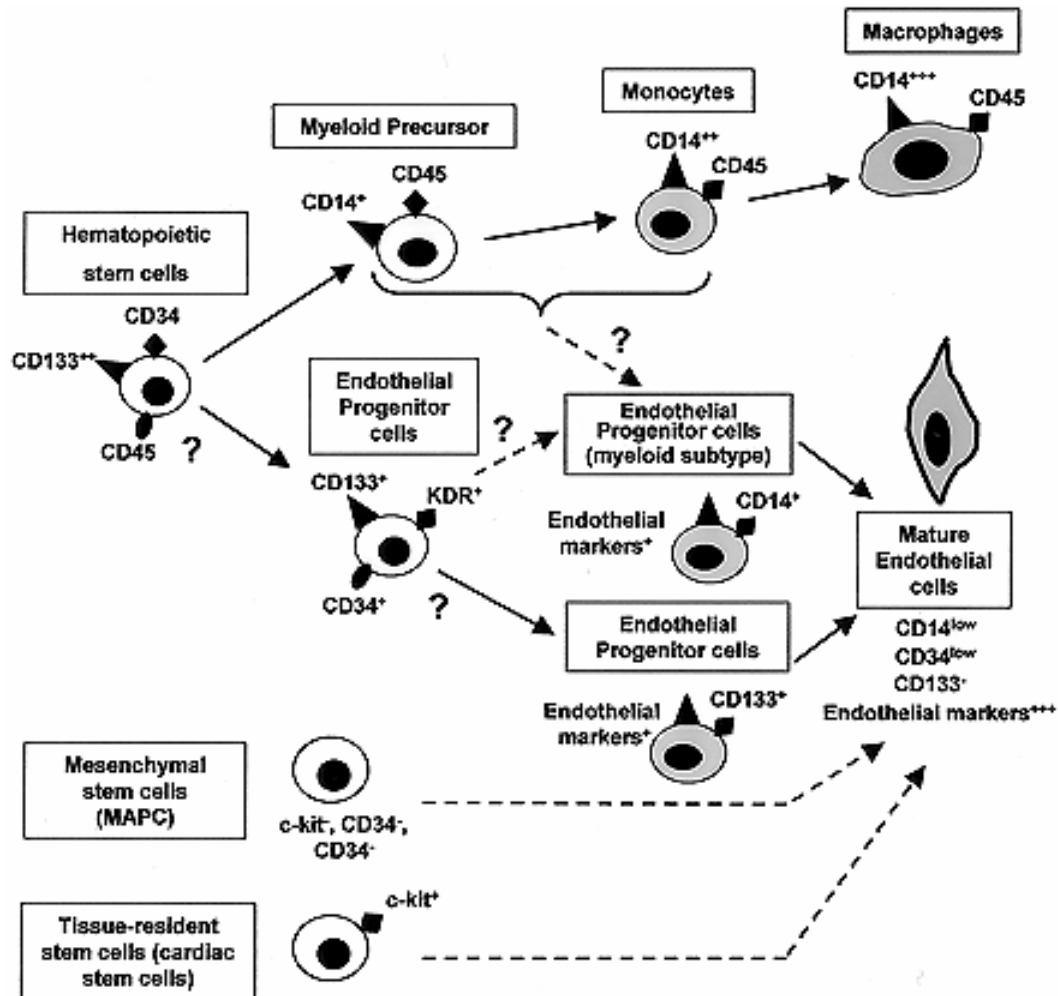


Figure 8: Origin and differentiation of endothelial progenitor cells. Scheme depicts the potential origin and differentiation of EPCs from HSCs and nonhematopoietic cells. (Urbich and Dimmeler, 2004)

To further complicate that topic, several studies showed that stem cell populations beside the HSCs can generate endothelial cells (Figure 8). For example, Reyes and colleagues identified nonhematopoietic multipotent adult progenitor cells (MAPC) which copurified with the mesenchymal stem cells isolated out of the postnatal bone marrow. When the MAPCs (CD34⁻, CD133⁺, vascular endothelial cadherin⁻ (VE-cadherin)) were cultured in presence of VEGF, expression of endothelial markers like CD34 and VE-cadherin were detected and the respective

MACs could be found in sites of neoangiogenesis in tumors (Reyes et al., 2002). Another cell type – the tissue-resident stem cell isolated out of the heart – has also been shown to give rise to endothelial cells (Beltrami et al., 2003).

Different isolation methods and sources of CD34⁺ EPCs have been described so far (Asahara et al., 1997; Fan et al., 2003; Gehling et al., 2000; Hur et al., 2004; Lin et al., 2000; Reyes et al., 2002; Shi et al., 1998; Wijelath et al., 2004). CD34⁺ cells can be isolated either out of the bone marrow (BM), peripheral blood (PB) or umbilical cord blood (CB). The amount of HSCs in the PB is lower (around 0.1 %) compared to the CB and BM where about 1 % of the total mononuclear fraction is CD34⁺ (Hao et al., 1995; Kinniburgh and Russell, 1993; Sutherland et al., 1994). The fraction of circulating HSCs in the PB increases upon ischemia or under treatment with cytokines which are known to mobilize bone marrow-derived progenitors (Gill et al., 2001; Takahashi et al., 1999). Compared to the highly primitive populations of CD34⁺CD38⁻ cells isolated out of BM, the cord blood-derived cells show a much higher cloning efficiency, proliferate more rapidly upon cytokine stimulation and generate a higher number of progeny cells (Cardoso et al., 1993; Hao et al., 1995; Lu et al., 1993). For these reasons, CB is an ideal source for isolation of HSCs.

3.2.2 Bone marrow stem cell niche, mobilization and homing

Quiescence and activity of HSCs in their bone marrow niche are tightly regulated by the microenvironment. This is a necessity to maintain tissue homeostasis and to prevent exhaustion of the stem cell pool or tumor formation. Important components of the bone marrow stem cell niche are osteoblasts and stromal cells (Moore and Lemischka, 2006; Visnjic et al., 2001). The membrane-bound stem cell factor (SCF, c-Kit ligand, steel factor S1F) on stromal cells immobilizes HSCs by its SCF-receptor c-Kit. In general, adhesion between these two cell types is regulated by cytokines. Secretion of proteolytic enzymes like elastase, cathepsin G or matrix metalloproteinase (MMP) is playing a major role in this process. One important mechanism for the mobilization of stem cells is the cleavage of membrane-bound SCF by MMP9 which is induced by stromal cell-derived factor-1 (SDF-1) thus diminishing chemoattraction to the bone marrow (Heissig et al., 2002). Also other factors like vascular endothelial growth factor (VEGF) and granulocyte macrophage colony-stimulating factor (GM-CSF) have been shown to

augment EPC levels in the blood and promote neovascularization (Asahara et al., 1999; Takahashi et al., 1999). Moreover, a number of proangiogenic factors including angiopoietin-1, placental growth factor and erythropoietin had similar effects (Dimmeler et al., 2001; Hattori et al., 2001; Hattori et al., 2002; Heeschen et al., 2003). Systemic treatment with HMG CoA reductase inhibitors (statins), estrogens, certain cytotoxic drugs (cyclophosphamide, hydroxyurea, 5-fluorouracil) and cytokines (e.g. G-CSF, GM-CSF, IL-11, IL-3, IL-8, SCF, Flt3L) as well as physical exercise enhanced HSC mobilization (Dimmeler et al., 2001; Iwakura et al., 2003; Laufs et al., 2004; Papayannopoulou et al., 2003). Incorporation of EPCs into newly formed vessels assumes not only EPC mobilization, but also a complex process composed of chemoattraction, adhesion, transmigration and finally differentiation into mature endothelial cells (Figure 9). The term “homing” which is often used in the context of stem cells comprises thereby the steps of adhesion, transmigration through the activated endothelium and migration to the target site. Besides homing to the ischemic or injured tissue also homing to the bone marrow occurs. This process which is far better understood than the homing to ischemic or injured tissue (Papayannopoulou, 2003).

Physiologically, ischemia seems to be an important egress signal for EPCs from the bone marrow. As possible mechanisms, upregulation of VEGF and SDF-1 have been proposed which could lead to induction of MMP9-mediated mobilization of EPCs (Aicher et al., 2003; Gill et al., 2001; Heissig et al., 2002; Takahashi et al., 1999; Wysoczynski et al., 2005). It has also been shown that SDF-1 levels are enhanced during the first days after myocardial infarction (Askari et al., 2003). Moreover, the circulating EPCs are attracted by a SDF-1 and VEGF gradient to sites of ischemia or tissue injury (Shintani et al., 2001; Yamaguchi et al., 2003). Together with directly induced hypoxia-responsive genes, immune competent cells which are accumulating in the ischemic tissue may enhance the level of chemokines such as MCP-1 or interleukins to further recruit circulating EPCs (Fujiyama et al., 2003). Another probable homing signal could be given by necrosis through release of high mobility group box protein 1 (HMGB1). This chromatin-binding protein is mediating extracellular danger signals thus promoting homing of EPCs (Scaffidi, Misteli, and Bianchi, 2002).

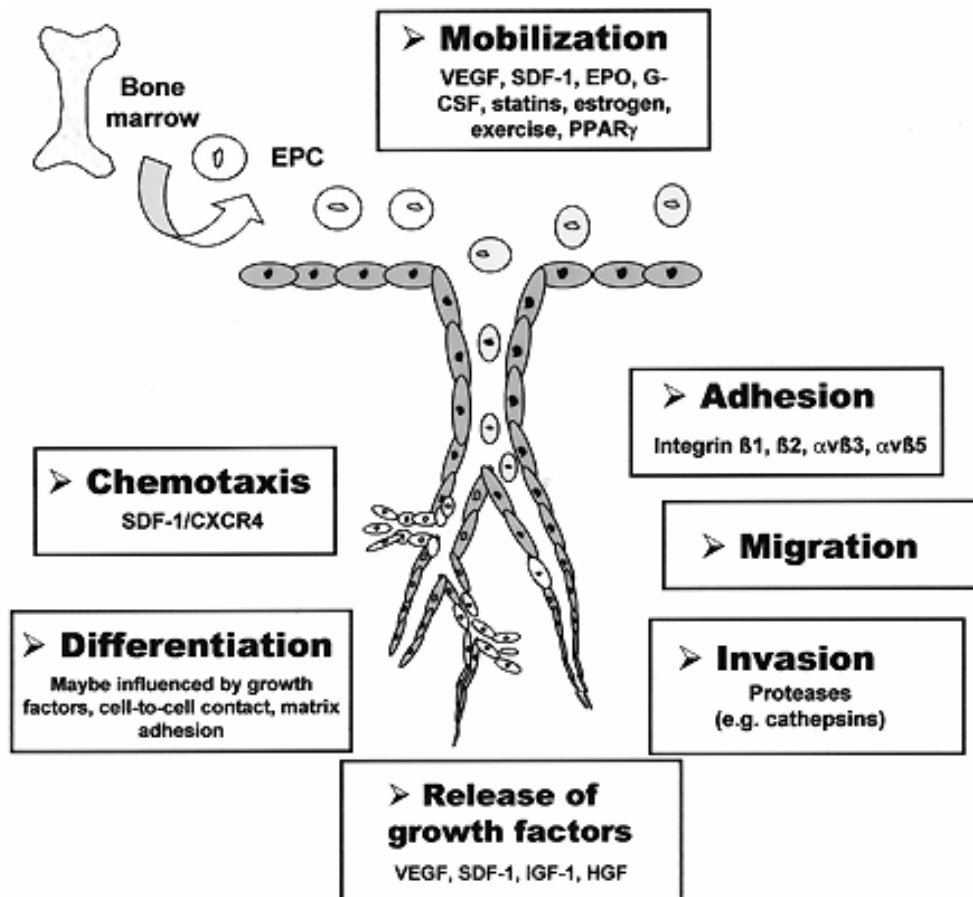


Figure 9: Mechanisms of EPC homing and differentiation. Recruitment and incorporation of EPCs into ischemic tissues requires a coordinated multistep process including mobilization, chemoattraction, adhesion, transmigration, migration, tissue invasion and in situ differentiation. Factors that are proposed to regulate the distinct steps are indicated. (Urbich and Dimmeler, 2004)

Adhesion and migration processes of diverse cell types including HSCs and leukocytes are controlled by integrins (Carlos and Harlan, 1994; Springer, 1994). This is, for example, a mechanism by which SDF-1 acts (De Falco et al., 2004). First step is the adhesion of HSCs to the activated endothelium. Integrins have been identified as potential mediators for homing as they are able to form cell-cell interactions (Chavakis et al., 2005; Soligo et al., 1990). In fact, there are evidences for the importance of different integrins depending on the target tissue (Scott, Priestley, and Papayannopoulou, 2003). Final attachment of embryonic progenitor cells to tumor endothelium was proposed to be mediated by P- and E-selectin and P-selectin glycoprotein ligand-1 (Vajkoczy et al., 2003).

In contrast to homing into sites of ischemia, incorporation of EPCs into denuded arteries seems to be less dependent on cell-cell interaction and transmigration.

Instead, adhesion to the extracellular matrix via vitronectin receptors ($\alpha_v\beta_3$ - and $\alpha_v\beta_5$ -integrins) is a more important mechanism. This has also been shown *in vivo* by inhibiting vitronectin receptors using cyclic RGD peptides which blocked reendothelialization of injured carotid arteries (Walter et al., 2002). Furthermore, other sorts of integrins like the β_1 -subtype might play a role in adhesion to extracellular matrix proteins of denuded arteries (Fujiyama et al., 2003).

Concerning migration and invasion through the endothelial monolayer to the site of ischemia little is known so far, but different proteases like cathepsins or metalloproteinases may take part in these processes.

Mechanisms influencing differentiation of EPCs into endothelial cells also remain largely unknown. However, VEGF and its receptors have been shown to mediate endothelial differentiation in embryonic development (Ferrara et al., 1996; Fong et al., 1995; Shalaby et al., 1995). Also for various adult progenitor cells, this crucial role for VEGF in *ex vivo* endothelial differentiation could be approved (Dimmeler et al., 2001; Kalka et al., 2000).

3.2.3 Therapeutic potentials of EPC transplantation and gene therapy

CD34⁺ cells gained attention as a population of endothelial progenitor cells having the ability to self-renew, proliferate and differentiate into endothelial cells. Moreover, as hematopoietic stem cells they give rise to all blood cells thus being interesting for therapy of hematopoietic and autoimmune diseases. Especially, induction of neovascularization in sites of ischemia and reendothelialization after endothelial injury brought these cells into focus for the treatment of chronic heart disease and acute myocardial infarction. Increased mobilization of stem cells from the bone marrow stem cell niche and proliferation of these cells is an effective means to support self-regenerative processes (Figure 10).

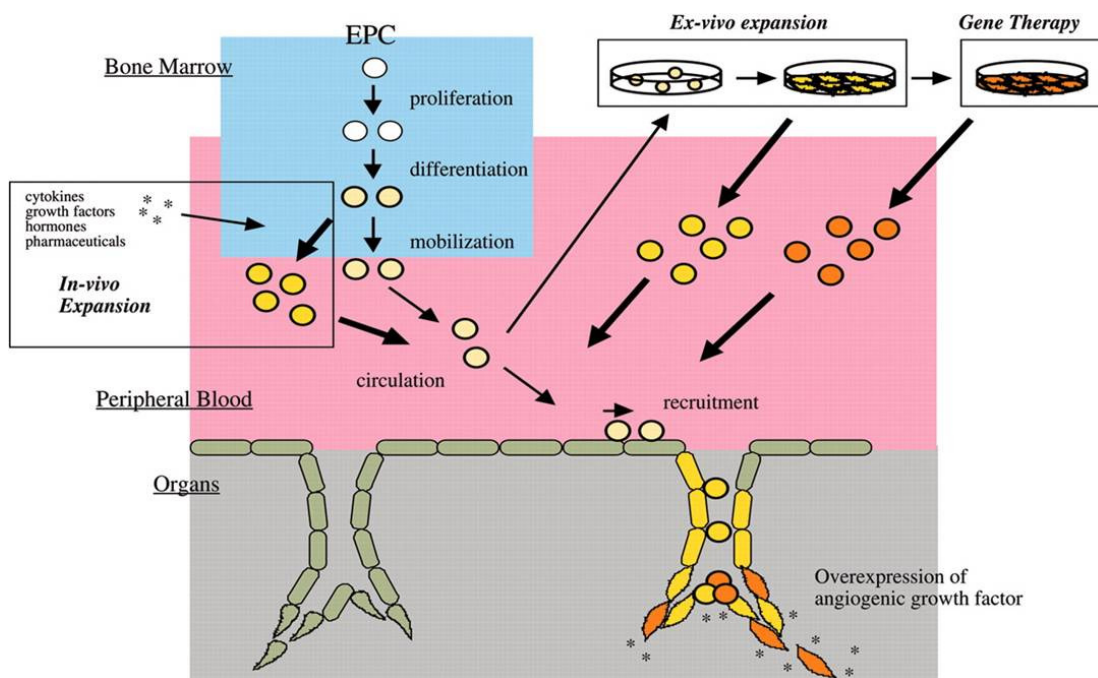


Figure 10: Therapeutic application of EPCs for neovascularization. (Asahara and Kawamoto, 2004)

In vivo expansion can be induced by application of growth factors, cytokines and pharmaceuticals like statins. Therapeutical success has been stated in several studies also in patients by treatment with VEGF (Kalka et al., 2000). Another possibility is the *ex vivo* expansion of CD34⁺ cells followed by transplantation. Asahara's group published that transplantation of *ex vivo* expanded human CD34⁺ cells in a hind limb model of immunodeficient mice augmented blood flow and led to a 50 % reduction in autoamputation and limb necrosis (Asahara et al., 1999). In nude rat myocardial ischemia the positive effects of transplanted human CD34⁺ cells comprised their incorporation into neovessels and differentiation into endothelial cells, enhancement of neovascularization and prevention of fibrosis and ventricular dysfunction (Kawamoto et al., 2001). Most convincingly are currently ongoing clinical trials where *ex vivo* expanded progenitor cells are transplanted successfully into patients suffering from acute myocardial infarction (TOPCARE-AMI study) or chronic heart disease (TOPCARE-CHD study) improving different parameters pointing to heart regeneration (Assmus et al., 2007; Assmus et al., 2006a; Assmus et al., 2002; Assmus et al., 2006b; Britten et al., 2003; Kissel et al., 2007; Schachinger et al., 2004; Schachinger et al., 2006a; Schachinger et al., 2006b; Schachinger et al., 2006c). The subsequently described strategy – together with *ex vivo* expansion – might be meaningful in patients where progenitor cell function is dysregulated like in hypercholesterolemia, type II

diabetes or in aged persons (Chauhan et al., 1996; Chen et al., 2004; Cosentino and Luscher, 1998; Heiss et al., 2005; Thum et al., 2007). Combination of cell- and gene-based strategies, e.g for the expression of angiogenic growth factors or genes favoring the differentiation along a certain lineage could improve the success of endothelial progenitor cell transplantation.

Their easy accessibility and *ex vivo* expansion capability makes CD34⁺ cells an auspicious aim for gene therapy. Different approaches have already been made using adenovirus- (Ad), lentivirus-, retrovirus- or AAV-based vector systems as described (Evans et al., 1999; Iwaguro et al., 2002; Santat et al., 2005; Schmidt et al., 2002). First experiments report increased neovascularization and a 63.7 % reduction in limb necrosis and autoamputations after application of Ad-VEGF in a mouse hind limb model (Iwaguro et al., 2002). For curing different hematological disorders like X-linked severe combined immunodeficiency or adenosine deaminase deficiency, several clinical trials using retroviral vector systems to transduce CD34⁺ cells have been successful (Aiuti et al., 2002; Cavazzana-Calvo et al., 2000; Gaspar et al., 2006; Hacein-Bey-Abina et al., 2002). Also in two primate models, different clones of retrovirus-transduced CD34⁺ cells were still detectable in peripheral blood leukocytes after 33 months (Schmidt et al., 2002). Despite these promising results, retroviral vectors imply the risk of insertional mutagenesis (Hacein-Bey-Abina et al., 2003). In the case of AAV, a rarely integrating vector, transgene expression declines over time being ideal for purposes where only transient gene expression is required as for example in myocardial diseases (Nathwani et al., 2000). This makes the AAV2-based vector system an attractive alternative. However, published *in vitro* data concerning transduction of CD34⁺ cells by rAAV2 are conflicting. Transduction efficiencies are reported to vary from 0 % (Alexander, Russell, and Miller, 1997) to higher expression levels using high (multiplicity of infection (MOI) >10⁶) or relatively low (MOI >100) vector to cell ratios (Chatterjee et al., 1999; Hargrove et al., 1997; Malik et al., 1997; Nathwani et al., 2000; Ponnazhagan et al., 1997; Zhou et al., 1994). Different protocols for isolation and culturing of EPCs as well as differing vector production techniques, titration methods and applied vector amounts impair a direct comparison of results. So, prestimulation of EPCs with cytokines enhances AAV-mediated transgene expression while freshly isolated cells are resistant to transduction (Nathwani et al., 2000). Transduction efficiencies could be

enhanced from 10 to 51 % by using higher cytokine concentrations and addition of TNF α (MOI 10⁶) (Nathwani et al., 2000). Early investigations reported transduceability of HSCs by rAAV, but using crude vector lysates (Fisher-Adams et al., 1996; Goodman et al., 1994; Zhou et al., 1994). These low purified preparations contain adenoviral contaminations which might persist in the vector preparation using Ad as helpervirus (Alexander, Russell, and Miller, 1997). Moreover, donor-depending differences in transgene expression have been reported varying from 0 to 80 % 48 h p.i. or 5 to 100 % in long-term culture-initiating cells after 5 weeks (Chatterjee et al., 1999; Ponnazhagan et al., 1997). Nevertheless, transplantation of rAAV2-transduced CD34⁺ cells into immune-deficient mice showed the potential to engraft. A certain amount of bone marrow cells was transgenic and remained stable as well as several blood cell lineages (Santat et al., 2005). Also in a rhesus monkey model a high amount of vector modified blood cells could be detected 15 months after transplantation demonstrating that transduction of CD34⁺ cells by rAAV leads to long-term expression of the transgene (Schimmenti et al., 1998).

3.2.4 Aim of the study

Despite considerable therapeutic advances heart diseases remain the main cause of premature death in the human population world-wide. Heart transplantation often represents the only possibility to rescue the patient, but this is limited by organ shortage and the risk of graft rejection. Due to recent improvements in vector technology and in identification of potential therapeutic genes for the treatment of heart diseases, gene therapeutical strategies have become an option. Another approach is presented by the use of stem and progenitor cells which has gained increasing attention. Endothelial progenitor cells, for example, have already been demonstrated to be promising tools to achieve revascularization in ischemic regions as they possess the ability to differentiate into endothelial cells and home to sites of ischemia. The combination of cell- and gene-based strategies offers clear advantages for certain applications as revascularization of ischemic sites, and is thus a topic of many pre- and clinical studies.

Both parts of this thesis focus on heart diseases. The first part aimed to establish the rAAV-based gene transfer system for modification of heart tissue before transplantation. This included the identification of potential limitations for efficient

use of this system, and – if possible – the development of strategies for their solution. As heterotopic heart transplantation models served the Sprague Dawley rats as small and the German landrace piglets as large animal model. While the rodent model ought to be established to later allow a fast screening for transgenes which might prolong graft survival, the studies in pigs should be used as preclinical model. Firstly, conditions enabling vector entry without harming the graft had to be assessed. In this regard, efficiency of intracoronary vector delivery under normothermic and hypothermic conditions should be compared in the rat model and findings shall then be translated into the pig model.

In the second part, a protocol for efficient rAAV-mediated transduction of CD34⁺ cells ought to be established. The great potential of these cells for the treatment of heart diseases is widely accepted. Furthermore, they are ideal targets for genetic modification as they can be isolated, cultivated *ex vivo* and reapplied into the patient where they home to ischemic regions. Since currently used vector systems bear – despite their efficiency – certain risks like insertional mutagenesis, rAAV is discussed as valid alternative. Thus, comparative analyses of different serotypes as well as single-stranded and self-complementary genome conformation ought to be performed. Furthermore, it should be determined which cellular receptors are engaged for vector entry. Since genetically modified CD34⁺ cells have to maintain their ability to differentiate into endothelial cells to be of use in the patient, a potential inhibitory effect of the rAAV-mediated gene transfer had to be excluded.

4 Results

4.1 rAAV transfer into heart

Numerous strategies for gene transfer into the heart have been developed. In most cases, investigators aimed to transduce the myocardium either by direct intramyocardial injection or intracoronary delivery of the gene transfer vector (see also chapter 3.1.5.1). In the latter case, additional attempts are necessary to overcome the endothelial barrier. Successful examples are elevated vascular pressure or administration of capillary-modulating substances (e.g. histamine) to increase vascular permeability (Beeri et al., 2002; Donahue et al., 1998; Logeart et al., 2001).

However, also the endothelium itself is a therapeutic target since it is an important determinant in endothelial dysfunction-associated disorders such as cardiovascular diseases (Cooke, 2000; Melo et al., 2004). Moreover, being the first donor-derived tissue encountered by the recipient's circulating immune cells, the endothelium has major impact on successful organ transplantation and could thus serve as target for gene therapy to reduce graft rejection, e.g. graft arteriopathy (Vassalli et al., 2003) (for more details please refer to chapter 3.1.5.1).

4.1.1 rAAV transfer into rodent heart

4.1.1.1 Heterogenic rat heart transplantation

Heart transplantation experiments with piglets are very time-consuming and complicated and large vector amounts are needed. Thus, a Sprague-Dawley rat heart transplantation model was established by our colleagues of the Department of Heart Surgery at the Ludwig-Maximilians University Munich aiming to use this model for a fast screening of potentially useful therapeutic genes transferred into the donor organ by rAAV-mediated gene transfer. Based on published results at the start of our project, which described successful applications of AAV2 vectors in rodent heart models we decided to use this serotype (Asfour et al., 2002; Hoshijima et al., 2002; Iwanaga et al., 2004; Li et al., 2003; Svensson et al., 1999). Firstly, we aimed to identify a transplantation technique allowing to transplant the heart as unharmed as possible providing at the same time the most feasible conditions for AAV-mediated gene transfer. Therefore, we compared the following techniques summarized in chapter 7.5.1: A) heart transplantations performed with

Results

a non-beating, hypothermic heart after cardiac arrest by ice-cold cardioplegic solution and B) a beating heart at normothermia. Whereas hypothermia should preserve better from ischemic injury the low temperature may impair receptor-mediated endocytosis of cell surface-bound AAV vectors. In contrast, normothermia might allow direct vector entry, but may harm the heart tissue. As depicted in Table 1, each group consisted of 3 animals.

| Operation technique | Vector application | Animal | Vector amount |
|---------------------|--------------------|--------|----------------------|
| normothermia | intracoronary | A1 | 5.2×10^{11} |
| | | A2 | 3.4×10^{11} |
| | | A3 | 8.5×10^{11} |
| hypothermia | intracoronary | B1 | 5.2×10^{11} |
| | | B2 | 5.0×10^{10} |
| | | B3 | 3.1×10^{11} |
| w/o transplantation | systemic | C1 | 5.2×10^{11} |
| | | C2 | 3.0×10^{11} |
| ----- | | | |
| | intramuscular | M1 | 3.4×10^9 |
| | | M2 | 5.6×10^9 |

Table 1: Experimental scheme of heteropic rat heart transplantations. 2 groups consisting of 3 animals were transplanted and rAAV2ssLacZ was applied intracoronary either into a normothermic, beating heart (A1-A3) or into a non-beating, hypothermic heart (B1-B3). In addition, two animals (C1 and C2) received rAAV2ssLacZ systemically via tail vein injection to determine the ability of rAAV2 vectors to target the heart. Moreover, the animals B2 and B3 received additionally a vector injection into skeletal muscle (M2 and M1, respectively) in order to control vector function. (rAAV2ssLacZ = AAV serotype 2 based vector encoding beta-galactosidase in the single-stranded vector genome conformation)

For gene transfer, rAAV2 encoding for the transgene β -galactosidase (LacZ) in the commonly used single-stranded (ss) vector genome conformation was produced as described in 7.3.6.1, purified by iodixanal gradient centrifugation (7.3.6.2) and further by heparin affinity chromatography (7.3.6.3) to minimize inflammatory responses to vector preparation impurities. Before use, genomic titers of vector preparations were determined by qPCR (7.3.6.4). Subsequently, between 5×10^{10} and 8.5×10^{11} DNA containing particles were applied into the coronaries of the grafts either in the normo- or hypothermia transplantation model (Table 1). In

addition, skeletal hind limb muscle injections and systemic application were performed to control vector function and to determine vector tropism for the heart tissue, respectively.

To minimize organ rejection, all animals received Tacrolimus (0.3 mg/kg body weight) daily for immunosuppression. All rats recovered well from transplantation and showed palpable contractions of the graft. With exception of animal A2, all animals were healthy, behaved and ate normally until the time point of explantation. The rat A2 had to be explanted at day 22 while all other animals were sacrificed 28 d post transplantation. Transplanted heart, native heart and liver were harvested for histological analyses and extraction of DNA and mRNA. Only the transplanted heart was analyzed in the animal A2. From the systemically injected rats, also spleen and lung were analyzed. From the two animals (B3 and B2) receiving an additional injection of rAAV2 into the the left and right hind limb muscle, total DNA and mRNA were isolated from the sample M1 (animal B3), while sample M2 (animal B2) was analyzed histologically.

4.1.1.1.1 Delivery of vector genomes into transplanted hearts

Heart transplantations and vector applications were performed as described in the previous chapter. To determine the applicability of the AAV vector technology for genetic modification of heart transplants we first assessed the presence of vector genomes using the therefor established quantitative real-time PCR protocols (qPCR) as described in 7.2.8. Briefly, DNA was extracted from shock-frozen organs of rAAV- and non-treated animals. The Quantitect SYBR Green PCR Kit (Qiagen) was then used to analyze 100 ng DNA of each sample by qPCR. Additionally, negative controls only containing the elution buffer (Tris, 10 mM, pH 8.0) (N1) or the PCR mix (N2) were included. The plasmid pZNL, the vector plasmid during rAAV packaging, served as positive control. For normalization, the housekeeping gene GAPDH was included to ensure that equal levels of DNA were used. PCR products were assayed by melting curve analyses and by agarose gel electrophoreses. Melting curve analyses showed no unspecific signals in the samples. The intensities of all GAPDH bands detected after electrophoretical separation and visualization were similar as expected from the values obtained by qPCR (qPCR data not shown) (Figure 11 A and B). Only in Figure 11 C, the

skeletal muscle probe M1 showed a stronger intensity of the band than the non-transduced muscle sample.

Quantification of vector-specific PCR products was not possible due to the low transgene DNA amounts in our samples. An increase in cycle numbers above 40 resulted in measurable PCR products, but also in the untreated animals. Based on melting curve analysis and agarose gel electrophoresis specific transgene DNA was detected in the non-treated controls. Therefore, only presence or absence of transgene DNA could be determined in samples undergoing 40 PCR cycles by agarose gel electrophoresis.

Amplification of LacZ genomes was clearly detectable in transplanted hearts (HTX) of the animals A1 and A2 (Figure 11 A). A3 only showed a faint band for LacZ (Figure 11 A). With exception of B2 (received the lowest vector amount), in all transplanted rat heart samples of group B LacZ amplification could be visualized (Figure 11 A). In contrast, native heart samples (H) of transplanted rats were devoid of transgene DNA (Figure 11 A). However, vector DNA was detectable in the liver of A1, A3 and B1 and of both animals receiving systemic vector administration. While the latter result was expected from previous reports, the former reveals that rAAV was transported from the transplanted heart into other parts of the body. Following systemic vector administration (without heart transplantation; Figure 11 B), LacZ DNA could clearly be detected in the liver as already outlined, but also in the spleen of C1 and C2. Moreover, a faint band was visible in both lung samples. Neither of the two heart samples showed LacZ DNA in the heart after systemic vector delivery. Transgene DNA was detectable in skeletal muscle after vector injection (Figure 11 C).

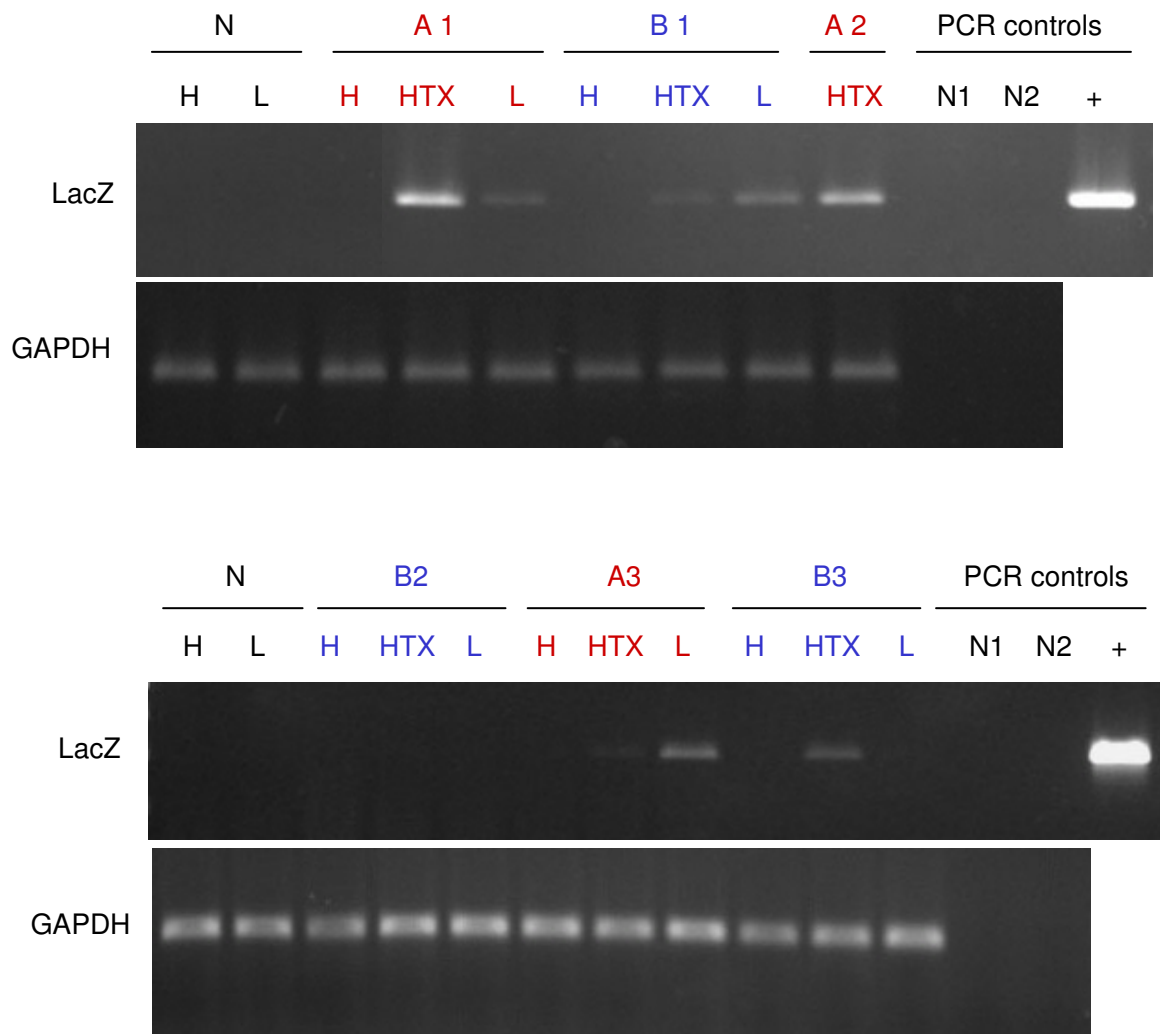
Vector genomes were neither detectable in untreated animals nor in PCR buffers while specific amplification products were obtained with pZNL which served as positive control.

Thus, rAAV-mediated gene transfer into the transplanted heart was observed with both operation techniques revealing that vector entry in cells of the heart tissue is not impaired. However, the transplanted heart samples in the normothermia group showed better results in the amount of vector DNA (3/3 animals were positive) compared to the group of rats receiving vector upon hypothermia. In the latter group transgene DNA could be detected as faint bands in transplanted hearts (3/2

Results

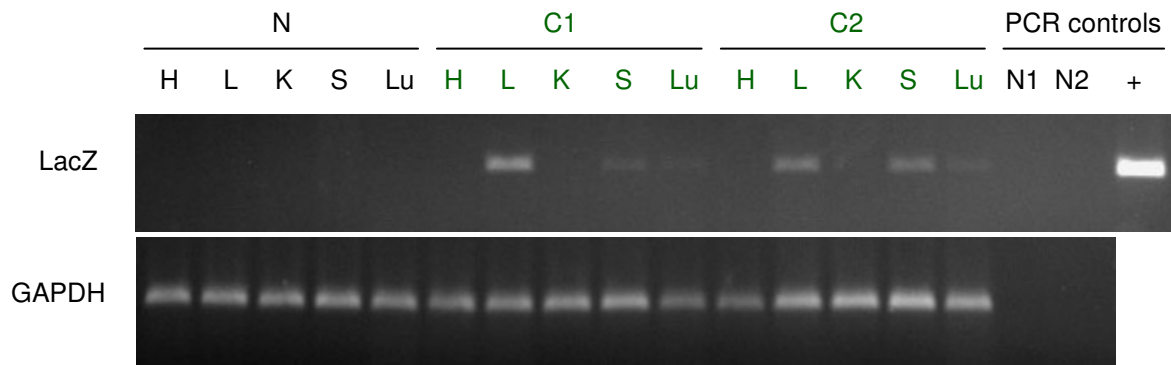
animals were positive). In contrast, no transgene DNA was measured in any of the systemically injected rats, revealing that rAAV2 does not possess a native tropism for this tissue. The liver tropism observed after systemic application is also obvious in the transplanted animals where vector genomes were detected in 50 % of the liver samples.

A



Results

B



C

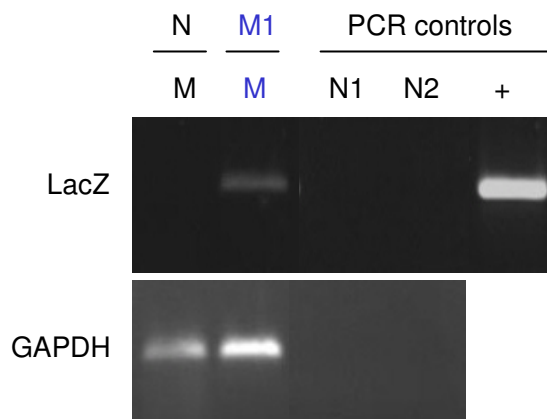


Figure 11: DNA analyses of rat organs. Total DNA was analyzed by qPCR for transgene (LacZ) and housekeeping gene (GAPDH) followed by agarose gel electrophoresis. Shown are representative pictures of 2 independent tissue extractions and 3 PCR runs. In (A), gel pictures of the 2 different groups receiving vectors in a transplantation model are depicted whereas results of animals with systemic vector application without transplantation are shown in (B). Intramuscularly injected samples are indicated in (C). Animal groups: N, negative animal; A, normothermia; B, hypothermia; C, systemic vector administration; M1, skeletal muscle after vector application; samples: H, native heart; HTX, transplanted heart; L, liver; K, kidney; S, spleen; Lu, lung; M, skeletal muscle; N1, negative control for DNA extraction; N2, non-template control for PCR; +, LacZ plasmid as positive control.

4.1.1.1.2 *Transgene mRNA expression cannot be detected in transplanted hearts*

Next, we determined the amount of transgene mRNA as assumption of a successful transport of the vector genomes into the nucleus and transgene transcription. The same animals described in the previous chapter were analyzed by qPCR.

First, RNA was isolated by phenol / chloroform extraction (7.2.6). Potential DNA contaminations were removed by DNase I digest and cDNA was synthesized using oligo-dT primer and the Transcriptor First Strand cDNA Synthesis Kit (Roche) as explained in 7.2.7. Around 140 ng cDNA were analyzed by qPCR to determine if transgene expression has occurred. For normalization, expression of the housekeeping gene GAPDH was used.

The level of specific cDNA was lower than the amount of transgene DNA. Thus, quantification of LacZ mRNA expression was impossible and conclusions could only be drawn after visualization of PCR products by agarose gel electrophoreses according to the previous chapter. Based on results obtained for the transgene DNA (4.1.1.1.1) which revealed the absence of transgene in native heart of all transplanted animals, only transplanted heart and liver were analyzed for mRNA. In the case of A2, only the transplanted heart was available as described before. B3 only showed detectable transgene DNA in the transplanted heart, thus liver was not analyzed.

Synthesis of cDNA from isolated mRNA was successful as GAPDH products were detectable in all samples. However, as the basal levels for GAPDH activity differ between the analyzed organs, band intensities are only comparable between the respective tissue samples. Nevertheless, amplified cDNA for LacZ could not be detected in transplanted hearts or livers in group A and B. Regarding the 2 rats having received systemic vector injection, only the second animal (C2) showed a faint band indicating LacZ expression in the liver. In contrast, injection into skeletal muscle resulted in well detectable signals for transgene-specific cDNA revealing that our vector preparation is functional and rAAV2 genomes can in principle be expressed in rats.

Results

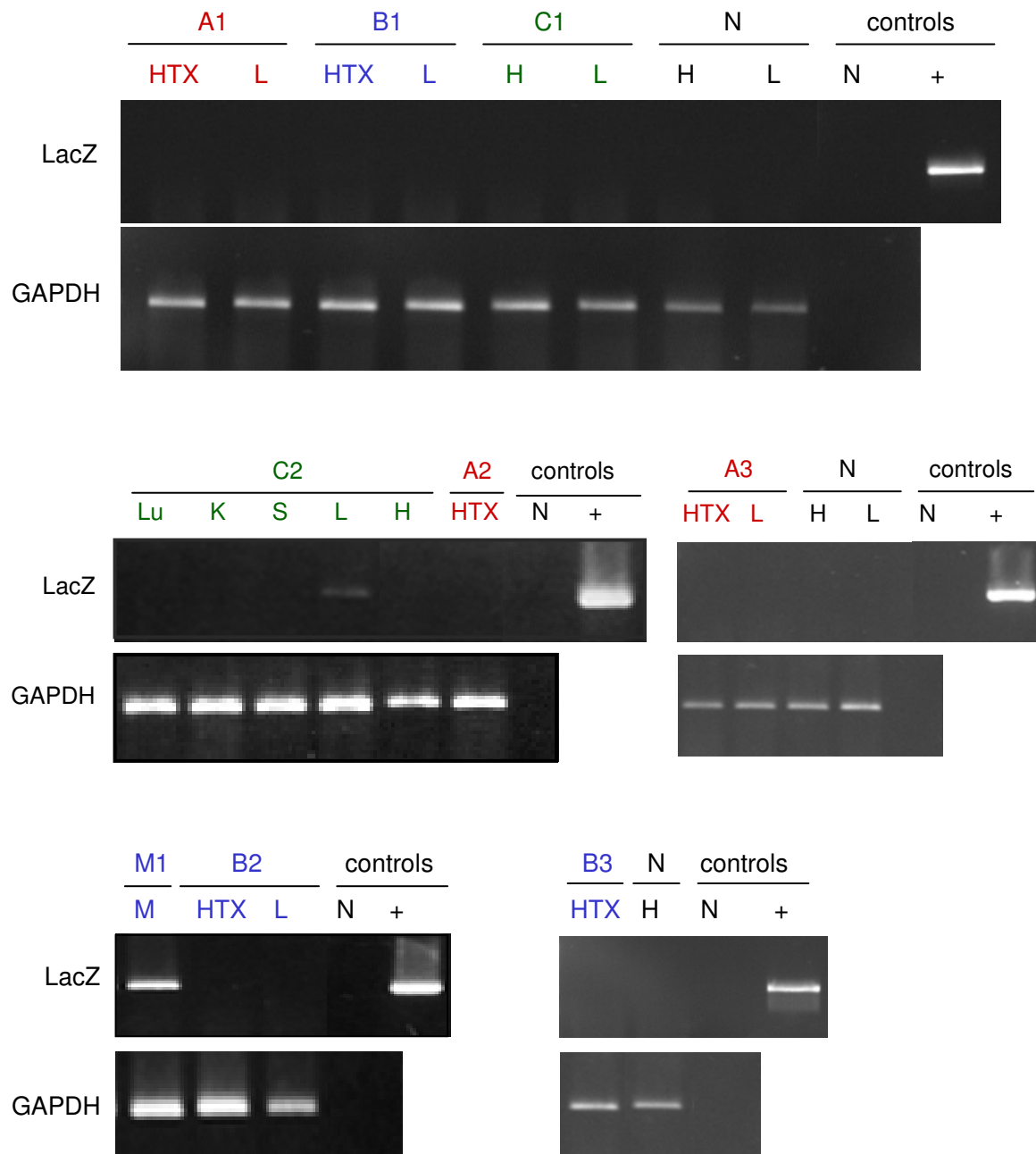


Figure 12: Agarose gel electrophoreses of amplified cDNA. RNA was extracted by phenol / chloroform extraction and digested with DNase I. Reverse Transcription was performed by Transcriptor First Strand cDNA Synthesis Kit (Roche). Then, qPCR analyses were performed and products were analyzed by agarose gel electrophoreses. Representative pictures are depicted here. Animal groups: N, negative animal; A, normothermia; B, hypothermia; C, systemic vector administration; M1, skeletal muscle after vector application; samples: H, native heart; HTX, transplanted heart; L, liver; K, kidney; S, spleen; Lu, lung; M, skeletal muscle; N, non-template control for PCR; +, LacZ plasmid as positive control.

4.1.1.1.3 *Beta-Galactosidase activity is not detectable in tissue sections of transplanted hearts*

After evaluation of transgene DNA in the animal groups introduced above, we determined if transgene expression has occurred in native heart, liver and in transplanted heart (HTX) of groups A and B, despite undetectable LacZ cDNA levels. Therefore, tissue sections were stained for X-Gal activity as described in 7.4.1. As already mentioned in 4.1.1.1, only the transplanted heart was analyzed in the case of A2 as this animal was explanted after 22 d instead of 28 d. Additionally, as positive control, we stained sections of a liver transduced with adenovirus coding for LacZ which was kindly provided by M. Odenthal (Institute of Pathology, Cologne).

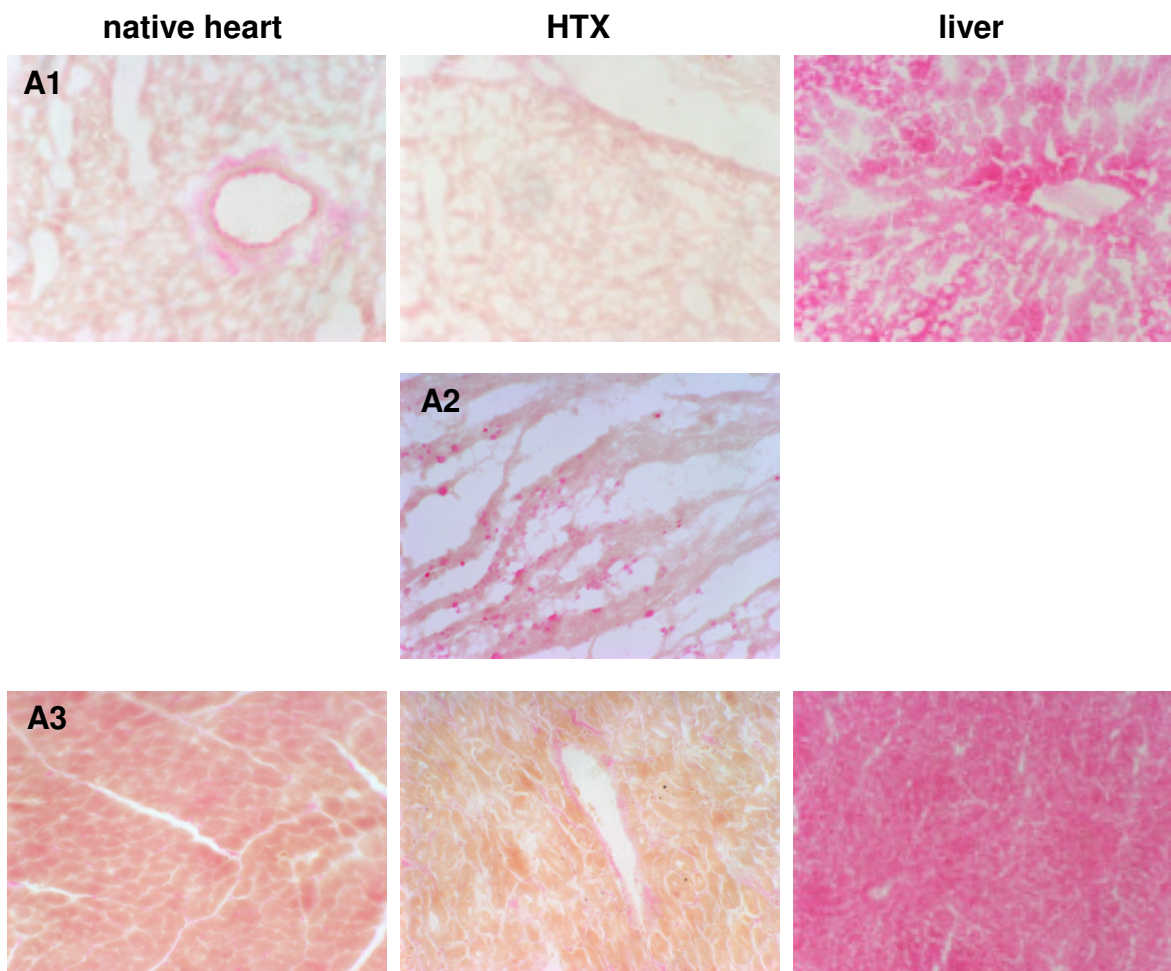


Figure 13: X-Gal and eosin stained tissue sections of rats receiving vector into the transplanted heart at normothermia. Organs were shock-frozen in isopentane and liquid nitrogen. The samples were prepared by cryotome tissue dissection and stained with X-Gal solution (2 d) and 0.5 % eosin solution (8 min). Shown are representative images of native heart, transplanted heart (HTX) and liver sections. Of animal A2, only HTX was available. In none of the samples, X-Gal activity was detected by microscope analyses (200x magnification; Olympus Vanox-S AH-2 microscope).

Following explantation, the organs were put into isopentane to preserve tissue structure and were immediately shock-frozen in liquid nitrogen. Cryotom tissue dissection was performed in the Institute of Pathology (Cologne). Thereby, several sections of 3 different planes were collected, air-dried overnight and stored at -80 °C. Without thawing, the sections were fixed in 1.5 % glutaraldehyde and stained for 2 d in X-Gal solution. Tissue sections were counterstained with 0.5 % eosin solution (no counterstaining in B3 and skeletal muscle sections) before dehydration. Object slides were covered and X-Gal staining was determined by microscopy (Olympus Vanox-S AH-2 microscope) (7.4.1).

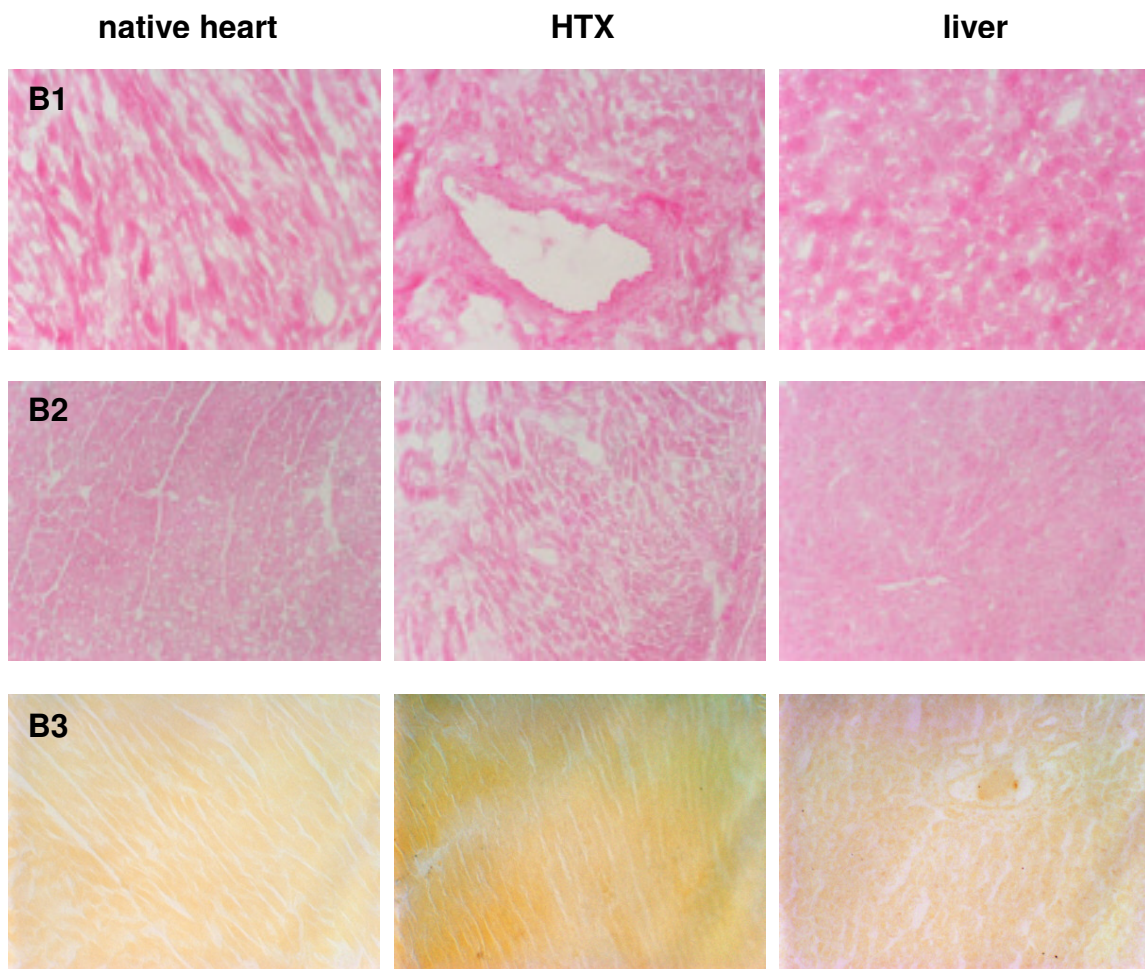


Figure 14: X-Gal and eosin stained tissue sections of transplanted animals after vector application into the hypothermic heart. Explanted organs were directly frozen in isopentane and liquid nitrogen before preparing by cryotom tissue dissection. Sections were stained for X-Gal activity (2 d) and counterstained with eosin (0.5 %, 8 min) (excluding B3) and analyzed by microscopy (200x magnification; Olympus Vanox-S AH-2 microscope). Representative images are shown here.

Microscope images of organs including vessels were analyzed for transgene expression in the endothelium. Neither the animals of the normothermic nor the hypothermic heart transplantation group showed X-Gal positive signals in any organ (Figure 13, Figure 14). A damaged morphological structure was visible in the transplanted heart of A2. Regarding the group that received a systemic vector administration into the tail vein, no positive staining for X-Gal could be detected in heart and liver despite detection of cDNA in the liver of C2 as depicted in 4.1.1.1.2 (Figure 15). In contrast, intramuscular injection of rAAV2ssLacZ resulted in transgene expression and protein production (verifying cDNA analyses) since this tissue showed detectable β -Gal activity (blue color) as depicted in Figure 16. Also in our positive control, the adenovirus-transduced liver, positively stained cells were found while our non-treated controls were negative for X-Gal staining.

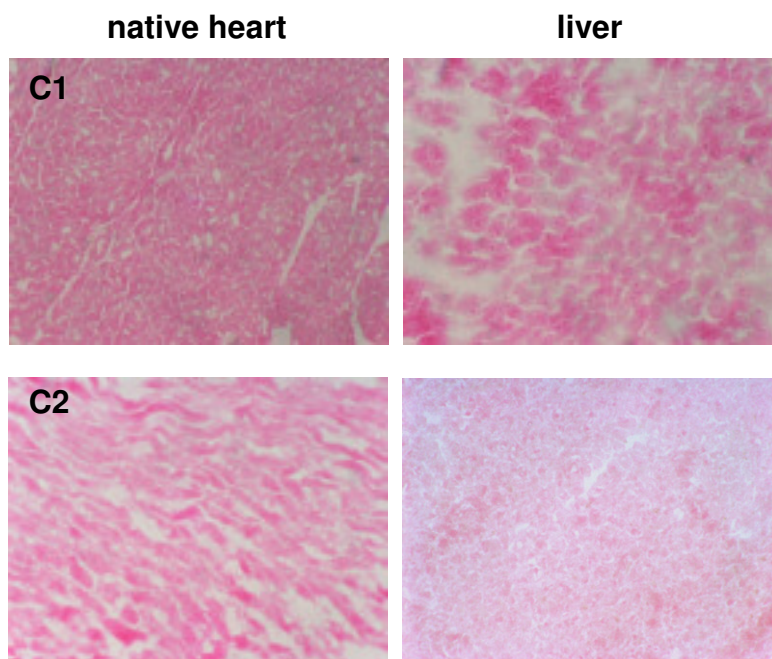


Figure 15: X-Gal and eosin stained tissue sections of animals receiving vector via the tail vein (systemic application). Isopentan frozen liver and heart of 2 rats were analyzed for X-Gal activity and counterstained with eosin after organs were cryotom dissected. Shown are representative microscope images (200x magnification; Olympus Vanox-S AH-2 microscope). X-Gal could not be detected in any of the sections.

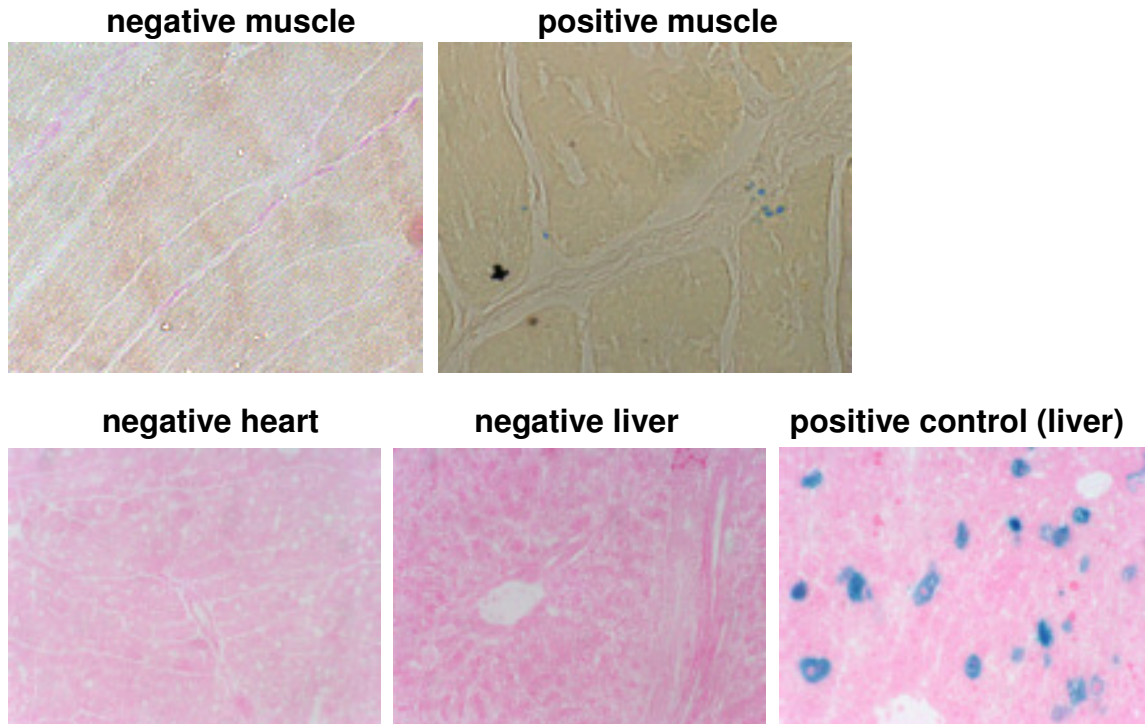


Figure 16: X-Gal stained tissue sections of control animals. X-Gal activity was determined in skeletal muscle of a rat having received rAAV2 intramuscular injection and a non-transduced control animal (skeletal muscle, heart and liver). The positive control of an adenovirus-transduced liver was kindly provided by M. Odenthal. After shock-freezing and cryotom tissue dissection, the tissue sections were stained for X-Gal (2 d) and eosin (8 min; no counterstaining in muscle) and microscope images were taken (200x magnification; Olympus Vanox-S AH-2 microscope). X-Gal activity (blue signals) could be detected in vector injected muscle and the positive control of adenovirus-transduced liver. LacZ in the positive control did not retain a nuclear localization signal in contrast to our transgene construct, thus displaying a positive X-Gal staining within the cytoplasm.

4.1.1.2 *In vitro* analyses of rAAV-mediated rat cell transduction

Since rAAV2 vector administration in both heterotopic rat heart transplantation models did not result in measurable transgene expression although vector DNA could be detected, we aimed to identify limiting factors by *in vitro* analyses. As *in vitro* model for rAAV-mediated rat endothelial cell transduction, primary rat aortic endothelial cells (RAECs) were used. Cells were kindly provided by M. Seifert (Charité, Berlin).

To reconfirm the endothelial character of the obtained RAECs the acetylated low-density lipoprotein (AcLDL) uptake assay was performed. Briefly, the acetylated form of the LDL complex is unable to bind its receptor. Instead it is taken up by

macrophages and endothelial cells by “scavenger” receptors specific for AcLDL. This method is routinely performed to identify endothelial cells. Representative images of fluorescence and light microscopy of AcLDL-treated RAECs are shown in Figure 17 demonstrating an efficient uptake of red fluorescence-labeled AcLDL in all cells, thereby confirming the endothelial character of the RAECs.

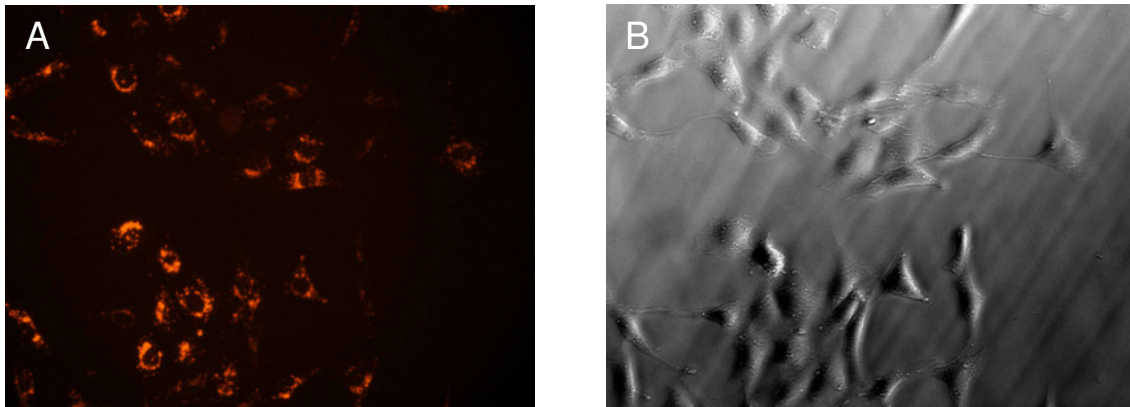


Figure 17: Dil-AcLDL uptake of RAEC. RAECs were incubated in Dil-AcLDL containing medium for 4 h. After washing and fixation, fluorescence (A) and light microscope (B) images were taken (200x; Zeiss Axiovert S100).

4.1.1.2.1 AAV2 capsids are detectable in the cytoplasm and perinuclear area of RAECs

Considering the presence of transgene DNA, but the absence of β -Gal activity in transplanted rat hearts, we first investigated if entry and intracellular transport of the vector might represent a limitation for endothelial cell transduction.

According to results published by us and others rAAV2 particles accumulate in the perinuclear area (Bartlett, Wilcher, and Samulski, 2000; Lux et al., 2005). First particles are detectable 15 min p.i. and remain visible for at least 24 hours (Lux et al., 2005; Seisenberger et al., 2001). RAECs were transduced with a GOI of 5×10^4 rAAV2ssGFP and fixed 4 h p.i.. They were stained with antibodies against intact AAV2 capsids (A20 antibody and a secondary RRX-labeled antibody) and the nuclear membrane (anti-Lamin B and a Cy5-labeled secondary antibody) and were analyzed by confocal laser scanning microscopy (LSM 510 Meta, Zeiss). As depicted in Figure 18 A, signals for intact AAV2 particles were detected within the cell. Although fluorescent signals may suggest the presence of AAV particles

within the nucleus, vertical sectioning revealed that vector particles were detectable in the perinuclear region, but not in the nucleus (Figure 18 A and B). The latter result is in line with our observation on HeLa cells, where entry of viral genomes, but not of intact capsids into the nucleus could be detected. Thus, it can be assumed that rAAV2 vectors entered RAECs which is consistent with our *in vivo* results, and are trafficked to the perinuclear area.

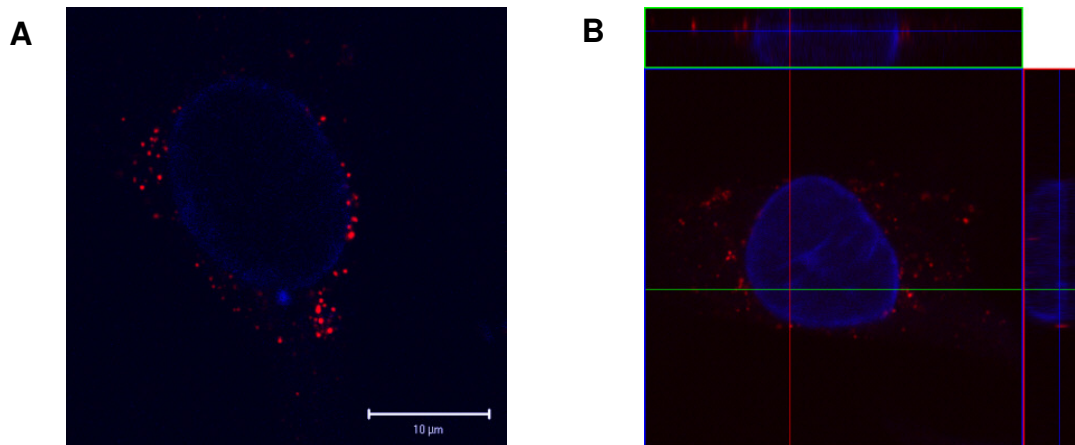


Figure 18: Visualization of RAEC transduced with rAAV2. RAECs were transduced with a GOI of 5×10^4 rAAV2ssGFP and fixed 4 h p.i.. Nuclear membrane was stained by anti-lamin B (blue: Cy5-labeled secondary antibody), while intact capsids were detected by A20 antibody (red: RRX-conjugated secondary antibody). Analyses were performed by confocal microscopy (LSM 510 Meta, Zeiss). Shown are representative confocal microscope images, one superimposed (A) and one image plane out of a z-stack stain of a horizontal section ($0.2 \mu\text{m}$).

4.1.1.2.2 CMV promoter induces transgene expression after transfection

Next, we investigated if lack of transgene expression in transplanted hearts might be due to inefficiency of the chosen strong viral CMV promoter. Therefore, two different plasmids both containing LacZ as transgene, but differing in the promoter were transfected into RAECs. We compared the endothelial cell-specific *fms*-like tyrosine kinase (FLT1) promoter described to mediate transgene expression in endothelial cells with “our” CMV promoter (Morishita, Johnson, and Williams, 1995; Nicklin et al., 2001b). RAECs cultured in medium without penicillin and streptomycin were transfected with Lipofectamin 2000 and $0.8 \mu\text{g}$ plasmid DNA according to the manufacturer’s instructions. One day thereafter, the cells were

fixed and stained for 4 h with X-Gal solution, the substrate for β -galactosidase activity (LacZ). Light microscope pictures were taken with an Olympus Vanox-S AH-2 microscope. Representative images are shown in Figure 19. In both cases only marginal LacZ activity was detectable pointing towards a low transfectability of these cells at least with the chosen method. However, β -galactosidase activity was visualized with both constructs revealing that the CMV promoter is in principle able to express transgenes in RAECs. Moreover, repeated experiments showed no clear difference between CMV- (A) and FLT1-(B) driven transgene expression with regard to efficiency.

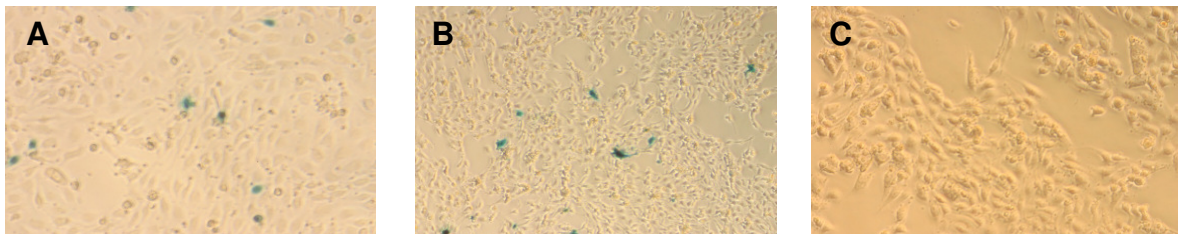


Figure 19: Transfection of RAECs with pZNL or pMV10-FLT1. RAECs were transfected with plasmids (0.8 μ g) coding for LacZ under the control of either a CMV promoter (pZNL) (A) or a FLT1 promoter (pMV10-FLT1) (B). The following day, cells were fixed and stained for LacZ activity for 4 h. Pictures were taken with an Olympus Vanox-S AH-2 microscope. Figure C shows control cells transfected without DNA in the transfection mix.

4.1.1.2.3 RAECs are poorly transduceable with AAV serotypes 1 to 5, but show enhanced expression by administration of MG132

As shown by experiments in the previous chapters, rAAV2 is able to enter RAECs and is transported to the perinuclear area. In addition, CMV promoter seems to be suited to control transgene expression in RAECs. Thus, we aimed to determine the efficiency of rAAV2-mediated transduction in RAECs. In order to identify a potentially more efficient serotype for transduction of these cells we included other serotypes, namely rAAV1 and rAAV3 to 5.

Moreover, we were interested to investigate if second-strand synthesis may limit transduction efficiency as we and others have shown for cell lines as well as for primary cells (Hacker et al., 2005; McCarty et al., 2003; McCarty, Monahan, and Samulski, 2001; Wang et al., 2003). Therefore, we compared the five different

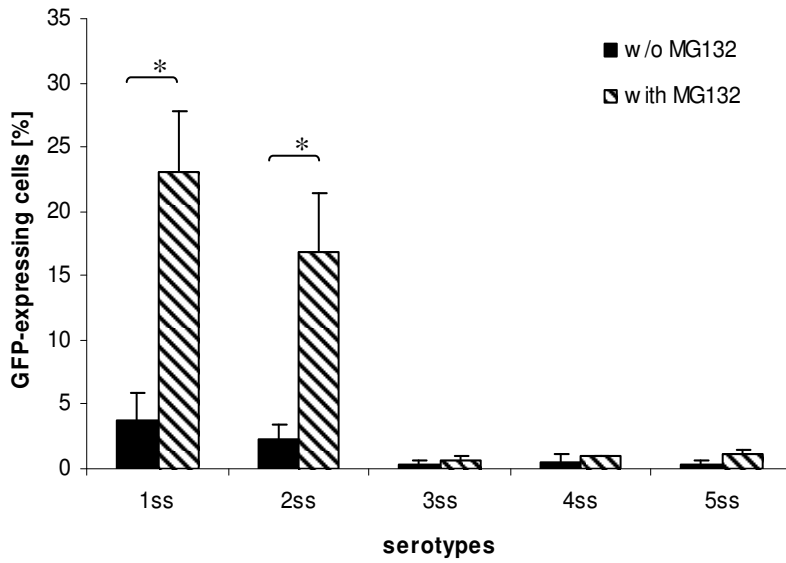
serotypes for their efficiencies encoding the transgene cassette in the self-complementary (sc) or the natural single-stranded genome conformation (ss).

Furthermore, we assessed the effect of the proteasome inhibitor MG132 (also Carbobenzoxyl-L-leucyl-L-leucyl-Leucinal; Z-LLL) on AAV-mediated transduction of primary RAECs. Although the mechanism of action remains to be elucidated, the enhancement in transduction efficiency *in vitro* and *in vivo* has been reported in various cell types (Hacker et al., 2005; Nicklin et al., 2001a; Pajusola et al., 2002; Yan et al., 2004).

Briefly, cells were transduced with 5×10^4 genomic particles per cell (GOI) of rAAV1 to 5 encoding for ssGFP or scGFP vector genomes, respectively. The proteasome inhibitor MG132 (40 μ M diluted in medium) or the solvent (DMSO) were applied at the time of transduction. Cells were washed intensely 3 times with PBS after 4 h. Flow cytometric analyses were performed 3 d p.i. (Figure 20). Comparisons between the serotypes identified rAAV1 as the most efficient serotype followed by rAAV2, whereas rAAV3, rAAV4 and rAAV5 showed only marginal GFP expression with a maximum of 1.5 ± 0.7 % (mean \pm standard error of the mean (SEM)) for rAAV5scGFP. The ranking of the serotypes was consistent between the group of rAAV encoding for scGFP and for ssGFP as depicted in Figure 20 A and B. Nonetheless, the absolute values for transduction with rAAV1 (16.6 ± 7.5 %) and rAAV2 (4.2 ± 0.7 %) scGFP vectors exceeded the efficiencies for rAAV1 (3.8 ± 2.0 %) and rAAV2 (2.3 ± 1.1 %) ssGFP vectors, respectively.

Interestingly, administration of the proteasome inhibitor MG132 resulted in a significant enhancement of transgene expression for serotype 1 as well as for serotype 2. An increase of 6-fold for rAAV1ssGFP (23.0 ± 4.7 %) and of 7.3-fold for rAAV2ssGFP (16.8 ± 1.1 %) was measured after addition of MG132 (Figure 20 A). Also, albeit less pronounced, an increase in transgene expression was observed for the vectors carrying self-complementary vector genomes, namely a 2.8-fold enhancement with rAAV1 (46.5 ± 10.1 %) and a 4.4-fold with rAAV2 (18.4 ± 2.2 %) in presence of MG132. No significant enhancement of transgene expression was detected when combining rAAV3 to 5 transductions and the addition of proteasome inhibitors.

A



B

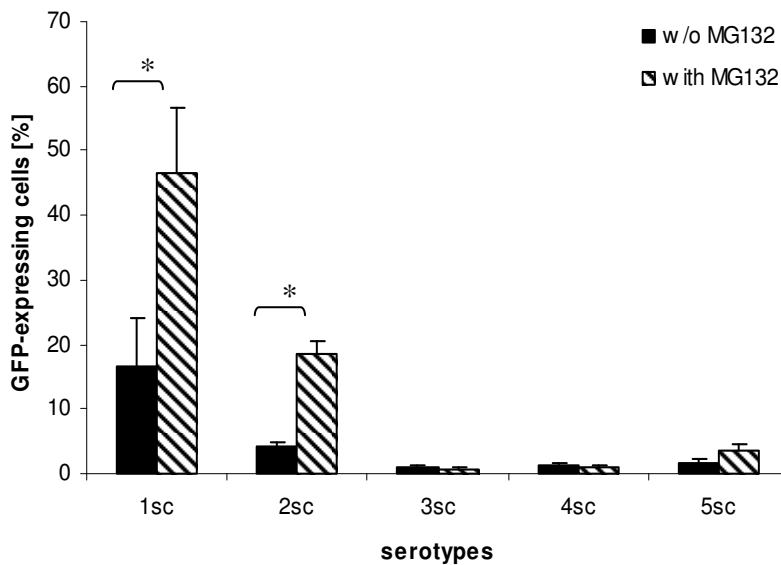


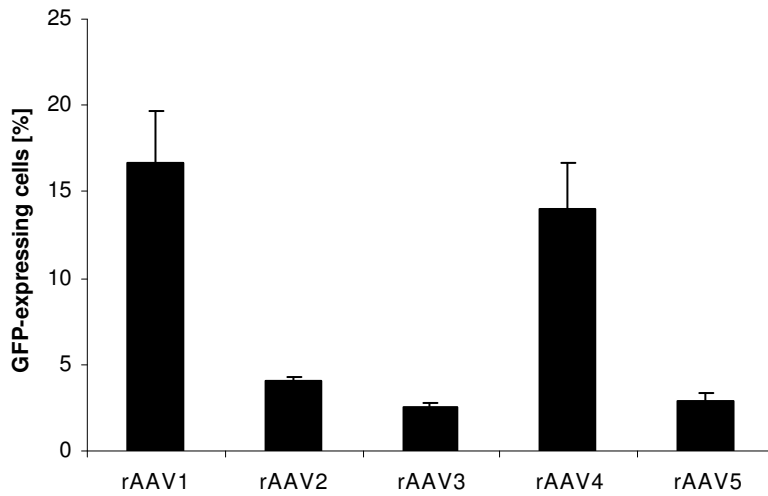
Figure 20: Transduction efficiency of rAAV1 to 5 (single-stranded and self-complementary vector genome conformation) in RAECs with and without MG132 treatment. RAECs were transduced with rAAV1 to 5 ($GOI\ 5 \times 10^4$) encoding either for GFP as transgene in either a single-stranded (ss) (A) or a self-complementary (sc) (B) vector genome conformation, respectively. Transduction was performed in presence or absence of 40 μ M MG132. After 4 h of incubation, cells were washed and analyzed by flow cytometry 3 d p.i. Shown are the results (means + SEM) of 3 (rAAV3, rAAV4, rAAV5) and 6 (rAAV1, rAAV2) independent experiments. (A) $*=P<0.002$ (B) $*=P<0.02$.

4.1.1.2.4 Neonatal rat cardiomyocytes show highest transgene expression after transduction with rAAV1 and rAAV4

As described in the previous chapters, the rAAV-mediated transduction efficiency in RAECs is rather low. Also *in vivo* no transgene expression was detectable in transplanted hearts (4.1.1.1.3). Alternatively, intramyocardial injection as well as enhancement of the vascular permeability has been reported to result in measurable transgene expression. In these cases, cardiomyocytes have been the target cell population thus being maybe a more suitable target for our application.

In order to evaluate the most efficient serotype for transduction of rat cardiac muscle cells and to compare that result with transduction of rat aortic endothelial cells, we investigated rAAV1 to rAAV5 on neonatal rat cardiomyocytes. Neonatal rat cardiomyocytes were kindly provided by B. Bölck (University Hospital of Cologne), but due to cell shortage only 2 experiments could be performed. On the first day, cells were cultured in medium containing 10 % horse serum and 5 % FCS. The following day, the cells were transduced with rAAV1 to 5 carrying the single-stranded GFP (ssGFP) genome. A GOI of 10^4 was chosen due to the high cell number per well (6×10^5 , 6-well) and the limiting amount of applicable vector volume. Cells were analyzed for GFP expression 3 d p.i. by flow cytometry (Figure 21 A) and fluorescence microscopy (Figure 21 B). Regarding the mean percentage for transgene-expressing cells, rAAV1 and rAAV4 showed the highest transduction efficiencies with 17.7 ± 3.0 % (mean \pm SEM) and 14.0 ± 2.7 %, respectively. The widely used serotype 2 only reached 4.1 ± 0.2 % whereas the serotypes 3 and 5 were even less efficient (rAAV3 2.6 ± 0.2 % and rAAV5 2.9 ± 0.5 %). Representative pictures of non-transduced and transduced (with rAAV1 or rAAV4) neonatal rat cardiomyocytes are shown in Figure 21 B. GFP-positive cells could only be detected in rAAV1 and rAAV4 transduced cells.

A



B

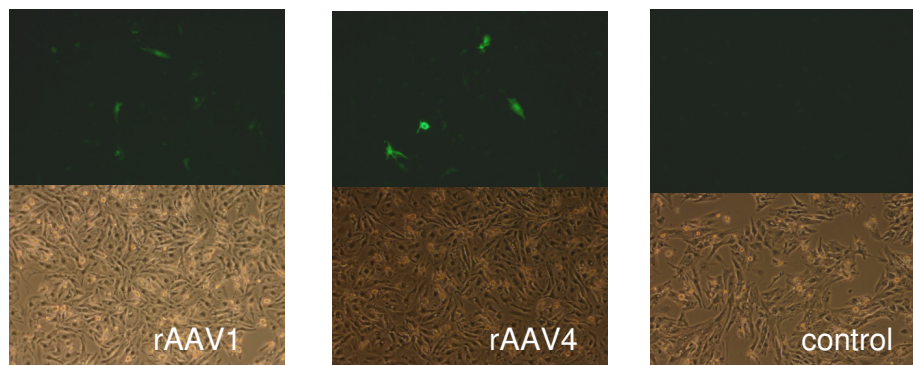


Figure 21: Transduction efficiency of rAAV1 to 5 in neonatal rat cardiomyocytes. Primary neonatal rat cardiomyocytes were transduced with 10^4 genomic particles per cell of rAAV2ssGFP. Transduction efficiency was evaluated 3 d p.i. by FACS analysis (A) and microscopy (B). In A, the results of 2 independent experiments are shown as mean + standard error of the mean (SEM).

In Figure 22 transduction efficiencies of RAECs and primary rat cardiomyocytes were compared. Hence, mean values obtained for transduced cardiomyocytes were divided by the ones for RAECs as described in 4.1.1.2.3 and results are shown as fold change. Whereas rat cardiomyocytes have been transduced with rAAV1 to rAAV5ssGFP at a GOI of 10^4 , RAECs received 5-fold higher vector amounts, but both flow cytometric analyses have been performed 3 d p.i.. As can be seen in Figure 22, more primary rat cardiomyocytes were successfully

transduced compared to RAECs. Despite the 5 times lower vector amount applied on cardiomyocytes, 4.4-fold more cardiomyocytes than RAECs expressed GFP when rAAV1 was used and 1.8-fold more in the case of rAAV2. For the serotypes rAAV3 to rAAV5 an even higher fold change has been calculated as a consequence of the nearly background transgene expression in RAECs (maximum 0.4 % GFP expressing cells). Also in rat cardiomyocytes, transduction efficiencies using rAAV3 and rAAV5 were very low while rAAV4 resulted in 14 % transgene-expressing cells.

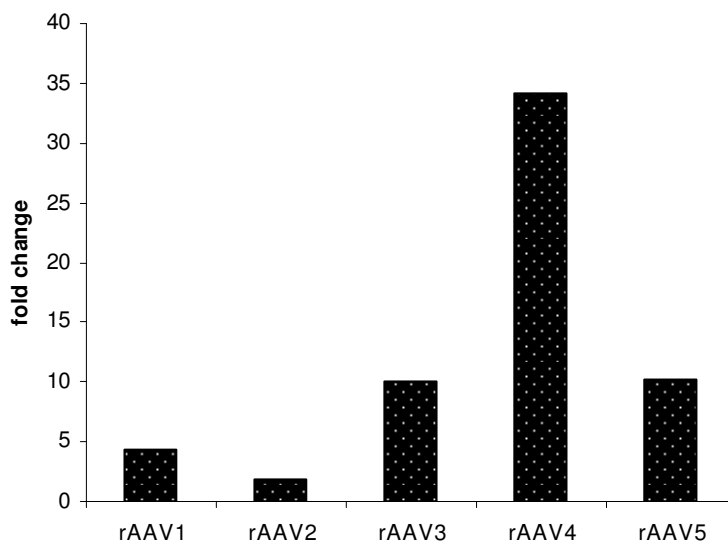


Figure 22: Comparison of transduction efficiencies between RAECs and primary rat cardiomyocytes. Shown are the fold changes of the mean transduction efficiencies of rat cardiomyocytes (GOI 10^4) divided by the amount of transgene expressing RAECs (GOI 5×10^4) 3d after transduction by the serotypes rAAV1 to rAAV5 encoding for ssGFP. The values are based on Figure 20 A and Figure 21 A.

4.1.2 rAAV-mediated gene transfer into porcine heart

4.1.2.1 Identification of the most suited serotype using PAECs as *in vitro* model

Concerning the choice of the serotype, we did not rely on literature for the pig heterotopic heart transplantation experiments unlike for the rat model. Therefore, we first aimed to assess the most feasible serotype for this purpose as comparative studies in porcine cells have not been published. Porcine aortic endothelial cells (PAECs) were chosen as *in vitro* model to investigate rAAV-

mediated transduction and potential intracellular barriers. PAECs were kindly provided by W. Kues (Institute of Farm Animal Genetics, Mariensee).

Corresponding to chapter 4.1.1.2, we reconfirmed the endothelial character of the provided PAECs by the ability to take up the endothelial-specific marker Dil-AcLDL. Therefore, PAECs were stained for 4 h with 1 $\mu\text{g/ml}$ Dil-AcLDL in medium at 37 °C. After washing and fixing the cells for 15 min in 3 % paraformaldehyde, fluorescence and light microscope images were taken (200x magnification; Zeiss Axiovert S100). As can be seen in Figure 23, PAECs take up Dil-AcLDL efficiently thus confirming their endothelial character.

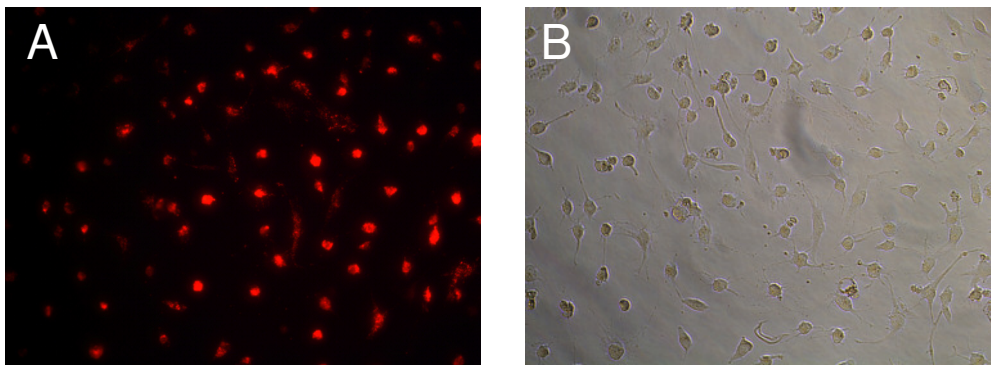


Figure 23: Dil-AcLDL uptake of PAECs. PAECs were incubated in Dil-AcLDL for 4 h, washed and fixed in 3 % paraformaldehyde before fluorescence (A) and light microscope (B) images were taken (Zeiss Axiovert S100).

4.1.2.1.1 PAECs are efficiently transducible with rAAV2

Endothelial cells are commonly described to be transducible by AAV only at low efficiencies compared to HeLa cells and the human glioma cell line LN-229 (Pajusola et al., 2002). In addition, comparative studies of different AAV serotypes in porcine endothelial cells are lacking. Therefore, we determined their permissiveness for the serotypes 1 to 5 and transduced PAECs with different amounts of the respective vectors (1×10^4 , 5×10^4 or 1×10^5). Moreover, we investigated if second-strand synthesis of the natural single-stranded (ss) vector genome in PAECs impairs efficient transduction as published for other cell lines (McCarty et al., 2003). Thus, we compared transduction efficiencies of rAAV1 to rAAV5 vectors encoding for the transgene in the single-stranded or double-stranded vector genome conformation, respectively. Transduction efficiency was

determined 3 d p.i. by flow cytometry and shown as mean + standard deviation in Figure 24.

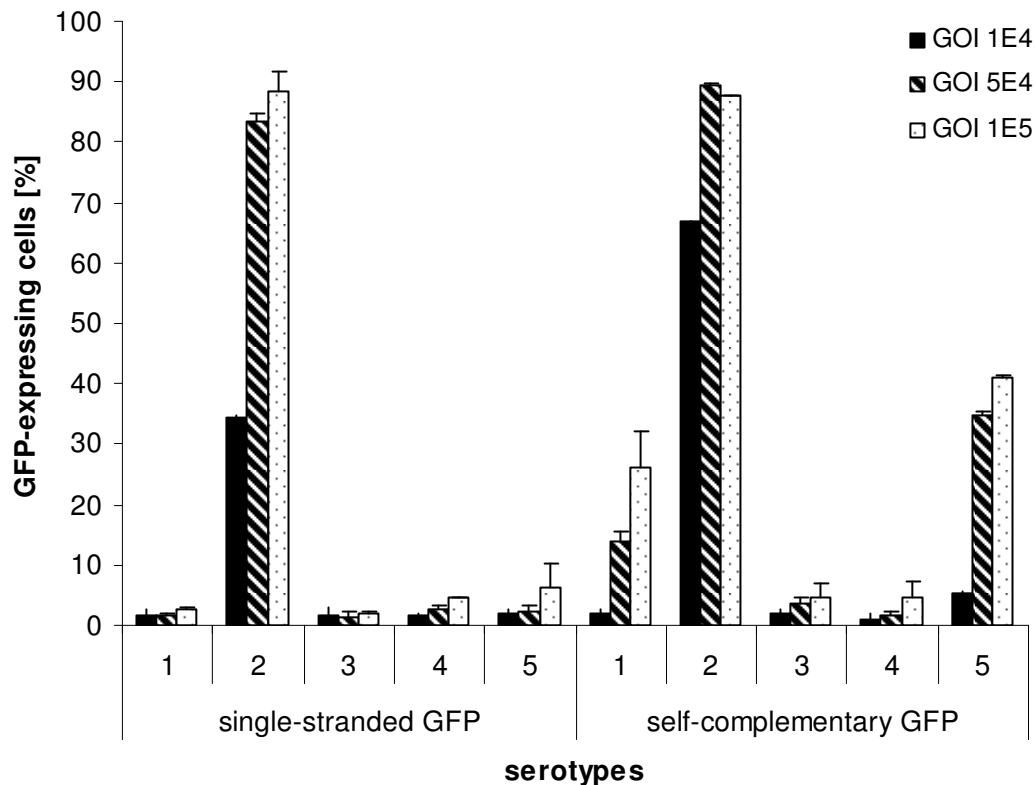


Figure 24: Transduction of PAECs with rAAV1 to 5 carrying single-stranded (ss) or self-complementary (sc) GFP genomes. For transduction 3 different vector-to-cell ratios (GOI of 10^4 , 5×10^4 or 10^5) were used shown as differently colored bars. PAECs were transduced by the serotypes 1 to 5 coding either for ssGFP or scGFP. The number of GFP-expressing cells was determined 3 d p.i. by FACS analysis and shown as mean + standard deviation.

As can be clearly seen, rAAV2 is the most efficient serotype for PAEC transduction. Comparing the means after administration of 10^4 genomic particles per cell (GOI) of rAAV2, scGFP (67.0 ± 0.02 %) vectors showed 2 times higher values than ssGFP-containing (34.5 ± 0.4 %) particles. Use of 5 times higher vector amounts per cell further increased the number of transgene-expressing cells to 83.4 ± 1.4 % for ssGFP- and 89.5 ± 0.3 % for scGFP-encoding rAAV2 vectors. These values changed minimally by administration of even higher vector concentrations (10^5 GOI) (ssGFP 88.4 ± 3.2 % and scGFP 87.6 ± 0.03 %) indicating saturation.

The serotypes 1 and 3 to 5 coding for ssGFP showed very low transduction efficiencies even at highest vector concentrations (GOI 10^5) (rAAV4 4.5 ± 0.1 %; rAAV5 6.1 ± 4.2 %). Also for scGFP vectors of the serotypes 3 and 4 only a low number of transduced cells could be detected with efficiencies of maximal 4.8 ± 2.2 % for rAAV3 and 4.5 ± 2.8 % for rAAV4 at a GOI of 10^5 . The second efficient scGFP-containing vector at this GOI with a transduction efficiency of 41.1 ± 0.1 % was rAAV5 which showed initially 5.2 ± 0.3 % transgene-expressing cells at a GOI of 10^4 and 34.9 ± 0.5 % (GOI 5×10^4). Also for rAAV1scGFP the number of transgene-expressing cells could be enhanced by use of higher GOIs, namely from 2.1 ± 0.6 % (GOI 10^4) to 26.2 ± 6.0 % (GOI 10^5).

| | rAAV1 | rAAV2 | rAAV3 | rAAV4 | rAAV5 |
|---------------------|-------|-------|-------|-------|-------|
| GOI 10^4 | 1.4 | 1.9 | 1.1 | 0.6 | 2.7 |
| GOI 5×10^4 | 8.3 | 1.1 | 2.5 | 0.7 | 14.8 |
| GOI 10^5 | 9.8 | 1 | 2.5 | 1 | 6.7 |

Table 2: Transgene expression using scGFP compared to ssGFP vectors. Shown are the fold changes of the means of transduction efficiencies of scGFP vectors divided by the means of the ssGFP vectors of the respective serotype and vector amount.

In conclusion, application of rAAV1scGFP and rAAV5scGFP vectors resulted in higher transduction efficiencies compared to the corresponding ssGFP vectors as shown in Table 2. For rAAV3 an up to 2.5-fold higher amount of GFP-expressing cells was obtained using rAAV3scGFP. In contrast, the generally low transgene expression after rAAV4ssGFP transduction was not enhanced by application of rAAV4scGFP. For rAAV2, an effect of vector genome conformation was only observable at a GOI of 10^4 as higher vector amounts resulted in maximal transduction efficiencies of around 90 %. In summary, serotype 2 showed the highest expression in PAECs.

4.1.2.1.2 Visualization of rAAV2 capsids in the cytoplasm of PAECs

By confocal microscopy, we aimed to visualize the highly efficient transduction of PAECs by rAAV2 (4.1.2.1.1). We were especially interested to compare these results with confocal images of the RAEC transduction which showed only low transgene expression (4.1.1.2.1 and 4.1.1.2.1). Therefore, PAECs were prepared like RAECs. Cells were transduced by rAAV2ssGFP at a GOI of 5×10^4 and fixed

4 h p.i.. Intact AAV2 vector capsids were stained with A20 antibody and RRX-conjugated secondary antibody (red), while the nuclear membrane was visualized by anti-Lamin B and Cy5-conjugated secondary antibody (blue) staining.

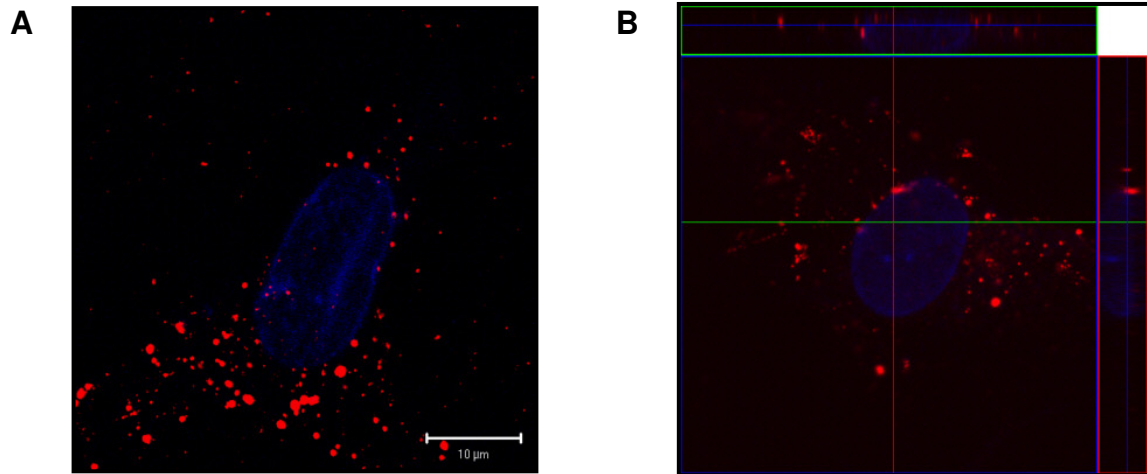


Figure 25: Visualization of PAEC transduction by rAAV2. PAECs were transduced by a GOI of 5×10^4 rAAVssGFP and fixed 4 h p.i.. Intact capsids were stained with A20 antibody and RRX-conjugated secondary antibody (red), whereas nuclear membrane was visualized by anti-Lamin B and Cy5-conjugated secondary antibody (blue). Shown are representative images of a superimposed (A) and a horizontal section ($0.2 \mu\text{m}$) (B) taken by confocal laser scanning microscopy (LSM 510 Meta, Zeiss).

In the superimposed picture in Figure 25 A, large aggregates of vector signals were visible distributed all over the cell. A representative image of a vertical plane section is depicted in Figure 25 B and reveals that signals are located within the cytoplasm. This picture differs from the one obtained for RAECs and a perinuclear accumulation – as seen with other cell types – could not be detected.

4.1.2.2 Heterogenic pig heart transplantation

Despite the existence of small animal models, species-specific large animal models are needed for preclinical evaluation. Porcine hearts are physically and physiologically closely related to human hearts thus being ideal as xenografts. Moreover, pigs serve as preclinical models to develop gene therapy approaches for cardiovascular diseases or organ transplantations. Unfortunately, large animal models require huge vector amounts to achieve significant transduction.

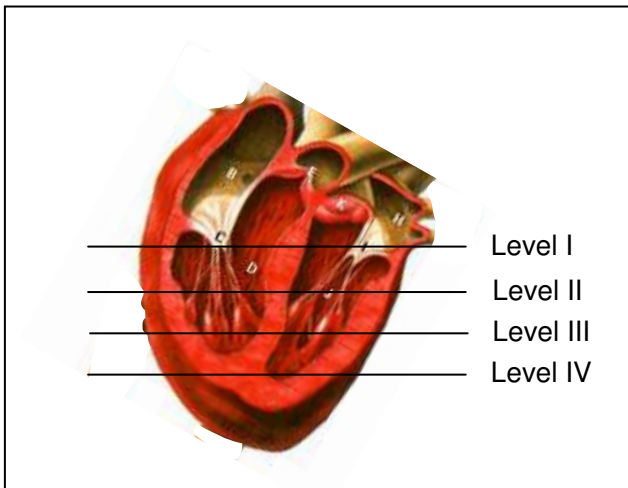
Heterotopic pig heart transplantations were performed by L. Burdorf and colleagues (Department of Heart Surgery, Ludwig-Maximilians-University Munich)

as described in 7.5.2. In order to prolong vector circulation in the heart after intracoronary vector application, an *in situ* Langendorff perfusion system was developed. Thus, the warmed and oxygenated blood containing the vector solution recirculated for about 40 min in the warm and beating heart enhancing the chance of vector entry as shown by our results obtained for the normothermic transplantation in the rat model. As immunosuppressive therapy the animals received 1.5 mg/kg body weight Tacrolimus per day.

As rAAV2 was revealed as the most efficient serotype in *in vitro* experiments of PAECs, we used this serotype *in vivo*. Large vector amounts had to be produced by triple transfection of HEK293 cells. Cell lysates were purified by iodixanol gradient centrifugation followed by heparin affinity chromatography to further purify and additionally concentrate the vector preparation (7.3.6). Genomic titers have been determined by qPCR.

In a first approach, we used 2×10^{12} genomic particles rAAV2ssLacZ, assessed the amount of vector genomes within the heart samples by qPCR and eventual transgene expression by X-Gal staining of cryosections. In a second experimental setting, we applied 2.3×10^{13} genomic particles of rAAV2scLuci. Also here, transgene DNA levels of the heart were analyzed by qPCR. Luciferase was evaluated by a luciferase detection assay. Both times histamine (100 μ g in 10 ml volume over 4 min injected into the perfusion system) was administered to render vessels permeable thus allowing to overcome endothelial barrier and to transduce endothelial as well as cardiac muscle cells. This was in contrast to our rat transplantations where we focused on endothelial cells as target and observed that the transduction efficiency obtained for the endothelium is very limited *in vivo* as well as *in vitro*. However, the situation in the porcine model might be different as we observed a very efficient transduction (up to 90 %) of PAECs *in vitro*.

A



B

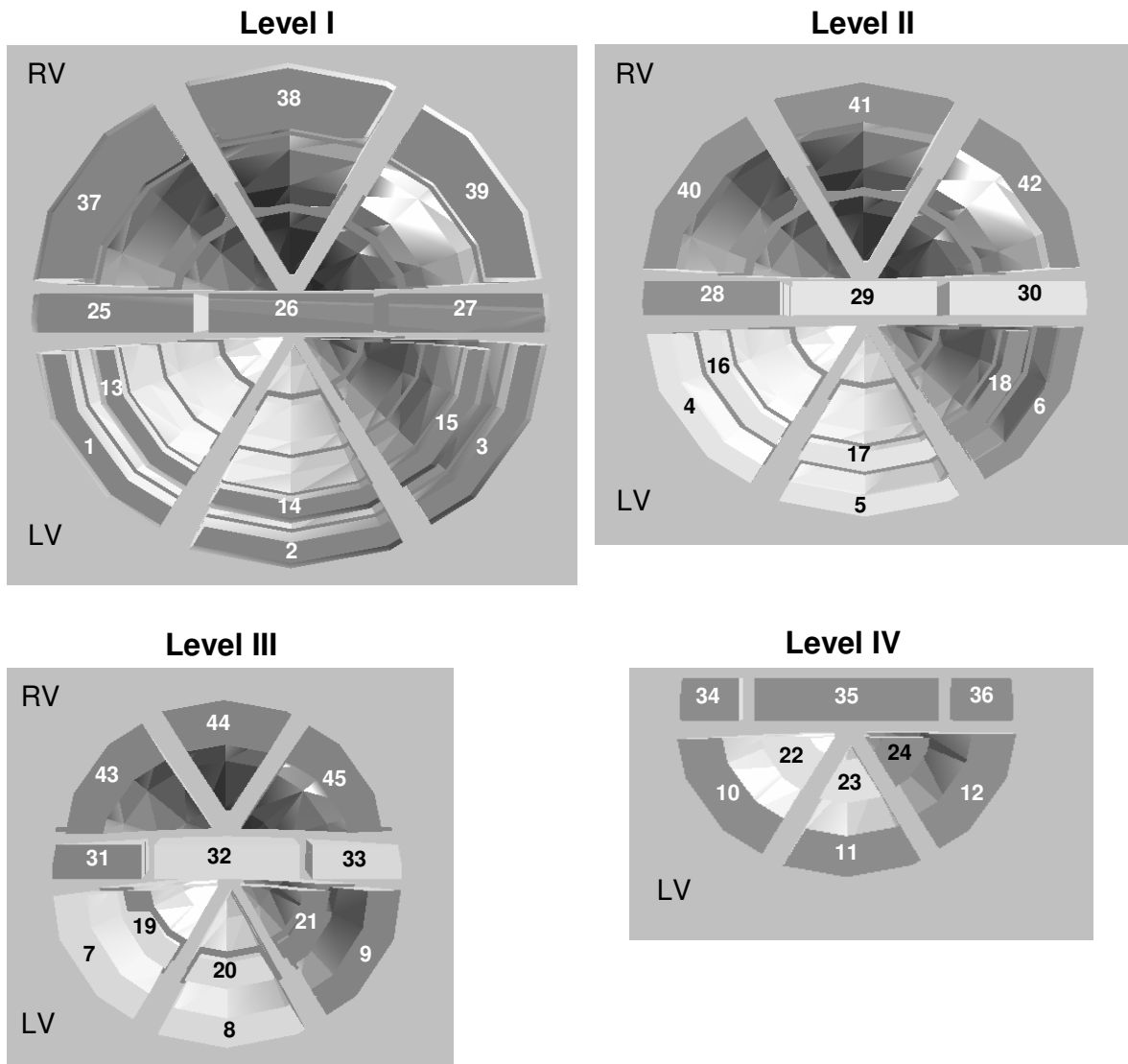


Figure 26: Dissection scheme for analysis of the transplanted porcine heart. As depicted, organ samples were taken from 4 different horizontal levels of the myocardium (A). Mapping of the numbers are shown whereas left side of each level represents the ventral and right the dorsal part of the heart (B). The numbers 37 to 45 account for samples of the right ventricle (RV), whereas 25 to 36 are taken from the septum region at the different planes. Samples of the left ventricle (LV) are divided into origin of outer (1 to 12) and inner (13 to 24) myocardial wall.

The hearts were explanted after 21 d and dissected following the scheme depicted in Figure 26. Samples were taken from 4 different levels from the very superior part of the ventricle (level I) to the apex cordi (level IV). The right ventricular (RV) samples were numbered 37 to 45, the septum region 25 to 36 in respect to the level. Regarding the left ventricle (LV), samples were taken from the outer (1 to 12) and inner (13 to 24) regions. For the first time, such a detailed and complete analysis of a vector perfused heart has been done as previous reports only analyzed the perfusion bed of the left anterior coronary (Kaspar et al., 2005; Raake et al., 2008). The main regions supplied by the coronaries correspond to the numbers 37, 39, 27 on level I, 40, 42 and 30 on level II and 43 and 45 on level III. Minor branches of the coronaries are located in the regions 7, 9, 11, 12 and 34 of the levels III and IV.

4.1.2.2.1 Successful vector delivery, but no transgene expression from single-stranded vector genomes in porcine heart

The first animal had received 2×10^{12} rAAV2 encoding for β -galactosidase in a single-stranded vector genome conformation intracoronarily while connected for 38 min to the *in situ* Langendorff perfusion system (7.5.2). Additionally, histamine (100 μ g in 10 ml volume over 4 min) was infused to increase permeability of the vessel wall. 21 d after transplantation, native heart, kidney, spleen, lung and liver as well as the transplanted heart were explanted whereas the latter was dissected following the above described scheme (4.1.2.2). Total DNA was extracted (7.2.5) and 100 ng were analyzed by qPCR for the presence of vector genomes and porcine GAPDH which was used for normalization (7.2.8). In contrast to our results in the rat model where we could not quantify the amount of vector genomes, gene transfer efficiency could be quantified in the pig model. The PCR products were verified by melting curve analyses and agarose gel electrophoreses (data not shown). In Figure 27 the results of 2 independent qPCRs for both genes are

depicted as copy number per μl DNA solution \pm standard deviation whereas 1 μl corresponds to 50 ng DNA.

The highest background signal for samples of an untreated animal was 31 copies/ μl . In all samples obtained from the transplanted heart LacZ DNA was detectable exceeding our detection limit and varying from 146 ± 58 (sample 5) to $26,147 \pm 4,715$ (sample 40) copies/ μl . Of note, 66.7 % of the samples were in the range of 1,000 to 10,000 copies/ μl .

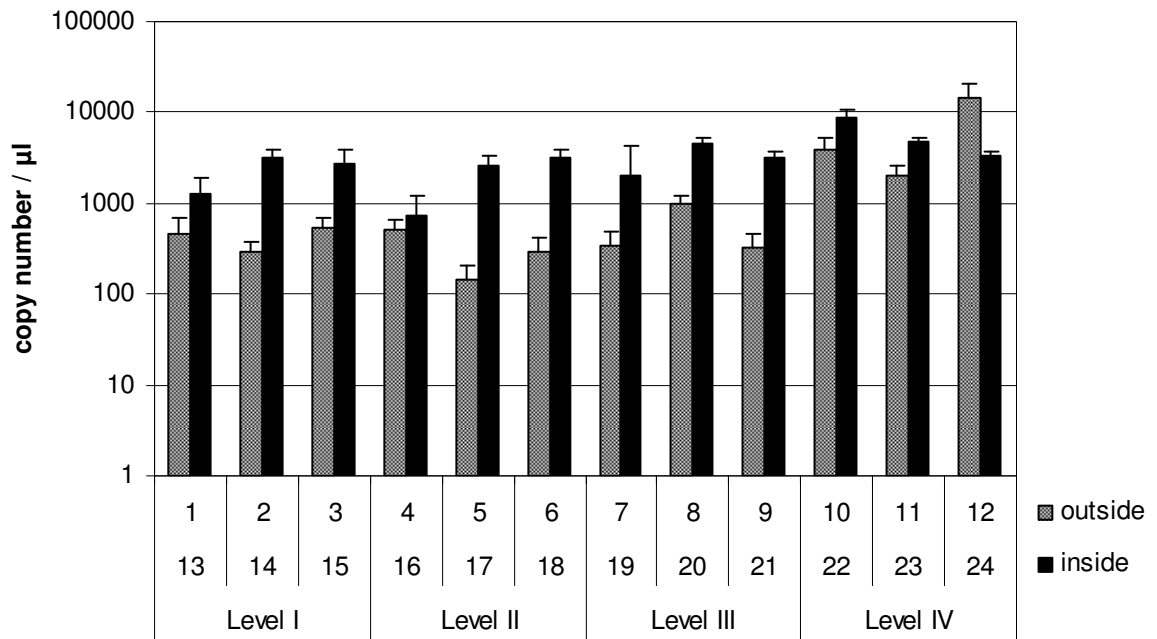
The outer parts of the left ventricle showed the lowest overall amount of vector DNA of all heart regions with an average copy number of 431 (146 ± 58 to 974 ± 230) for levels I to III. Level IV showed higher values ranging from $1,988 \pm 548$ (sample 11) to $14,484 \pm 6871$ (sample 12) copies/ μl . Inner regions of the left ventricle tended to result in higher amounts of vector genomes, namely between 739 ± 476 and $8,753 \pm 1,857$ copies/ μl .

Within the septum area, all samples yielded between 1,000 and 10,000 copies/ μl with a mean of $3,677 \pm 2,085$ copies/ μl . Lowest amount of transgene DNA was measured in sample 32 (961 ± 131), while the highest value was detected in sample 31 ($8,585 \pm 2,023$). However, no preference for a certain dissection level could be determined. For each level, the first value (ventral part of the septum) was the highest, while means decreased more and more towards the dorsal parts (with exception of sample 32).

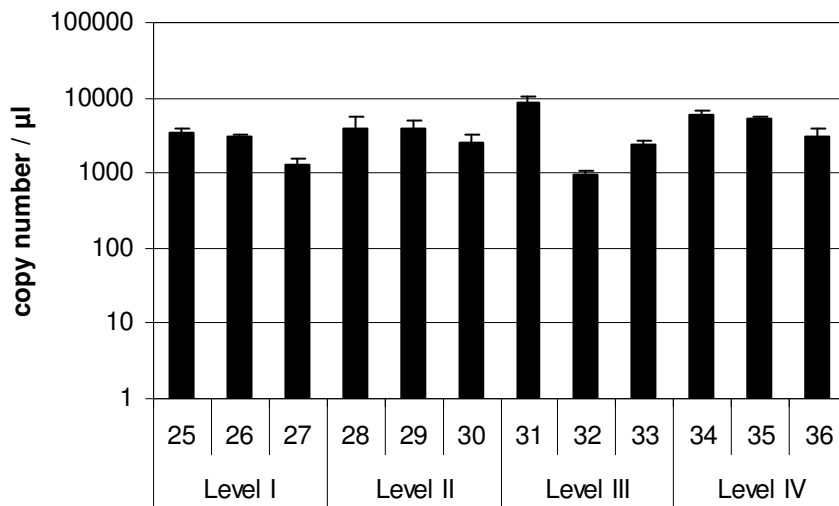
The same tendencies could be seen in the right ventricle levels I and II. Thus, the vector DNA amounts detectable in the area neighbouring the septum in the ventral part was also in this case higher than the 2 other samples of the same plane. The highest values of all heart samples were measured in the right ventricle with $26,147 \pm 4,715$ copies/ μl for sample 40 and $19,503 \pm 7,424$ for number 44. Minimal transgene DNA amounts were detected in sample 39 with 989 ± 106 copies/ μl . The overall average copy number in the right ventricle was $8,324 \pm 8,766$ copies/ μl .

Regarding extracardiac organs for determination of vector excess after transplantation, none of the analyzed organs exceeded the values for the negative control animal. Thus, no transduction could be measured in non-target tissues of the transplanted and rAAV-treated pig.

Left ventricle



Septum



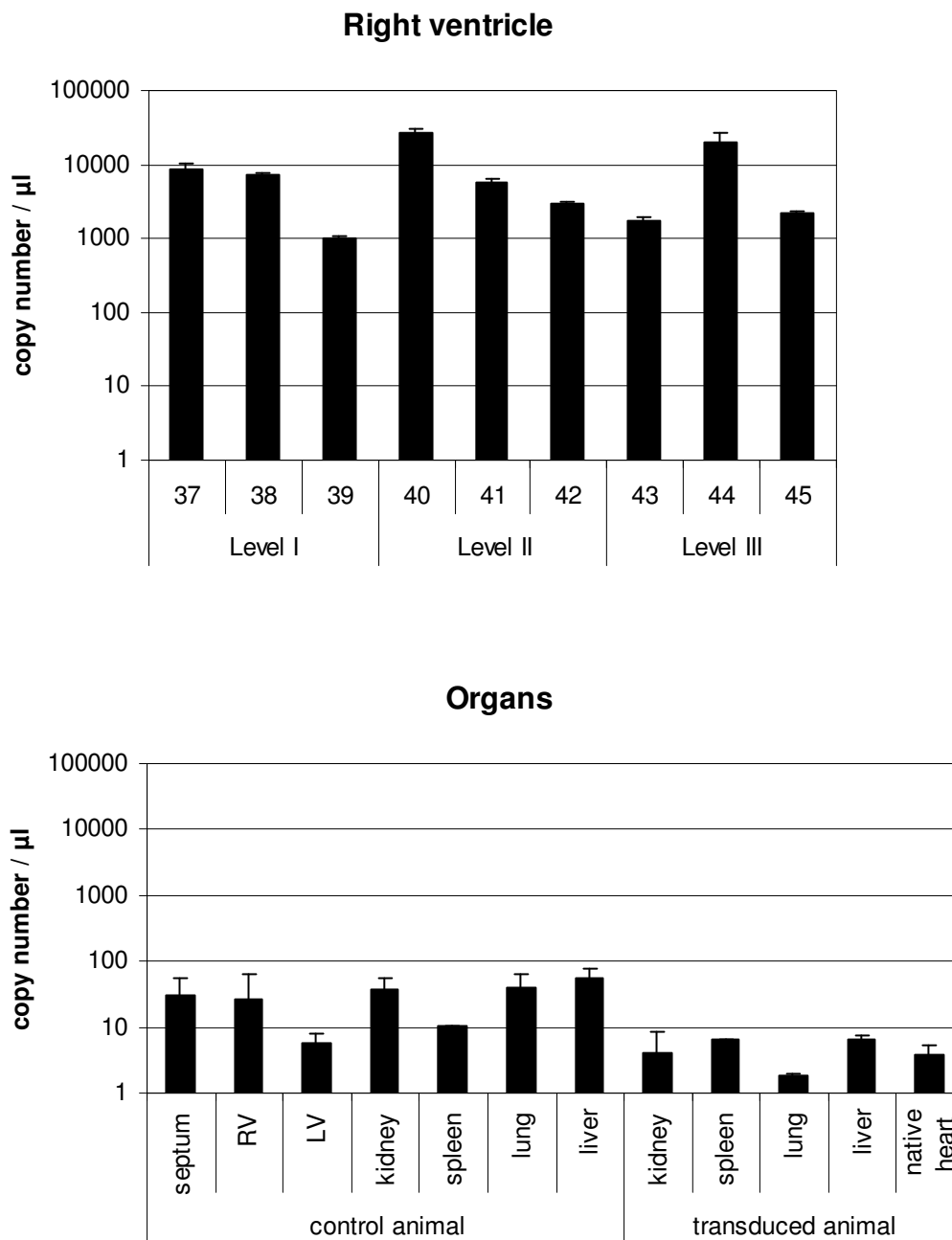


Figure 27: Distribution of vector genomes in the transplanted pig. The piglet received 2×10^{12} genomic particles of rAAV2ssLacZ intracoronary and was explanted after 21 d. The control animal did not receive any vector. The amount of LacZ DNA in the respective heart regions (right ventricle; left ventricle; septum) and organs was determined by qPCR and normalized to GAPDH. Shown are the results of 2 independent PCR runs for each gene as transgene copy number per μl DNA (1 μl equals 50 ng DNA) (+ standard deviation). RV, right ventricle; LV, left ventricle.

Additionally, tissue sections were performed by cryotom tissue dissection to investigate if transgene expression had occurred (M. Odenthal, Institute of Pathology, Cologne). The same protocol was used as described for rat heart

transplanted organs (4.1.1.1.3, 7.4.1). Briefly, sections were stained with X-Gal (2 d), counterstained by 0.5 % eosin solution (8 min) and analyzed by light microscopy. Despite the detection of vector genomes, X-Gal activity could not be detected in any of the samples (data not shown).

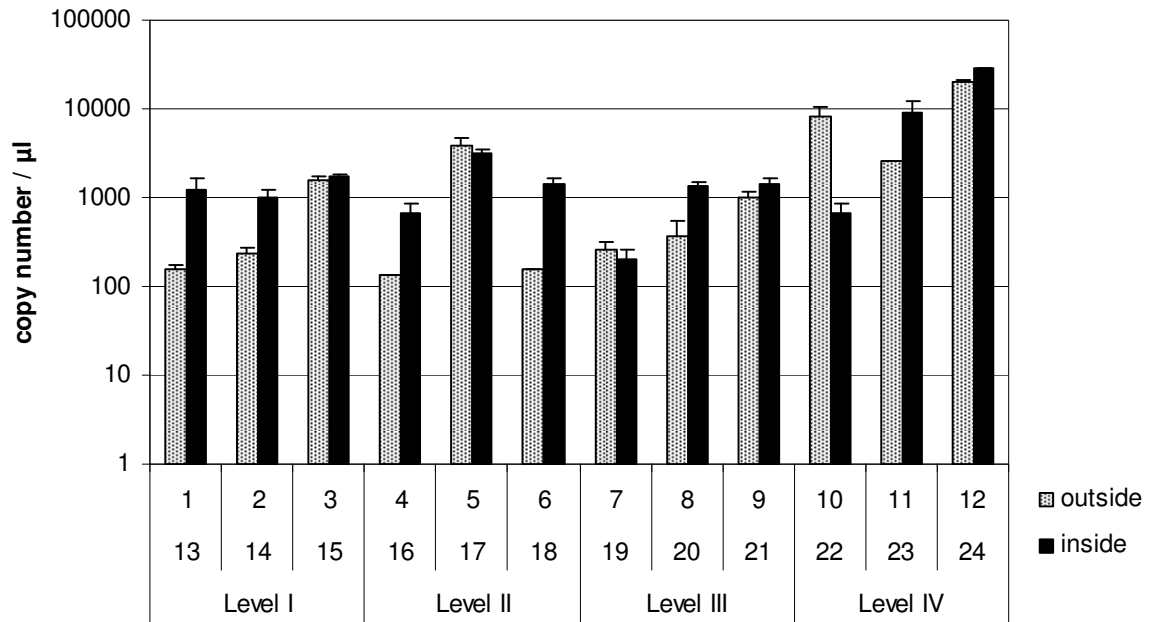
4.1.2.2.2 Successful vector delivery and transgene expression from self-complementary vector genomes in porcine heart

Self-complementary (sc) vector genome conformation is known to enhance transgene expression *in vitro* and *in vivo* (McCarty et al., 2003). Also in PAECs, the efficiency of transgene expression by rAAV2scGFP was higher than for single-stranded (ss) rAAV2 which was most obvious at lower vector-to-cell ratios (4.1.2.1.1). Therefore, we assayed if use of a sc vector would result in detectable transgene product levels *in vivo*. We chose luciferase (Luci) as transgene. Vector production, operation including use of Langendorff perfusion system (recirculation time 39 min), vector administration and histamine injection were performed as described in chapter 7.5.2. It was possible to produce rAAV2scLuci at high titers, thus 2.3×10^{13} genomic particles were administered. The organs were explanted 21 d later and the heart was dissected following the scheme depicted in Figure 26.

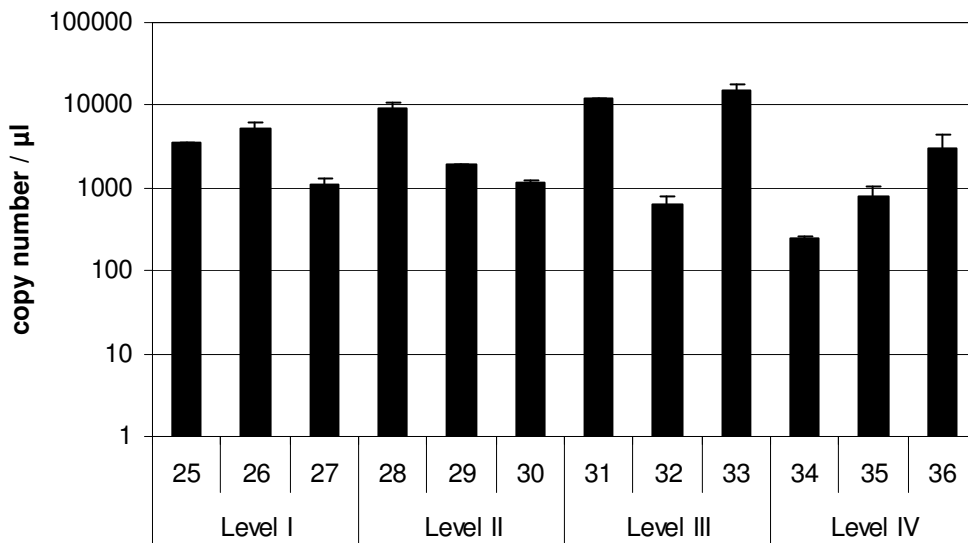
At first, DNA was extracted (7.2.5) and the level of transgene and housekeeping gene in 100 ng DNA by qPCR using the LightCycler Fast Start DNA Master SYBR Green I Kit (Roche) was evaluated as described in 7.2.8. PCRs were performed 2 times independently. As the amount of luciferase was quantifiable, the level of luciferase DNA could be normalized to the porcine GAPDH gene as shown in Figure 28. The PCR products were verified by melting curve analysis and agarose gel electrophoresis (data not shown). Values are given as copy number/ μ l whereas 1 μ l corresponds to 50 ng DNA.

As can be seen in Figure 28, luciferase PCR did not result in transgene-specific background signals in organs of the control animal.

Left ventricle



Septum



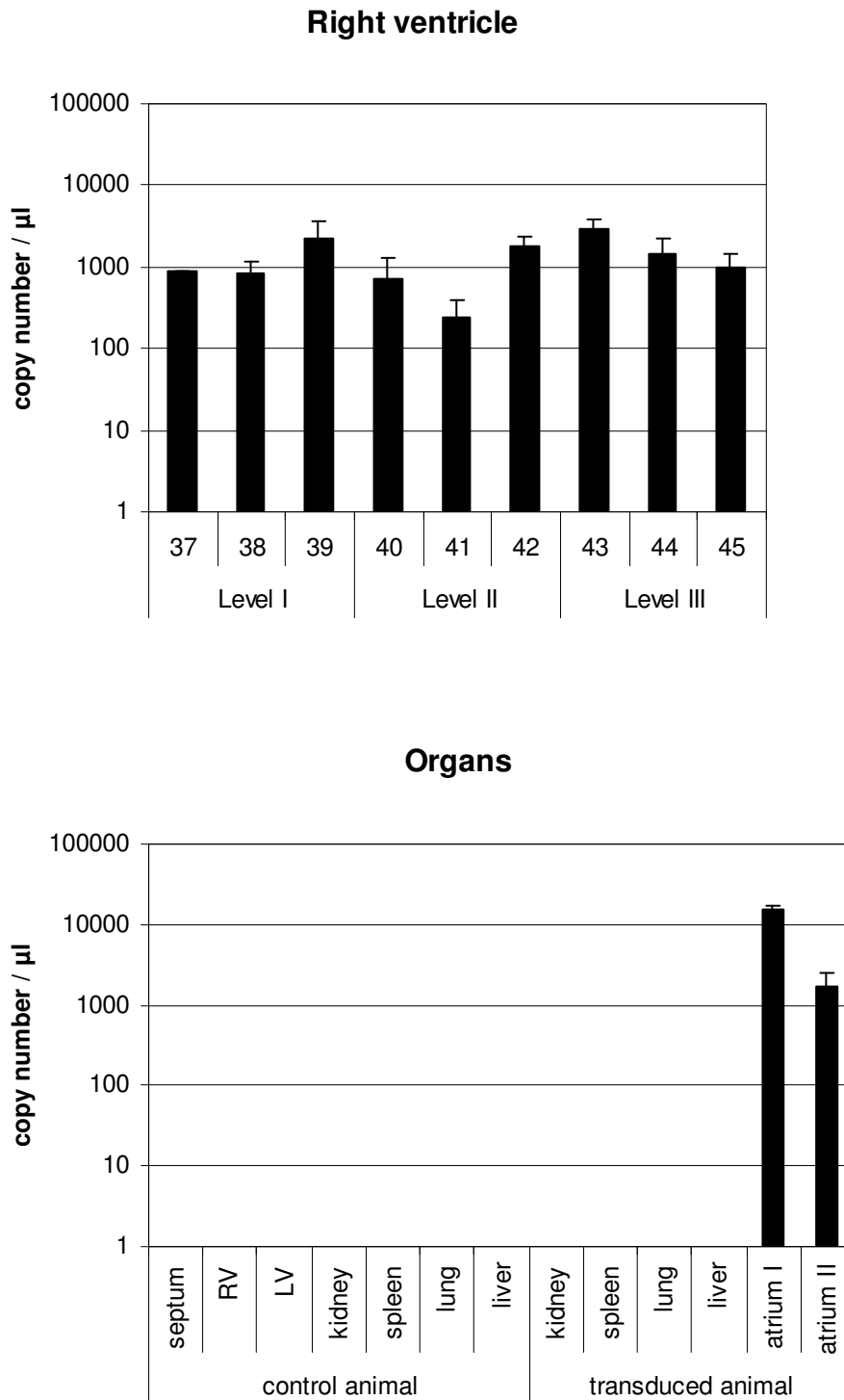


Figure 28: Distribution of vector genomes in the transplanted animal. The pig received 2.3×10^{13} genomic particles of rAAV2 encoding luciferase in the self-complementary vector genome conformation intracoronary and was explanted after 21 d while the control animal was non-transduced. The amount of transgene DNA in the septum, left and right ventricle and organs was determined by qPCR and normalized to the housekeeping gene GAPDH. Shown are the results of 2 independent PCR runs for each gene as normalized transgene copies/ μl DNA (1 μl corresponds to 50 ng DNA) (+ standard deviation). RV, right ventricle; LV, left ventricle.

Evidently, luciferase DNA was detected in every sample albeit at different levels. The highest overall values were observed in the samples 12 and 24 of the left ventricle with $20,601 \pm 335$ copies/ μl (mean \pm standard deviation) and $28,985 \pm 197$, respectively. Also the lowest transgene DNA amount was detected in this area with 136 ± 1 copies/ μl in sample 4. No tendencies could be observed in the left ventricle regarding distribution of transgene DNA. In most cases (9 out of 12) the levels of luciferase DNA was higher in the inner regions compared to the outer counterparts. The highest values within the outer regions were measured in level IV ($10,493 \pm 9,215$ copies/ μl ; 852 ± 1211 for levels I to III).

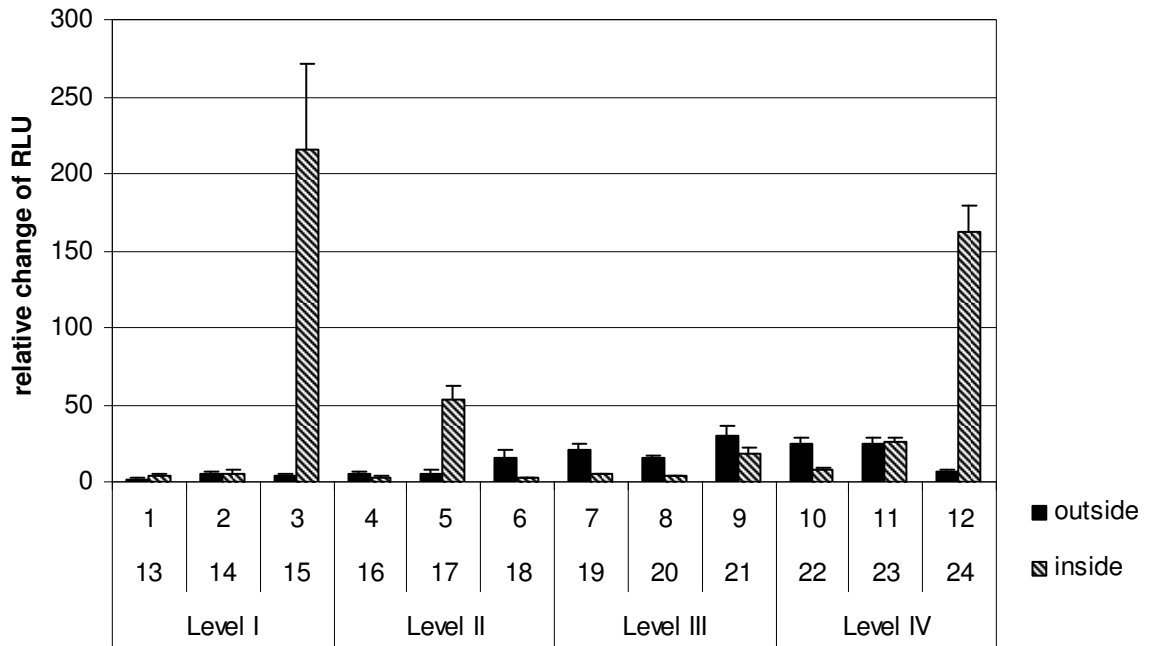
Within the septum region, in sample 33 the highest amount of luciferase DNA with $15,281 \pm 2,622$ was detected, while sample 34 showed the lowest with 251 ± 14 copies/ μl . Within the level IV the average amount of transgene DNA was the lowest compared to the other levels. Nevertheless, mean luciferase DNA level in the septum (4,519) was higher than in the ventricular regions (left ventricle 3,262; right ventricle 1,343).

As already stated, the lowest transgene DNA amount was detected in the right ventricle. The copy numbers ranged from 237 ± 149 (sample 41) to $2,935 \pm 957$ (sample 43).

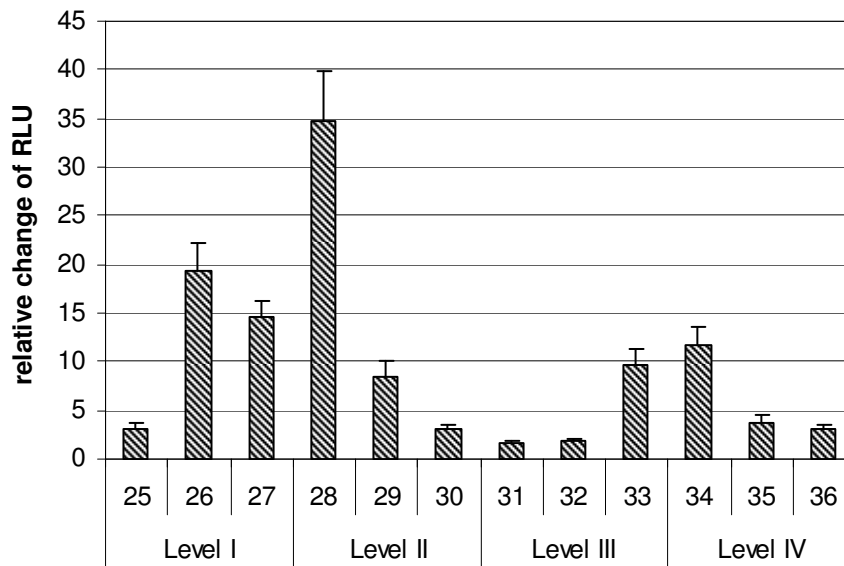
Additionally to the ventricular and septum samples, 2 parts of the atrium were analyzed showing high transgene copy numbers with $15,541 \pm 2,051$ (atrium I) and $1,728 \pm 742$ copies/ μl (atrium II).

After confirming the existence of transgene DNA in the transplanted and transduced heart, we evaluated the presence of transgene product by luciferase detection assay (7.4.4). Therefore, the amount of protein per sample was determined by Bradford assay to allow normalization of the luciferase signal. Approximately 20 mg of tissue was homogenized in 400 μl lysis buffer (*Renilla* Luciferase Assay System, Promega) by ball mill, incubated for 1 h on ice and pelleted (30 min, 16,000 \times g, 4 °C). 5 μl of the supernatant was measured by Bradford assay in an ELISA reader at a wavelength of 595 nm 3 times independently (7.4.3).

Left ventricle



Septum



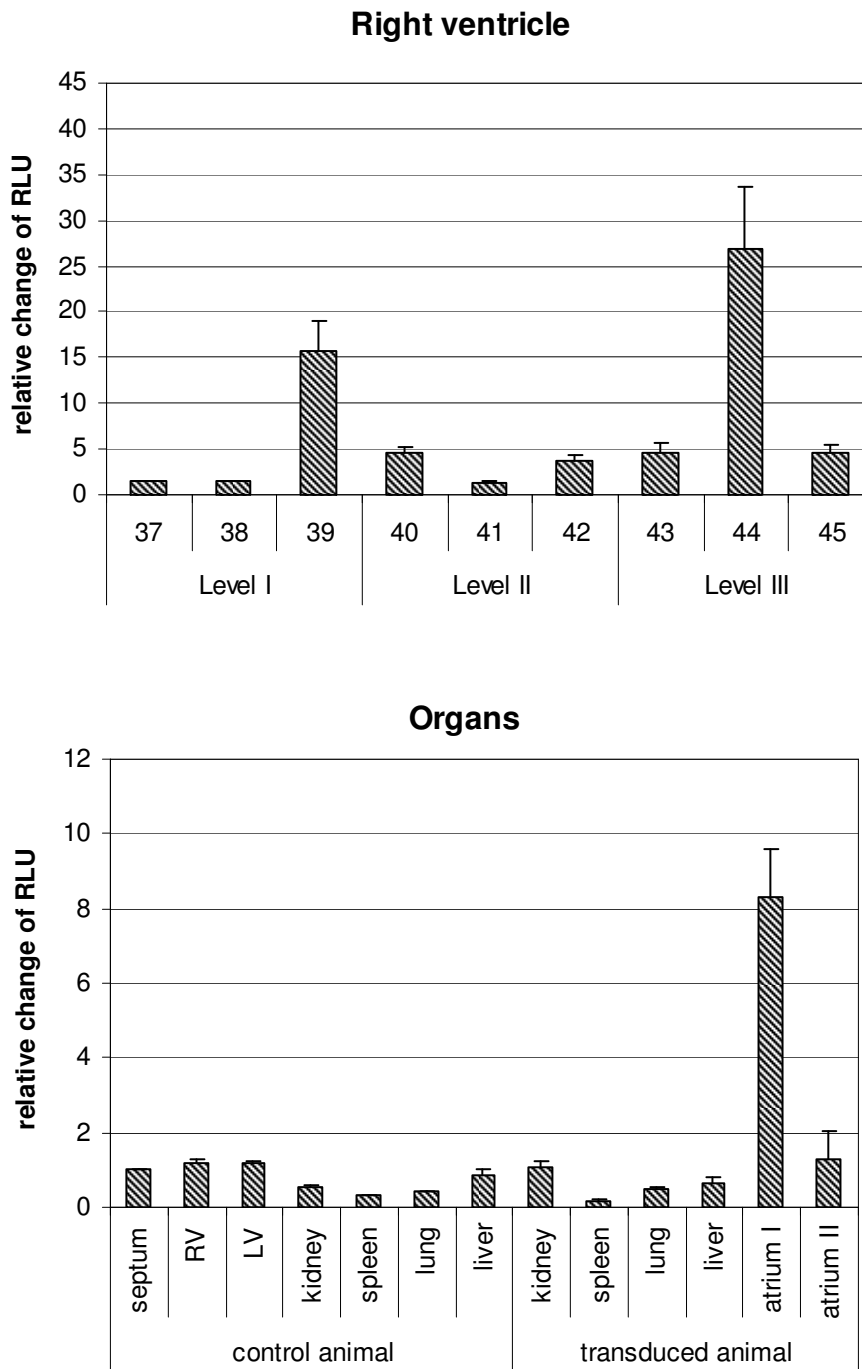


Figure 29: Luciferase activity in transplanted porcine heart and other organs after intracoronary vector injection of rAAV2Luci or without vector treatment (control animal). The animal organs of the transduced and non-transduced pigs were explanted 21 d after transplantation and analyzed for luciferase activity. Protein amount was determined 3 times by Bradford assay for normalization of luciferase signal. Shown are the normalized results of 3 independent luciferase assays as relative change of relative light units (RLU) + standard deviation compared to the septum of the control animal. RV, right ventricle; LV, left ventricle.

For detection of luciferase activity 20 μ l protein lysate was mixed with 100 μ l assay buffer and 1 μ l substrate (*Renilla* Luciferase Assay System, Promega) and measured by luminometer. Only a limited amount of samples was measured at once as chemiluminescence fades fast. The measurement was repeated 3 times independently. Normalization to total protein amount of 110 μ g followed to allow comparison of relative light units (RLU). In Figure 29 the relative changes in RLU (mean \pm standard deviation) in comparison to a sample obtained from the septum area of a transplanted, but non-treated pig are shown.

Remarkably, all cardiac samples showed detectable luciferase activity. Interestingly, variances were immense reaching from 1.4-fold (\pm 0.1) (sample 41) to 215.0-fold (\pm 56.4) (sample 15). Sites of high expression were heterogeneously distributed. Whereby, the 3 samples showing the highest activity were located in the inner wall of the left ventricle (sample 15: 215.0 \pm 56.4; sample 17: 53.1 \pm 9.4; sample 24: 162.1 \pm 17.4). The levels of the remaining samples of the inner ventricular region were similar to the outer regions. Regarding the outer part of the left ventricle, luciferase activity varied from 1.9 \pm 0.3 fold to 29.5 \pm 6.7 fold with a mean change of 13.1-fold.

Also in the septum region, the luciferase activity ranged from 1.7 \pm 0.1 fold (sample 31) to 34.8 \pm 5.1 fold (sample 28) with an overall mean of 9.6-fold.

In the right ventricle, only 2 out of 9 samples showed a more than 5-fold increase in luciferase activity, namely sample 39 with 15.7 \pm 3.3 fold and sample 44 with 26.8 \pm 6.7 fold.

Analyses of extracardiac organs revealed absence of detectable amounts of luciferase. The separately analyzed samples of the cardiac atrium showed an increase of 8.3 \pm 1.3 fold for atrium I, but only a marginal change of 1.3 \pm 0.8 fold for atrium II.

4.2 Establishment of rAAV-mediated gene transfer into CD34⁺ cells

4.2.1 Second-strand synthesis is a limiting step in CD34⁺ cell transduction

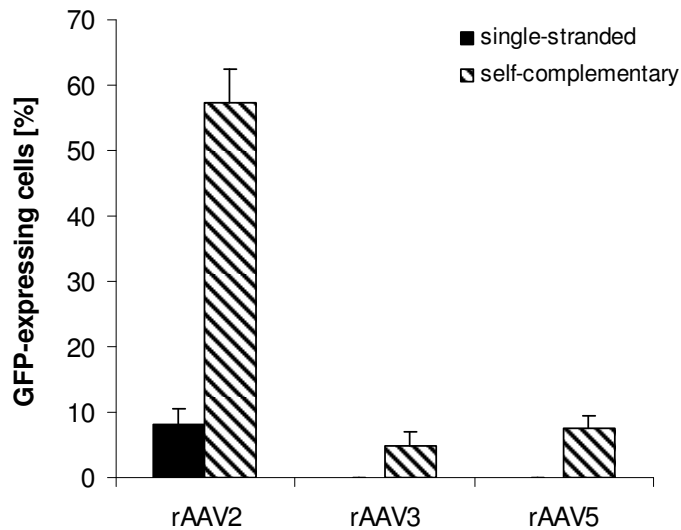
As already summarized in 3.2.3, publications on rAAV-mediated transduction of human CD34⁺ cells are hardly comparable due to differences in vector production, titration and applied vector amounts in addition to varying cell origin and isolation techniques. So far, only rAAV2 has been evaluated in human CD34⁺ cells, but with conflicting results regarding their transduction efficiencies. In this study we aimed to develop a protocol for efficient transduction of CD34⁺ cells by making use of the now available improvements in AAV vector technology. Thus, we compared rAAV2 which is the most commonly used AAV serotype in *ex vivo* and *in vivo* gene transfer applications with rAAV3 known for its tropism for hematopoietic cells and rAAV5 which is the most divergent serotype for their applicability in CD34⁺ cell transduction (Bantel-Schaal et al., 1999; Chiorini et al., 1999; Handa et al., 2000; Lu, 2004). All three serotypes were produced as pseudotypes with single-stranded (ss) or self-complementary (sc) vector genomes by a helper virus-free packaging method to exclude any assistance of helper virus particles in transduction and to determine the role of vector genome conformation (McCarty, Monahan, and Samulski, 2001; Xiao, Li, and Samulski, 1998) (7.3.6.1, 7.3.6.2). As the various serotypes differ in their tropism, we did not use transducing titers for normalization of the vector preparations, but equal vector genomes per cell (GOI). The genomic titers of all rAAV vector preparations were determined by quantitative PCR and ranged between 6.6×10^{10} (rAAV5scGFP) and 1.1×10^{12} (rAAV2ssGFP) genomic particles/ml as shown in Table 3, thus revealing that all vectors could be produced with a reasonable efficiency (7.3.6.4) (Theiss et al., 2003).

| | rAAV2 | | rAAV3 | rAAV5 | |
|-------|----------------------|----------------------|----------------------|----------------------|----------------------|
| | 1. preparation | 2. preparation | 1. preparation | 1. preparation | 2. preparation |
| ssGFP | 4.9×10^{11} | 1.1×10^{12} | 8.6×10^{11} | 3.1×10^{11} | |
| scGFP | 5.3×10^{11} | 2.0×10^{11} | 1.7×10^{11} | 6.7×10^{10} | 6.6×10^{10} |

Table 3: Genomic titers of rAAV vector preparations. The serotypes rAAV2, rAAV3 and rAAV5 encoding either for single-stranded (ss) or self-complementary (sc) GFP have been produced as described in chapter 7.3.6.1 and 7.3.6.2. Genomic titers were determined by qPCR and are indicated as vector genomes per ml.

CD34⁺ cells were isolated out of cord blood by separating peripheral mononuclear cells by Ficoll-density gradient centrifugation and subsequent magnetic cell sorting for CD34 (Direct CD34 Progenitor Cell Isolation Kit, Miltenyi Biotech) as described in 7.3.7.1. After pre-expansion of the cells for 2 to 4 days in serum-free culture medium (Stem Span, CellSystems) containing Flt3-ligand (100 ng/ml), SCF (100 ng/ml), IL-3 (20 ng/ml) and IL-6 (20 ng/ml), cells were transduced with a GOI of 10^5 of rAAV2, rAAV3 or rAAV5 coding for GFP in a single-stranded or self-complementary vector genome conformation. Cells were washed 3 h p.i. cultured for 3 additional days and assayed for transgene expression by flow cytometry. Results are shown in Figure 30 as mean + standard error of the mean (SEM) of 3 (rAAV3, rAAV5) and 8 (rAAV2) experiments of different donors.

As depicted in Figure 30, neither transduction with rAAV3ssGFP nor rAAV5ssGFP, both encoding for GFP in a single-stranded vector genome conformation, resulted in a detectable amount of transgene expression, although vector genomes were detected in these CD34⁺ cells by qPCR experiments as shown in Figure 31. AAV2ssGFP transduction resulted in GFP expression, but only a marginal transduction efficiency of 8 ± 2.5 % (mean \pm SEM) was achieved. In contrast, use of self-complementary instead of the naturally occurring single-stranded vector genome conformation resulted in a significant increase in transduction efficiency for all three serotypes. Also in this case rAAV2 was the most efficient serotype reaching a transduction efficiency of 57.2 ± 2.6 %. Thus, second-strand synthesis is a limiting step in rAAV-mediated transduction of CD34⁺ cells.



| | single-stranded vector genomes | self-complementary vector genomes |
|-------|--------------------------------|-----------------------------------|
| rAAV2 | 8.0 ± 2.5 | 57.2 ± 5.2 |
| rAAV3 | 0 ± 0.1 | 4.8 ± 2.2 |
| rAAV5 | 0 ± 0.1 | 7.4 ± 2.2 |

Figure 30: Transduction efficiencies of CD34⁺ cells by rAAV2, rAAV3 and rAAV5 coding for GFP in single-stranded (ss) or self-complementary (sc) vector genome conformation. Pre-expanded CD34⁺ cells were transduced with a GOI of 10⁵. 3 h p.i. medium was exchanged and 3 d p.i. 2x10⁴ cells were analyzed by flow cytometry. Bar graph shows the mean of 3 (rAAV3 and rAAV5) and 8 (rAAV2) independent experiments with cells obtained from umbilical cord blood of different donors. The data in the enclosed table are given as mean percentage of positive cells ± standard error of the mean (SEM).

In order to investigate if the differential transgene expression observed for the 3 serotypes was due to potential limitations in cell entry, we determined the amount of transgene DNA isolated from rAAV-treated CD34⁺ cells. Therefore, cells were thawed, expanded and transduced as described above with a GOI of 10⁴ of rAAV2, 3 or 5 encoding for ssGFP or scGFP. Cells were washed and extensively trypsinized to remove non-internalized vectors 3 h p.i.. The extracted DNA samples were analyzed by qPCR for GFP and normalized to human GAPDH gene. For all samples the crossing points for GAPDH showed a comparable value ranging from 23.4 to 24.4 cycles thus confirming that equal DNA amounts have been analyzed. Results of 2 independent experiments are shown in Figure 31 as normalized copy number + standard deviation. Melting curve analyses revealed

one specific PCR amplification product for all rAAV-treated cell samples, while non-transduced controls showed only unspecific products. Therefore, only values obtained for the rAAV-treated cell samples are shown in Figure 31.

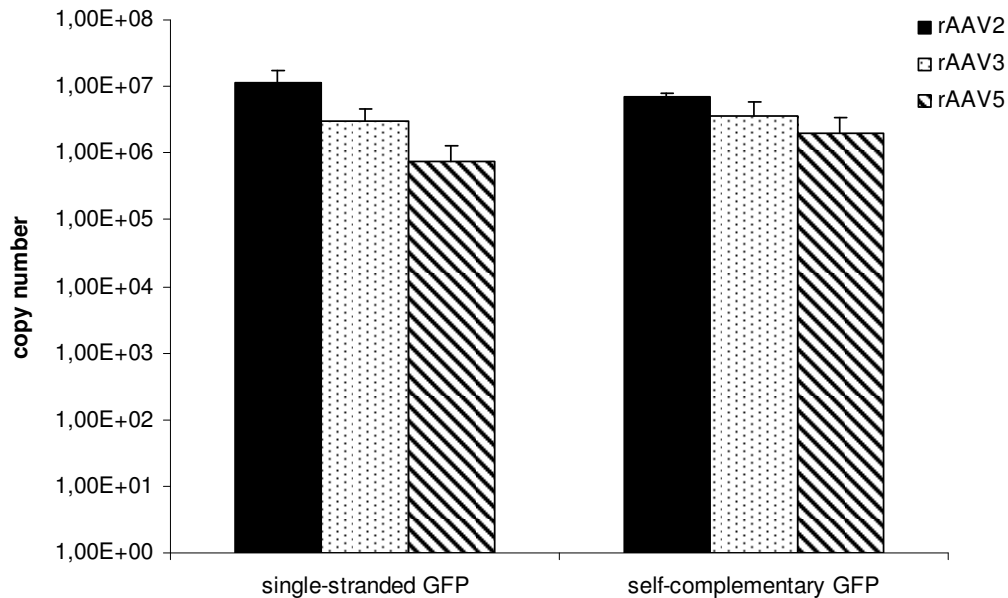


Figure 31: Quantitative analysis of transgene DNA isolated from CD34⁺ cells 3 h p.i. with the indicated vectors. Thawed cells were pre-expanded for 3 d and transduced with a GOI of 10^4 of rAAV2, 3 or 5 encoding ssGFP or scGFP. 3 h p.i., cells were washed and extensively trypsinized and total DNA was extracted. Quantitative PCR analyses were performed for GFP and normalized to human GAPDH. Results are shown as copy number + standard deviation.

As depicted in Figure 31, serotype 2 was most efficient in entering CD34⁺ cells. Entry was independent of the genome conformation ($1.1 \times 10^7 \pm 6.8 \times 10^6$ copies for ssGFP and $7.1 \times 10^6 \pm 6.9 \times 10^5$ copies for scGFP), as expected. The value for rAAV2scGFP was only 0.6-fold lower than for the rAAV2ssGFP. Also for rAAV3 which was the second efficient serotype in entry, the values obtained for scGFP ($3.0 \times 10^6 \pm 1.5 \times 10^6$ copies) were only 1.2-fold higher than for ssGFP vectors ($3.7 \times 10^6 \pm 2.1 \times 10^6$ copies). Serotype 5 entered the cell with the lowest efficiency. In comparison with rAAV5ssGFP ($7.7 \times 10^5 \pm 5.3 \times 10^5$ copies), 2.6-fold more vector genomes were detected after transduction with rAAV5scGFP ($2 \times 10^6 \pm 1.3 \times 10^6$ copies). These observations reveal that all serotypes are in principle able to enter CD34⁺ cells, however, they differ in their efficiency. For rAAV2ssGFP, e.g. 3.7 and 14.4-fold higher amounts of vector genomes were intracellularly detected than for

rAAV3 and rAAV5, respectively. Thus, the higher transduction efficiency of rAAV2 compared to rAAV3 and rAAV5 might be explained at least in part by variations in cell entry efficiency.

4.2.2 Loss of transgene expression during prolonged cultivation times

A transduction efficiency of almost 60 % was commonly reached in human CD34⁺ cells 3 d p.i. with rAAV2scGFP (GOI 10⁵). At least for certain applications stable gene expression would be desirable, e.g. for expression of anti-thrombotic or cytoprotective factors for maintenance and survival of colonized vascular prosthetic grafts and cardiac valves. Thus, we determined if expression level persisted. Briefly, CD34⁺ cells were either freshly isolated or thawed (CellSystems), pre-expanded and transduced with rAAV2 coding either for ssGFP or scGFP. Cells were washed 3 h p.i., further cultivated and analyzed for GFP-expression by FACS analyses 3 d p.i.. One week thereafter, flow cytometric analyses were repeated. Results are summarized in Figure 32 as mean percentages of GFP expressing cells + standard error of the mean of 5 independent experiments.

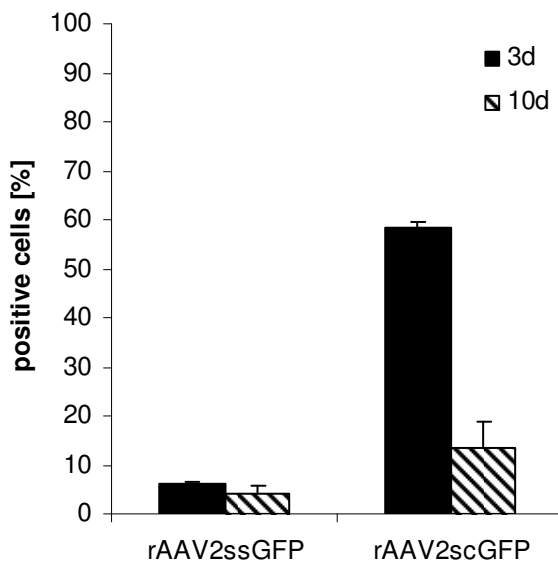


Figure 32: Transgene expression in CD34⁺ cells 3 and 10 d p.i.. Pre-expanded fresh or thawed CD34⁺ cells were transduced with a GOI of 10⁵ of rAAV2ssGFP or rAAV2scGFP and 2x10⁴ cells were analyzed for GFP expression 3 and 10 d after transduction. Shown are the mean percentages of transgene expressing cells + standard error of the mean of 5 independent experiments.

Comparably to the values obtained in 4.2.1, transduction with rAAV2scGFP resulted in 58.5 ± 1.3 % with rAAV2ssGFP in 5.9 ± 0.5 % transgene-expressing cells 3 d p.i.. However, GFP expression declined strongly in the case of rAAV2scGFP treated cells (13.3 ± 5.3 %) when the cells were further cultivated. The already low level of transgene expression by rAAV2ssGFP after 3 d changed only marginally (4.1 ± 1.7 %) within 7 days of further cultivation.

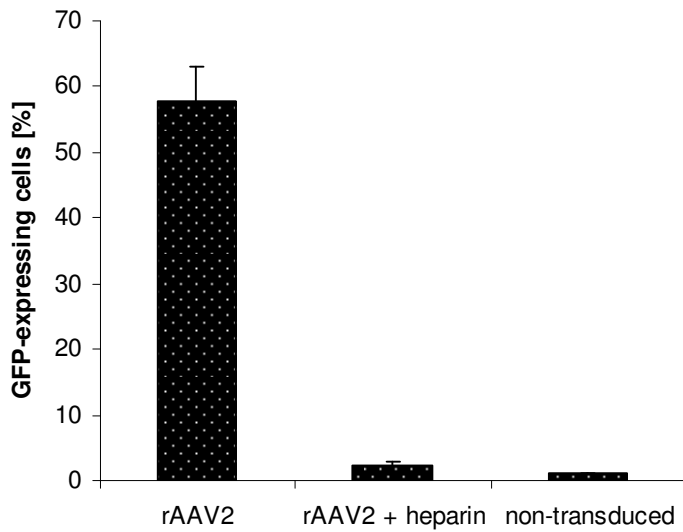
4.2.3 Heparin inhibits transduction with rAAV2 approving HSPG as primary receptor

Heparan sulfate proteoglycan (HSPG) has been described as primary receptor for AAV2 (Summerford and Samulski, 1998). To investigate if HSPG is also involved in rAAV2-mediated CD34⁺ cell transduction, competition studies using heparin, a soluble analogue of HSPG, were performed (Figure 33). In addition, this experiment allows to distinguish between vector and pseudotransduction since addition of heparin is unable to impair GFP protein transduction.

Therefore, CD34⁺ cells were freshly isolated from cord blood. Peripheral mononuclear cells were separated by Ficoll-density gradient centrifugation and sorted for CD34 by MACS (Direct CD34 Progenitor Cell Isolation Kit, Miltenyi Biotech) as described more detailed in 7.3.7.1. After pre-expansion for 2 to 4 d, cells were transduced with a GOI of 10^5 rAAV2scGFP in presence or absence of 971 units of heparin. Cells were washed 3 h p.i.. Transduction efficiency was analyzed 3 d p.i. by flow cytometry (Figure 33 A) and fluorescence microscopy (Figure 33 B). Results of 3 independent experiments obtained with cells of different donors are shown as mean percentage of GFP-expressing cells + standard error of the mean (mean \pm SEM).

Comparable to results presented in 4.2.1, transduction efficiencies over 50 % (56.7 ± 5.3 %) were obtained with rAAV2scGFP (Figure 33 A). In contrast, transduction was almost completely abolished by adding heparin (1.2 ± 0.7 %; $P < 0.0003$) (Figure 33 A). In line with these results, fluorescence microscopy revealed GFP-expressing cells when only rAAV2 was applied while no GFP expression was detected when rAAV2 transductions were performed in presence of heparin and in non-transduced controls (Figure 33 B). These results show clearly that HSPG acts as a primary receptor for rAAV2 transduction. Moreover, pseudotransduction in CD34⁺ cells can be excluded.

A



B

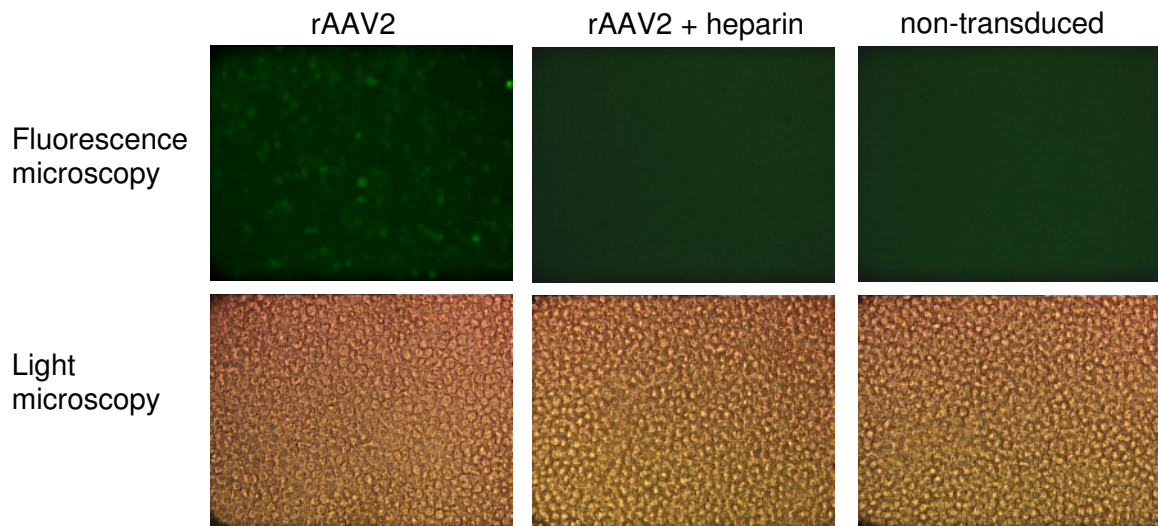


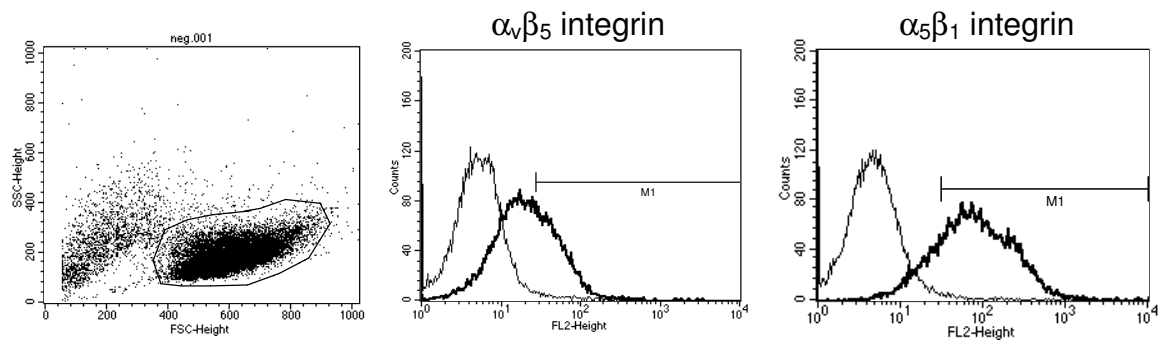
Figure 33: Inhibition of rAAV2scGFP-mediated transduction by heparin. 971 units of heparin (Sigma) were applied to 8×10^4 pre-expanded CD34⁺ cells, followed by 10^5 genomic particles of rAAV2scGFP per cell. In parallel, cells were transduced with the same amount of vector in the absence of heparin. Cells were incubated for 3 h at 37 °C and 5 % CO₂, followed by a washing step. 3 d p.i. 2×10^4 cells were analyzed by flow cytometry (A) and fluorescence microscopy (B). Results presented in (A) are the mean of 3 independent experiments using CD34⁺ cells isolated from umbilical cord blood from 3 different donors. Data are shown as mean percentage of GFP-expressing cells, error bars as standard error of the mean (SEM).

4.2.4 Transduction efficiency correlated with the availability of $\alpha_5\beta_1$ integrins

Thus far, in addition to the primary receptor HSPG, 5 cellular receptors have been described for AAV2 (Akache et al., 2006; Asokan et al., 2006; Kashiwakura et al., 2005; Qing et al., 1999; Summerford, Bartlett, and Samulski, 1999; Summerford and Samulski, 1998). Fibroblast growth factor receptor (FGFR) or hepatocyte growth factor receptor (HGFR, c-met) and possibly laminin receptor may enhance AAV2 binding to the cell surface. The subsequent interaction with the coreceptor $\alpha_v\beta_5$ integrin induces endocytosis and most likely a rearrangement of the cytoskeleton, thus enabling AAV to enter the cell and be trafficked towards the nuclear area (Sanlioglu et al., 2000). Recently, $\alpha_5\beta_1$, a second integrin molecule, functioning as an alternative AAV coreceptor has been identified (Asokan et al., 2006). Therefore, we determined the surface expression level of $\alpha_v\beta_5$ and $\alpha_5\beta_1$ on CD34⁺ cells isolated from human cord blood (freshly isolated (CB1) or cells by CellSystems (CB2)) or human bone marrow (kindly provided by N. Fein and H. Abken, University Hospital of Cologne) by flow cytometry at the day of transduction (after 2 to 4 d of expansion) to assess which of these two integrins is likely available to allow AAV2 entry into CD34⁺ cells. In addition, these cells were transduced with a GOI of 10⁵ rAAV2scGFP, washed 3 h later and determined for transgene expression at 3 d p.i. by flow cytometry.

As shown in Figure 34 A, independent of the source of CD34⁺ cells, transduction efficiencies above 50 % were obtained. Also irrespective of the source, high expression of $\alpha_5\beta_1$ integrin was observed at the day of transduction, whereas the expression of $\alpha_v\beta_5$ was strongly depending on the donor and ranged between 0.5 % and 59.5 %. Representative FACS plots are depicted in Figure 34 A, demonstrating the shift of CD34⁺ cells stained either with anti- $\alpha_5\beta_1$ or anti- $\alpha_v\beta_5$ antibody and secondary antibody (PE-labeled) compared to the isotype control. This result indicates that transduction efficiency most obviously correlated with the availability of $\alpha_5\beta_1$ integrin.

A



B

| source of CD34 ⁺ cells | $\alpha_v\beta_5$ [%] | $\alpha_5\beta_1$ [%] | GFP expression [%] |
|-----------------------------------|-----------------------|-----------------------|--------------------|
| CB1 | 59.5 | n.d. | 58.0 |
| | 43.8 | n.d. | 66.5 |
| | 39.5 | n.d. | 65.0 |
| CB2 | 33.4 | 78.8 | 62.7 |
| | 2.4 | 91.8 | 55.2 |
| | 22.8 | 96.2 | 60.3 |
| | 0.5 | 82.8 | 68.8 |
| BM | 3.5 | 84.4 | 52.0 |

Figure 34: Correlation between availability of $\alpha_v\beta_5$ and $\alpha_5\beta_1$ integrins and transduction efficiency. (A) Representative FACS plots (cells stained with 1st and 2nd antibody (bold lines), isotype control (normal lines) (B) Percentages of $\alpha_v\beta_5$ and $\alpha_5\beta_1$ integrin (primary antibodies MAB1961 and MAB1999 by Chemicon) expressing cells within CD34⁺ cell preparations from 3 different sources as assessed by flow cytometry. Subsequently, these cells were transduced with a GOI of 10⁵ of rAAV2scGFP and transgene expression was determined by FACS analysis 3 d p.i. Three different sources were used: Freshly isolated cord blood CD34⁺ cells (CB1) from 3 different donors, 4 different samples of cord blood CD34⁺ cells purchased from CellSystems (CB2), and one sample of CD34⁺ cells isolated from bone marrow (BM); n.d.= not determined.

Moreover, we determined integrin levels on freshly thawed cells which have been reported to be not transducible (Nathwani et al., 2000). According to Hart and colleagues, $\alpha_5\beta_1$ integrin expression becomes upregulated in CD34⁺ cells by pre-expansion of CD34⁺ cells in SCF-containing medium (Hart et al., 2004). In line with this, FACS analyses of freshly thawed CD34⁺ cells (prior to expansion) showed no

expression of $\alpha_v\beta_5$ and a maximum of 3.3 % $\alpha_5\beta_1$ integrins, while more than 77 % $\alpha_5\beta_1$ integrin and less than 2 % $\alpha_v\beta_5$ integrin-expressing cells were detectable at 3 d after expansion (Table 4).

| w/o pre-expansion | | pre-expanded | |
|-----------------------|-----------------------|-----------------------|-----------------------|
| $\alpha_v\beta_5$ [%] | $\alpha_5\beta_1$ [%] | $\alpha_v\beta_5$ [%] | $\alpha_5\beta_1$ [%] |
| 0 | 3.3 | 0.5 | 82.8 |
| 0 | 0 | 1.6 | 77.4 |

Table 4: Amount of CD34⁺ cells displaying integrins before and after pre-expansion. CD34⁺ cells were freshly thawed and directly stained for $\alpha_v\beta_5$ and $\alpha_5\beta_1$ integrins (w/o pre-expansion). The amount of integrins was determined by FACS analyses. The procedure was repeated with pre-expanded cells after 3 d. Shown are the results of 2 independent experiments with pooled donors.

We further aimed to support the assumption that $\alpha_5\beta_1$ integrin serves as coreceptor in CD34⁺ cell transduction. Wild type AAV2 contains a NGR motif associated with $\alpha_5\beta_1$ integrin binding (Asokan et al., 2006). Therefore, we used an AAV2 mutant described to be deficient for $\alpha_5\beta_1$ integrin binding due to an arginine to alanine substitution at the amino acid position 513 in the respective NGR motif (NGR R513A) (Asokan et al., 2006). Assuming that rAAV2 transduction relies on $\alpha_5\beta_1$ integrins, CD34⁺ cell transduction by a non- $\alpha_5\beta_1$ binding mutant should be significantly impaired. Thus, CD34⁺ cells were analyzed for the amount of both integrins at the time of vector administration by flow cytometry (Figure 35 B). $\alpha_v\beta_5$ integrins were not detectable on the pre-expanded cells in this experiment. In contrast, more than 90 % of the cells displayed $\alpha_5\beta_1$ integrins. Hence, only $\alpha_5\beta_1$ integrins were available to potentially assist vector entry and results on transduction studies can directly be correlated with this coreceptor. The pre-expanded CD34⁺ cells (CellSystems) were transduced with a GOI of 10⁴ of rAAV2 or NGR R513A encoding scGFP. Washing and trypsinization of the cells 3 h p.i. should eliminate non-internalized vectors. Cells were cultivated for 3 further days before transgene expression was determined by FACS analyses. As depicted in Figure 35 A, the amount of GFP-expressing cells after transduction with NGR R513A (4.6 ± 0.4 %) was 5.6 times lower than with rAAV2 (25.9 ± 3.3 %). This result strongly supports our assumption that $\alpha_5\beta_1$ and not $\alpha_v\beta_5$ integrins mediate cell entry of rAAV2 into CD34⁺ cells.

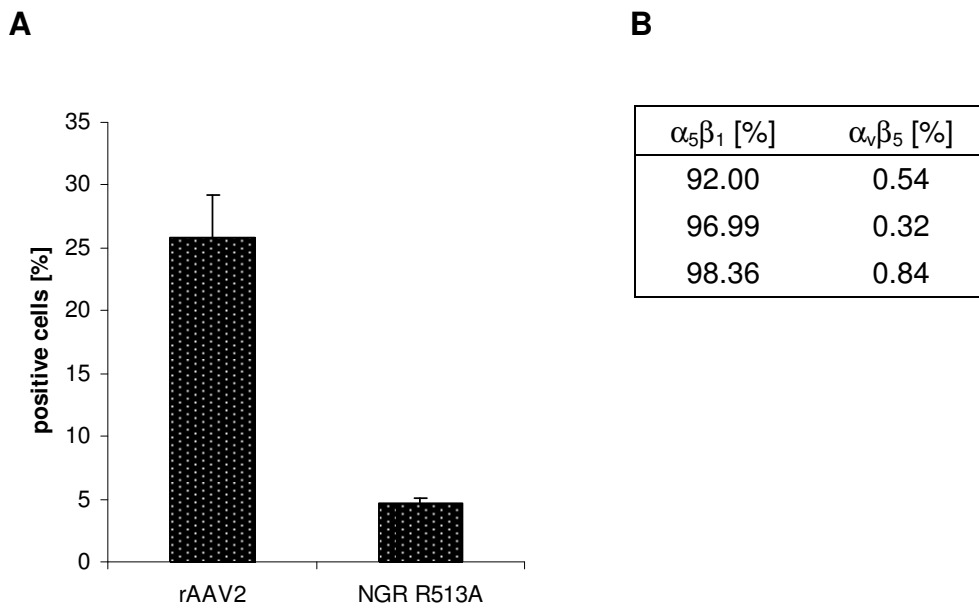


Figure 35: Transgene expression in CD34⁺ cells transduced with rAAV2 and NGR R513A. CD34⁺ cells (CellSystems) were thawed and pre-expanded for 3 d. The amount of integrins was determined by FACS analyses (B) at the day of transduction with a GOI of 10⁴ of either rAAV2 or NGR R513A encoding scGFP. 3 h p.i., cells were washed, extensively trypsinized to remove non-internalized vectors and further cultivated. Flow cytometric analyses for GFP expression were performed 3 d p.i. (A). Shown are the means + SEM of 3 independent experiments.

4.2.5 Enhancement of transgene expression using retinoic acid and Trichostatin A

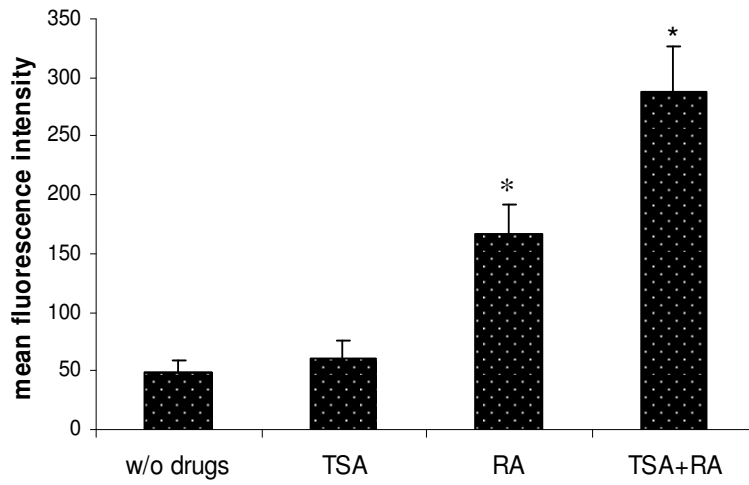
Various attempts have been made to increase transgene expression after viral or non-viral gene transfer. A widely used promoter which also found application in our study is derived from the immediate-early region of cytomegalovirus (CMV) gene. The CMV promoter induces high transgene expression levels in various tissues and cells likely due to a number of *cis*-regulatory elements mediating to which binding of transcription factors like NF- κ B, CREB, AP-1 and retinoic acid receptor (RARs, RXRs) can occur (Angulo et al., 1996; Boshart et al., 1985; Ghazal et al., 1992; Guo et al., 1996; Loser et al., 1998; Rideg et al., 1994; Rotondaro, Mele, and Rovera, 1996; Wade, Klucher, and Spector, 1992). The latter is of special interest, since addition of retinoic acid was shown to enhance transcription from CMV promoters, e.g. in endothelial cells after adenoviral transgene delivery (Angulo et al., 1996; Gaetano et al., 2000). Despite the high transcriptional activity

that is normally achieved with CMV promoters at early times after transduction with viral vectors, promoter silencing after a longer period represents a major hurdle that impairs a long lasting transgene expression *in vivo*, *in vitro* and in stem cells (Xia et al., 2007). Recently, the histone-deacetylase inhibitors (HDACi) Trichostatin A (TSA) and FR901228 have been shown to enhance adenovirus-mediated transgene expression in hematopoietic and endothelial cells (Gaetano et al., 2000; Kitazono et al., 2002). Thus, we intended to determine the effect of single or combined treatment with TSA and RA on AAV-mediated transgene expression in CD34⁺ cells. CD34⁺ cells (CellSystems) were thawed and pre-expanded as described in 7.3.7.2.

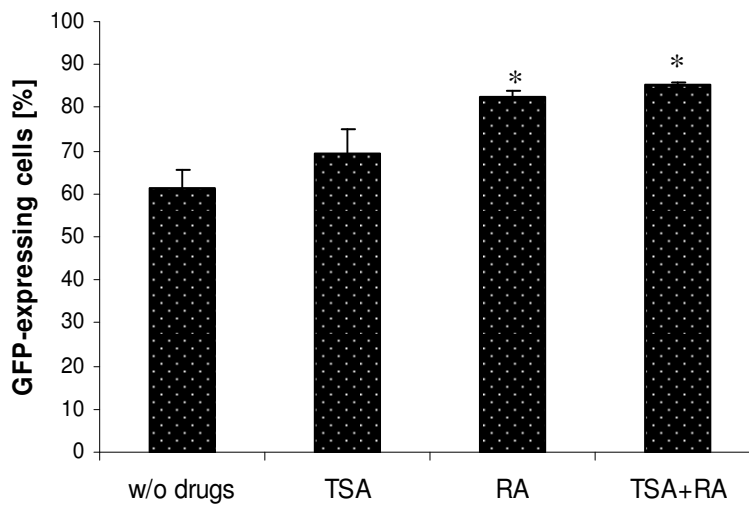
In a first series of experiments, we incubated pre-expanded CD34⁺ cells with rAAV2scGFP at a GOI of 10⁵ in the presence of different RA (5-5000 nM) and/or TSA (3.125-500 ng/ml) concentrations to determine the most suited amount of these drugs for our experiments. Cells were washed 3 h p.i., cultured for 3 d in medium supplemented with the respective drug and then analyzed by flow cytometry (data not shown). These analyses revealed an optimal concentration of 10 μM for RA and of 25 ng/ml for TSA.

Next, we incubated pre-expanded CD34⁺ cells with rAAV2scGFP at a GOI of 10⁵ of either drugs, alone or in combination, and determined the percentage of GFP-expressing cells as well as the mean fluorescence intensity (MFI) as a value for transduction efficiency and transcriptional activity, respectively, at 3 d p.i. by flow cytometry (Figure 36). On average, a 3.4-fold (mean ± 0.2 SEM; P=0.006) increase in the MFI was observed when RA was administered, while addition of TSA resulted in 1.3-fold increased MFI (mean ± 0.3 SEM; P<0.25). Further, when RA and TSA were added in combination, the highest increase in the MFI value (5.9-fold ± 1.1; P=0.002) was observed, thus revealing a synergistic effect of the two drugs. As a consequence of the increased transcriptional activity, more CD34⁺ cells reached a high transgene expression level. Thus, by adding these two transcriptionally active drugs, the amount of cells with a reasonable transgene expression could be increased from 61.4 ± 4 % to 85.6 ± 0.3 % (mean ± SEM; n=3; P<0.002) (Figure 36).

A



B



C

| | transgene expression GFP-expressing cells \pm SEM [%] | mean fluorescence intensity MFI \pm SEM |
|-----------|--|--|
| w/o drugs | 61.4 \pm 4.0 | 48.8 \pm 9.7 |
| TSA | 69.5 \pm 5.4 | 61.4 \pm 13.8 |
| RA | 82.7 \pm 1.0 | 166.8 \pm 25.3 |
| TSA+RA | 85.6 \pm 0.3 | 288.2 \pm 39.1 |

Figure 36: Enhancement of rAAV2scGFP-mediated transgene expression by Trichostatin A (TSA) and retinoic acid (RA). 8×10^4 pre-expanded CD34⁺ cells (CellSystems) were treated with either 25

ng/ml TSA (Sigma) and/or 10 μ M RA (Sigma) at the time of transduction with rAAV2scGFP. In parallel, cells were transduced with the same amount of vector in the absence of the drugs (only solvent). 3 h p.i. cells were washed and fresh medium containing the drugs or solvent without drugs as control were added. 3 d p.i. transgene expression was measured of 2×10^4 cells by cell cytometry. (A) Bar graph indicates the mean fluorescence intensity as detected by FACS analysis; (B) Bar graph showing the increase in the percentage of GFP-expressing cells in the presence of the two drugs. (n=3; error bars= SEM; *= $P \leq 0.006$). (C) Indicated is the correlation between increase in the percentage of GFP expressing cells and the enhancement of MFI in the four tested conditions.

4.2.6 CD34⁺ cells are able to take up Dil-AcLDL after endothelial differentiation assay

CD34⁺ cells are also known as endothelial progenitor cells defined by their ability to differentiate into endothelial cells. Therefore, we evaluated the potential of CD34⁺ cells to take up acetylated low-density lipoproteins (Dil-AcLDL) as endothelial cell marker after pre-expansion, rAAV2 transduction and subsequent incubation in endothelial differentiation medium. Cells were seeded onto fibronectin-coated plates to enable attachment. For coating, the plates were incubated with 10 μ g/ml fibronectin in PBS over night at 4 $^{\circ}$ C. Subsequently solution was taken off and plates were dried.

CD34⁺ cells (CellSystems) were thawed, pre-expanded for 2 to 4 d and transduced with a GOI of 10^5 rAAV2 encoding either single-stranded or self-complementary GFP vector genomes. Transduction efficiency was determined by FACS analysis 3 d p.i.. At the same time, these cells were seeded onto fibronectin-coated plates in endothelial basal medium (EBM-2 + supplements) including 20 % FCS and 50 ng/ μ l VEGF for induction of endothelial differentiation. Every 3 d, half of the medium was exchanged carefully. 10 d after initiation of differentiation, adherent cells showed a spindle-shaped morphology and were incubated with 1 μ g/ml Dil-AcLDL diluted in medium for 4 h at 37 $^{\circ}$ C. Cells were fixed with 3 % paraformaldehyde and analyzed for Dil-AcLDL uptake by fluorescence microscopy (200x magnification; Zeiss Axiovert S100). Representative images of 3 independent experiments are shown in Figure 37. Red fluorescence could be detected in nearly all of the non-transduced and previously transduced cells indicating differentiation into endothelial cells. These results

indicate that the rAAV transduction process did not interfere with differentiation and endothelial cell-specific Dil-AcLDL uptake.

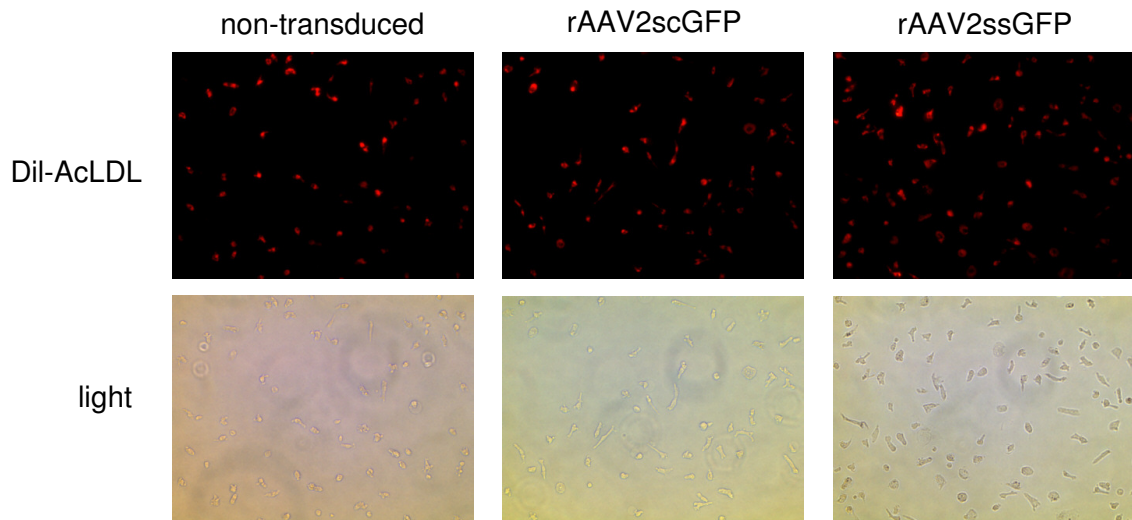


Figure 37: Dil-AcLDL uptake of CD34⁺ cells after 10 d of incubation in endothelial differentiation medium. CD34⁺ cells were pre-expanded and transduced with a GOI of 10⁵ of rAAV2 coding for single-stranded (ss) or self-complementary (sc) GFP. 3 d p.i., cells were seeded onto fibronectin-coated plates and cultivated in endothelial differentiation medium for 10 d before incubation in 1 µg/ml Dil-AcLDL containing medium for 4 h. Cells were fixed and analyzed by fluorescence microscopy (200x magnification; Zeiss Axiovert S100). Shown are representative images of 3 independent experiments for endothelial differentiation.

For later applications, differentiation of transduced endothelial progenitor cells into endothelial cells is required. Therefore, we investigated the potential correlation between transduced cells and cells which have taken up Dil-AcLDL. As GFP fluorescence was not detectable after 10 d we analyzed the adherent cells for presence of vector genomes. After intense washing, the adherent cells were trypsinized and DNA was extracted using the DNeasy Blood & Tissue Kit (Qiagen). 100 ng DNA of the samples were analyzed by qPCR for the transgene GFP and normalized to the housekeeping gene GAPDH. Mean values for GFP DNA of 3 independent experiments are depicted in Figure 38 and shown as copy number per 50 ng DNA + standard deviation. The background level for GFP DNA in the non-transduced control was $1.1 \times 10^3 + 1.5 \times 10^3$ copies/50 ng DNA, but this value was based on amplification of unspecific and specific products as revealed by melting curve analyses. Therefore, the background level is supposed to be much lower and is depicted as striped bar in Figure 38. In contrast, DNA samples

Results

from transduced cells showed only the GFP-specific PCR product in the respective melting curve analyses.

Interestingly, the amount of transgene after transduction with rAAV2ssGFP ($5.9 \times 10^5 + 5 \times 10^5$ copies/50 ng DNA) equalled the level of rAAV2scGFP transduction ($6.1 \times 10^5 + 4.2 \times 10^5$ copies/50 ng DNA) (GOI 10^5). Both values exceeded the background signal more than 500 fold which clearly indicates presence of vector genomes within the DNA of the adherent cells. As nearly all cells were positive for Dil-AcLDL uptake as shown in Figure 37, this result strongly suggests that transduced CD34⁺ cells maintained their ability to differentiate into endothelial cells.

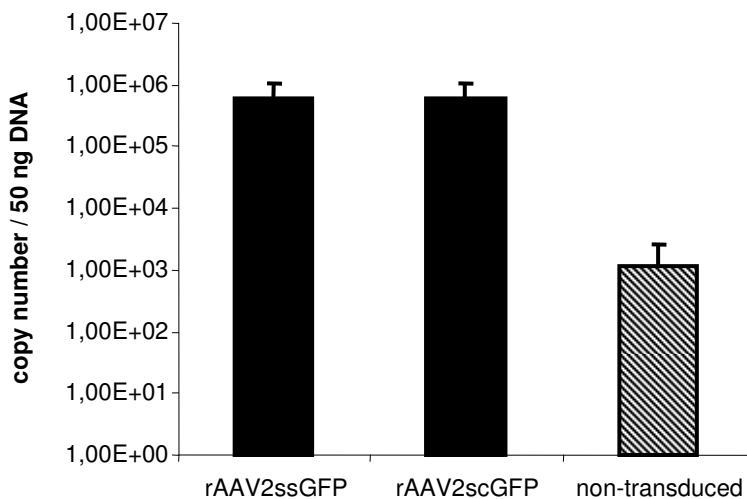


Figure 38: Level of transgene DNA in transduced and non-transduced cells after endothelial differentiation assay. CD34⁺ cells were pre-expanded and transduced with rAAV2 coding either for ssGFP or scGFP with a GOI of 10^5 . 3 d after, cells were seeded onto fibronectin-coated plates in endothelial differentiation medium und cultivated for 10 d. After repeated washing, DNA was extracted from the adherent cells and 100 ng were analyzed in qPCR. Values were normalized to GAPDH and shown as GFP copy numbers per 50 ng DNA + standard deviation. In contrast to the transduced samples, melting curve analyses of the non-transduced samples revealed also other PCR products beside GFP and are therefore depicted as striped bar. Summarized are results from 3 independent experiments.

4.3 Further applications of serotypes

4.3.1 Serotype 2 is superior in transduction of primary melanoma cells

As part of a publication on tumor cell directed gene transfer, primary melanoma cells from three different patients (MediGene, Martinsried) were transduced with the serotypes 1 to 5 to compare the transduction profiles of primary tumor cells and tumor cell lines (Hacker et al., 2005). Tumor cell lines have been grown in long-term culture and might therefore show differences. Primary melanoma cells were transduced with a GOI of 1×10^4 rAAV1 to rAAV5 encoding the transgene in the commonly used single-stranded vector genome conformation (ssGFP). Since rAAV2 was the most efficient serotype on the melanoma cell line MV3 primary cells were additionally transduced with a lower GOI of 1×10^3 for this serotype. Transgene expression was determined 48 h p.i. by FACS analysis.

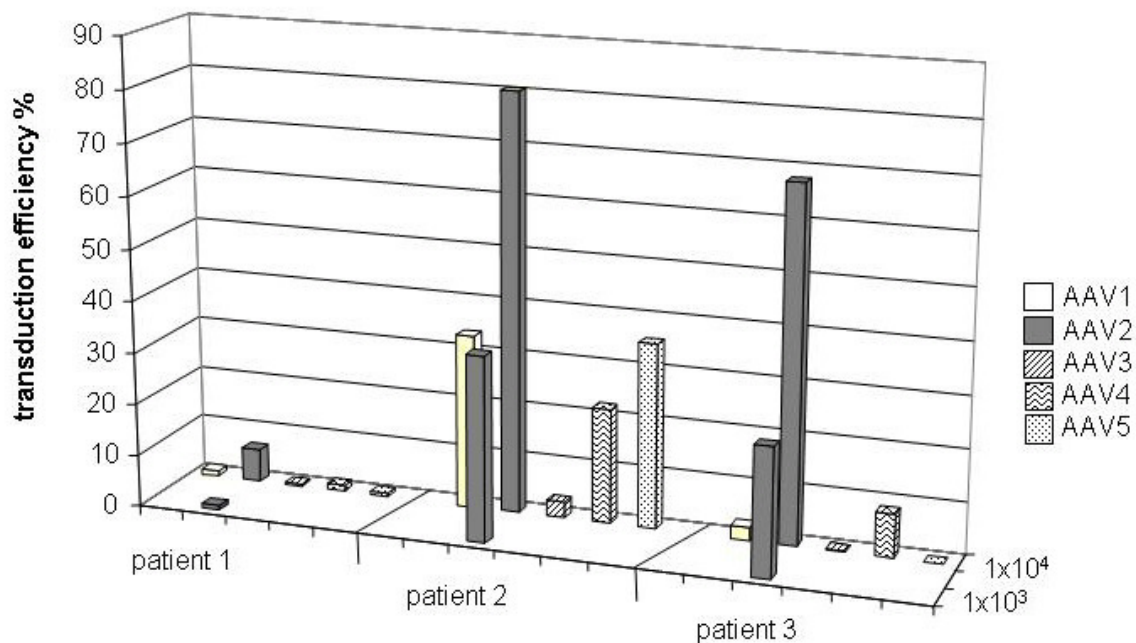


Figure 39: rAAV-mediated gene transfer in primary melanoma cells. Primary melanoma cells from 3 different patients were transduced with rAAV1 to rAAV5 at a GOI of 1×10^4 . Additionally, a transduction experiment was performed using rAAV2 at a GOI of 1×10^3 . 48 h later, the amount of GFP-expressing cells was determined by FACS analysis.

Although patient-specific variations in transduction efficiencies were observed, rAAV2 was superior in all cases compared to rAAV1, rAAV3 and rAAV5 (Figure 39). The level of transgene expression ranged from 6.4 % (patient 1) to 80.5 % (patient 2) at a GOI of 1×10^4 . Even at tenfold lower vector amounts reasonable transduction efficiencies of 35.6 % (patient 2) and 24.6 % (patient 3) were obtained with rAAV2ssGFP. Interestingly, for the other serotypes no unique order of transduction efficiencies could be observed; it was rather depended on the patient. Whereas tumor cells derived from patient 1 and 3 were nearly resistant to rAAV5 transduction, 35.6 % of the cells from patient 2 were GFP-positive. A comparable picture was obtained for rAAV1 transduction. In contrast, rAAV4 was revealed as second best serotype for transduction of melanoma cells derived from patient 3.

4.3.2 Serotype 2 is superior in transduction of primary porcine fibroblasts and HeLa cells

Besides porcine endothelial cells, primary porcine fibroblasts have been evaluated for their permissiveness of rAAV transduction. These cells are of special interest for somatic cell nuclear transfer in pigs, a procedure which is carried out by our cooperation partners in the Institute of Farm Animal Genetics, Mariensee (B. Petersen, H. Niemann) (Betthausen et al., 2000; Onishi et al., 2000). Transgenes are introduced into porcine fibroblasts which are then screened for the occurrence of stable integration events. These cells are fused to enucleated oocytes and transferred surgically into the foster mother. This technology greatly improved the generation of transgenic animals, however, the efficiency (born piglet/transferred embryos) is still low. The ability of wild-type AAV2 to integrate site-specifically could be favorable for this application as it minimizes the risk of deleterious insertions.

First, we assessed the efficiency of fibroblast transduction by the serotypes 1 to 5. Therefore, primary porcine fibroblasts were transduced by 3 different vector concentrations of rAAV1 to 5 encoding for the transgene GFP in a single-stranded (ss) or self-complementary (sc) vector genome conformation, respectively. The amount of GFP-expressing cells was determined by flow cytometry 2 d p.i.. rAAV2 was the most efficient serotype in fibroblast transduction reaching 87.8 ± 5.3 % with ssGFP and 96.3 ± 1 % with scGFP at a GOI of 10^5 . Also serotype 5 was highly efficient with 75.7 ± 1.2 % (ssGFP) and 84.1 ± 11.6 % (scGFP) at the

highest vector concentration. The serotypes 1 and 3 showed similar transduction efficiencies of about 5 % for the ssGFP and of 30 % for scGFP vectors. AAV4 displayed the lowest transgene expression levels of 2.1 % (ssGFP) and 8 % (scGFP). At a GOI of 10^3 only rAAV2ssGFP (13.6 ± 4.9 %), rAAV2scGFP (64.9 ± 8.7 %) and rAAV5scGFP (22.9 ± 1.4 %) resulted in transduction levels above 0.5 %. Overall, transduction with scGFP vectors at GOI 10^4 and 10^5 resulted in higher transduction efficiencies compared to ssGFP vectors in all serotypes.

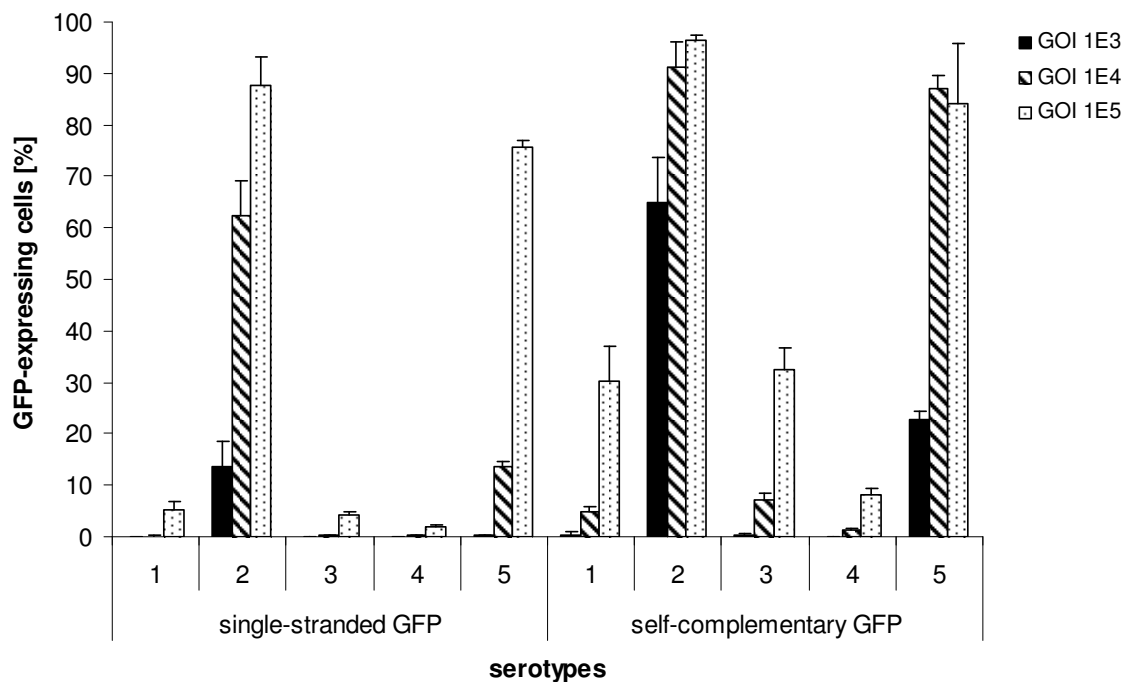


Figure 40: Transduction efficiencies of rAAV1 to rAAV5 on porcine fibroblasts. Primary porcine fibroblasts were transduced with 3 different GOIs (10^3 , 10^4 or 10^5) of the serotypes 1 to 5 coding either for single-stranded or self-complementary GFP. The amount of GFP-expressing cells was determined 2 d p.i. by FACS analysis. Results are shown as mean + standard deviation of 3 independent experiments.

The same experiments have been performed in parallel with the highly permissive tumor cell line HeLa to correlate these transduction efficiencies to those of porcine fibroblasts and other cell types. HeLa cells were transduced with rAAV1 to rAAV5 coding for ssGFP or scGFP at a GOI of 10^3 and 10^4 . The amount of GFP-expressing cells was determined 2 d p.i. by flow cytometry. Also in these cells, rAAV2 was the most efficient serotype whereas already 90 ± 1.8 % GFP-positive cells were detected at a GOI of 10^3 of the ssGFP vector. In the case of

rAAV2scGFP nearly every cell expressed GFP (about 99 %) (both GOIs). In contrast to porcine fibroblasts, rAAV3 was revealed as the second efficient serotype followed by rAAV1. At a GOI of 10^3 rAAV3ssGFP resulted in only 4.9 ± 4.2 % GFP-expressing cells while 55.4 ± 2 % were measured at a GOI of 10^4 . Regarding rAAV3scGFP these values were 48.3 ± 4.7 % and 93.9 ± 0.5 % for the respective vector amounts. Although transduction with rAAV1scGFP (GOI 10^4) resulted in comparable transgene expression levels (93.7 ± 1 %), 35.9 ± 3.5 % GFP-expressing cells were measured when tenfold less vectors were applied. As expected, transduction with rAAV1ssGFP showed a transduction efficiency of maximal 43.2 ± 5.1 %. In contrast to transduction of porcine fibroblasts, serotype 5 showed much lower transgene expression levels in HeLa cells with 17.9 ± 4 % (ssGFP) and 68.5 ± 7.7 % (scGFP) at GOI 10^4 . On the other hand, rAAV4 was the vector with the lowest efficiency among these 5 serotypes in transduction of both cell types. In HeLa cells, a GFP-expression of 11.9 ± 4.7 % (ssGFP) and 24.2 ± 6.7 % (scGFP) was determined for rAAV4 at a GOI of 10^4 .

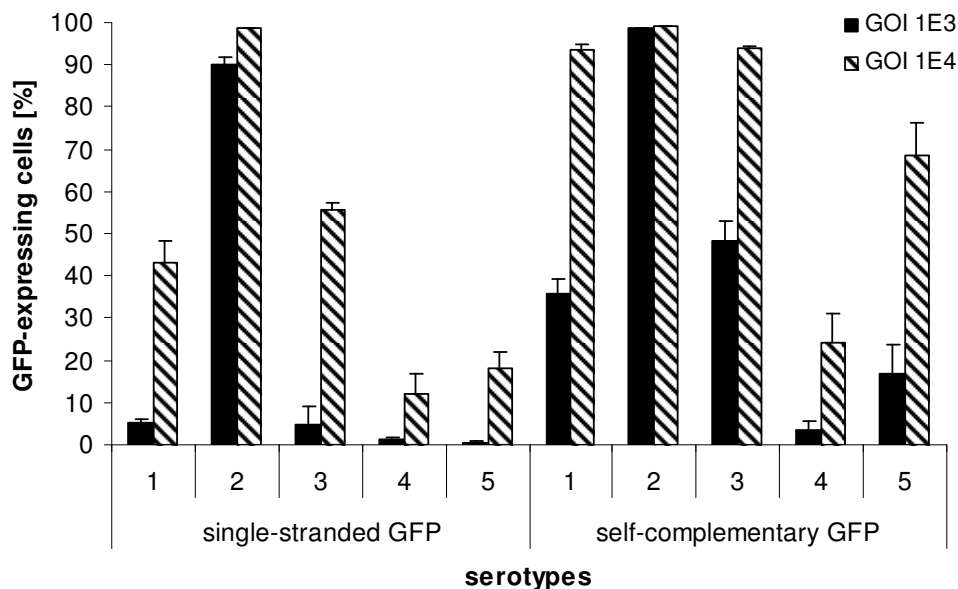


Figure 41: Transduction efficiencies of rAAV1 to rAAV5 on HeLa cells. HeLa cells were transduced with rAAV1 to rAAV5 encoding for ssGFP or scGFP at GOI 10^3 and 10^4 . Transgene expression levels were determined 2 d p.i. by flow cytometry. Results are shown as mean + standard deviation of 3 independent experiments.

4.4 Vector genomes are detected in spleen following intracerebral injection of rAAV2

Results summarized in this chapter are part of a publication in which rAAV2 was used to express single-chain antibodies against prion receptor intracerebrally in a scrapie mouse model (Zuber, et al., in press). This work was performed in collaboration with C. Zuber and S. Weiss (Gene Center, Munich).

As reported by our cooperation partners, the 37/67 kDa laminin receptor acts as a receptor for internalization of prions and is potentially involved in propagation and pathogenesis (Ludewigs et al., 2007; Vana et al., 2007; Zuber, Ludewigs, and Weiss, 2007). Its level has been shown to be increased in spleen and brain of scrapie infected hamsters and mice - the organs where the abnormal form of the prion protein is mainly found (Rieger et al., 1997). Therefore, different approaches have been done to block laminin receptor in order to reduce binding and internalization of the abnormal prion protein (Gauczynski et al., 2006; Leucht et al., 2003; Vana and Weiss, 2006). In this recent report, the efficiency of single-chain antibodies (scFv) (S18 and N3) against the laminin receptor has been investigated. S18 and N3 have been selected by phage display. An unrelated single-chain scFv (C9, a scFv directed against the HBV coat protein) served as control. These antibodies had prior been assayed for their protective effect *in vivo* by passive immunotransfer into scrapie infected mice (Zuber et al., 2008). AAV2 has been chosen as vector system to provide the transgene. The rAAV2 vectors (5×10^9 genomic particles) encoding S18, N3 or C9 were microinjected intracerebrally into the hippocampus followed by injection of scrapie homogenate into the same site 2 weeks after vector application. Expression of the scFv N3 in the brain was detected pointing to a successful transduction of neuronal cells. The second organ known to contain elevated amounts of prion protein is the spleen. Thus, spleens were analyzed for a potential therapeutic effect of single-chain antibodies with regard to proteinase K resistant prion protein level, which is associated with the infectious prion agent. Both groups having received therapeutic vectors (rAAV2-S18 and rAAV2-N3) showed lower prion protein levels than control animals after rAAV2-C9 injection (90 d p.i.). We analyzed 100 ng DNA of the spleen samples for the respective transgene (S18 and C9) and housekeeping gene (GAPDH) DNA by qPCR followed by agarose gel

electrophoresis of the PCR product (Figure 42). As depicted in Figure 42, we could demonstrate the presence of the therapeutic (S18, samples B and C) and control (C9, sample A) DNA in mouse spleens. An unrelated animal having received PBS was used as negative control (N). In the C9-PCR, the rAAV2-C9 injected animal (A) clearly showed a C9-specific band, whereas the unrelated control (N) was negative. Also in the S18-PCR, S18-specific DNA was detected in both rAAV2-S18 treated mice (B and C). An unspecific signal was amplified in sample C and the control N as shown in Figure 42. GAPDH levels were comparable between the samples confirming that equal DNA amounts have been analyzed.

These results point to a crossing of the blood-brain barrier of the vectors and subsequent transduction of the spleen.

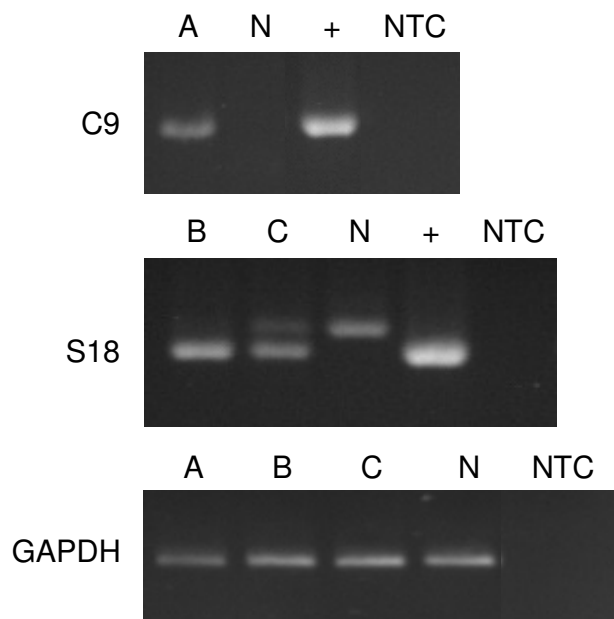


Figure 42: Detection of C9, S18 and GAPDH DNA within mouse spleens. 5×10^9 genomic particles of rAAV2-S18 or rAAV2-C9 were microinjected intracerebrally. 2 weeks after, scrapie homogenate was administered to the same site. 90 d p.i., spleen DNA was extracted and analyzed for GAPDH, S18 or C9 DNA, respectively. PCR products were analyzed by agarose gel electrophoresis. A, rAAV2-C9 injected mouse; B and C, rAAV2-S18 injected mice; N, unrelated mouse having received PBS; +, plasmid DNA containing the respective transgene as positive control; NTC, non-template control.

5 Discussion

5.1 Heterotopic heart transplantations

5.1.1 Approaches for endothelial transduction in rat model

We assessed the feasibility of rAAV2-mediated transduction of endothelium in a heterotopic rat heart transplantation model after intracoronary injection either in normothermic (n=3) or hypothermic (n=3) hearts (4.1.1.1). In addition, vector was applied into the tail vein without transplantation (n=2). PCR analyses revealed the presence of transgene DNA in transplanted hearts (HTX) independent of the operation technique. Only one animal (B2) did not show any transgene DNA which might be due to the 10-fold lower vector amount that has been injected. The existence of vector DNA in several liver samples (A1, A3 and B1) indicates that considerable amounts of vector did not enter cardiac cells, but were transported to other organs. This is in line with a comparable rat transplantation model of intracoronary vector injection where the transgene could also be detected in the liver (Kaspar et al., 2005). Interestingly, transgene DNA was measurable in the livers of both transplantation groups (A and B). In the hypothermia group, where the vector was injected into the cold and cardioplegic heart, rAAV is able to bind to its receptor, but cell entry is likely to be impaired due to the low temperature. After transplantation and flooding with blood, a loss of vectors might occur before the heart has reached physiologic temperature which is likely to vector entry. In contrast, administration into the normothermic heart allows immediate cell entry of the vector. Therefore, we expected that injection into the normothermic heart could be supportive of gene transfer into the heart. Our results indeed showed stronger signals corresponding to our vector DNA in transplanted heart samples of the normothermia than of the hypothermia group. Therefore, we suggest performing further gene transfer experiments in normothermic hearts.

Vector DNA was detectable in all animals (besides B2) in the transplanted heart. Thus, rAAV2 can enter cardiac cells. However, neither transgene mRNA nor β -Gal activity were detected. Based on our detailed *in vitro* analyses, discussed in the next chapter, this impairment is most likely due to an inadequate intracellular processing of the vector.

Concordantly with our *in vivo* results, Byrne's group observed that a transc coronary single-shot vector injection into cardioplegically arrested rat hearts followed by transplantation does not result in a detectable transgene expression (Asfour et al., 2002). They solved this problem by introducing an atrial septal defect which allowed the *ex vivo* recirculation of the vector (rAAV2ssLacZ). This was performed for 20 min at 15 °C in oxygenated Krebs-Henseleit solution. Analyses of the transplanted heart revealed a successful transduction with a significant X-Gal staining. Thus, prolonging the contact time between viral vectors and target cells seems to affect transduction efficiencies positively and would be one of the options to improve transduction efficiencies in our model.

Successful heart transduction by injection of 1.5×10^9 infectious units of AAV2CMV-LacZ intracoronary into the cardioplegic heart was reported for a mouse model (Svensson et al., 1999). Critical for the success of this approach performing a 15 min *ex vivo* perfusion was most likely the high volume to conquer the endothelial barrier due to the high pressure. Numerous attempts have been made to increase vascular permeability and thereby overcoming the endothelial barrier since endothelial cells seem to be inadequate cell types for achieving high levels of transgene expression. In line, intracoronary administration of histamine and vector (using amounts comparable to our experiments) resulted in 20 - 32 % transgene expression in cardiomyocytes as demonstrated by Kaspar and colleagues (Kaspar et al., 2005). These publications point out that increased vascular permeability (e.g. histamine, high pressure) could be another possibility which alone or in combination with a prolonged incubation time may improve *in vivo* transduction efficiencies of heart tissue.

Iwanaga and colleagues reported that less than 1 % of cardiomyocytes were positively stained for X-Gal activity after injection of rAAV2ssLacZ into hypothermic rat hearts despite administration of the vasoactive substance P (as alternative to overcome the endothelial barrier) in a big volume (Iwanaga et al., 2004). The clamping of the vessels and the vector amount were similar to our approach with the exception that we additionally transplanted the heart. This emphasizes that *in vivo* gene transfer into heart tissue is still an experimental approach and many controversial results have been described. Previous studies in hamsters performed by the same group also revealed absence of β -galactosidase activity, but observed immune reactions which were also observed in their rat model

(Hoshijima et al., 2002). In both studies, absence of signs of inflammation, but transgene expression was detected when phospholamban was used as transgene instead of LacZ. The same technique of pulmonary and aortic artery occlusion and administration of substance P in addition to intra-aortic injection of rAAV2LacZ did not lead to inflammation, but resulted in high myocardial transduction after 4 weeks in a mouse model (Iwatate et al., 2003).

Predominantly myocardial not endothelial transgene expression was detected. Observations by Li and colleagues demonstrated high β -Gal activity in the myocardium and its complete absence in the vessels after intracoronary vector delivery in heterotopic heart transplantation in a hamster model (Li et al., 2003). On the other hand, transgene expression was detected in endothelial cells and the perivascular area in a comparable approach in a rat model after injection of 1×10^{12} rAAV2GFP vector genomes, but storage of the graft in Histidine-Tryptophan-Ketoglutarate (HTK) solution for 6 h prior to implantation (Tsui et al., 2003). However, in this case the amount of transduced endothelial cells was not quantified and leaves room for discussion.

As an alternative, direct rat myocardial injections have been published to be successful (Dandapat et al., 2007; Liu et al., 2006; Palomeque et al., 2007). Especially, the administration of a vector construct identical to the here used rAAV2ssLacZ at comparable vector amounts (4×10^{11} particles) indicates the potential difference in efficiencies between intramyocardial and intracoronary vector injections (Liu et al., 2006).

Injection into skeletal muscle resulted in successful cDNA detection and X-Gal staining in our experiments. Consistent with our results, Xiao and colleagues published long-term rAAV2-mediated gene expression in mouse skeletal muscle (Xiao, Li, and Samulski, 1996).

In summary, reports on successful transgene expression emphasize vascular permeability and a prolonged exposition time of the vector as critical factors. Furthermore, cardiomyocytes seem to be the more suited target cells in contrast to our setting where we aimed to transduce endothelial cells which are the first target in graft rejection by intracoronary vector injection. Taking into account previous publications and our here reported results, the inefficient *in vivo* transgene expression is most likely due to endothelial cell-based intracellular restrictions (see

below) impairing efficient rAAV2-mediated transgene expression. In further experiments, the use of histamine or other vasoactive substances are recommended in order to transduce also cardiomyocytes. Ideally, vectors should be injected into the normothermic heart to improve cell entry as suggested from our results.

5.1.2 *In vitro* studies of RAECs

5.1.2.1 Superiority of rAAV1 in rat cardiac endothelial and cardiomyocyte transduction

Since our *in vivo* application of AAV2-based vectors did not result in transgene expression, we aimed to identify a more suited AAV serotype for transduction of cardiac endothelium using primary rat aortic endothelial cells (RAECs) as *in vitro* model. However, all analyzed serotypes were inefficient. Nevertheless, rAAV1 seems to be superior in comparison to rAAV2 to 5. Our results are in line with observations reported by Chen and colleagues comparing the same serotypes at 7 d p.i. (Chen et al., 2005). In our hands, rAAV2 was the second efficient vector in contrast to Chen and colleagues who described a stronger effect for rAAV5 which even surpassed the efficiency of rAAV1 at 14 d p.i.. Thus, our results are consistent with these observations, although describing transduction efficiencies at an earlier time point.

In order to estimate the efficiency of rAAV-mediated gene transfer into rat myocardium – the alternative target cell population in heart tissue – we compared transduction efficiencies for rAAV1 to 5 on primary neonatal cardiomyocytes. Best transgene expression levels were obtained by serotype 1 followed by rAAV4. Comparative *in vitro* analyses of neonatal cardiomyocyte transduction have not been published so far. Only rAAV2-mediated transductions have been reported in several publications (Kaspar et al., 2005; Maeda et al., 2000; Svensson et al., 1999). Kaspar and colleagues for instance, transduced primary cells with 10^4 DNase-resistant particles/cell which likely correspond to “our” 10^4 genomic particles/cell approach (Kaspar et al., 2005). In contrast to our observations (4.1 % after 3 d) they were able to reach transgene expression in 60 % of the cells 2 d p.i.. Also Maeda and colleagues reported similarly high transduction efficiencies (Maeda et al., 2000). The discrepancy to our results (4.1 % with rAAV2ssGFP at a GOI of 10^4) is not clear and due to variations in the experimental details not easily explainable.

The relevance of our *in vitro* studies in cardiomyocytes can be estimated from recent reports (Palomeque et al., 2007; Su et al., 2006). Intramyocardial injection of rAAV1 in rat resulted in higher transgene expression than rAAV2 corresponding to transduction efficiencies in primary cardiomyocytes (Palomeque et al., 2007). Also in a mouse model of myocardial injection rAAV1 was revealed as superior serotype in comparison to rAAV2 to 5 (Su et al., 2006). However, these efficiencies can be exceeded by other serotypes like rAAV6 or the recently identified rAAV8 (Palomeque et al., 2007). Of note, recent publications point towards a possibility to target the heart *in vivo* as rAAV9 seems to possess at least a preferential tropism for heart tissue (Inagaki et al., 2006; Pacak et al., 2006). These experiments have been performed in mice and nonhuman primates and showed superior effects for rAAV9 than for rAAV8 which was described before as the serotype of choice in mice (Wang et al., 2005).

In conclusion, the application of rAAV1 compared to rAAV2 showed higher transduction efficiencies in endothelial cells in our as well as in published experiments. Also *in vivo* the superior effect of rAAV1 compared to rAAV2 after intramyocardial injection has been reported. Therefore, we recommend the use of alternative serotypes, e.g. rAAV1 or – based on the most recent reports – rAAV9 instead of rAAV2.

5.1.2.2 Barriers in endothelial cells impair rAAV-mediated transgene expression

Obtained levels for rAAV-mediated transgene expression in endothelial cells are low *in vivo* and *in vitro* (Nicklin et al., 2001a; Pajusola et al., 2002). Therefore, we intended to investigate this problem in detail using rAAV2-mediated transduction of rat aortic endothelial cells (RAECs) as model system. Until establishment of a successful transduction, vectors have to overcome multiple barriers such as cell membrane, endosomal compartment, cellular protein degradation machinery and nuclear membrane. Of these numerous steps, we investigated the question of entry and perinuclear accumulation. Moreover, the effects of a proteasome inhibitor and second-strand synthesis were studied.

Laser scanning microscope studies in transduced RAECs revealed AAV-specific perinuclear accumulation of incoming particles (4.1.1.2.1). This results points to occurrence of vector entry and intracellular trafficking towards the nucleus in RAECs. Also Sipo and colleagues reported vector entry into human microvascular

endothelial cells albeit they observed that 50 % of the vectors stayed on the cell surface as they could be removed by trypsinization (Sipo et al., 2007). It can be assumed that the vectors are sequestered at the cell surface since endothelial cells express high levels of extracellular matrix including HSPG, which serves as primary receptor for AAV2 (Pajusola et al., 2002). Although we cannot comment on the efficiency of entry and perinuclear accumulation processes we conclude that vector entry is maybe to some extent, but not primarily, the reason for the low transduction efficiency in RAECs. Other steps like endosomal processing or nuclear translocation of vector genomes might contribute as well.

We observed a significant enhancement (7.3-fold for rAAV2ssGFP; $P < 0.002$; 4.4-fold for rAAV2scGFP; $P < 0.02$) in transgene-expressing RAECs transduced with a GOI of 5×10^4 in presence of 40 μM of the proteasome inhibitor MG132 3 d p.i. (4.1.1.2.1). In line with this result, we could also demonstrate an enhancement in transduction efficiency in the colon carcinoma cell line HT29 after application of the tripeptidyl aldehyde proteasome inhibitor MG132 which reversibly blocks the catalytic centre of the 26 S proteasome (Hacker et al., 2005; Oka et al., 2004). Interestingly, MG132 was published to enhance transduction efficiency significantly in human endothelial cells at 10^4 transducing particles/cell of rAAV2ssGFP (Nicklin et al., 2001a). In contrast to our results in RAECs, Pajusola and colleagues reported only a minor increase of GFP-expressing cells in human umbilical vascular endothelial cells (HUVEC; 1.3-fold) and human saphenous vein endothelial cells (SVEC; 3.2-fold) *in vitro* and in rabbit carotid artery assay *in vivo* (Pajusola et al., 2002). The mechanism by which proteasome inhibitors enhance rAAV-mediated transduction remains to be elucidated. Thus, proteasome inhibitors seem not to act simply by preventing the degradation of internalized virions or vector DNA (Douar et al., 2001; Duan et al., 2000; Yan et al., 2002). Interestingly, treatment with proteasome inhibitors increased the amount of ubiquitin detected on rAAV2 and rAAV5 capsids allowing to hypothesize that ubiquitin might serve as signal for uncoating or it possibly assists nuclear translocation of rAAV or vector genomes (Yan et al., 2002). Indeed, it is known that ubiquitin also gains proteasome-independent functions in regulation of cellular processes such as cell division, differentiation, signal transduction and protein trafficking (Mukhopadhyay and Riezman, 2007).

Once the vector genomes are located in the nucleus, natural single-stranded vector genomes first have to undergo second-strand synthesis. This step has been determined as rate-limiting process for efficient transduction by rAAV in certain cell types (Ferrari et al., 1996; Fisher et al., 1996). However, use of rAAV2scGFP only marginally enhanced the transduction efficiency in RAECs (1.8-fold increase compared to rAAV2ssGFP). Thus, we assume that this conversion is maybe not as efficiently performed as in certain cell types like HeLa, but has not to be considered as the main reason for impaired transgene expression as it was observed in the case of CD34⁺ cells (see chapter 4.2.1).

An enhancement of the amount of transgene-expressing cells by using self-complementary vector genomes and addition of MG132 demonstrated that RAECs are in principle able to induce transgene expression. Thus, it can be assumed that the CMV promoter as reason for impaired transduction efficiency can be excluded at least in short term assays *in vitro*. Other groups also support this assumption as strong activities in human endothelial cells could be observed (Pajusola et al., 2002). However, CMV promoter silencing processes *in vivo* cannot be excluded. Therefore, the choice of endothelial cell-specific promoters, e.g. the FLT-1 promoter which also would guarantee selective expression, would be a reasonable variation in our future experiments (Nicklin et al., 2001b). Nonetheless, in our *in vitro* model, we rather tend to exclude a contributory effect of the CMV promoter on the low level of transgene expression.

In summary, the intracellular detection of vector particles and the significantly enhanced transgene expression achieved by co-application of MG132 reveal that rAAV vectors are able to enter rat endothelial cells. Furthermore, intracellular transport of viral vectors towards the nucleus is not impaired albeit we cannot comment on its efficiency. Conversion of single-stranded vector genomes into a transcriptionally active vector genome conformation occurs maybe less efficiently than in other cells, but is also not the main limiting step. By the addition of proteasome inhibitors, however, a yet unknown limiting step could be overcome. Since no details about the mechanism by which proteasome inhibitors enhance AAV transduction are clear, it is currently impossible to speculate which intracellular events/steps are hampered. As outlined above, use of alternative serotypes or of targeting vectors seems to be currently the best way to cope with the observed limitation.

5.1.3 Porcine endothelial cells are highly permissive for AAV

As preparation for our *in vivo* gene transfer into porcine hearts, primary porcine aortic endothelial cells (PAECs) were used as *in vitro* model to estimate the efficiency of rAAV-mediated gene transfer into endothelial cells of this species in order to determine the best suited serotype among rAAV1 to rAAV5. This study, which is indeed the first report on a comparative analysis of different serotypes on PAECs revealed that AAV vectors are suitable for transduction of this cell type. Actually, results obtained with PAECs exceeded the efficiencies for rodent and human endothelial cells (Nicklin et al., 2001a; Pajusola et al., 2002). Serotype 2 was superior in transduction efficiency in comparison with rAAV1 and rAAV3 to rAAV5 and yielded about 90 % transgene-expressing cells using rAAV2 encoding GFP in the single-stranded as well as in the self-complementary vector genome conformation at a GOI of 10^5 (4.1.2.1.1). As expected, at lower vector-to-cell ratios rAAV2 containing the self-complementary vector genomes achieved higher transduction efficiencies. Concerning the other serotypes, rAAV5 was revealed as the second and rAAV1 as third efficient serotype for PAEC transduction. According to rAAV2, higher transduction efficiencies were measured for vectors containing the self-complementary vector genome conformation.

Our results reveal rAAV2 as the ideal serotype among rAAV1 to rAAV5 for porcine endothelial transduction. These high transduction efficiencies in PAECs are astonishing as endothelial cell transduction has commonly been reported to be low (Pajusola et al., 2002).

Further analyses of transduction by confocal laser scanning microscopy revealed large aggregates of intact capsids in PAECs in contrast to RAECs transduced at equal GOIs. This observation suggests a more efficient entry of rAAV2 into PAECs than into RAECs. In both cell types intact capsids were detected exclusively within the cytoplasm indicating occurrence of vector uncoating before or during nuclear entry in line with Lux and colleagues (Lux et al., 2005).

5.1.4 AAV vector mediated transgene expression in porcine hearts

Although gene transfer into the heart has been assessed in rodents, large animal models are indispensable for preclinical evaluation. Only a limited number of reports on rAAV-mediated gene transfer in porcine heart has been published so far (Kaplitt et al., 1996; Kaspar et al., 2005; Raake et al., 2008). Here, we

determined the efficiencies of heart transduction by intracoronarily injected rAAV2 vectors, which had turned out to be the most efficient serotype on PAECs. To increase vascular permeability, histamine was applied simultaneously. The two transplanted animals received different amounts of particles. Moreover, the vectors differed in the encoded transgene and in the vector genome conformation (2×10^{12} rAAV2ssLacZ and 2.3×10^{13} rAAV2scLuci) (4.1.2.2). Although this precludes a direct comparison, we decided to change the transgene since packaging efficiency and thereby the amount of applicable vector amount could be greatly enhanced by the use of luciferase instead of β -galactosidase. In both experiments, vector genomes were detected in all cardiac sections 21 d after transplantation as determined by qPCR. However, transgene expression could only be detected in the second animal that received a higher vector dose and a vector encoding luciferase in a self-complementary genome conformation.

Based on our own results and on published reports it is likely that a substantial contribution to the successful rAAV-mediated transgene expression is attributable to the self-complementary vector genome conformation used in this approach (Andino et al., 2007; McCarty et al., 2003). Moreover, the applied vector amount was ten times higher in the second animal. The assumption that vector amounts are crucial even in local applications like intracoronary vector injections is supported by results described by Kaspar and colleagues (Kaspar et al., 2005). They reported a successful gene expression in 3 of 4 pigs when a ten times higher vector amount was applied than we used in our first animal. Furthermore, considerably higher transduction efficiency was detected using 5.28×10^{13} vectors which correspond to about the same vector amount per kilogram body weight that we used.

Since both transgenes were controlled by the same promoter (CMV) this option can be excluded. However, low expression of β -Gal might have remained undetected due to the less sensitive quantification methods (X-Gal staining of tissue sections followed by microscopical analyses) while even tiny amounts of luciferase activity were measurable. Nevertheless, as already stated a direct comparison of both approaches is not possible and further experiments have to be performed to elucidate which of the discussed points solely or in combination are responsible for the successful gene transfer that was achieved in the second pig.

5.1.5 Distribution of transgene DNA and product in the two animals

In contrast to previous studies we performed the cardiac gene transfer in a heart transplantation setting as large animal model for xenotransplantation. Thereby, the vector-modified heart was transplanted into the abdomen of the recipient pig resulting in altered blood flow namely through the coronaries into the right atrium and ventricle and through the pulmonary arteries into the donor circulation excluding the left ventricle from the blood flow. To evaluate transduction efficiencies we dissected the heart into 4 levels and numerous samples of the left and right ventricle as well as of the septum region as depicted in Figure 26.

Comparing vector distribution in the left ventricle, both animals showed tendentially higher levels in the inner wall than in the outer part (4.1.2.2.1, 4.1.2.2.2). Moreover, highest values were obtained in the apex cordi (level IV) of both pigs. The region of highest mean copy numbers was the septum whereby the two ventral samples in level I and II (25, 26, 28, 29) revealed higher transgene DNA amounts than the third sample (27, 30). The only difference between both animals in the left ventricle was observed in level IV where the ranking of vector amount in the samples was inverted. Concerning level III, the DNA distribution was again similar, whereas lowest DNA amount was detected in the middle sample. Furthermore, the two animals showed no correlation regarding vector genome distribution in the heart tissue. While in the rAAV2ssLacZ injected pig in all regions of level I and II the copy number decreased from the ventral to the dorsal part, this was only the case in level III of the rAAV2scLuci transduced animal.

Yet unexplained is the fact that regions of highest amounts in transgene DNA did not correspond to areas located at the assumptive course of the left anterior coronary which should be represented by the regions 27, 30, 37, 39, 40, 42, 43 and 44 as well as smaller branches supplying the regions 7, 9, 11, 12 and 34. However, an individual variation in course of the vessels may serve as an explanation (the course of vessels in our two animals has not been recorded by our cooperation partners).

We were interested to which extent transgene DNA levels correspond to the transgene expression level. Due to the lack of expression in the first animal, this question could only be addressed to the second animal that had received rAAV2scLuci. Luciferase levels varied from 1.4-fold (sample 41) to 215-fold

(sample 15) when normalized to a non-treated porcine sample. With some exceptions the variation in vector DNA amount did not mirror the luciferase levels of the respective samples. Solely for all levels of the inner wall of the left ventricle, levels I to III in the septum region and level I of the right ventricle, the highest DNA sample correlated with the corresponding highest luciferase activity. Since similar studies have not been performed yet, we cannot compare our results with published reports.

In contrast to the published observations in non-transplanted animals, thus in hearts with a nature course of blood circulation, we detected transgene expression in the entire heart not only in the region of the left anterior coronary (Kaplitt et al., 1996; Kaspar et al., 2005; Raake et al., 2008). In relevant publications only the territory of the left anterior descending (LAD) coronary was analyzed (Kaspar et al., 2005; Raake et al., 2008). Kaplitt and colleagues also analyzed other regions of the heart, but observed transgene expression exclusively within the LAD territory (Kaplitt et al., 1996). Also the vector application methods differed from our approach of indirect (into the aorta) antegrade (with natural blood flow) intracoronary vector application while connected to a newly developed *in situ* Langendorff reperfusion system for prolonged exposure of the vector to the heart. Closest to our setting were experiments by Kaspar and colleagues who applied heparin affinity purified rAAV2 vectors encoding for CMV promoter-controlled GFP at comparable vector amounts ($2.6 - 5.3 \times 10^{13}$ DNase resistant particles rAAV2ssGFP) (Kaspar et al., 2005). However, we have to take into account that their pigs were double in weight compared to our animals. Also in their approach, histamine was administered to increase vascular permeability followed by catheter-based vector injection directly into the left circumflex coronary. In contrast to our experiments, pigs were analyzed after 8 weeks and the central core of the perfusion bed showed gene-expression in 12 % of the cells. Since we detected luciferase activity by luminometer a direct comparison between the 12 % GFP-expressing cells and our relative light units (RLU) is impossible. However, the high luciferase activity detected in some of our samples may point to a higher level of gene transfer efficiency.

Recently, Raake and colleagues published a comparative analysis for transgene expression using rAAV6 and a heparin binding mutant of rAAV2 after pressure-regulated retrograde (into the anterior cardiac vein) intracoronary vector injection

(Raake et al., 2008). Serotype 6 was determined as superior to the rAAV2 mutant, but it was not compared to rAAV2. Moreover, another recent publication revealed rAAV1 as more efficient than rAAV2 at least in intramyocardial injection into the porcine heart (Su et al., 2008).

Regarding extracardiac organs, no transgene DNA or expression was detected in any of the pigs. Therefore, we conclude that the major part of the vector entered cardiac cells efficiently without measureable systemic distribution. Especially the novelty of the *in situ* Langendorff reperfusion system for recirculation of oxygenated blood at normothermic conditions after vector injection over a longer time might have enhanced the transduction of cardiac cells and therefore limited gene transfer into extra-cardiac organs. This is in line with Kaspar and colleagues who used a direct catheter-based vector delivery in presence of histamine and analyzed the organs 8 weeks p.i. and observed no signs of transgene expression in non-cardiac pig organs (Kaspar et al., 2005). However, a biodistribution analysis for transgene DNA was not performed (Kaspar et al., 2005).

Altogether, transgene DNA distribution coincides only partially between the two pigs. Also the amount of transgene DNA did not correlate with the level of transgene expression. Moreover, the transgene-containing regions were not consistent with the course of the left anterior coronary as reported by other groups. Instead, we detected transgene expression in the entire heart albeit at different levels.

5.1.6 Potential of rAAV2 for animal cloning

As already described in 4.3.2, porcine fibroblasts are used by our cooperation partners of the Institute of Farm Animal Genetics (Mariensee) for somatic cell nuclear transfer. We evaluated the feasibility of rAAV vectors for mediating gene transfer into these cells. The high efficiency of rAAV2 transduction qualifies this vector for further analyses. In order to achieve site-specific integration, the transfection of a Rep-coding plasmid or addition of Rep protein could be an option. So far, transgenes have been transfected into fibroblasts and analyzed for integration events. Interestingly, porcine fibroblasts and the highly permissive human tumor cell line HeLa showed the same transduction profile concerning the serotypes rAAV1 to rAAV5.

Insertion of transgene into the oocyte is another approach, which was used here for the generation of genetically manipulated cattle. Our partners observed that addition of rAAV2 to the medium is sufficient for transduction. Thus, the vector is able to overcome the zona pellucida of the oocyte. Moreover, they injected a plasmid coding for Rep into the oocyte. Intense GFP expression of the blastocysts has been observed. Although transfer of the embryos into cows and maintenance of pregnancies are difficult and expensive, one calf treated with rAAVscGFP was born. Unfortunately, it did not show any transgene DNA which might be due to lack of vector integration.

Although not completed, these preliminary experiments suggest rAAV2 as potential vector for production of transgenic animals.

5.2 Investigations on CD34⁺ cells

5.2.1 Most efficient serotype rAAV2 is limited by second-strand synthesis

CD34⁺ cells gained increasing attention for the treatment of hematopoietic diseases as well as for induction of neovascularization in ischemic regions or sites of endothelial injury. Beneficial effects of combined cell and gene therapeutical approaches are now being evaluated (Melo et al., 2004). So far, only the serotype 2 coding for single-stranded (ss) vector genomes has been studied in human CD34⁺ cell transduction, but with controversial results. Comparative analyses of several serotypes as well as the influence of second-strand synthesis using self-complementary (sc) vectors have exclusively been performed in murine CD34⁺ cells (Zhong et al., 2006). Therefore, we assessed the most efficient serotype among rAAV2, rAAV3 and rAAV5 (4.2.1). AAV2 was clearly revealed as the most suitable serotype. While single-stranded genomes containing vectors only resulted in a minor transduction efficiency for rAAV2 (8 %), rAAV3 and rAAV5 did not show any transgene expression 3 d after transduction with a GOI of 10⁵. The use of scGFP vectors could enhance GFP-expression for those serotypes only slightly (4.8 % for rAAV3 and 7.4 % for rAAV5). In contrast, almost 60 % transduction efficiency was obtained by rAAV2scGFP. This immense difference in the amount of transgene-expressing cells after administration of either scGFP or ssGFP vector genomes can be explained by limitations in second-strand synthesis as previously described for other cell types (Hacker et al., 2005; McCarty, Monahan, and

Samulski, 2001). The only comparative analysis of both vector conformations in transduction of hematopoietic progenitor cells – even though of murine origin – also approved this step as limitation of transduction pathway (Zhong et al., 2006). In transduction of murine hematopoietic progenitor cells rAAV1 has been described as most efficient serotype.

In order to determine if the differential expression levels of the serotypes 2, 3 and 5 are based on unequal entry, we determined the amount of vector genomes in the total DNA of CD34⁺ cells 3 h p.i. with ssGFP and scGFP vectors at a GOI of 10⁴ (4.2.1). Serotype 2 clearly entered the cell most efficiently, followed by rAAV3 and then rAAV5. Thus, a less efficient entry is at least one reason for the lower level of transgene expression obtained by rAAV3 and 5. Moreover, similar transgene levels of scGFP and ssGFP vectors of the respective serotype confirmed that the difference in their transgene expression is only accounted by the different vector conformations.

The high transgene expression level observed 3 d p.i. with rAAV2scGFP declined by 4.4-fold within one further week of cultivation. This is in line with observations of transient gene expression over a period of 10 to 14 d p.i. as reported by Nathwani and colleagues (Nathwani et al., 2000). One explanation could be a downregulation of promoter activity as previously described for CMV promoter in hematopoietic and mesenchymal progenitor cells in comparative promoter analyses (Byun et al., 2005). For that reason, use of vectors containing promoters distinct from CMV promoter should be considered. Moreover, loss of non-integrated vector genomes during cell divisions might also contribute to the decreasing amount of GFP-expressing cells.

As discussed in the introduction, publications on rAAV2-mediated transduction of CD34⁺ cells present conflicting results. Early experiments have been performed with low purified crude vector lysates which have been generated by use of adenovirus as helper virus (Fisher-Adams et al., 1996; Goodman et al., 1994; Hargrove et al., 1997; Zhou et al., 1994). Thus, helper virus contaminations could have assisted second-strand synthesis thereby enabling transgene expression (Alexander, Russell, and Miller, 1997). As we produced our vectors in a helper-free method with subsequent iodixanol gradient centrifugation as described in 3.1.4 we could exclude this effect. Besides vector production, also titration,

isolation and cultivation of CD34⁺ cells varied in the different reports. Our conditions were most comparable to experimental settings as described by Nathwani and colleagues (Nathwani et al., 2000). They reported an efficient gene transfer into human cord blood-derived CD34⁺ and CD34⁺CD38⁻ cells using highly purified helper virus-free rAAV2 preparations. Isolation of the cells was performed corresponding to our protocol and also the choice of cytokines (albeit not the concentrations and medium) for cultivation and the use of pre-expanded (2 d) cells for transduction was equal to our approach. In contrast, they used a multiplicity of infection of 10⁶ which corresponds to a GOI of approximately 10⁷ representing about 100 times higher vector amounts of rAAV2ssGFP than in our experimental setting. Nonetheless, they only observed low transduction efficiencies of 10 to 23 % after vector incubation over night and further cultivation for 24 to 48 h using high or low dose cytokine concentrations. Our results showed 8 % GFP-positive cells 3 d p.i. with rAAV2ssGFP at a GOI of 10⁵. Cells were only incubated with vector for 3 h and the used cytokine concentrations lied in between the reported ones. This emphasizes a more efficient transduction in our hands. Even though they showed that transduction efficiencies could be enhanced from 10 to 51 % by using higher cytokine concentrations and addition of TNF α (MOI of 10⁶) this value did not reach efficiencies obtained for rAAV2scGFP transduction (57 %) at lower GOI in our experiments. Moreover, we could demonstrate a significant enhancement in transgene-expressing cells (85.6 %) by coadministration of rAAV2scGFP, Trichostatin A and retinoic acid as described in 4.2.5 and discussed more detailed in 5.2.4 which was not reported before. In conclusion, we reported highly efficient transduction of cord blood-derived CD34⁺ cells.

5.2.2 Transduction procedure does not interfere with endothelial differentiation

The ability to differentiate into endothelial cells is a prerequisite for successful neovascularization and engraftment of CD34⁺ cells. In order to investigate if this ability is affected by AAV transduction, we evaluated the differentiation potential of transduced and non-transduced CD34⁺ cells 3 d p.i.. After 10 d of cultivation in differentiation medium on fibronectin-coated plates, the cells showed a spindle-shaped morphology and took up Dil-AcLDL efficiently independent of the vector application. This experiment verified that our CD34⁺ cells could differentiate into endothelial cells. However, it was – most likely due to promoter silencing events –

not possible to visualize GFP expression to correlate definitely differentiated and transduced cells. Therefore, we analyzed the DNA from differentiated cells for presence of transgene DNA by qPCR. Equal amounts of GFP DNA in samples of cells transduced with rAAV2ssGFP and rAAV2scGFP vectors (about 6×10^5 copies after normalization to GAPDH) confirmed the presence of vector DNA within cells after 10 d of differentiation assay. As can be seen in the microscope images, nearly all cells showed Dil-AcLDL uptake. Thus, it seems likely that also transduced cells maintained their ability for differentiation.

5.2.3 Receptor and coreceptor studies

Heparan sulfate proteoglycan (HSPG) has been described as primary receptor for rAAV2 transduction (Summerford and Samulski, 1998). However, Handa and colleagues reported that certain cell types like mutants of the CHO-K1 cell line deficient for glycosaminoglycan can be transduced by AAV2 (Handa et al., 2000). Therefore, we were interested to evaluate if HSPG is involved in rAAV2-mediated CD34⁺ cell transduction by competitive inhibition with the soluble analogue of HSPG, heparin (4.2.3). Studies on hematopoietic progenitor cell lines suggested the presence of HSPG on the cell surface (Drzeniek et al., 1999; Stocker et al., 1996). Whereas rAAV2scGFP-transduced cells showed again almost 60 % transduction efficiency, presence of heparin reduced the number of GFP-expressing cells to background level. This confirms the involvement of HSPG in CD34⁺ cell transduction and thereby also the presence of that receptor on the cell.

The abundance of receptors and coreceptors on the cell is a factor which determines susceptibility of the respective cell type to rAAV transduction. Ponnazhagan and colleagues observed large differences in transgene expression of rAAV2-transduced bone marrow-derived human CD34⁺ cells of 12 donors (Ponnazhagan et al., 1997). Half of the donor cells were refractory to rAAV2 transduction at a MOI of 100, while the others showed efficiencies ranging from 15 to 80 %. This difference was attributed to the differential susceptibility of the cells as assessed by virus-binding assays with radiolabeled virus. In contrast, we observed transduceability of CD34⁺ cells of all donors whereas much lower variations in transgene expression were detected (lowest 24.1 % and highest 69.4 % values; SEM 5.2 %; n=8) as depicted in Figure 30. Absence of a significant variation in transduction efficiency in individual cell samples was also reported by

Nathwani and colleagues (Nathwani et al., 2000). Since Ponnazhagan's publication, HSPG was described as primary receptor for rAAV2 as well as 5 more coreceptors. FGFR, HGFR and eventually laminin receptor were proposed to enhance AAV2 binding to the cell (Akache et al., 2006; Kashiwakura et al., 2005; Qing et al., 1999). Subsequently, AAV2 interacts with $\alpha_v\beta_5$ integrin thus inducing endocytosis and probably cytoskeletal rearrangements necessary for efficient trafficking (Sanlioglu et al., 2000). Recently, $\alpha_5\beta_1$ integrin has been identified as an alternative AAV coreceptor (Asokan et al., 2006). In order to investigate which of the integrins most likely assists vector entry, we evaluated the abundance of the two integrin coreceptors on CD34⁺ cells in relation to the transduction efficiency. Therefore, we measured the level of integrins at the day of transduction (after 2 to 4 d of pre-expansion) by FACS analysis and determined GFP-fluorescence of transduced cells 3 d p.i. (4.2.4). These experiments were performed with bone marrow-derived and freshly isolated or bought (pooled from different donors) cord blood-derived CD34⁺ cells. The amount of $\alpha_v\beta_5$ integrin varied largely from 0.5 % to 59.5 % whereas the level of $\alpha_5\beta_1$ integrin was generally higher (78.8 – 96.2 %) and more evenly distributed. Analyses of transduction efficiencies 3 d later revealed a minimum of 52 % GFP-expressing cells. Comparing the amount of the two integrins with the transgene expression point to a correlation of $\alpha_5\beta_1$ integrin and transgene expression. Especially, the examples of extremely low $\alpha_v\beta_5$ integrin levels of 0.5 and 2.5 % together with high $\alpha_5\beta_1$ integrin amounts and more than 55 % GFP expression emphasizes this assumption. These observations would support $\alpha_5\beta_1$ integrin as coreceptor.

To further confirm the role of this integrin for transduction, we compared transduction efficiencies of rAAV2 and a mutant, NGR R513A, deficient for $\alpha_5\beta_1$ integrin binding (Asokan et al., 2006). As the amount of $\alpha_v\beta_5$ integrin displayed on the cells was below 1 % and above 90 % for $\alpha_5\beta_1$ integrin at the time of transduction, the obtained result could be correlated solely with the activity of $\alpha_5\beta_1$ integrin. The NGR R513A mutant was 5.6 times less efficient than rAAV2 which allows the conclusion that $\alpha_5\beta_1$ integrin serves as coreceptor in CD34⁺ cell transduction. For CD34⁺ cells, a physiological role of $\alpha_5\beta_1$ integrins has been assigned as attachment receptor to fibronectin which is part of the extracellular

matrix of the bone marrow stroma (Dao et al., 1998; Hurley, McCarthy, and Verfaillie, 1995).

Interestingly, surface expression of at least $\alpha_5\beta_1$ integrins seemed to be induced by culturing in cytokine-containing medium as both $\alpha_v\beta_5$ and $\alpha_5\beta_1$ integrins were nearly undetectable on freshly thawed cells as determined in 2 independent experiments. After 3 d of pre-expansion in medium supplemented with SCF, IL-3, IL-6 and Flt3L, less than 2 % of the cells displayed $\alpha_v\beta_5$ integrins while on more than 77 % $\alpha_5\beta_1$ integrins were detectable. This is in line with Hart and colleagues who reported an upregulation of $\alpha_5\beta_1$ integrins upon cultivation in SCF-containing medium (Hart et al., 2004). The absence of $\alpha_5\beta_1$ integrins on freshly isolated CD34⁺ cells might explain the untransduceability by rAAV2 vectors as previously reported (Nathwani et al., 2000). Therefore, pre-expansion of CD34⁺ prior to transduction might be favourable not only in terms of the growing cell number.

5.2.4 Effects of the transcriptionally active drugs TSA and RA

Although we already obtained a high transgene expression of about 60 % in CD34⁺ cells after transduction with rAAV2scGFP, we assessed the potential of further increasing this value by transcriptionally active drugs. Therefore, we followed the report of Gaetano and colleagues who observed an enhancement of transgene expression in adenovirus-transduced endothelial cells by the histone deacetylase inhibitor (HDACi) Trichostatin A (TSA) and retinoic acid (RA) (Gaetano et al., 2000; Kitazono et al., 2002). FACS analyses 3 d p.i. revealed an increase in transgene-expressing cells by the use of TSA and RA. The use of TSA alone only showed a minor increase from 61.4 % to 69.5 % GFP-positive cells. In contrast, RA induced a stronger enhancement up to 82.7 % transgene-expressing cells and 3.4-fold higher values in mean fluorescence intensity (MFI). However, the combination of both drugs resulted in highest transgene expression (85.6 %) and 5.9-fold increased in MFI. These results are in line with observations in adenoviral-mediated transgene expression by Gaetano and colleagues (Gaetano et al., 2000). Thus, we recommend the treatment of CD34⁺ cells with TSA and RA in gene transfer experiments with rAAV vectors containing a CMV-promoter for enhancement of transgene expression.

The effect of these drugs is in part based on the influence on the strong viral CMV promoter containing numerous *cis*-regulatory elements mediating binding of

transcription factors such as retinoic acid receptors (RARs, RXRs) (Angulo et al., 1996; Ghazal et al., 1992). Retinoic receptors bind to retinoic acid response elements (RARE) on promoters of RA-target genes and recruit protein complexes including HDACs (Chambon, 1996). The induced remodelling processes result in transcriptional repression. Binding of RA causes release of the HDAC activities and HATs are subsequently recruited to the RAREs leading to reactivation of transcription due to increased DNA accessibility to the transcriptional machinery. Thereby, the enhancement in transgene expression by rAAV containing a CMV-promoter controlled transgene upon RA coadministration can be explained (Fazi et al., 2005).

On the other hand, HDACi act in multiple ways (Dokmanovic and Marks, 2005). Most obviously, they inhibit the deacetylation of histones thus inducing enhanced accessibility of the DNA to transcriptional processes. As AAV DNA has been proposed to be complexed with histone-like structures, it is imaginable that HDACi might influence these structures as well (Marcus-Sekura and Carter, 1983). CMV promoter silencing has been shown to occur frequently *in vitro* and *in vivo*, thus impairing efficient transgene expression for longer periods (Xia et al., 2007). Interestingly, Chen and colleagues reported reactivation of silenced CMV promoter in rAAV- and retrovirus-transduced cells by use of TSA (Chen et al., 1997). Additionally, HDACs and HATs also regulate non-histone proteins which are involved in the control of cell-cycle progression, differentiation and apoptosis (Dokmanovic and Marks, 2005). Therefore, HDACi might be implicated in the regulation of these targets. Especially the participation of HDACi and RA in the control of RA-target genes might explain their synergistic effect in our experiments (Minucci et al., 1997). These drugs are also evaluated for tumor therapy whereas several groups reported enhanced effects of combined TSA and RA treatment *in vitro* and *in vivo* (De los Santos et al., 2007; Touma et al., 2005).

5.2.5 Outlook

This work aimed to contribute to gene- and cell-based strategies for the treatment of heart diseases. Modification of heart tissue by rAAV gene transfer prior to transplantation was the focus of the first part of this thesis. The ultimate goal of this approach in our rat model was its use as screening platform for factors impairing transplant rejection. As outlined above, none of the investigated serotypes resulted in reasonable transduction efficiencies on RAECs although rAAV1 was more efficient than rAAV2. If rAAV1 is also more efficient *in vivo* as it has recently been published, remains to be determined (Palomeque et al., 2007; Su et al., 2006). Based on recent reports, rAAV9 could even be better suited (Inagaki et al., 2006; Pacak et al., 2006). An alternative to the change in serotype are targeting strategies. AAV peptide libraries containing rAAV capsid mutants that differ from each other only by 7mer peptides with random sequences displayed in cell surface-exposed regions have been developed (Perabo et al., 2003; Muller et al., 2003). These libraries are used to select for capsid mutants that enter the cell specifically via the inserted peptide and are processed efficiently with the respective target cells. Our group has already developed in close collaboration with A. Baker (University of Glasgow, UK) rAAV targeting vectors for human and mouse endothelial cells using the phage display technology (Nicklin et al., 2001). Furthermore, in two different approaches we could prove *in vivo* targeting ability and transgene expression as well (Work et al., 2006; White et al. 2004). Thus, the targeting technology holds promise to design vectors overcoming the intracellular barriers hampering rAAV-mediated gene expression in endothelial cells.

Crucial for the *in vivo* transduction efficiency is maybe the use of self-complementary vector genome conformation of rAAV vectors. This can be assumed from our results in pig studies, but remains to be demonstrated. Overall, the results on gene transfer into porcine heart were quite promising. However, the number of analyzed pigs is very low and additional transplantation experiments have to be performed before proceeding to the evaluation of therapeutically relevant genes, e.g. immunomodulatory genes for their ability to prolong graft survival. The requirement of large vector amounts, however, will remain the major hurdle in transduction of porcine heart. Therefore, the search for potentially more efficient serotypes or the selection for vector targeting is reasonable.

The second part focused on the rAAV-mediated transduction of CD34⁺ cells for which an efficient protocol was established. Vector safety is a principal concern for clinical applications. Especially the tumor development in two patients during a retrovirus-based clinical SCID trial caused by insertional tumorigenesis has revealed this risk (Hacein-Bey-Abina et al., 2003). Even though AAV2 is rarely integrating, it has to be determined if vector genomes possess an integrating ability in CD34⁺ cells (Kotin, Linden, and Berns, 1992). These ongoing experiments are performed by ligation-mediated PCR (LM-PCR) in close collaboration with B. Fehse (Johann Wolfgang Goethe-University Frankfurt) (Kustikova et al., 2007). Actually, especially if long-term expression is needed, it would be favorable to induce vector genome integration. The AAV system offers the possibility to direct vector integration to a specific region in the human genome, e.g. by addition of Rep protein or Rep-encoding sequences, an approach which is clearly in the focus of the future work in this project (Kotin et al., 1990).

6 Materials

6.1 Chemicals and Solutions

| Product | Company |
|---|----------------------------------|
| 5-bromo-4-chloro-3-indolyl-beta-D-galactopyranoside (X-Gal) | Roth, Karlsruhe |
| Agar-Agar | Roth, Karlsruhe |
| Agarose | Invitrogen, Karlsruhe |
| all trans-Retinoic Acid (RA) | Sigma, Deisenhofen |
| Aqua bidest. (Ampuwa) | Fresenius Kabi, Homburg |
| Biotin Conjugate Streptavidin | Dianova, Hamburg |
| Boric Acid | Merck, Darmstadt |
| Bovine Serum Albumine | AppliChem, Darmstadt |
| Bovine Serum Albumine (BSA) Standard Set | BioRad, München |
| Calcium Chloride | Sigma, Deisenhofen |
| Chloroform | Merck, Darmstadt |
| Dil-AcLDL | CellSystems, St. Katharinen |
| Dimethylsulfoxide (DMSO) | Riedel-de Haën, Seelze |
| DPX Mountant for Histology | Fluka, Neu-Ulm |
| EDTA | Roth, Karlsruhe |
| Eosin G-Solution 0.5 % aqueous | Merck, Darmstadt |
| Ethanol | Roth, Karlsruhe |
| Ethidium Bromide | Roth, Karlsruhe |
| Fibronectin from Human Plasma | Sigma, Deisenhofen |
| Gelatine | Sigma, Deisenhofen |
| Glycerol | Roth, Karlsruhe |
| Heparin | B. Braun Melsungen AG |
| Heparin (used for CD34 ⁺ cells) | Sigma, Deisenhofen |
| HEPES | Roth, Karlsruhe |
| Hydrochloric acid | Roth, Karlsruhe |
| Isopropanol | Roth, Karlsruhe |
| Lipofectamin 2000 | Invitrogen, Karlsruhe |
| Lymphoprep (Ficoll) | Sentinel, Milan, Italy |
| Magnesium Chloride | Roth, Karlsruhe |
| Mangan Chloride | Merck, Darmstadt |
| MassRuler DNA Ladder Mix | MBI Fermentas GmbH, St. Leon-Rot |
| MG132 | Sigma, Deisenhofen |
| MOPS | Sigma, Deisenhofen |
| OptiMEM | Invitrogen, Karlsruhe |
| Optiprep Density Gradient Medium (Iodixanol) | Sigma, Deisenhofen |
| Paraformaldehyde | Sigma, Deisenhofen |
| PBS 10x | Biochrom, Berlin |
| Peptone/Tryptone | Roth, Karlsruhe |
| Potassium Acetate | Merck, Darmstadt |
| Potassium hexacyanoferrat II trihydrat | Fluka, Neu-Ulm |
| Potassium hexacyanoferrat III | Sigma, Deisenhofen |
| Quick Start Bradford Dye Reagent | BioRad, München |

| | |
|----------------------|------------------------------------|
| Sodium Chloride | Roth, Karlsruhe |
| Sodium Hydroxide | Roth, Karlsruhe |
| Sodium Phosphate | Roth, Karlsruhe |
| Trichostatin A (TSA) | Sigma, Deisenhofen |
| Tris | Merck, Darmstadt |
| Triton X-100 | Sigma, Deisenhofen |
| Trizol Reagent | Invitrogen, Karlsruhe |
| Vectashield | Vector Laboratories, Burlingame |
| X-Tra Solv | Mediate Histotechnic, Burgdorf |
| Yeast Extract | Roth, Karlsruhe |

6.2 Enzymes and Kits

| Product | Company |
|--|------------------------------------|
| DNA restriction enzymes | MBI Fermentas, St. Leon-Rot |
| Benzonase | Merck, Darmstadt |
| Direct CD34 Progenitor Cell Isolation Kit | Miltenyi Biotec, Bergisch-Gladbach |
| <i>Renilla</i> Luciferase Assay System | Promega, |
| DNeasy Blood & Tissue Kit | Qiagen, Hilden |
| EndoFree Plasmid Kits | Qiagen, Hilden |
| PCR Purification Kit | Qiagen, Hilden |
| Gel Extraction Kit | Qiagen, Hilden |
| Quantitect SYBR Green PCR Kit | Qiagen, Hilden |
| RNase A (100 mg) | Roche, Mannheim |
| Transcriptor First Strand cDNA Synthesis Kit | Roche, Mannheim |
| DNase I | Roche, Mannheim |
| LightCycler Uracil-DNA Glycosylase (UNG) | Roche, Mannheim |

6.3 Plasmids

pXX6:

Adenoviral helper plasmid encoding for VA, E2A and E4 and ampicillin resistance; pXX6 was kindly provided by J. Samulski (University of North Carolina, Chapel Hill, USA).

pXR1, pXR2, pXR3, pXR4 and pXR5:

The plasmids encoded for the capsids of the respective serotypes and the Rep proteins of AAV2 (Rabinowitz et al., 2002). For the serotypes 3 to 5 a portion of the serotype-specific *Rep* gene was substituted for that of AAV2. The Rep proteins are able to package transgenes flanked by the ITRs of AAV2 into the capsids. These plasmids were kindly provided by J. Samulski (University of North Carolina, Chapel Hill, USA).

pGFP single-stranded:

The GFP plasmid consists of AAV ITR sequences flanking the hygromycin selectable marker gene controlled by the thymidine kinase promoter and the *Aequorea victoria* enhanced Green Fluorescent Protein (GFP) gene regulated by the Cytomegalovirus (CMV) promoter (Hacker et al., 2001).

pGFP self-complementary:

The enhanced GFP gene is controlled by the human CMV promoter. A deletion in one of the terminal resolution sites interferes with strand displacement resulting in a self-complementary genome, which is packaged into the viral capsid (Hacker et al., 2005).

pLuci:

The transgene cassette encoding for the CMV promoter controlled Luciferase gene is flanked by one intact ITR and one containing a mutated terminal resolution site. As in the pGFP self-complementary plasmid also this plasmid is packaged as pseudo double-stranded genome. The plasmid was constructed and kindly provided by my colleague Sibille Quadt-Humme.

pZNL:

This plasmid carries a CMV and an EM-7 promoter followed by a Zeocin-resistance gene. After a fusion sequence the LacZ gene containing a nuclear localization sequence (NLS) and SV40pA follows. The transgene cassette is flanked by ITRs (Girod et al., 1999).

pMV10-FLT-1:

This construct contains a FLT-1 promoter, a LacZ gene and a CMVpA. The plasmid was kindly provided by A. Baker (University of Glasgow, Glasgow, UK).

pNGR R513A:

The plasmid based on pRC99 encoding for the Rep and Cap proteins of AAV2, contains a mutation within the *cap* sequence leading to a substitution at the amino acid position 513 (R→A). The construct was generated according to Asokan and colleagues and kindly provided by my colleague Anke Huber (Asokan et al., 2006).

6.4 Primers

Primers were synthesized by Sigma-Genosys.

GAPDH (Glycerinaldehyde-3-Phosphate Dehydrogenase)

Human GAPDH forward: 5'-GAG TCC ACT GGC GTC TTCA
Human GAPDH reverse: 5'-TTC AGC TCA GGG ATG ACC TT
Porcine GAPDH forward: 5'-ACA TGG CCT CCA AGG AGT AAGA
Porcine GAPDH reverse: 5'-GAT CGA GTT GGG GCT GTG ACT
(Duvigneau et al., 2005)
Rat GAPDH forward: 5'-ATC CCA GAG CTG AAC G
Rat GAPDH reverse: 5'-GAA GTC GCA GGA GAC A

eGFP (enhanced green fluorescent protein)

eGFP 1 forward: 5'-GCT ACC CCG ACC ACA TGA AG
eGFP 1 reverse: 5'-GTC CAT GCC GAG AGT GAT CC

LacZ (Beta-Galactosidase)

LacZ forward: 5'-ATC CTC TGC ATG GTC AGG TC
LacZ reverse: 5'-CTG GGC CTG ATT CAT TCC

Luciferase

Luci forward: 5'-CGT GCT GGA CTC CTT CAT CA
Luci reverse: 5'-TTG CGG ACA ATC TGG ACG AC

C9

C9 forward: 5'-GAA GCA CGC GTA TCC TAT GA
C9 reverse: 5'-ATT ATT AGT CGG CCT CAT CC

S18

S18 forward: 5'-AGG GAG ACA GCC TCA GAA ACT TTT
S18 reverse: 5'-CGC CGA ATA GCA CAT TTA CAT GAT

6.5 Antibodies

Primary antibodies

- Anti- $\alpha_v\beta_5$ (MAB1961): monoclonal; mouse α -human; Chemicon
- Anti- $\alpha_5\beta_1$ (MAB1999): monoclonal; mouse α -human; Chemicon
- Anti-Lamin B (M-20; sc6217): polyclonal; α -mouse; SantaCruz Biotechnology
- Anti-AAV intact capsid (A20): monoclonal; mouse IgG1 hybridoma supernatant; DKFZ Heidelberg, J. Kleinschmidt

Secondary antibodies

- PE-conjugated goat α -mouse IgG (ab7002-500); monoclonal; abcam
- Cy5-conjugated AffiniPure donkey α -goat IgG (H+L); Jackson ImmunoResearch
- Rhodamine Red-X- (RRX-) conjugated AffiniPure goat α -mouse IgG (H+L); Jackson ImmunoResearch

6.6 Bacteria Strains

E. coli DH5 α :

F-, *lac1*-, *recA1*, *endA1*, *hsdR17*, Δ (*lacZYA-argF*), U169,F80d/*lacZ* Δ M15, *supE44*, *thi-1*, *gyrA96*, *relA1*; (Hanahan, 1983)

6.7 Eukaryotic Cells

For culturing and media conditions please refer to the chapters 6.8 and 7.3

6.7.1 Immortalized Cell Lines

HEK293

Human embryonic kidney cells, transformed with Ad5 DNA and containing the adenoviral genes *E1a* and *E1b*; American Type Culture Collection (ATCC); (Graham et al., 1977)

HeLa

Human epithelial cervix adenocarcinoma cells; ATCC; (Scherer, Syverton, and Gey, 1953)

6.7.2 Primary cells

Rat aortic endothelial cells (RAEC)

These cells were isolated by a non-enzymatic outgrowth method of thoracic aortic rings as described by Nicosia and colleagues (Nicosia, Villaschi, and Smith, 1994). Adult Lewis rats were used as donors. After isolation the cells were characterized by their ability to take up Dil-AcLDL and to stain for von Willebrand Factor (vWF) as well as endothelial markers like CD31 by FACS analysis. Morphologically the endothelial cells can be identified by their cobblestone formation. The cells were kindly provided by M. Seifert (Charité Berlin).

Rat neonatal cardiomyocytes

Neonatal cardiomyocytes were isolated from 1 to 3 d old Wistar rats by E. Saygili as described before (Saygili et al., 2007; Zobel et al., 2007) and provided by B. Bölck (University Hospital Cologne). Hearts were digested with collagenase and trypsin. Afterwards, the myocytes were purified by passage through a Percoll gradient. Cells were grown in DMEM/Ham's F-12 supplemented with 10 % horse serum and 5 % fetal bovine serum. After 1 or 2 d depending on the cells, the medium was removed and the cells were washed and maintained in serum-free DMEM/Ham's F-12. Then, the neonatal cardiomyocytes were transduced directly.

Porcine aortic endothelial cells (PAEC)

Porcine aortic endothelial cells were provided by W. Kues (Institute of Farm Animal Genetics, Mariensee). First, the piece of porcine aorta was rinsed with PBS and antibiotics to remove erythrocytes. For isolation of endothelial cells, prewarmed Collagenase type II solution (1 mg/ml in PBS) was injected into the aorta. After 15 min incubation at 37 °C the solution was aspirated and centrifuged in the same volume of DMEM (5 min, 1000 rpm). The pelleted cells were grown in DMEM, 10 % FCS and ECGF and seeded into gelatin-coated flasks. Endothelial cells can then be recognized by their cobblestone morphology.

Porcine fibroblasts

Fetale porcine fibroblasts were isolated by outgrowth of fibroblasts of explant culture and kindly provided by B. Petersen (Institute of Farm Animal Genetics, Mariensee).

Human CD34⁺ cells

CD34⁺ cells were either freshly isolated as described in chapter 7.3.7 or purchased as frozen cells from CellSystems (7.3.7.2).

Melanoma cells

Primary melanoma cells from 3 different patients were kindly provided by MediGene AG (Martinsried).

6.8 Culture Media and Supplements

| <u>Product</u> | <u>Company</u> |
|--|-----------------------------|
| Ampicillin | Sigma, Deisenhofen |
| Ascorbic acid | Sigma, Deisenhofen |
| Bovine apo-transferrin | Sigma, Deisenhofen |
| Bovine insuline | Sigma, Deisenhofen |
| DMEM/Ham's F-12 | PAA, Pasching |
| Dulbecco's MEM + Glutamax-I (DMEM) | Invitrogen, Karlsruhe |
| Endothel Basal Medium | PAA, Pasching |
| Endothelial Cell Basal Medium-2 + supplements (EBM-2) | Lonza |
| Fetal Calf Serum (FCS) | Invitrogen, Karlsruhe |
| Hygromycin B | Roche, Mannheim |
| Lithium chloride | Sigma, Deisenhofen |
| Penicillin/Streptomycin (P/S) | Invitrogen, Karlsruhe |
| Phosphate-buffered saline (PBS) | Invitrogen, Karlsruhe |
| recombinant human Fms-related tyrosine kinase 3 ligand (Flt3L) | Dunnlab, Asbach |
| recombinant human Interleukin 3 (IL3) | Dunnlab, Asbach |
| recombinant human Interleukin 6 (IL6) | Endogen |
| recombinant human Stem Cell Factor (SCF) | Endogen |
| recombinant human VEGF 165 | R&D Systems |
| Sodium selenate | Sigma, Deisenhofen |
| StemSpan serum-free expansion medium | CellSystems, St. Katharinen |
| Trypsin-EDTA | Invitrogen, Karlsruhe |

Media compositions for cell types are listed below:

HeLa, HEK293, melanoma cells and porcine aortic endothelial cells (PAEC):

- Dulbecco's-MEM and Glutamax-I
- 10 % FCS
- 100 U/ml penicillin and 100 mg/ml streptomycin

Materials

Porcine fibroblasts:

- Dulbecco's-MEM and Glutamax-I
- 20 % FCS
- 100 U/ml penicillin and 100 mg/ml streptomycin

Rat aortic endothelial cells (RAEC):

- Endothel Basal Medium (PAA)
- 10 % FCS
- 5 µg/ml gentamycin

Neonatal rat cardiomyocytes:

- DMEM/Ham's F-12
- 10 mg/ml ampicillin
- 1 µg/ml bovine insuline
- 5 µg/ml bovine apo-transferrin
- 1 nM sodium selenate
- 1 nM lithium chloride
- 25 µg/ml ascorbic acid
- (10 % horse serum and 5 % FCS only during the first 1 to 2 d after isolation)

CD34⁺ cells (expansion medium):

- Stem Span serum-free expansion medium
- IL-3 20 ng/ml
- IL-6 20 ng/ml
- SCF 100 ng/ml
- Flt3-ligand 100 ng/ml

CD34⁺ cells (endothelial differentiation medium):

- Endothelial Cell Basal Medium-2 + supplements as provided
- 20 % FCS
- 50 ng/ml VEGF 165

6.9 Laboratory Equipment and Disposables

| Product | Company |
|---|--|
| µQuant Microplate Spectrophotometer | BioTek Instruments, Bad Friedrichshall |
| Axiovert 25 CFL | Carl Zeiss, Göttingen |
| Axiovert S100 | Carl Zeiss, Göttingen |
| Balance Adventure Pro | Ohaus, NJ, USA |
| Blood collecting bag | MacoPharma |
| Cell Culture Plastic Ware | Beyer, Düsseldorf |
| Centrifuge 5415D | Eppendorf, Hamburg |
| Centrifuge 5-6B | Beckman, München |
| Centrifuge 5810R | Eppendorf, Hamburg |
| FACScalibur | Becton Dickinson, Heidelberg |
| Filter (0.22 µm, 0.45 µm) | Schleicher & Schuell Micro Science, Dassel |
| General laboratory ware | VWR, Darmstadt |
| Heater/Magnetic Shaker Heidolph MR 3001 | Heidolph Instruments, Schwabach |
| Hera -80 °C freezer | Heraeus |
| Heraeus Lamina | Heraeus |
| HiTrap Heparin Affinity Columns (1 ml) | Amersham Pharmacia Biotech, Freiburg |
| Incubator Hera Cell 150 | Heraeus |
| Incubator Shaker Innova 4430 | New Brunswick Scientific, NJ |
| LightCycler 1 | Roche, Mannheim |
| LightCycler Capillaries | Roche, Mannheim |
| LightCycler carousel centrifuge | Roche, Mannheim |
| LSM 510 Meta | Carl Zeiss, Göttingen |
| Microplate Luminometer LB 96 V | EG&G Berthold, Bad Wildbad |
| Mini Sub GT Gel Electrophoresis Unit | BioRad, München |
| MiniMACS system | Miltenyi Biotech |
| Mixer Mill MM300 | Retsch, Haan |
| Olympus Vanox-S AH-2 | Olympus, Hamburg |
| pH Meter Seven Easy | Mettler-Toledo, Schwerzenbach |
| Pipettes and Filtertips | Sarstedt |
| Power Supply | Renner, Dannstadt |
| Pump P-1 | Amersham Pharmacia Biotech, Freiburg |
| Reaction tubes (1.5 ml, 2 ml) | Eppendorf, Hamburg |
| Sorvall T-865 rotor | Thermo Scientific |
| Sorvall Ultracentrifuge OTD Combi | Thermo Scientific |
| Spectrophotometer BioRad SmartSpec 3000 | BioRad, München |
| Syringes and Needles | B. Braun Melsungen, Melsungen |
| Thermomixer Comfort | Eppendorf, Hamburg |
| Vortex Genie 2 | Scientific Industries, NY, USA |
| Waterbath Medingen W6 | Medingen, Freital |

6.10 Data Treating Software

Microsoft Office Excel 2003; Micrografx Picture Publisher 8; Clone Manager 3;
Adobe Photoshop CS2; specific software for the respective instruments

7 Methods

7.1 *Bacteria Culture*

7.1.1 Cultivation of Bacteria

Bacteria were grown in LB medium at 37 °C under vigorous shaking over night. For generating single clones, bacteria were plated on plates containing LB and agar.

LB medium: 10 g tryptone
 5 g yeast
 5 g NaCl
 15 g agar
 ad 1 l distilled H₂O

7.1.2 Preparation of Competent Bacteria

One bacterial colony of the strain DH5 α was picked from an LB-agar plate and grown over night in LB at 37 °C. The following day the bacteria suspension was diluted 1:100 and grown till an optical density (OD) between 0.7 and 0.8 was reached. 50 ml of the suspension was cooled down for 10 min in an ice-cold water bath before pelleting the bacteria 10 min, 3200 rpm at 4 °C. The pellet was resuspended in 15 ml TFB I buffer and incubated 10 min at 4 °C. After centrifuging the bacteria (10 min, 800 x g, 4 °C), they were resuspended in 2 ml TFB II buffer. 200 μ l aliquots of the chemo-competent bacteria were shock-frosted in liquid nitrogen and stored at -80 °C.

TFB I buffer (200 ml): 30 mM potassium acetate
 100 mM CaCl₂
 15 % glycerol
 ad 190 ml H₂O

Autoclavation, than addition of sterile filtered:
 50 mM MnCl₂

TFB II buffer (50 ml): 10 mM MOPS
 75 mM CaCl₂
 10 mM KCl
 15 % glycerol
 ad 50 ml H₂O

7.1.3 Transformation of Bacteria

Chemo-competent bacteria were thawed on ice. 100 to 500 ng DNA were added to 50 µl bacterial suspension and agitated carefully. The mixture was incubated 30 min on ice before heat shock treatment for 30 s at 37 °C. Immediately, bacteria were put back on ice. 5 min later 450 µl LB medium was added and mixed gently. 250 µl of the suspension could then be distributed on LB agar plates containing ampicillin (50 µg/ml). Bacteria grew over night at 37 °C. Single colonies were picked and analyzed the next day.

7.2 Working with nucleic acids

7.2.1 Plasmid amplification and extraction

For plasmid amplification and extraction the “Qiagen EndoFree Plasmid Mega Kit” was used according to the manufacturer’s instructions.

Starter bacteria cultures were inoculated from either glycerol stocks or picked as single clones from selective plates and grown in selective LB medium. This culture should then be diluted 1:500 in an absolute volume of 2.5 l and grown shaking over night at 37 °C. Harvesting followed at 6000 x g for 30 min at 4 °C. For efficient alkaline lysis, the pellet was resuspended in 50 ml P1 buffer then inverted several times after adding 50 ml of buffer P2 and incubated 5 min at room temperature. Lysis was stopped and precipitation of genomic DNA, proteins and cell debris was enhanced by adding 50 ml of chilled buffer P3 and shaking vigorously until a white fluffy material has formed. The lysate was poured into the QIAfilter Cartridge which has been screwed onto a glass bottle and incubated for 10 min. A vacuum source pulled the liquid through the filter. 50 ml of FWB2 buffer should then be added to the Cartridge, stirred and filtered again. Endotoxins could be removed from the filtrate by 12.5 ml ER buffer, inverting the bottle and incubation on ice for 30 min. The QIAGEN-tip 2500 was equilibrated by 35 ml QBT buffer before the lysate was applied to the column. 200 ml of washing buffer QC

were used to rinse the column before DNA was finally eluted in 35 ml buffer QN. DNA precipitation followed by adding 24.5 ml isopropanol, mixing and pelleting at 3200 x g at 4 °C for a minimum of 30 min. Supernatant was removed and the pellet was washed with 7 ml 70 % ethanol and another centrifugation step for 10 min. Again, the supernatant was taken off and the pellet was allowed to dry for some minutes before a suitable volume of endotoxin-free buffer TE was added. To minimize the risk of shearing events, the suspension was left over night in the fridge to let solve the DNA before quantification and analysis.

7.2.2 DNA and RNA Quantification

DNA and RNA samples were diluted in H₂O before they were measured in a BioRad SmartSpec 3000 spectrophotometer. The measured wavelength is 260 nm, concentrations are calculated by the conversion factors 50 µg/ml for double-stranded DNA and 40 µg/ml for RNA. The purity of the DNA preparation is given by the ratio Abs 260 nm / Abs 280 nm. While 1.8 is ideal, lower values point to contaminations with proteins and aromatic substances whereas higher ratios indicate possible contaminations with RNA.

7.2.3 Restriction Enzyme Digest

Digestion with restriction enzymes was performed according to the manufacturer's instructions in a 20 µl solution containing 1 µg of DNA, 1-10 units of restriction enzyme per 1 µg DNA and 1 x buffer.

7.2.4 Agarose Gel Electrophoresis

Restriction enzyme digests as well as PCR products were analyzed by agarose gel electrophoresis to verify the size of the fragments or products.

Therefore, 1 x TBE buffer was boiled with the desired amount of agarose, mixed with the intercalating substance ethidium bromide (0.25 µg/ml) and poured into the gel chamber. The comb was directly inserted and taken out when solidification occurred before the chamber was put into the electrophoresis chamber containing 1 x TBE. For large fragments 0.8 % agarose, for smaller ones 2 % was used. 300 to 500 ng of restriction digested DNA or 10 µl of the PCR products were mixed with loading dye filled up with H₂O to a final volume of 10 µl and loaded onto the gel. Depending on the size of the gel between 80 and 140 V and 200 mA was chosen for electrophoresis.

TBE Buffer (10 x): 540 g Tris base
 275 g boric acid
 200 ml 0.5 M EDTA pH 8.0
 ad 5 l H₂O

7.2.5 Tissue DNA extraction

Frozen animal tissue samples of about 50 mg were cut into small pieces and DNA was extracted using the DNeasy Blood & Tissue Kit (Qiagen) according to the manufacturer's instructions with small modifications.

360 µl of the buffer ATL was added to the tissue samples as well as 40 µl of the Proteinase K (double amount of what is recommended). Tissue lysis was induced at 56 °C in a thermomixer for some hours up to over night incubation. After 15 s of vortexing, first 400 µl of buffer AL was added, vortexed, then 400 µl ethanol. Only fluid and very small precipitates were applied to the DNeasy Mini spin column in order to prevent blocking. DNA stuck to the column and the rest of the lysate was removed by centrifugation at 10,000 x g for 1 min. Salts and proteins were eliminated by two washing steps: The first time using buffer AW1 (centrifugation for 1 min at 16,000 x g) the second with buffer AW2 and 3 min of centrifugation for drying the membrane completely. DNA was eluted in 50 µl Tris (10 mM, pH 8.0) after 1 min of incubation on the membrane and 1 min of centrifugation at 10,000 x g. DNA concentration was measured as described in 7.2.2 and diluted to a final concentration of 100 ng/µl prior to quantitative PCR analysis. DNA was stored at -20 °C.

7.2.6 Tissue RNA extraction

RNA was extracted using the Trizol / Chloroform method. Briefly, 1 ml of Trizol was pipetted into a 2 ml safe-lock tube containing one small metal ball. Tubes were put on ice after adding around 50 mg of organ. Homogenization was performed using a ball mill (Mixer Mill MM300, Retsch) at 30 Hertz for 3 min. The lysate was then incubated for 5 min at room temperature before 200 µl of chloroform were pipetted and vortexed. After 3 min of incubation at room temperature the mixture was centrifuged 15 min at 16,000 x g at 4 °C. After centrifugation 2 phases are visible, the lower Trizol phase and the upper aqueous phase containing the RNA. Carefully, the supernatant was pipetted into a fresh 1.5

ml tube without touching the protein interphase. For pelleting the RNA 500 μ l of isopropanol was added, vortexed and incubated for 10 min at room temperature then centrifuged 15 min at 16,000 x g at 4 °C. Further washing of the pellet was done with 1 ml of 75 % ethanol and centrifugation (7,500 x g, 5 min, 4 °C). After removing the supernatant the pellet should be air-dried and resuspended in 30 (heart) to 150 μ l (liver) RNase-free water depending on the size of the pellet. RNA concentration was measured as described in 7.2.2 and stored at -80 °C.

7.2.7 DNase I digest and cDNA synthesis

To prevent unspecific signals in the cDNA PCR reaction due to remaining DNA in the RNA preparation, DNase I digest was done before Reverse Transcriptase (RT) reaction.

RNA was thawed on ice and 10 μ g were taken out. The RNA was mixed with the same volume of PBS, 1 U/ μ g RNA DNase I and 0.1 mg/ml BSA and 2.5 mM MgCl₂ as end concentration. Incubation for 30 min at 37 °C was stopped by adding 2.5 mM EDTA end concentration and heating for 10 min at 65 °C. Samples were then put on ice.

Transcriptor First Strand cDNA Synthesis Kit (Roche) was used to transcribe mRNA into cDNA according to the manufacturer's instructions. Therefore, 1 μ l Oligo dT-primer (50 μ M) were added to around 3 μ g of DNase I-digested RNA and filled up with RNase-free water up to 13 μ l. Incubation at 65 °C for 10 minutes denatured the secondary structure. For starting the RT reaction the following reagents supplied with the kit were pipetted into the RNA-primer-mix to a final volume of 20 μ l:

- 4 μ l RT buffer (5x)
- 0.5 μ l RNase Inhibitor (40 U/ μ l)
- 0.5 μ l RT (20 U/ μ l)
- 2 μ l dNTPs (each of 10 mM)

The mix was incubated 1 h at 42 °C followed by a heating step (85 °C, 5 min). Afterwards, samples were put on ice or if not used immediately stored at -20 °C.

7.2.8 Quantitative Polymerase-Chain-Reaction

For analyzing the DNA amount by quantitative polymerase-chain reaction (PCR) in a LightCycler 1 system (Roche) either a kit by Roche (LightCycler Fast Start DNA Master SYBR Green I) or by Qiagen (Quantitect SYBR Green PCR Kit) was used depending on the ability to accomplish the particular amplification in the most sensitive and specific way. The kit purchased from Roche was used to quantify GFP, Luciferase and porcine GAPDH genes whereas the Qiagen kit was applied for rat GAPDH and LacZ coding sequences.

100 to 200 ng of DNA and cDNA were analyzed per capillary. For determination of genomic titer of AAV vector preparation 2 μ l of the extracted DNA (7.3.6.4) was analyzed.

Pipetting scheme using LightCycler Fast Start DNA Master SYBR Green I:

| | |
|-------------------------------|---------------------------|
| 2 μ l | DNA or cDNA |
| 2 μ l | Mix 1 |
| 2 μ l | MgCl ₂ (25 mM) |
| 0.1 μ l | Primer forward (0.1 mM) |
| 0.1 μ l | Primer reverse (0.1 mM) |
| <u>13.8 μl</u> | H ₂ O |
| 20 μ l | |

If Qiagen's kit was applied, the following scheme was pipetted:

| | |
|------------------------------|--------------------------------------|
| 2 μ l | DNA or cDNA |
| 10 μ l | Quantitect SYBR Green PCR Master Mix |
| 0.1 μ l | Primer forward (0.1 mM) |
| 0.1 μ l | Primer reverse (0.1 mM) |
| <u>7.8 μl</u> | H ₂ O |
| 20 μ l | |

For eliminating potential contaminations with PCR products of previous amplifications, LightCycler Uracil-DNA (UNG) Glycosylase was added. Its effect is based on cutting of Uracil-containing DNA. This nucleotide is only inserted during PCR where it is supplied in the mix. The enzyme works for 10 min at 40 °C and is inactivated during the denaturation step for 5 min at 95 °C. We used UNG

Methods

glycosylase in very sensitive PCRs – here LacZ for analyzing material out of animals.

| | |
|-------------------------------|--------------------------------------|
| 2 μ l | DNA or cDNA |
| 10 μ l | Quantitect SYBR Green PCR Master Mix |
| 0.1 μ l | Primer forward (0.1 mM) |
| 0.1 μ l | Primer reverse (0.1 mM) |
| 0.25 μ l | UNG (2 U/ μ l) |
| <u>7.55 μl</u> | H ₂ O |
| 20 μ l | |

Usually a supermix for all samples was prepared. First, the mix was pipetted into the glass capillaries followed by the DNA. Then the capillaries were closed. The following protocols were established:

GFP-PCR protocol:

| Program | Cycles | Analysis mode | Temp (°C) | Time (s) | slope (°C/s) | Acquisition mode |
|---------------|--------|----------------|-----------|----------|--------------|------------------|
| Denaturation | 1 | None | 95 | 900 | 20 | none |
| Amplification | 40 | Quantification | 95 | 10 | " | " |
| | | | 63 | 3 | " | " |
| | | | 72 | 20 | " | single |
| Melting curve | 1 | Melting curves | 95 | 0 | " | " |
| | | | 66 | 10 | " | " |
| | | | 95 | 0 | 0.1 | continuous |
| Cooling | 1 | None | 40 | 30 | 20 | none |

Luciferase-PCR protocol:

| Program | Cycles | Analysis mode | Temp (°C) | Time (s) | slope (°C/s) | Acquisition mode |
|---------------|--------|----------------|-----------|----------|--------------|------------------|
| Denaturation | 1 | None | 95 | 900 | 20 | none |
| Amplification | 40 | Quantification | 95 | 10 | " | " |
| | | | 69 | 5 | " | " |
| | | | 72 | 12 | " | single |
| Melting curve | 1 | Melting curves | 95 | 0 | " | " |
| | | | 66 | 10 | " | " |
| | | | 95 | 0 | 0.1 | continuous |
| Cooling | 1 | None | 40 | 30 | 20 | none |

Methods

Porcine GAPDH-PCR protocol:

| Program | Cycles | Analysis mode | Temp (°C) | Time (s) | slope (°C/s) | Acquisition mode |
|---------------|--------|----------------|-----------|----------|--------------|------------------|
| Denaturation | 1 | None | 95 | 900 | 20 | none |
| Amplification | 40 | Quantification | 95 | 10 | " | " |
| | | | 68 | 10 | " | " |
| | | | 72 | 15 | " | single |
| Melting curve | 1 | Melting curves | 95 | 0 | " | " |
| | | | 66 | 10 | " | " |
| | | | 95 | 0 | 0.1 | continuous |
| Cooling | 1 | None | 40 | 30 | 20 | none |

LacZ and rat GAPDH-PCR protocol:

| Program | Cycles | Analysis mode | Temp (°C) | Time (s) | slope (°C/s) | Acquisition mode |
|---------------|--------|----------------|-----------|----------|--------------|------------------|
| Denaturation | 1 | None | 95 | 900 | 20 | none |
| Amplification | 40 | Quantification | 95 | 10 | " | " |
| | | | 68 | 10 | " | " |
| | | | 72 | 15 | " | single |
| Melting curve | 1 | Melting curves | 95 | 0 | " | " |
| | | | 66 | 10 | " | " |
| | | | 95 | 0 | 0.1 | continuous |
| Cooling | 1 | None | 40 | 30 | 20 | none |

S18-PCR protocol:

| Program | Cycles | Analysis mode | Temp (°C) | Time (s) | slope (°C/s) | Acquisition mode |
|---------------|--------|----------------|-----------|----------|--------------|------------------|
| Denaturation | 1 | None | 95 | 600 | 20 | none |
| Amplification | 45 | Quantification | 95 | 10 | " | " |
| | | | 62 | 5 | " | " |
| | | | 72 | 10 | " | single |
| Melting curve | 1 | Melting curves | 95 | 0 | " | " |
| | | | 60 | 10 | " | " |
| | | | 95 | 0 | 0.1 | continuous |
| Cooling | 1 | None | 40 | 30 | 20 | none |

C9-PCR protocol:

| Program | Cycles | Analysis mode | Temp (°C) | Time (s) | slope (°C/s) | Acquisition mode |
|---------------|--------|----------------|-----------|----------|--------------|------------------|
| Denaturation | 1 | None | 95 | 600 | 20 | none |
| Amplification | 38 | Quantification | 95 | 10 | " | " |
| | | | 61 | 10 | " | " |
| | | | 72 | 10 | " | single |
| Melting curve | 1 | Melting curves | 95 | 0 | " | " |
| | | | 60 | 10 | " | " |
| | | | 95 | 0 | 0.1 | continuous |
| Cooling | 1 | None | 40 | 30 | 20 | none |

To verify the amplified products, melting curves of the LightCycler runs were analyzed. Moreover, they could be analyzed in Agarose Gel electrophoresis.

7.3 Eukaryotic cell culture

7.3.1 Cultivation of Cells

Cells were cultured at 37 °C in humid atmosphere containing 5 % CO₂. For culture media please refer to chapter 6.8.

7.3.2 Trypsinization

To detach cells from the culture dishes, medium was taken off and cells were washed with PBS to remove rests of the medium. Then they were incubated in a small volume of trypsin in the incubator until detachment was visible. The reaction was stopped by addition of medium containing 10 % FCS.

7.3.3 Counting

After trypsinizing the cells, 10 µl of the suspension was transferred into a “Neubauer” chamber. Four squares were counted and an average was calculated. The number of cells (n) in one square equals $n \times 10^4$ per ml.

7.3.4 Seeding / Passaging

Cells were transferred into a new culture dish in a suitable dilution of prewarmed, fresh medium. Agitation of the culture plates and flasks should guarantee homogenous distribution of the cells.

7.3.5 Freezing and Thawing Cells

Cells were trypsinized and pelleted before resuspending them in 1 ml freezing solution containing 90 % FCS and 10 % DMSO. Immediately, the suspension was put on ice and then stored in liquid nitrogen.

For thawing cells, the freezing vial was taken out of the liquid nitrogen tank and transported on ice. Carefully, the suspension was thawed in a water bath at 37 °C until only some rests of ice were left. Then, the cells were transferred into a 15 ml plastic tube containing prewarmed medium before pelleting the cells at 400 x g for 5 min at room temperature in order to remove toxic DMSO. After resuspension in fresh medium, the cells were plated in culture dishes. For CD34⁺ cells another thawing protocol was followed (7.3.7.2).

7.3.6 Vector production and purification

7.3.6.1 AAV-Vector Packaging

AAV particles were produced in HEK293 cells by the adenovirus-free production method using pXX6 to supplement the adenoviral helper functions (Xiao, Li, and Samulski, 1998). Briefly, 7.5×10^6 HEK293 cells were seeded in 15 cm² cell culture plates. 24 h later (at an approximate confluence of 80 %) medium was exchanged and 2 h afterwards cotransfection was performed with the three packaging plasmids by the calcium phosphate method with a total of 37.5 µg plasmid DNA per 15 cm² cell culture plate:

7.5 µg pXR1 (or pXR2/ pXR3/ pXR4/ pXR5 coding for the respective capsid)

7.5 µg transgene-encoding plasmid (contains ITRs)

22.5 µg pXX6 (encodes for E2A, E4 and VA of Ad5)

For each plate a solution of 1 ml CaCl₂ (250 mM) was mixed with the plasmid DNA then 1 ml of the HBS buffer (50mM HEPES, 280mM NaCl, 1.5 mM NaP) was dropped onto the solution incubated for 2 min and pipetted onto the plate while cautious mixing with the medium. After 24 h incubation at 37 °C/ 5 % CO₂ medium was exchanged with DMEM containing only 2 % FCS to reduce further cell divisions. The transfected cells were harvested and pelleted by low-speed centrifugation on the following day (48 h post transfection). The pellet was resuspended in lysis buffer (150 mM NaCl, 50 mM Tris-HCl (pH 8.5)) and the cellular and nuclear membranes were destroyed by repeated freeze and thaw

cycles. To abolish genomic and plasmid DNA or RNA contaminants in the vector preparation, the suspension was treated with 50 U/ml Benzonase for 30 minutes at 37 °C. Then, the suspension was centrifuged 30 min at 4 °C and 3,220 x g. The supernatant was taken off carefully and centrifuged again.

7.3.6.2 Iodixanol Gradient Purification

Discontinuous iodixanol gradient centrifugation was used to remove cellular debris. Full capsids are concentrated in the 40 % phase of the iodixanol gradient.

Vector suspension was inserted into an ultracentrifugation tube. The different phases of the iodixanol gradient - beginning with 15 % - were sub layered by using a syringe connected to an Amersham Biosciences Pump P-1. 8, 6, 5 and 6 ml of the respective solutions were applied. The tube was filled up with PBS/MgCl₂(1 mM)/KCl(2.5 mM), closed and centrifuged at 63,000 rpm at 4 °C for 2 h (Sorvall Ultracentrifuge OTD Combi). Subsequently, the 40 % iodixanol phase was harvested.

| | 15% | 25% | 40% | 60% |
|-----------------------|----------|----------|----------|----------|
| 10x PBS | 5 ml | 5 ml | 5 ml | / |
| 1 M MgCl ₂ | 50 µl | 50 µl | 50 µl | 50 µl |
| 2.5 M KCl | 50 µl | 50 µl | 50 µl | 50 µl |
| 5 M NaCl | 10 ml | / | / | / |
| Optiprep | 12.5 ml | 20 ml | 33.3 ml | 50 ml |
| 0.5% Phenolred | 75 µl | 75 µl | / | 25 µl |
| H ₂ O | ad 50 ml | ad 50 ml | ad 50 ml | ad 50 ml |

7.3.6.3 Heparin Affinity Chromatography

For purification of vectors which are able to bind to heparin, e.g. rAAV2 and rAAV3, affinity chromatography using heparin columns (1ml) from Amersham Pharmacia Biotec might be performed instead or additional to iodixanol gradient centrifugation. Therefore the Amersham Biosciences Pump P-1 was used. First, the column was equilibrated with PBS/MgCl₂(1 mM)/KCl(2.5 mM), while the vector solution was diluted 1:10 in the same buffer and applied to the column. After a washing step with 20 ml PBS/Mg/K, vector was eluted with PBS/Mg/K plus 1 M NaCl in 500 µl steps.

7.3.6.4 Vector titration

For extraction of the vector genome from the viral particles the Qiagen DNeasy Blood & Tissue Kit was used according to the protocol for Isolation of Total DNA from Cultured Animal Cells. For alkaline lysis, 10 µl of the vector solution was mixed with 190 µl PBS, 200 µl buffer ATL and 20 µl Proteinase K and incubated for 10 min at 56 °C. Subsequently, the samples were vortexed and 200 µl of buffer AL and ethanol (96-100 %) were added. The solution was applied to a DNeasy Mini Spin column, centrifuged and washed in AW1 and AW2 buffer before the DNA was eluted in 200 µl Tris 10 mM pH 8.0.

The genomic titer was then determined by quantitative PCR as described in 7.2.8. To quantify the amount of vector genomes within the extracted DNA, defined dilutions (1×10^8 to 1×10^5 genomic particles/µl) from the respective transgene-encoding plasmid were prepared and used as standards in the quantitative PCR.

7.3.7 Working with CD34⁺ cells

7.3.7.1 Isolation and culturing of CD34⁺ cells

Only the cord blood of mothers who gave their written agreement was recovered in heparin-containing bags directly after birth. The purification steps consist of an isolation of mononuclear blood cells (MBC) by Ficoll-density gradient followed by magnetic cell sorting of CD34⁺ cells. This work has been accomplished by Michele Cadau (Centro Cardiologico, Monzino, Italy).

First, the blood was diluted in two volumes phosphate-buffered saline (PBS without Ca⁺⁺ and Mg⁺⁺). Two volumes of diluted blood were layered carefully over one volume of Ficoll. After 30 min of centrifugation at 400 x g in a swinging rotor without brake at room temperature, the MBC-containing ring between plasma and Ficoll was collected. Afterwards, the cells were washed twice in PBS/2 mM EDTA/5 % FCS by centrifugation (10 min, 400 x g, 4 °C) and resuspended in the precedent buffer solution.

For the following positive selection with immunomagnetic beads the Direct CD34 Progenitor Cell Isolation Kit (Miltenyi Biotech) was used according to the manufacturer's instructions. MBCs were shaken for 30 min on ice with 100 µl Fc receptor blocking reagent per 10^8 cells before adding monoclonal mouse anti-human CD34 antibody-coupled magnetic beads (IgG1 isotype). After an additional washing step like above, cells were resuspended in 500 µl PBS/ 2 mM EDTA/ 5 %

FCS and sorted on an activated column placed in the magnetic field of a MACS separator (miniMACS system, Miltenyi Biotec). The labelled cells are bound to the column and therefore separated from other cell populations. After rinsing the column with 1 ml PBS/ 2 mM EDTA/ 5 % FCS and removal of the column from the magnetic field, the magnetically retained cells can be eluted as positively selected cell fraction. The purity of the obtained cell fraction used to be more than 80 % as assessed by FACS analysis for CD34 expression.

Cells were expanded prior to use for a 2 to 4 days in 300 µl medium in 96-well plates at 37 °C and 5 % CO₂. Serum-free culture medium (Stem Span, CellSystems) was supplemented with Flt3-ligand (100 ng/ml), SCF (100 ng/ml), IL-3 (20 ng/ml), IL-6 (20 ng/ml) and sterile filtrated. Medium was exchanged every 2 to 3 d.

7.3.7.2 Thawing of CD34⁺ cells

Purchased cells from CellSystems were thawed according to the manufacturer's instructions. Cells were almost completely thawed by putting them into a water bath (37 °C). 1 ml of pre-warmed StemSpan medium without cytokines was applied to the cells and then transferred into a 50 ml tube containing 50 µl DNase I (10,000 U/ml) for prevention of cell clumping. Fresh medium was dropped slowly to an end volume of 15 ml while turning the tube. Cells were pelleted (200 x g, 22 °C, 15 min), the supernatant was taken off carefully and the procedure was repeated. Cells were counted and seeded in StemSpan medium containing cytokines into 96-well plates (for culture media see 7.3.7.1).

7.3.7.3 Transduction of CD34⁺ cells with AAV

After expanding the cells for 2 to 4 days, 8×10^4 cells per well were seeded in a 96-well plate. Later, cells were incubated in medium with half-cytokine concentration containing the vector solution or iodixanol over a period of 3 h. Then a washing step with PBS was performed to remove the iodixanol. Cells were centrifuged at 400 x g for 10 min at 4 °C und resuspended in fresh medium with normal cytokine concentration.

7.3.7.4 Analysis of transduced CD34⁺ cells by FACS

Cells were harvested, centrifuged at 400 x g for 10 min at 4 °C and resuspended in 250 µl PBS. The cells were directly used if GFP fluorescence should be

measured. For the analysis of $\alpha_v\beta_5$ integrins, cells were harvested and washed as above, but resuspended in 50 μ l PBS and 1 μ l of primary antibody (mouse anti-human monoclonal antibody, 1 mg/ml, Chemicon). After 15 min incubation on ice and a following washing step, 1 μ l of secondary antibody (goat anti-mouse IgG-PE labelled polyclonal antibody, abcam) was added to 50 μ l cell suspension in PBS. FACS analysis started after 15 min incubation on ice and an additional washing step. Unstained cells and cells that were only treated with secondary antibody were used as controls.

7.3.8 Dil-AcLDL uptake

Endothelial cells can be characterized by their ability to take up acetylated low-density lipoproteins (AcLDL). Acetylation of lysine rests inhibits binding to the LDL-receptor. Instead the fluorescence (Dil-) labeled substance can be bound and taken up efficiently by scavenger receptors of endothelial cells and macrophages.

Endothelial cells were incubated 4 to 5 h in 1 μ g/ml Dil-AcLDL (CellSystems) diluted in medium at 37 °C. Then the supernatant was taken off and cells were rinsed twice with PBS prior to fixation in 3 % paraformaldehyde at room temperature for 15 min. After two more rinsing steps the plates were stored at 4 °C and analyzed by fluorescence microscopy (Zeiss Axiovert S100).

7.4 Determination of protein

7.4.1 Detection of beta-Galactosidase activity in tissue sections

Cryosections were done in the Institute of Pathology (M. Odenthal, University Hospital of Cologne). Sections were dried over night and kept at -80 °C. For staining, they were put directly in 1.5 % glutaraldehyde/ PBS for 5 min and washed 3 times for 30 s in distilled water. Then the object slides were incubated 2 min in PBS before changing to LacZ staining solution which consists of:

- 2 ml X-Gal in DMSO (20 mg/ml)
- 100 μ l 1M MgCl₂
- 20 ml 50 mM Potassium hexacyanoferrat II trihydrat (50 mM)
- 20 ml 50 mM Potassium hexacyanoferrat III (50 mM)
- 160 ml PBS

The cryosections were incubated for 2 d at 37 °C in the dark. The following day the object slides were washed 2 times for 30 s in distilled water. If no counterstaining with eosin was performed, water was removed by an ascending ethanol series of 70, 80 and 2 times 100 % for 2 min each. X-tra solv (Medite) was used as xylol substitute 2 times for 2 min before covering the object slides with DPX mounting medium for histology (Fluka). For counterstaining cryosections were incubated for 8 min in 0.5 % eosin solution followed by 2 washing steps in 100 % ethanol for 2 min. As above incubation with X-tra solv and covering were the last steps. Pictures were taken with an Olympus Vanox-S AH-2 microscope.

7.4.2 Staining for beta-Galactosidase activity in cells

The following values are calculated for a 1 cm² well. Medium was taken off and cells were washed with PBS. Cells were fixed 5 min in 300 µl 1.5 % glutaraldehyde diluted in PBS and washed again for 5 min in PBS. Then 500 µl of LacZ staining solution were added to the cells and incubated at 37 °C for 3 to 7 h depending on the developing blue color intensity.

LacZ staining solution for 10 ml:

- 500 µl X-Gal in DMSO (20 mg/ml)
- 6.5 ml PBS
- 1 ml MgCl₂ (20 mM)
- 1 ml Potassium hexacyanoferrat II trihydrat (50 mM)
- 1 ml Potassium hexacyanoferrat III (50 mM)

Then LacZ solution was exchanged against 3 % DMSO/ PBS in order to stabilize staining and cells for some days.

7.4.3 Bradford Assay

To determine protein amount of tissue samples around 20 mg tissue were added to 400 µl lysis buffer (*Renilla* Luciferase Assay System, Promega) and one small metal ball to homogenize the tissue sample in a ball mill (Mixer Mill MM300, Retsch) at 30 Hertz for 3 min. After an incubation step of 1 h on ice the lysates were centrifuged for 30 min at 4 °C at 16,000 x g and the supernatant was transferred into a new Eppendorf tube. In double, 5 µl of the lysates (or adequate dilutions) and the BSA standards were pipetted into a 96-well plate. Then 250 µl room-temperature Bradford Dye 1 x were added and incubated 5 to 60 min. The

plate was be measured at a wavelength of 595 nm in an ELISA reader and analyzed by Microsoft Excel.

7.4.4 Luciferase Assay

20 µl of protein lysates (see 7.4.3) were put into a 96-well plate (Nunc) before a mixture of 100 µl assay buffer and 1 µl of the substrate (*Renilla* Luciferase Assay System, Promega) per well were added to the sample. Because the chemoluminescence is fading relatively fast, a maximum of 24 samples were measured at once. To compare relative light units these results were normalized to the total protein amount determined by Bradford assay.

7.5 Heterotopic heart transplantation

7.5.1 Rat heart transplantation

Transplantations were performed by Lars Burdorf (B. Reichart, M. Schmöckel, Department of Cardiac Surgery, Ludwig-Maximilians University Munich). Described is the operation method using cardioplegic solution, the so-called cold heart transplantation, in contrast to transplantation of a warm and beating heart. The technique is the same, but without the use of cardioplegic solution.

Male Sprague-Dawley rats were first narcotized by ether and then by peritoneal injection of Pentobarbital (60 mg/kg body weight). Organ recipients and donors were prepared in the same way, but only the recipients were layered onto a heating pad. After reaching chirurgical tolerance the animals were shaved and disinfected. Organ donors were prepared by abdominal incision. The intestines were put extraabdominal so that preparation of the infrarenal parts of the Vena cava inferior (V. cava inf.) and the Aorta abdominalis could proceed. The intestines and the opened abdomen had to be covered with moist tissues.

For explantation of the heart, the anticoagulans hirudin (30 mg/kg body weight) was applied into the V. cava inf. two minutes prior to opening of the sternum and application of 10 ml ice-cold cardioplegic solution (Custodiol/HTK Bretschneider) in the V. cava inf., respectively. Aorta abdominalis and V. cava inf. were cut through. When reaching asystoly, Truncus pulmonalis was disconnected and cut through. For cardioprotection another 2 ml of cardioplegic solution was injected into the Aorta ascendens and then the vector solution was applied very slowly. Finally, the

Venae cavae were ligated and cut through together with the Aorta. The explanted heart is kept in ice-cold physiological saline solution until implantation.

For implantation of the donor heart, the aorto-caval vessels are branched off infrarenally. Basically, incisions are made in these two vessels and then the donor Aorta ascendens was ligated to the Aorta abdominalis and the donor Truncus pulmonalis was anastomosed to the recipient V. cava inf.. Thus, blood flow was only circulating through the right part of the donor heart by entering through the aorta, flowing through the coronaries, the right atrium and ventricle to pass the pulmonary artery and then return into the circulation of the recipient.

To prevent hypovolemia, 2 ml of warm physiological saline solution was given into the abdominal cavity, intestines are layered back and the abdomen was closed.

As immunosuppressive therapy the animals received 0.3 mg/kg body weight Tacrolimus each day.

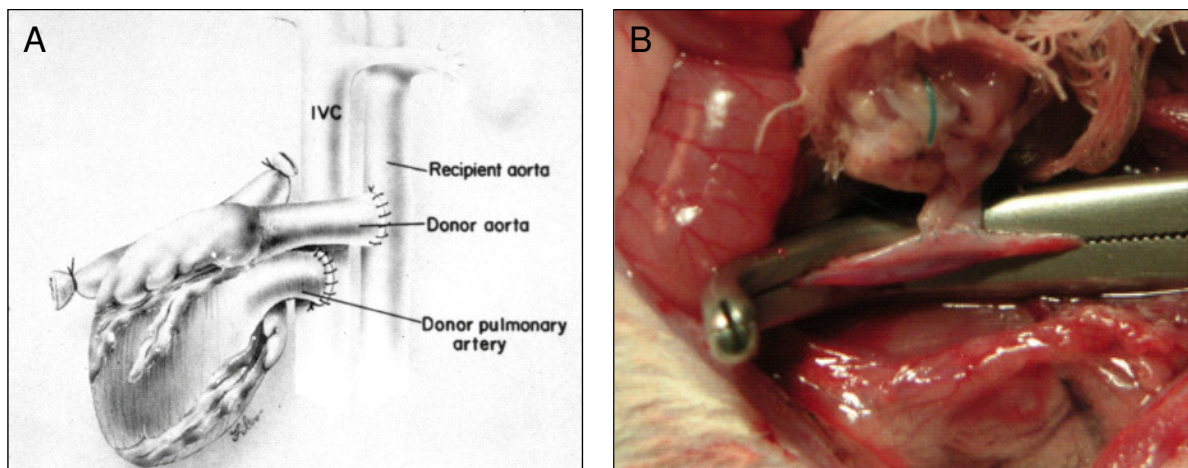


Figure 43: Anastomoses of the donor heart vessels with the aorta-caval vessels in the recipient abdomen. First showed schematic (A) and as picture taken during operation (B). The donor aorta ascendens is ligated to the recipient Aorta abdominalis and the donor pulmonary artery (Truncus pulmonalis) is ligated to the recipient Vena cava inferior. (Figures were kindly provided by L. Burdorf)

7.5.2 Pig heart transplantation

Transplantations were done by Lars Burdorf and colleagues (B.Reichart, Department of Cardiac Surgery, Ludwig-Maximilians-University Munich).

Only piglets of the same litter and blood group found application. Narcosis of recipient and donor was performed in the same way. Midazolam (0.75 – 1.5 mg/kg

body weight), Azaperon (25 mg/kg body weight), Ketamin (25 mg/kg body weight) and 0.5 mg Atropin were injected intramuscularly. Further drugs were applied by the ear vein like the anesthetic Propofol/Disoprivan (60-120 mg/h). Additionally, Enfluran (0.6 %) was given by inhalation.

The pigs were fixed on the operation table. They were intubated and artificial respiration was induced (Servo 900). Vital parameters were observed by a central-nervous catheter (V. jugularis) as well as electrocardiogram, analysis of saturation with oxygen and blood gas.

In contrast to rat cardiac transplantation, where the vector was injected either in the warm and beating heart or in the cardioplegic heart followed directly by transplantation, our colleagues in Munich applied here a new system. This method, called *in situ* Langendorff perfusion system, allows recirculation of the vector solution in warmed and oxygenated blood through the beating heart *in situ* over a longer period (Figure 44). It might be of advantage that vectors are passing more than once the heart and having the opportunity for transduction, before circulating through other organs and binding there.

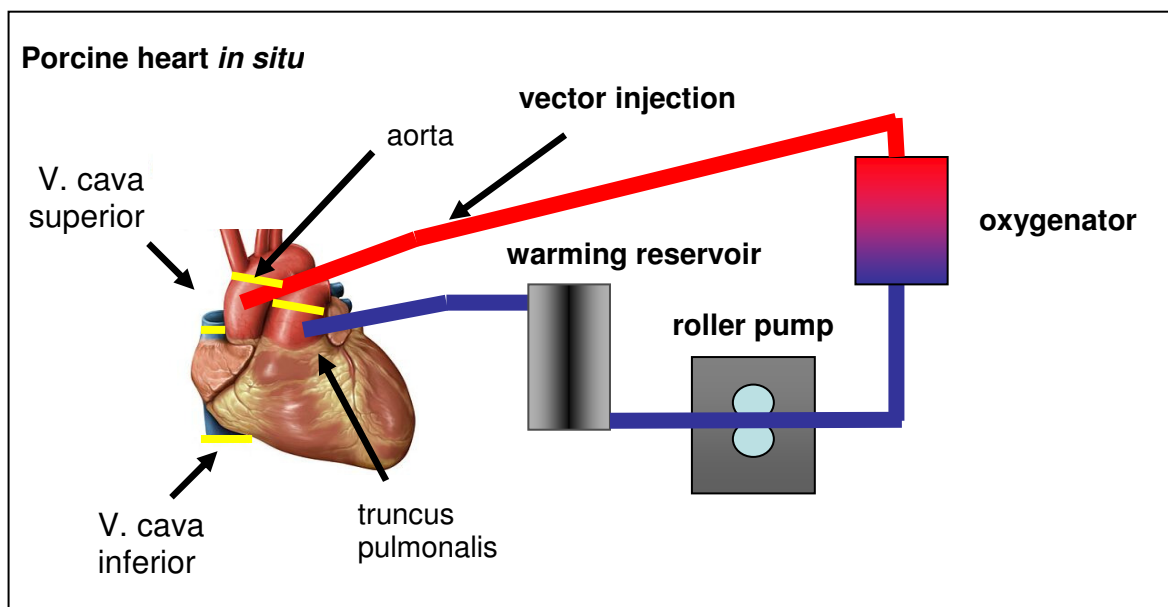


Figure 44: Scheme of an *in situ* Langendorff perfusion system. All vessels are clamped (marked in yellow) while the blood circulates through the truncus pulmonalis in a reservoir to warm the blood. A roller pump supports blood flow whereas an oxygenator provides oxygen for gas substitution. The blood enters the heart via the aorta and passes the coronaries. Vector is injected shortly before the entry into the heart. (Figure was modified and kindly provided by L. Burdorf)

In brief, the thorax of the donor pig was opened and the vessels and heart were made accessible. Hirudin (0.4 mg/kg body weight) was injected as anticoagulant. To connect the heart to the Langendorff perfusion system, needles were set into the aorta and the truncus pulmonalis. After clamping these vessels and the Venae cavae and after opening the needles connected to the Langendorff perfusion system, the blood circulates exclusively through the system. First, the blood is brought into a reservoir where it is warmed to 38 °C (physiological temperature). A roller pump supports blood flow and prevents stasis. As third element an artificial lung (oxygenator) enriches the blood with oxygen which goes back into the aorta. As this system pumps the blood retro gradually, it flows into the coronaries, from there into the right heart, takes the truncus pulmonalis and passes the perfusion system. Histamine (100 µg in 10 ml volume) was applied over a period of 4 min into the system in order to increase vascular permeability. Vector was injected shortly before the blood entered the heart via the aorta. Blood was circulating about 40 min before the heart was infused with cardioplegic solution (30 ml/kg body weight) to stop circulation.

The following explantation and implantation of the donor heart was performed in a comparable way as described for the rat heart transplantation (7.5.1). The recipient V. cava inferior was ligated to the donor A. pulmonalis and the recipient Aorta abdominals to the donor Aorta ascendens, respectively. The blood flow is as follows: from the donor Aorta abdominalis through the Aorta ascendens into the sinus coronaries. Then, it flows into the right atrium and ventricle to leave then the graft by the A. pulmonalis. The myocard is supplied by the coronaries.

For immunosuppression, Tacrolimus (0.3 mg/kg body weight) was already given during narcosis. From the second postoperative day on, 1.5 mg/kg body weight Tacrolimus was administered. Regularly, immunosuppression levels and other blood parameters were monitored. Functionality of the transplant was controlled by palpation and by electrocardiogram.

21 d after operation, the organ recipient was anesthetized like before, intubated and catheterized. Color, contractions and morphology of the donor heart were assessed before explantation.

8 Abbreviations

Amino acids

| | |
|---|---------------|
| A | alanine |
| C | cysteine |
| D | aspartate |
| E | glutamate |
| F | phenylalanine |
| G | glycine |
| H | histidine |
| I | isoleucine |
| K | lysine |
| L | leucine |
| M | methionine |
| N | asparagine |
| P | proline |
| Q | glutamine |
| R | arginine |
| S | serine |
| T | threonine |
| V | valine |
| W | tryptophan |
| Y | tyrosine |

Bases

| | |
|---|----------|
| A | adenine |
| C | cytosine |
| G | guanine |
| T | thymine |

| | |
|-------------|--|
| AAV | adeno-associated virus |
| Dil-AcLDL | acetylated low density lipoprotein |
| Ad | adenovirus |
| APC | antigen-presenting cell |
| bp | base pair |
| Bcl-2 | B-cell lymphoma 2 |
| LacZ | β -galactosidase |
| BM | bone marrow |
| ch | chromosome |
| CD | cluster of differentiation |
| CB | cord blood |
| CTLA4 | cytotoxic T-lymphocyte antigen 4 |
| d | day |
| EPC | endothelial progenitor cell |
| ELISA | enzyme-linked immunosorbent assay |
| Flk-1 | fetal liver kinase |
| FGF | fibroblast growth factor |
| FACS | fluorescence-activated cell sorting |
| Flt3-ligand | Fms-related tyrosine kinase 3 ligand |
| e.g. | for example |
| GAPDH | glyceraldehyde-3-phosphate dehydrogenase |

Abbreviations

| | |
|-------------|--|
| GM-CSF | granulocyte macrophage colony stimulating factor |
| GFP | green fluorescent protein |
| HSC | hematopoietic stem cell |
| HO-1 | heme oxygenase 1 |
| HSPG | heparan-sulfate proteoglycan |
| HGF | hepatocyte growth factor |
| HSV | herpes simplex virus |
| h | hour |
| HCMV | human cytomegalie virus |
| HPV | human papilloma virus |
| IL | Interleukin |
| ITR | inverted terminal repeat |
| kDa | kilo Dalton |
| MMP | matrix metalloproteinase |
| min | minute |
| MOI | multiplicity of infection |
| MAPC | multipotent adult progenitor cells |
| NPC | nuclear pore complex |
| nt | nucleotide |
| ORF | open reading frame |
| PNRE | perinuclear recycling endosome |
| RBS | Rep binding site |
| RA | retinoic acid |
| RRX | Rhodamine Red-X |
| rpm | rounds per minute |
| s | second |
| SC | stem cell |
| Sca-1 | stem cell antigen 1 |
| c-Kit | stem cell factor receptor |
| SDF-1 | stromal cell-derived factor 1 |
| TRS | terminal resolution site |
| TLR | toll-like receptor |
| TGF β | transforming growth factor β |
| CFTR | transmembrane conductance regulator |
| TSA | Trichostatin A |
| VE-caherin | vascular endothelial cadherin |
| VEGF | vascular endothelial growth factor |
| vIL-10 | viral Interleukin 10 |
| VP | viral protein |
| vWF | von Willebrand factor |
| w/o | without |

9 References

- Aicher, A., Heeschen, C., Mildner-Rihm, C., Urbich, C., Ihling, C., Technau-Ihling, K., Zeiher, A. M., and Dimmeler, S. (2003). Essential role of endothelial nitric oxide synthase for mobilization of stem and progenitor cells. *Nat Med* **9**(11), 1370-6.
- Aiuti, A., Slavin, S., Aker, M., Ficara, F., Deola, S., Mortellaro, A., Morecki, S., Andolfi, G., Tabucchi, A., Carlucci, F., Marinello, E., Cattaneo, F., Vai, S., Servida, P., Miniero, R., Roncarolo, M. G., and Bordignon, C. (2002). Correction of ADA-SCID by stem cell gene therapy combined with nonmyeloablative conditioning. *Science* **296**(5577), 2410-3.
- Akache, B., Grimm, D., Pandey, K., Yant, S. R., Xu, H., and Kay, M. A. (2006). The 37/67-kilodalton laminin receptor is a receptor for adeno-associated virus serotypes 8, 2, 3, and 9. *J Virol* **80**(19), 9831-6.
- Alexander, I. E., Russell, D. W., and Miller, A. D. (1997). Transfer of contaminants in adeno-associated virus vector stocks can mimic transduction and lead to artifactual results. *Hum Gene Ther* **8**(16), 1911-20.
- Alexander, I. E., Russell, D. W., Spence, A. M., and Miller, A. D. (1996). Effects of gamma irradiation on the transduction of dividing and nondividing cells in brain and muscle of rats by adeno-associated virus vectors. *Hum Gene Ther* **7**(7), 841-50.
- Andino, L. M., Conlon, T. J., Porvasnik, S. L., Boye, S. L., Hauswirth, W. W., and Lewin, A. S. (2007). Rapid, widespread transduction of the murine myocardium using self-complementary Adeno-associated virus. *Genet Vaccines Ther* **5**, 13.
- Angulo, A., Suto, C., Heyman, R. A., and Ghazal, P. (1996). Characterization of the sequences of the human cytomegalovirus enhancer that mediate differential regulation by natural and synthetic retinoids. *Mol Endocrinol* **10**(7), 781-93.
- Asahara, T., and Kawamoto, A. (2004). Endothelial progenitor cells for postnatal vasculogenesis. *Am J Physiol Cell Physiol* **287**(3), C572-9.
- Asahara, T., Masuda, H., Takahashi, T., Kalka, C., Pastore, C., Silver, M., Kearne, M., Magner, M., and Isner, J. M. (1999). Bone marrow origin of endothelial progenitor cells responsible for postnatal vasculogenesis in physiological and pathological neovascularization. *Circ Res* **85**(3), 221-8.
- Asahara, T., Murohara, T., Sullivan, A., Silver, M., van der Zee, R., Li, T., Witzenbichler, B., Schatteman, G., and Isner, J. M. (1997). Isolation of putative progenitor endothelial cells for angiogenesis. *Science* **275**(5302), 964-7.
- Asfour, B., Baba, H. A., Scheld, H. H., Hruban, R. H., Hammel, D., and Byrne, B. J. (2002). Uniform long-term gene expression using adeno-associated virus (AAV) by ex vivo recirculation in rat-cardiac isografts. *Thorac Cardiovasc Surg* **50**(6), 347-50.
- Askari, A. T., Unzek, S., Popovic, Z. B., Goldman, C. K., Forudi, F., Kiedrowski, M., Rovner, A., Ellis, S. G., Thomas, J. D., DiCorleto, P. E., Topol, E. J., and Penn, M. S. (2003). Effect of stromal-cell-derived factor 1 on stem-cell homing and tissue regeneration in ischaemic cardiomyopathy. *Lancet* **362**(9385), 697-703.
- Asokan, A., Hamra, J. B., Govindasamy, L., Agbandje-McKenna, M., and Samulski, R. J. (2006). Adeno-associated virus type 2 contains an integrin

- alpha5beta1 binding domain essential for viral cell entry. *J Virol* **80**(18), 8961-9.
- Assmus, B., Fischer-Rasokat, U., Honold, J., Seeger, F. H., Fichtlscherer, S., Tonn, T., Seifried, E., Schachinger, V., Dimmeler, S., and Zeiher, A. M. (2007). Transcoronary transplantation of functionally competent BMCs is associated with a decrease in natriuretic peptide serum levels and improved survival of patients with chronic postinfarction heart failure: results of the TOPCARE-CHD Registry. *Circ Res* **100**(8), 1234-41.
- Assmus, B., Honold, J., Schachinger, V., Britten, M. B., Fischer-Rasokat, U., Lehmann, R., Teupe, C., Pistorius, K., Martin, H., Abolmaali, N. D., Tonn, T., Dimmeler, S., and Zeiher, A. M. (2006a). Transcoronary transplantation of progenitor cells after myocardial infarction. *N Engl J Med* **355**(12), 1222-32.
- Assmus, B., Schachinger, V., Teupe, C., Britten, M., Lehmann, R., Dobert, N., Grunwald, F., Aicher, A., Urbich, C., Martin, H., Hoelzer, D., Dimmeler, S., and Zeiher, A. M. (2002). Transplantation of Progenitor Cells and Regeneration Enhancement in Acute Myocardial Infarction (TOPCARE-AMI). *Circulation* **106**(24), 3009-17.
- Assmus, B., Walter, D. H., Lehmann, R., Honold, J., Martin, H., Dimmeler, S., Zeiher, A. M., and Schachinger, V. (2006b). Intracoronary infusion of progenitor cells is not associated with aggravated restenosis development or atherosclerotic disease progression in patients with acute myocardial infarction. *Eur Heart J* **27**(24), 2989-95.
- Atchison, R. W., Casto, B. C., and Hammon, W. M. (1965). Adenovirus-Associated Defective Virus Particles. *Science* **149**, 754-6.
- Auricchio, A., Kobinger, G., Anand, V., Hildinger, M., O'Connor, E., Maguire, A. M., Wilson, J. M., and Bennett, J. (2001). Exchange of surface proteins impacts on viral vector cellular specificity and transduction characteristics: the retina as a model. *Hum Mol Genet* **10**(26), 3075-81.
- Bantel-Schaal, U., Delius, H., Schmidt, R., and zur Hausen, H. (1999). Human adeno-associated virus type 5 is only distantly related to other known primate helper-dependent parvoviruses. *J Virol* **73**(2), 939-47.
- Bantel-Schaal, U., Hub, B., and Kartenbeck, J. (2002). Endocytosis of adeno-associated virus type 5 leads to accumulation of virus particles in the Golgi compartment. *J Virol* **76**(5), 2340-9.
- Bantel-Schaal, U., and zur Hausen, H. (1984). Characterization of the DNA of a defective human parvovirus isolated from a genital site. *Virology* **134**(1), 52-63.
- Bartlett, J. S., Wilcher, R., and Samulski, R. J. (2000). Infectious entry pathway of adeno-associated virus and adeno-associated virus vectors. *J Virol* **74**(6), 2777-85.
- Baumgartner, I., Pieczek, A., Manor, O., Blair, R., Kearney, M., Walsh, K., and Isner, J. M. (1998). Constitutive expression of phVEGF165 after intramuscular gene transfer promotes collateral vessel development in patients with critical limb ischemia. *Circulation* **97**(12), 1114-23.
- Becerra, S. P., Koczot, F., Fabisch, P., and Rose, J. A. (1988). Synthesis of adeno-associated virus structural proteins requires both alternative mRNA splicing and alternative initiations from a single transcript. *J Virol* **62**(8), 2745-54.

- Becerra, S. P., Rose, J. A., Hardy, M., Baroudy, B. M., and Anderson, C. W. (1985). Direct mapping of adeno-associated virus capsid proteins B and C: a possible ACG initiation codon. *Proc Natl Acad Sci U S A* **82**(23), 7919-23.
- Becker, A. J., Mc, C. E., and Till, J. E. (1963). Cytological demonstration of the clonal nature of spleen colonies derived from transplanted mouse marrow cells. *Nature* **197**, 452-4.
- Beeri, R., Guerrero, J. L., Supple, G., Sullivan, S., Levine, R. A., and Hajjar, R. J. (2002). New efficient catheter-based system for myocardial gene delivery. *Circulation* **106**(14), 1756-9.
- Bekeredjian, R., Chen, S., Frenkel, P. A., Grayburn, P. A., and Shohet, R. V. (2003). Ultrasound-targeted microbubble destruction can repeatedly direct highly specific plasmid expression to the heart. *Circulation* **108**(8), 1022-6.
- Beltrami, A. P., Barlucchi, L., Torella, D., Baker, M., Limana, F., Chimenti, S., Kasahara, H., Rota, M., Musso, E., Urbanek, K., Leri, A., Kajstura, J., Nadal-Ginard, B., and Anversa, P. (2003). Adult cardiac stem cells are multipotent and support myocardial regeneration. *Cell* **114**(6), 763-76.
- Berns, K. I. (1990). Parvovirus replication. *Microbiol Rev* **54**(3), 316-29.
- Berns, K. I., and Giraud, C. (1996). Biology of adeno-associated virus. *Curr Top Microbiol Immunol* **218**, 1-23.
- Berns, K. I., and Linden, R. M. (1995). The cryptic life style of adeno-associated virus. *Bioessays* **17**(3), 237-45.
- Betthausen, J., Forsberg, E., Augenstein, M., Childs, L., Eilertsen, K., Enos, J., Forsythe, T., Golueke, P., Jurgella, G., Koppang, R., Lesmeister, T., Mallon, K., Mell, G., Misica, P., Pace, M., Pfister-Genskow, M., Strelchenko, N., Voelker, G., Watt, S., Thompson, S., and Bishop, M. (2000). Production of cloned pigs from in vitro systems. *Nat Biotechnol* **18**(10), 1055-9.
- Blackburn, S. D., Steadman, R. A., and Johnson, F. B. (2006). Attachment of adeno-associated virus type 3H to fibroblast growth factor receptor 1. *Arch Virol* **151**(3), 617-23.
- Boshart, M., Weber, F., Jahn, G., Dorsch-Hasler, K., Fleckenstein, B., and Schaffner, W. (1985). A very strong enhancer is located upstream of an immediate early gene of human cytomegalovirus. *Cell* **41**(2), 521-30.
- Bossis, I., and Chiorini, J. A. (2003). Cloning of an avian adeno-associated virus (AAAV) and generation of recombinant AAAV particles. *J Virol* **77**(12), 6799-810.
- Brister, J. R., and Muzyczka, N. (2000). Mechanism of Rep-mediated adeno-associated virus origin nicking. *J Virol* **74**(17), 7762-71.
- Britten, M. B., Abolmaali, N. D., Assmus, B., Lehmann, R., Honold, J., Schmitt, J., Vogl, T. J., Martin, H., Schachinger, V., Dimmeler, S., and Zeiher, A. M. (2003). Infarct remodeling after intracoronary progenitor cell treatment in patients with acute myocardial infarction (TOPCARE-AMI): mechanistic insights from serial contrast-enhanced magnetic resonance imaging. *Circulation* **108**(18), 2212-8.
- Buning, H., Nicklin, S. A., Perabo, L., Hallek, M., and Baker, A. H. (2003a). AAV-based gene transfer. *Curr Opin Mol Ther* **5**(4), 367-75.
- Buning, H., Ried, M. U., Perabo, L., Gerner, F. M., Huttner, N. A., Enssle, J., and Hallek, M. (2003b). Receptor targeting of adeno-associated virus vectors. *Gene Ther* **10**(14), 1142-51.
- Byun, H. M., Suh, D., Jeong, Y., Wee, H. S., Kim, J. M., Kim, W. K., Ko, J. J., Kim, J. S., Lee, Y. B., and Oh, Y. K. (2005). Plasmid vectors harboring cellular promoters can induce prolonged gene expression in hematopoietic and

- mesenchymal progenitor cells. *Biochem Biophys Res Commun* **332**(2), 518-23.
- Byun, J., Huh, J. E., Park, S. J., Jang, J. E., Suh, Y. L., Lee, J. S., Gwon, H. C., Lee, W. R., Cosset, F. L., and Kim, D. K. (2000). Myocardial injury-induced fibroblast proliferation facilitates retroviral-mediated gene transfer to the rat heart in vivo. *J Gene Med* **2**(1), 2-10.
- Calabrese, F., and Thiene, G. (2003). Myocarditis and inflammatory cardiomyopathy: microbiological and molecular biological aspects. *Cardiovasc Res* **60**(1), 11-25.
- Cardoso, A. A., Li, M. L., Batard, P., Hatzfeld, A., Brown, E. L., Levesque, J. P., Sookdeo, H., Panterne, B., Sansilvestri, P., Clark, S. C., and et al. (1993). Release from quiescence of CD34+ CD38- human umbilical cord blood cells reveals their potentiality to engraft adults. *Proc Natl Acad Sci U S A* **90**(18), 8707-11.
- Carlos, T. M., and Harlan, J. M. (1994). Leukocyte-endothelial adhesion molecules. *Blood* **84**(7), 2068-101.
- Carter, P. J., and Samulski, R. J. (2000). Adeno-associated viral vectors as gene delivery vehicles. *Int J Mol Med* **6**(1), 17-27.
- Cassell, G. D., and Weitzman, M. D. (2004). Characterization of a nuclear localization signal in the C-terminus of the adeno-associated virus Rep68/78 proteins. *Virology* **327**(2), 206-14.
- Cavazzana-Calvo, M., Hacein-Bey, S., de Saint Basile, G., Gross, F., Yvon, E., Nusbaum, P., Selz, F., Hue, C., Certain, S., Casanova, J. L., Bousso, P., Deist, F. L., and Fischer, A. (2000). Gene therapy of human severe combined immunodeficiency (SCID)-X1 disease. *Science* **288**(5466), 669-72.
- Chambon, P. (1996). A decade of molecular biology of retinoic acid receptors. *Faseb J* **10**(9), 940-54.
- Chan, S. Y., Goodman, R. E., Szmuszkovicz, J. R., Roessler, B., Eichwald, E. J., and Bishop, D. K. (2000). DNA-liposome versus adenoviral mediated gene transfer of transforming growth factor beta1 in vascularized cardiac allografts: differential sensitivity of CD4+ and CD8+ T cells to transforming growth factor beta1. *Transplantation* **70**(9), 1292-301.
- Chatterjee, S., Li, W., Wong, C. A., Fisher-Adams, G., Lu, D., Guha, M., Macer, J. A., Forman, S. J., and Wong, K. K., Jr. (1999). Transduction of primitive human marrow and cord blood-derived hematopoietic progenitor cells with adeno-associated virus vectors. *Blood* **93**(6), 1882-94.
- Chauhan, A., More, R. S., Mullins, P. A., Taylor, G., Petch, C., and Schofield, P. M. (1996). Aging-associated endothelial dysfunction in humans is reversed by L-arginine. *J Am Coll Cardiol* **28**(7), 1796-804.
- Chavakis, E., Aicher, A., Heeschen, C., Sasaki, K., Kaiser, R., El Makhfi, N., Urbich, C., Peters, T., Scharffetter-Kochanek, K., Zeiher, A. M., Chavakis, T., and Dimmeler, S. (2005). Role of beta2-integrins for homing and neovascularization capacity of endothelial progenitor cells. *J Exp Med* **201**(1), 63-72.
- Chen, D., Sung, R., and Bromberg, J. S. (2002). Gene therapy in transplantation. *Transpl Immunol* **9**(2-4), 301-14.
- Chen, J. Z., Zhang, F. R., Tao, Q. M., Wang, X. X., Zhu, J. H., and Zhu, J. H. (2004). Number and activity of endothelial progenitor cells from peripheral blood in patients with hypercholesterolaemia. *Clin Sci (Lond)* **107**(3), 273-80.

- Chen, S., Kapturczak, M., Loiler, S. A., Zolotukhin, S., Glushakova, O. Y., Madsen, K. M., Samulski, R. J., Hauswirth, W. W., Campbell-Thompson, M., Berns, K. I., Flotte, T. R., Atkinson, M. A., Tisher, C. C., and Agarwal, A. (2005). Efficient transduction of vascular endothelial cells with recombinant adeno-associated virus serotype 1 and 5 vectors. *Hum Gene Ther* **16**(2), 235-47.
- Chen, W. Y., Bailey, E. C., McCune, S. L., Dong, J. Y., and Townes, T. M. (1997). Reactivation of silenced, virally transduced genes by inhibitors of histone deacetylase. *Proc Natl Acad Sci U S A* **94**(11), 5798-803.
- Chen, Z., Lu, L., Li, J., Xiao, X., Fung, J. J., and Qian, S. (2003). Prolonged survival of heart allografts transduced with AAV-CTLA4Ig. *Microsurgery* **23**(5), 489-93.
- Chiorini, J. A., Kim, F., Yang, L., and Kotin, R. M. (1999). Cloning and characterization of adeno-associated virus type 5. *J Virol* **73**(2), 1309-19.
- Chiorini, J. A., Yang, L., Liu, Y., Safer, B., and Kotin, R. M. (1997). Cloning of adeno-associated virus type 4 (AAV4) and generation of recombinant AAV4 particles. *J Virol* **71**(9), 6823-33.
- Chirmule, N., Propert, K., Magosin, S., Qian, Y., Qian, R., and Wilson, J. (1999). Immune responses to adenovirus and adeno-associated virus in humans. *Gene Ther* **6**(9), 1574-83.
- Clarke, J. K., McFerran, J. B., McKillop, E. R., and Curran, W. L. (1979). Isolation of an adeno associated virus from sheep. Brief report. *Arch Virol* **60**(2), 171-6.
- Collaco, R. F., Cao, X., and Trempe, J. P. (1999). A helper virus-free packaging system for recombinant adeno-associated virus vectors. *Gene* **238**(2), 397-405.
- Cooke, J. P. (2000). The endothelium: a new target for therapy. *Vasc Med* **5**(1), 49-53.
- Cosentino, F., and Luscher, T. F. (1998). Endothelial dysfunction in diabetes mellitus. *J Cardiovasc Pharmacol* **32 Suppl 3**, S54-61.
- Dai, Y., Roman, M., Naviaux, R. K., and Verma, I. M. (1992). Gene therapy via primary myoblasts: long-term expression of factor IX protein following transplantation in vivo. *Proc Natl Acad Sci U S A* **89**(22), 10892-5.
- Dandapat, A., Hu, C. P., Li, D., Liu, Y., Chen, H., Hermonat, P. L., and Mehta, J. L. (2007). Overexpression of TGFbeta(1) by adeno-associated virus type-2 vector protects myocardium from ischemia-reperfusion injury. *Gene Ther*.
- Daniel, T. O., Milfay, D. F., Escobedo, J., and Williams, L. T. (1987). Biosynthetic and glycosylation studies of cell surface platelet-derived growth factor receptors. *J Biol Chem* **262**(20), 9778-84.
- Dao, M. A., Hashino, K., Kato, I., and Nolte, J. A. (1998). Adhesion to fibronectin maintains regenerative capacity during ex vivo culture and transduction of human hematopoietic stem and progenitor cells. *Blood* **92**(12), 4612-21.
- David, A., Chetritt, J., Guillot, C., Tesson, L., Heslan, J. M., Cuturi, M. C., Soullillou, J. P., and Anegon, I. (2000). Interleukin-10 produced by recombinant adenovirus prolongs survival of cardiac allografts in rats. *Gene Ther* **7**(6), 505-10.
- Davidson, B. L., Stein, C. S., Heth, J. A., Martins, I., Kotin, R. M., Derksen, T. A., Zabner, J., Ghodsi, A., and Chiorini, J. A. (2000). Recombinant adeno-associated virus type 2, 4, and 5 vectors: transduction of variant cell types and regions in the mammalian central nervous system. *Proc Natl Acad Sci U S A* **97**(7), 3428-32.

- De Falco, E., Porcelli, D., Torella, A. R., Straino, S., Iachininoto, M. G., Orlandi, A., Truffa, S., Biglioli, P., Napolitano, M., Capogrossi, M. C., and Pesce, M. (2004). SDF-1 involvement in endothelial phenotype and ischemia-induced recruitment of bone marrow progenitor cells. *Blood* **104**(12), 3472-82 Epub.
- De los Santos, M., Zambrano, A., Sanchez-Pacheco, A., and Aranda, A. (2007). Histone deacetylase inhibitors regulate retinoic acid receptor beta expression in neuroblastoma cells by both transcriptional and posttranscriptional mechanisms. *Mol Endocrinol* **21**(10), 2416-26.
- Di Pasquale, G., Davidson, B. L., Stein, C. S., Martins, I., Scudiero, D., Monks, A., and Chiorini, J. A. (2003). Identification of PDGFR as a receptor for AAV-5 transduction. *Nat Med* **9**(10), 1306-12.
- Dimmeler, S., Aicher, A., Vasa, M., Mildner-Rihm, C., Adler, K., Tiemann, M., Rutten, H., Fichtlscherer, S., Martin, H., and Zeiher, A. M. (2001). HMG-CoA reductase inhibitors (statins) increase endothelial progenitor cells via the PI 3-kinase/Akt pathway. *J Clin Invest* **108**(3), 391-7.
- Ding, Z., Fach, C., Sasse, A., Godecke, A., and Schrader, J. (2004). A minimally invasive approach for efficient gene delivery to rodent hearts. *Gene Ther* **11**(3), 260-5.
- Dokmanovic, M., and Marks, P. A. (2005). Prospects: histone deacetylase inhibitors. *J Cell Biochem* **96**(2), 293-304.
- Donahue, J. K., Kikkawa, K., Thomas, A. D., Marban, E., and Lawrence, J. H. (1998). Acceleration of widespread adenoviral gene transfer to intact rabbit hearts by coronary perfusion with low calcium and serotonin. *Gene Ther* **5**(5), 630-4.
- Dong, J. Y., Fan, P. D., and Frizzell, R. A. (1996). Quantitative analysis of the packaging capacity of recombinant adeno-associated virus. *Hum Gene Ther* **7**(17), 2101-12.
- Douar, A. M., Poulard, K., Stockholm, D., and Danos, O. (2001). Intracellular trafficking of adeno-associated virus vectors: routing to the late endosomal compartment and proteasome degradation. *J Virol* **75**(4), 1824-33.
- Drzeniek, Z., Stocker, G., Siebertz, B., Just, U., Schroeder, T., Ostertag, W., and Haubeck, H. D. (1999). Heparan sulfate proteoglycan expression is induced during early erythroid differentiation of multipotent hematopoietic stem cells. *Blood* **93**(9), 2884-97.
- Duan, D., Li, Q., Kao, A. W., Yue, Y., Pessin, J. E., and Engelhardt, J. F. (1999). Dynamin is required for recombinant adeno-associated virus type 2 infection. *J Virol* **73**(12), 10371-6.
- Duan, D., Sharma, P., Yang, J., Yue, Y., Dudus, L., Zhang, Y., Fisher, K. J., and Engelhardt, J. F. (1998a). Circular intermediates of recombinant adeno-associated virus have defined structural characteristics responsible for long-term episomal persistence in muscle tissue. *J Virol* **72**(11), 8568-77.
- Duan, D., Yue, Y., and Engelhardt, J. F. (2001). Expanding AAV packaging capacity with trans-splicing or overlapping vectors: a quantitative comparison. *Mol Ther* **4**(4), 383-91.
- Duan, D., Yue, Y., Yan, Z., McCray, P. B., Jr., and Engelhardt, J. F. (1998b). Polarity influences the efficiency of recombinant adeno-associated virus infection in differentiated airway epithelia. *Hum Gene Ther* **9**(18), 2761-76.
- Duan, D., Yue, Y., Yan, Z., Yang, J., and Engelhardt, J. F. (2000). Endosomal processing limits gene transfer to polarized airway epithelia by adeno-associated virus. *J Clin Invest* **105**(11), 1573-87.

- Dubielzig, R., King, J. A., Weger, S., Kern, A., and Kleinschmidt, J. A. (1999). Adeno-associated virus type 2 protein interactions: formation of pre-encapsidation complexes. *J Virol* **73**(11), 8989-98.
- Duvigneau, J. C., Hartl, R. T., Groiss, S., and Gemeiner, M. (2005). Quantitative simultaneous multiplex real-time PCR for the detection of porcine cytokines. *J Immunol Methods* **306**(1-2), 16-27.
- Erles, K., Sebokova, P., and Schlehofer, J. R. (1999). Update on the prevalence of serum antibodies (IgG and IgM) to adeno-associated virus (AAV). *J Med Virol* **59**(3), 406-11.
- Evans, J. T., Kelly, P. F., O'Neill, E., and Garcia, J. V. (1999). Human cord blood CD34+CD38- cell transduction via lentivirus-based gene transfer vectors. *Hum Gene Ther* **10**(9), 1479-89.
- Fan, C. L., Li, Y., Gao, P. J., Liu, J. J., Zhang, X. J., and Zhu, D. L. (2003). Differentiation of endothelial progenitor cells from human umbilical cord blood CD 34+ cells in vitro. *Acta Pharmacol Sin* **24**(3), 212-8.
- Farkas, S. L., Zadori, Z., Benko, M., Essbauer, S., Harrach, B., and Tijssen, P. (2004). A parvovirus isolated from royal python (*Python regius*) is a member of the genus Dependovirus. *J Gen Virol* **85**(Pt 3), 555-61.
- Fazi, F., Travaglini, L., Carotti, D., Palitti, F., Diverio, D., Alcalay, M., McNamara, S., Miller, W. H., Jr., Lo Coco, F., Pelicci, P. G., and Nervi, C. (2005). Retinoic acid targets DNA-methyltransferases and histone deacetylases during APL blast differentiation in vitro and in vivo. *Oncogene* **24**(11), 1820-30.
- Feng, D., Chen, J., Yue, Y., Zhu, H., Xue, J., and Jia, W. W. (2006). A 16bp Rep binding element is sufficient for mediating Rep-dependent integration into AAVS1. *J Mol Biol* **358**(1), 38-45.
- Ferrara, N., Carver-Moore, K., Chen, H., Dowd, M., Lu, L., O'Shea, K. S., Powell-Braxton, L., Hillan, K. J., and Moore, M. W. (1996). Heterozygous embryonic lethality induced by targeted inactivation of the VEGF gene. *Nature* **380**(6573), 439-42.
- Ferrari, F. K., Samulski, T., Shenk, T., and Samulski, R. J. (1996). Second-strand synthesis is a rate-limiting step for efficient transduction by recombinant adeno-associated virus vectors. *J Virol* **70**(5), 3227-34.
- Fisher-Adams, G., Wong, K. K., Jr., Podsakoff, G., Forman, S. J., and Chatterjee, S. (1996). Integration of adeno-associated virus vectors in CD34+ human hematopoietic progenitor cells after transduction. *Blood* **88**(2), 492-504.
- Fisher, K. J., Gao, G. P., Weitzman, M. D., DeMatteo, R., Burda, J. F., and Wilson, J. M. (1996). Transduction with recombinant adeno-associated virus for gene therapy is limited by leading-strand synthesis. *J Virol* **70**(1), 520-32.
- Fisher, K. J., Jooss, K., Alston, J., Yang, Y., Haecker, S. E., High, K., Pathak, R., Raper, S. E., and Wilson, J. M. (1997). Recombinant adeno-associated virus for muscle directed gene therapy. *Nat Med* **3**(3), 306-12.
- Flotte, T. R., Afione, S. A., Conrad, C., McGrath, S. A., Solow, R., Oka, H., Zeitlin, P. L., Guggino, W. B., and Carter, B. J. (1993). Stable in vivo expression of the cystic fibrosis transmembrane conductance regulator with an adeno-associated virus vector. *Proc Natl Acad Sci U S A* **90**(22), 10613-7.
- Fong, G. H., Rossant, J., Gertsenstein, M., and Breitman, M. L. (1995). Role of the Flt-1 receptor tyrosine kinase in regulating the assembly of vascular endothelium. *Nature* **376**(6535), 66-70.

- French, B. A., Mazur, W., Geske, R. S., and Bolli, R. (1994). Direct in vivo gene transfer into porcine myocardium using replication-deficient adenoviral vectors. *Circulation* **90**(5), 2414-24.
- Fujiyama, S., Amano, K., Uehira, K., Yoshida, M., Nishiwaki, Y., Nozawa, Y., Jin, D., Takai, S., Miyazaki, M., Egashira, K., Imada, T., Iwasaka, T., and Matsubara, H. (2003). Bone marrow monocyte lineage cells adhere on injured endothelium in a monocyte chemoattractant protein-1-dependent manner and accelerate reendothelialization as endothelial progenitor cells. *Circ Res* **93**(10), 980-9.
- Gaetano, C., Catalano, A., Palumbo, R., Illi, B., Orlando, G., Ventrizzo, G., Serino, F., and Capogrossi, M. C. (2000). Transcriptionally active drugs improve adenovirus vector performance in vitro and in vivo. *Gene Ther* **7**(19), 1624-30.
- Gao, G., Vandenberghe, L. H., Alvira, M. R., Lu, Y., Calcedo, R., Zhou, X., and Wilson, J. M. (2004). Clades of Adeno-associated viruses are widely disseminated in human tissues. *J Virol* **78**(12), 6381-8.
- Gao, G. P., Alvira, M. R., Wang, L., Calcedo, R., Johnston, J., and Wilson, J. M. (2002). Novel adeno-associated viruses from rhesus monkeys as vectors for human gene therapy. *Proc Natl Acad Sci U S A* **99**(18), 11854-9.
- Gaspar, H. B., Björkegren, E., Parsley, K., Gilmour, K. C., King, D., Sinclair, J., Zhang, F., Giannakopoulos, A., Adams, S., Fairbanks, L. D., Gaspar, J., Henderson, L., Xu-Bayford, J. H., Davies, E. G., Veys, P. A., Kinnon, C., and Thrasher, A. J. (2006). Successful reconstitution of immunity in ADA-SCID by stem cell gene therapy following cessation of PEG-ADA and use of mild preconditioning. *Mol Ther* **14**(4), 505-13.
- Gauczynski, S., Nikles, D., El-Gogo, S., Papy-Garcia, D., Rey, C., Alban, S., Barritault, D., Lasmezas, C. I., and Weiss, S. (2006). The 37-kDa/67-kDa laminin receptor acts as a receptor for infectious prions and is inhibited by polysulfated glycanes. *J Infect Dis* **194**(5), 702-9.
- Gehling, U. M., Ergun, S., Schumacher, U., Wagener, C., Pantel, K., Otte, M., Schuch, G., Schafhausen, P., Mende, T., Kilic, N., Kluge, K., Schafer, B., Hossfeld, D. K., and Fiedler, W. (2000). In vitro differentiation of endothelial cells from AC133-positive progenitor cells. *Blood* **95**(10), 3106-12.
- Ghazal, P., DeMattei, C., Giulietti, E., Kliewer, S. A., Umesono, K., and Evans, R. M. (1992). Retinoic acid receptors initiate induction of the cytomegalovirus enhancer in embryonal cells. *Proc Natl Acad Sci U S A* **89**(16), 7630-4.
- Gill, M., Dias, S., Hattori, K., Rivera, M. L., Hicklin, D., Witte, L., Girardi, L., Yurt, R., Himel, H., and Rafii, S. (2001). Vascular trauma induces rapid but transient mobilization of VEGFR2(+)/AC133(+) endothelial precursor cells. *Circ Res* **88**(2), 167-74.
- Girod, A., Ried, M., Wobus, C., Lahm, H., Leike, K., Kleinschmidt, J., Deleage, G., and Hallek, M. (1999). Genetic capsid modifications allow efficient re-targeting of adeno-associated virus type 2. *Nat Med* **5**(9), 1052-6.
- Girod, A., Wobus, C. E., Zadori, Z., Ried, M., Leike, K., Tijssen, P., Kleinschmidt, J. A., and Hallek, M. (2002). The VP1 capsid protein of adeno-associated virus type 2 is carrying a phospholipase A2 domain required for virus infectivity. *J Gen Virol* **83**(Pt 5), 973-8.
- Goodman, S., Xiao, X., Donahue, R. E., Moulton, A., Miller, J., Walsh, C., Young, N. S., Samulski, R. J., and Nienhuis, A. W. (1994). Recombinant adeno-associated virus-mediated gene transfer into hematopoietic progenitor cells. *Blood* **84**(5), 1492-500.

- Gould, D. J., and Favorov, P. (2003). Vectors for the treatment of autoimmune disease. *Gene Ther* **10**(10), 912-27.
- Graham, F. L., Smiley, J., Russell, W. C., and Nairn, R. (1977). Characteristics of a human cell line transformed by DNA from human adenovirus type 5. *J Gen Virol* **36**(1), 59-74.
- Grimm, D., and Kay, M. A. (2003). From virus evolution to vector revolution: use of naturally occurring serotypes of adeno-associated virus (AAV) as novel vectors for human gene therapy. *Curr Gene Ther* **3**(4), 281-304.
- Grimm, D., and Kleinschmidt, J. A. (1999). Progress in adeno-associated virus type 2 vector production: promises and prospects for clinical use. *Hum Gene Ther* **10**(15), 2445-50.
- Grines, C. L., Watkins, M. W., Mahmarian, J. J., Iskandrian, A. E., Rade, J. J., Marrott, P., Pratt, C., and Kleiman, N. (2003). A randomized, double-blind, placebo-controlled trial of Ad5FGF-4 gene therapy and its effect on myocardial perfusion in patients with stable angina. *J Am Coll Cardiol* **42**(8), 1339-47.
- Guo, Z. S., Wang, L. H., Eisensmith, R. C., and Woo, S. L. (1996). Evaluation of promoter strength for hepatic gene expression in vivo following adenovirus-mediated gene transfer. *Gene Ther* **3**(9), 802-10.
- Guzman, R. J., Lemarchand, P., Crystal, R. G., Epstein, S. E., and Finkel, T. (1993). Efficient gene transfer into myocardium by direct injection of adenovirus vectors. *Circ Res* **73**(6), 1202-7.
- Hacein-Bey-Abina, S., Le Deist, F., Carlier, F., Bouneaud, C., Hue, C., De Villartay, J. P., Thrasher, A. J., Wulffraat, N., Sorensen, R., Dupuis-Girod, S., Fischer, A., Davies, E. G., Kuis, W., Leiva, L., and Cavazzana-Calvo, M. (2002). Sustained correction of X-linked severe combined immunodeficiency by ex vivo gene therapy. *N Engl J Med* **346**(16), 1185-93.
- Hacein-Bey-Abina, S., Von Kalle, C., Schmidt, M., McCormack, M. P., Wulffraat, N., Leboulch, P., Lim, A., Osborne, C. S., Pawliuk, R., Morillon, E., Sorensen, R., Forster, A., Fraser, P., Cohen, J. I., de Saint Basile, G., Alexander, I., Wintergerst, U., Frebourg, T., Aurias, A., Stoppa-Lyonnet, D., Romana, S., Radford-Weiss, I., Gross, F., Valensi, F., Delabesse, E., Macintyre, E., Sigaux, F., Soulier, J., Leiva, L. E., Wissler, M., Prinz, C., Rabbitts, T. H., Le Deist, F., Fischer, A., and Cavazzana-Calvo, M. (2003). LMO2-associated clonal T cell proliferation in two patients after gene therapy for SCID-X1. *Science* **302**(5644), 415-9.
- Hacker, U. T., Gerner, F. M., Buning, H., Hutter, M., Reichenspurner, H., Stangl, M., and Hallek, M. (2001). Standard heparin, low molecular weight heparin, low molecular weight heparinoid, and recombinant hirudin differ in their ability to inhibit transduction by recombinant adeno-associated virus type 2 vectors. *Gene Ther* **8**(12), 966-8.
- Hacker, U. T., Wingenfeld, L., Kofler, D. M., Schuhmann, N. K., Lutz, S., Herold, T., King, S. B., Gerner, F. M., Perabo, L., Rabinowitz, J., McCarty, D. M., Samulski, R. J., Hallek, M., and Buning, H. (2005). Adeno-associated virus serotypes 1 to 5 mediated tumor cell directed gene transfer and improvement of transduction efficiency. *J Gene Med* **7**(11), 1429-38.
- Hajjar, R. J., Schmidt, U., Matsui, T., Guerrero, J. L., Lee, K. H., Gwathmey, J. K., Dec, G. W., Semigran, M. J., and Rosenzweig, A. (1998). Modulation of ventricular function through gene transfer in vivo. *Proc Natl Acad Sci U S A* **95**(9), 5251-6.

- Hanahan, D. (1983). Studies on transformation of *Escherichia coli* with plasmids. *J Mol Biol* **166**(4), 557-80.
- Handa, A., Muramatsu, S., Qiu, J., Mizukami, H., and Brown, K. E. (2000). Adeno-associated virus (AAV)-3-based vectors transduce haematopoietic cells not susceptible to transduction with AAV-2-based vectors. *J Gen Virol* **81**(Pt 8), 2077-84.
- Hansen, J., Qing, K., and Srivastava, A. (2001a). Adeno-associated virus type 2-mediated gene transfer: altered endocytic processing enhances transduction efficiency in murine fibroblasts. *J Virol* **75**(9), 4080-90.
- Hansen, J., Qing, K., and Srivastava, A. (2001b). Infection of purified nuclei by adeno-associated virus 2. *Mol Ther* **4**(4), 289-96.
- Hao, Q. L., Shah, A. J., Thiemann, F. T., Smogorzewska, E. M., and Crooks, G. M. (1995). A functional comparison of CD34 + CD38- cells in cord blood and bone marrow. *Blood* **86**(10), 3745-53.
- Hargrove, P. W., Vanin, E. F., Kurtzman, G. J., and Nienhuis, A. W. (1997). High-level globin gene expression mediated by a recombinant adeno-associated virus genome that contains the 3' gamma globin gene regulatory element and integrates as tandem copies in erythroid cells. *Blood* **89**(6), 2167-75.
- Hart, C., Drewel, D., Mueller, G., Grassinger, J., Zaiss, M., Kunz-Schughart, L. A., Andreesen, R., Reichle, A., Holler, E., and Hennemann, B. (2004). Expression and function of homing-essential molecules and enhanced in vivo homing ability of human peripheral blood-derived hematopoietic progenitor cells after stimulation with stem cell factor. *Stem Cells* **22**(4), 580-9.
- Hattori, K., Heissig, B., Tashiro, K., Honjo, T., Tateno, M., Shieh, J. H., Hackett, N. R., Quitarano, M. S., Crystal, R. G., Rafii, S., and Moore, M. A. (2001). Plasma elevation of stromal cell-derived factor-1 induces mobilization of mature and immature hematopoietic progenitor and stem cells. *Blood* **97**(11), 3354-60.
- Hattori, K., Heissig, B., Wu, Y., Dias, S., Tejada, R., Ferris, B., Hicklin, D. J., Zhu, Z., Bohlen, P., Witte, L., Hendriks, J., Hackett, N. R., Crystal, R. G., Moore, M. A., Werb, Z., Lyden, D., and Rafii, S. (2002). Placental growth factor reconstitutes hematopoiesis by recruiting VEGFR1(+) stem cells from bone-marrow microenvironment. *Nat Med* **8**(8), 841-9.
- Hatzopoulos, A. K., Folkman, J., Vasile, E., Eiselen, G. K., and Rosenberg, R. D. (1998). Isolation and characterization of endothelial progenitor cells from mouse embryos. *Development* **125**(8), 1457-68.
- Hauswirth, W. W., and Berns, K. I. (1977). Origin and termination of adeno-associated virus DNA replication. *Virology* **78**(2), 488-99.
- Heeschen, C., Aicher, A., Lehmann, R., Fichtlscherer, S., Vasa, M., Urbich, C., Mildner-Rihm, C., Martin, H., Zeiher, A. M., and Dimmeler, S. (2003). Erythropoietin is a potent physiologic stimulus for endothelial progenitor cell mobilization. *Blood* **102**(4), 1340-6.
- Heilbronn, R., Burkle, A., Stephan, S., and zur Hausen, H. (1990). The adeno-associated virus rep gene suppresses herpes simplex virus-induced DNA amplification. *J Virol* **64**(6), 3012-8.
- Heiss, C., Keymel, S., Niesler, U., Ziemann, J., Kelm, M., and Kalka, C. (2005). Impaired progenitor cell activity in age-related endothelial dysfunction. *J Am Coll Cardiol* **45**(9), 1441-8.
- Heissig, B., Hattori, K., Dias, S., Friedrich, M., Ferris, B., Hackett, N. R., Crystal, R. G., Besmer, P., Lyden, D., Moore, M. A., Werb, Z., and Rafii, S. (2002).

- Recruitment of stem and progenitor cells from the bone marrow niche requires MMP-9 mediated release of kit-ligand. *Cell* **109**(5), 625-37.
- Hensley, S. E., and Amalfitano, A. (2007). Toll-like receptors impact on safety and efficacy of gene transfer vectors. *Mol Ther* **15**(8), 1417-22.
- Hermens, W. T., ter Brake, O., Dijkhuizen, P. A., Sonnemans, M. A., Grimm, D., Kleinschmidt, J. A., and Verhaagen, J. (1999). Purification of recombinant adeno-associated virus by iodixanol gradient ultracentrifugation allows rapid and reproducible preparation of vector stocks for gene transfer in the nervous system. *Hum Gene Ther* **10**(11), 1885-91.
- Hermonat, P. L. (1992). Inhibition of bovine papillomavirus plasmid DNA replication by adeno-associated virus. *Virology* **189**(1), 329-33.
- Herzog, R. W., Yang, E. Y., Couto, L. B., Hagstrom, J. N., Elwell, D., Fields, P. A., Burton, M., Bellinger, D. A., Read, M. S., Brinkhous, K. M., Podsakoff, G. M., Nichols, T. C., Kurtzman, G. J., and High, K. A. (1999). Long-term correction of canine hemophilia B by gene transfer of blood coagulation factor IX mediated by adeno-associated viral vector. *Nat Med* **5**(1), 56-63.
- Hinshaw, J. E., and Schmid, S. L. (1995). Dynamin self-assembles into rings suggesting a mechanism for coated vesicle budding. *Nature* **374**(6518), 190-2.
- Hoggan, M. D., Blacklow, N. R., and Rowe, W. P. (1966). Studies of small DNA viruses found in various adenovirus preparations: physical, biological, and immunological characteristics. *Proc Natl Acad Sci U S A* **55**(6), 1467-74.
- Hosang, M. (1988). Characterization of a platelet-derived growth factor receptor on Swiss 3T3 cells by affinity crosslinking. *J Recept Res* **8**(1-4), 455-66.
- Hoshijima, M., Ikeda, Y., Iwanaga, Y., Minamisawa, S., Date, M. O., Gu, Y., Iwatate, M., Li, M., Wang, L., Wilson, J. M., Wang, Y., Ross, J., Jr., and Chien, K. R. (2002). Chronic suppression of heart-failure progression by a pseudophosphorylated mutant of phospholamban via in vivo cardiac rAAV gene delivery. *Nat Med* **8**(8), 864-71.
- Hur, J., Yoon, C. H., Kim, H. S., Choi, J. H., Kang, H. J., Hwang, K. K., Oh, B. H., Lee, M. M., and Park, Y. B. (2004). Characterization of two types of endothelial progenitor cells and their different contributions to neovasculogenesis. *Arterioscler Thromb Vasc Biol* **24**(2), 288-93.
- Hurley, R. W., McCarthy, J. B., and Verfaillie, C. M. (1995). Direct adhesion to bone marrow stroma via fibronectin receptors inhibits hematopoietic progenitor proliferation. *J Clin Invest* **96**(1), 511-9.
- Huttner, N. A., Girod, A., Schnittger, S., Schoch, C., Hallek, M., and Buning, H. (2003). Analysis of site-specific transgene integration following cotransduction with recombinant adeno-associated virus and a rep encoding plasmid. *J Gene Med* **5**(2), 120-9.
- Im, D. S., and Muzyczka, N. (1990). The AAV origin binding protein Rep68 is an ATP-dependent site-specific endonuclease with DNA helicase activity. *Cell* **61**(3), 447-57.
- Inagaki, K., Fuess, S., Storm, T. A., Gibson, G. A., McTiernan, C. F., Kay, M. A., and Nakai, H. (2006). Robust systemic transduction with AAV9 vectors in mice: efficient global cardiac gene transfer superior to that of AAV8. *Mol Ther* **14**(1), 45-53.
- Iwaguro, H., Yamaguchi, J., Kalka, C., Murasawa, S., Masuda, H., Hayashi, S., Silver, M., Li, T., Isner, J. M., and Asahara, T. (2002). Endothelial progenitor cell vascular endothelial growth factor gene transfer for vascular regeneration. *Circulation* **105**(6), 732-8.

- Iwakura, A., Luedemann, C., Shastry, S., Hanley, A., Kearney, M., Aikawa, R., Isner, J. M., Asahara, T., and Losordo, D. W. (2003). Estrogen-mediated, endothelial nitric oxide synthase-dependent mobilization of bone marrow-derived endothelial progenitor cells contributes to reendothelialization after arterial injury. *Circulation* **108**(25), 3115-21.
- Iwanaga, Y., Hoshijima, M., Gu, Y., Iwatate, M., Dieterle, T., Ikeda, Y., Date, M. O., Chrast, J., Matsuzaki, M., Peterson, K. L., Chien, K. R., and Ross, J., Jr. (2004). Chronic phospholamban inhibition prevents progressive cardiac dysfunction and pathological remodeling after infarction in rats. *J Clin Invest* **113**(5), 727-36.
- Iwatate, M., Gu, Y., Dieterle, T., Iwanaga, Y., Peterson, K. L., Hoshijima, M., Chien, K. R., and Ross, J. (2003). In vivo high-efficiency transcortary gene delivery and Cre-LoxP gene switching in the adult mouse heart. *Gene Ther* **10**(21), 1814-20.
- Jacobson, E. R., Kopit, W., Kennedy, F. A., and Funk, R. S. (1996). Coinfection of a bearded dragon, *Pogona vitticeps*, with adenovirus- and dependovirus-like viruses. *Vet Pathol* **33**(3), 343-6.
- Jennings, K., Miyamae, T., Traister, R., Marinov, A., Katakura, S., Sowders, D., Trapnell, B., Wilson, J. M., Gao, G., and Hirsch, R. (2005). Proteasome inhibition enhances AAV-mediated transgene expression in human synoviocytes in vitro and in vivo. *Mol Ther* **11**(4), 600-7.
- Kalka, C., Masuda, H., Takahashi, T., Kalka-Moll, W. M., Silver, M., Kearney, M., Li, T., Isner, J. M., and Asahara, T. (2000). Transplantation of ex vivo expanded endothelial progenitor cells for therapeutic neovascularization. *Proc Natl Acad Sci U S A* **97**(7), 3422-7.
- Kaludov, N., Brown, K. E., Walters, R. W., Zabner, J., and Chiorini, J. A. (2001). Adeno-associated virus serotype 4 (AAV4) and AAV5 both require sialic acid binding for hemagglutination and efficient transduction but differ in sialic acid linkage specificity. *J Virol* **75**(15), 6884-93.
- Kapeller, R., and Cantley, L. C. (1994). Phosphatidylinositol 3-kinase. *Bioessays* **16**(8), 565-76.
- Kaplitt, M. G., Leone, P., Samulski, R. J., Xiao, X., Pfaff, D. W., O'Malley, K. L., and Durning, M. J. (1994). Long-term gene expression and phenotypic correction using adeno-associated virus vectors in the mammalian brain. *Nat Genet* **8**(2), 148-54.
- Kaplitt, M. G., Xiao, X., Samulski, R. J., Li, J., Ojamaa, K., Klein, I. L., Makimura, H., Kaplitt, M. J., Strumpf, R. K., and Diethrich, E. B. (1996). Long-term gene transfer in porcine myocardium after coronary infusion of an adeno-associated virus vector. *Ann Thorac Surg* **62**(6), 1669-76.
- Kashiwakura, Y., Tamayose, K., Iwabuchi, K., Hirai, Y., Shimada, T., Matsumoto, K., Nakamura, T., Watanabe, M., Oshimi, K., and Daida, H. (2005). Hepatocyte growth factor receptor is a coreceptor for adeno-associated virus type 2 infection. *J Virol* **79**(1), 609-14.
- Kaspar, B. K., Roth, D. M., Lai, N. C., Drumm, J. D., Erickson, D. A., McKirnan, M. D., and Hammond, H. K. (2005). Myocardial gene transfer and long-term expression following intracoronary delivery of adeno-associated virus. *J Gene Med* **7**(3), 316-24.
- Kawamoto, A., Gwon, H. C., Iwaguro, H., Yamaguchi, J. I., Uchida, S., Masuda, H., Silver, M., Ma, H., Kearney, M., Isner, J. M., and Asahara, T. (2001). Therapeutic potential of ex vivo expanded endothelial progenitor cells for myocardial ischemia. *Circulation* **103**(5), 634-7.

- Kay, M. A., Manno, C. S., Ragni, M. V., Larson, P. J., Couto, L. B., McClelland, A., Glader, B., Chew, A. J., Tai, S. J., Herzog, R. W., Arruda, V., Johnson, F., Scallan, C., Skarsgard, E., Flake, A. W., and High, K. A. (2000). Evidence for gene transfer and expression of factor IX in haemophilia B patients treated with an AAV vector. *Nat Genet* **24**(3), 257-61.
- Ke, B., Ritter, T., Kato, H., Zhai, Y., Li, J., Lehmann, M., Busuttil, R. W., Volk, H. D., and Kupiec-Weglinski, J. W. (2000). Regulatory cells potentiate the efficacy of IL-4 gene transfer by up-regulating Th2-dependent expression of protective molecules in the infectious tolerance pathway in transplant recipients. *J Immunol* **164**(11), 5739-45.
- Ke, B., Shen, X. D., Zhai, Y., Gao, F., Busuttil, R. W., Volk, H. D., and Kupiec-Weglinski, J. W. (2002). Heme oxygenase 1 mediates the immunomodulatory and antiapoptotic effects of interleukin 13 gene therapy in vivo and in vitro. *Hum Gene Ther* **13**(15), 1845-57.
- Kern, A., Schmidt, K., Leder, C., Muller, O. J., Wobus, C. E., Bettinger, K., Von der Lieth, C. W., King, J. A., and Kleinschmidt, J. A. (2003). Identification of a heparin-binding motif on adeno-associated virus type 2 capsids. *J Virol* **77**(20), 11072-81.
- Khan, T. A., Sellke, F. W., and Laham, R. J. (2003). Gene therapy progress and prospects: therapeutic angiogenesis for limb and myocardial ischemia. *Gene Ther* **10**(4), 285-91.
- King, J. A., Dubielzig, R., Grimm, D., and Kleinschmidt, J. A. (2001). DNA helicase-mediated packaging of adeno-associated virus type 2 genomes into preformed capsids. *Embo J* **20**(12), 3282-91.
- Kinniburgh, D., and Russell, N. H. (1993). Comparative study of CD34-positive cells and subpopulations in human umbilical cord blood and bone marrow. *Bone Marrow Transplant* **12**(5), 489-94.
- Kissel, C. K., Lehmann, R., Assmus, B., Aicher, A., Honold, J., Fischer-Rasokat, U., Heeschen, C., Spyridopoulos, I., Dimmeler, S., and Zeiher, A. M. (2007). Selective functional exhaustion of hematopoietic progenitor cells in the bone marrow of patients with postinfarction heart failure. *J Am Coll Cardiol* **49**(24), 2341-9.
- Kitazono, M., Rao, V. K., Robey, R., Aikou, T., Bates, S., Fojo, T., and Goldsmith, M. E. (2002). Histone deacetylase inhibitor FR901228 enhances adenovirus infection of hematopoietic cells. *Blood* **99**(6), 2248-51.
- Kotin, R. M., Linden, R. M., and Berns, K. I. (1992). Characterization of a preferred site on human chromosome 19q for integration of adeno-associated virus DNA by non-homologous recombination. *Embo J* **11**(13), 5071-8.
- Kotin, R. M., Siniscalco, M., Samulski, R. J., Zhu, X. D., Hunter, L., Laughlin, C. A., McLaughlin, S., Muzyczka, N., Rocchi, M., and Berns, K. I. (1990). Site-specific integration by adeno-associated virus. *Proc Natl Acad Sci U S A* **87**(6), 2211-5.
- Kronenberg, S., Bottcher, B., von der Lieth, C. W., Bleker, S., and Kleinschmidt, J. A. (2005). A conformational change in the adeno-associated virus type 2 capsid leads to the exposure of hidden VP1 N termini. *J Virol* **79**(9), 5296-303.
- Kronenberg, S., Kleinschmidt, J. A., and Bottcher, B. (2001). Electron cryo-microscopy and image reconstruction of adeno-associated virus type 2 empty capsids. *EMBO Rep* **2**(11), 997-1002.
- Kustikova, O. S., Geiger, H., Li, Z., Brugman, M. H., Chambers, S. M., Shaw, C. A., Pike-Overzet, K., de Ridder, D., Staal, F. J., von Keudell, G., Cornils, K.,

- Nattamai, K. J., Modlich, U., Wagemaker, G., Goodell, M. A., Fehse, B., and Baum, C. (2007). Retroviral vector insertion sites associated with dominant hematopoietic clones mark "stemness" pathways. *Blood* **109**(5), 1897-907.
- Kyostio, S. R., Owens, R. A., Weitzman, M. D., Antoni, B. A., Chejanovsky, N., and Carter, B. J. (1994). Analysis of adeno-associated virus (AAV) wild-type and mutant Rep proteins for their abilities to negatively regulate AAV p5 and p19 mRNA levels. *J Virol* **68**(5), 2947-57.
- Labow, M. A., and Berns, K. I. (1988). The adeno-associated virus rep gene inhibits replication of an adeno-associated virus/simian virus 40 hybrid genome in cos-7 cells. *J Virol* **62**(5), 1705-12.
- Laufs, U., Werner, N., Link, A., Endres, M., Wassmann, S., Jurgens, K., Miche, E., Bohm, M., and Nickenig, G. (2004). Physical training increases endothelial progenitor cells, inhibits neointima formation, and enhances angiogenesis. *Circulation* **109**(2), 220-6.
- Lemoli, R. M. (2005). Pegfilgrastim for mobilization of stem cells in allogeneic donors. *Haematologica* **90**(12), 1590A.
- Leucht, C., Simoneau, S., Rey, C., Vana, K., Rieger, R., Lasmezas, C. I., and Weiss, S. (2003). The 37 kDa/67 kDa laminin receptor is required for PrP(Sc) propagation in scrapie-infected neuronal cells. *EMBO Rep* **4**(3), 290-5.
- Li, E., Stupack, D., Bokoch, G. M., and Nemerow, G. R. (1998). Adenovirus endocytosis requires actin cytoskeleton reorganization mediated by Rho family GTPases. *J Virol* **72**(11), 8806-12.
- Li, J., Wang, D., Qian, S., Chen, Z., Zhu, T., and Xiao, X. (2003). Efficient and long-term intracardiac gene transfer in delta-sarcoglycan-deficiency hamster by adeno-associated virus-2 vectors. *Gene Ther* **10**(21), 1807-13.
- Limberis, M. P., and Wilson, J. M. (2006). Adeno-associated virus serotype 9 vectors transduce murine alveolar and nasal epithelia and can be readministered. *Proc Natl Acad Sci U S A* **103**(35), 12993-8.
- Lin, Y., Weisdorf, D. J., Solovey, A., and Hebbel, R. P. (2000). Origins of circulating endothelial cells and endothelial outgrowth from blood. *J Clin Invest* **105**(1), 71-7.
- Linden, R. M., Ward, P., Giraud, C., Winocour, E., and Berns, K. I. (1996). Site-specific integration by adeno-associated virus. *Proc Natl Acad Sci U S A* **93**(21), 11288-94.
- Linden, R. M., Winocour, E., and Berns, K. I. (1996). The recombination signals for adeno-associated virus site-specific integration. *Proc Natl Acad Sci U S A* **93**(15), 7966-72.
- Liu, X., Pachori, A. S., Ward, C. A., Davis, J. P., Gneccchi, M., Kong, D., Zhang, L., Murduck, J., Yet, S. F., Perrella, M. A., Pratt, R. E., Dzau, V. J., and Melo, L. G. (2006). Heme oxygenase-1 (HO-1) inhibits postmyocardial infarct remodeling and restores ventricular function. *Faseb J* **20**(2), 207-16.
- Logeart, D., Hatem, S. N., Heimbürger, M., Le Roux, A., Michel, J. B., and Mercadier, J. J. (2001). How to optimize in vivo gene transfer to cardiac myocytes: mechanical or pharmacological procedures? *Hum Gene Ther* **12**(13), 1601-10.
- Lois, C., and Alvarez-Buylla, A. (1993). Proliferating subventricular zone cells in the adult mammalian forebrain can differentiate into neurons and glia. *Proc Natl Acad Sci U S A* **90**(5), 2074-7.

- Loser, P., Jennings, G. S., Strauss, M., and Sandig, V. (1998). Reactivation of the previously silenced cytomegalovirus major immediate-early promoter in the mouse liver: involvement of NFkappaB. *J Virol* **72**(1), 180-90.
- Losordo, D. W., Vale, P. R., Hendel, R. C., Milliken, C. E., Fortuin, F. D., Cummings, N., Schatz, R. A., Asahara, T., Isner, J. M., and Kuntz, R. E. (2002). Phase 1/2 placebo-controlled, double-blind, dose-escalating trial of myocardial vascular endothelial growth factor 2 gene transfer by catheter delivery in patients with chronic myocardial ischemia. *Circulation* **105**(17), 2012-8.
- Lu, L., Xiao, M., Shen, R. N., Grigsby, S., and Broxmeyer, H. E. (1993). Enrichment, characterization, and responsiveness of single primitive CD34 human umbilical cord blood hematopoietic progenitors with high proliferative and replating potential. *Blood* **81**(1), 41-8.
- Lu, Y. (2004). Recombinant adeno-associated virus as delivery vector for gene therapy--a review. *Stem Cells Dev* **13**(1), 133-45.
- Ludewigs, H., Zuber, C., Vana, K., Nikles, D., Zerr, I., and Weiss, S. (2007). Therapeutic approaches for prion disorders. *Expert Rev Anti Infect Ther* **5**(4), 613-30.
- Lusby, E. W., and Berns, K. I. (1982). Mapping of the 5' termini of two adeno-associated virus 2 RNAs in the left half of the genome. *J Virol* **41**(2), 518-26.
- Lux, K., Goerlitz, N., Schlemminger, S., Perabo, L., Goldnau, D., Endell, J., Leike, K., Kofler, D. M., Finke, S., Hallek, M., and Buning, H. (2005). Green fluorescent protein-tagged adeno-associated virus particles allow the study of cytosolic and nuclear trafficking. *J Virol* **79**(18), 11776-87.
- Maeda, Y., Ikeda, U., Shimpo, M., Shibuya, M., Monahan, J., Urabe, M., Ozawa, K., and Shimada, K. (2000). Adeno-associated virus-mediated vascular endothelial growth factor gene transfer into cardiac myocytes. *J Cardiovasc Pharmacol* **36**(4), 438-43.
- Malik, P., McQuiston, S. A., Yu, X. J., Pepper, K. A., Krall, W. J., Podsakoff, G. M., Kurtzman, G. J., and Kohn, D. B. (1997). Recombinant adeno-associated virus mediates a high level of gene transfer but less efficient integration in the K562 human hematopoietic cell line. *J Virol* **71**(3), 1776-83.
- Manno, C. S., Chew, A. J., Hutchison, S., Larson, P. J., Herzog, R. W., Arruda, V. R., Tai, S. J., Ragni, M. V., Thompson, A., Ozelo, M., Couto, L. B., Leonard, D. G., Johnson, F. A., McClelland, A., Scallan, C., Skarsgard, E., Flake, A. W., Kay, M. A., High, K. A., and Glader, B. (2003). AAV-mediated factor IX gene transfer to skeletal muscle in patients with severe hemophilia B. *Blood* **101**(8), 2963-72.
- Manno, C. S., Pierce, G. F., Arruda, V. R., Glader, B., Ragni, M., Rasko, J. J., Ozelo, M. C., Hoots, K., Blatt, P., Konkle, B., Dake, M., Kaye, R., Razavi, M., Zajko, A., Zehnder, J., Rustagi, P. K., Nakai, H., Chew, A., Leonard, D., Wright, J. F., Lessard, R. R., Sommer, J. M., Tigges, M., Sabatino, D., Luk, A., Jiang, H., Mingozzi, F., Couto, L., Ertl, H. C., High, K. A., and Kay, M. A. (2006). Successful transduction of liver in hemophilia by AAV-Factor IX and limitations imposed by the host immune response. *Nat Med* **12**(3), 342-7.
- Marcus-Sekura, C. J., and Carter, B. J. (1983). Chromatin-like structure of adeno-associated virus DNA in infected cells. *J Virol* **48**(1), 79-87.
- Marsh, M., and Helenius, A. (1989). Virus entry into animal cells. *Adv Virus Res* **36**, 107-51.

- Mayor, H. D., Jamison, R. M., Jordan, L. E., and Melnick, J. L. (1965). Structure and Composition of a Small Particle Prepared from a Simian Adenovirus. *J Bacteriol* **90**(1), 235-42.
- McCarty, D. M., Fu, H., Monahan, P. E., Toulson, C. E., Naik, P., and Samulski, R. J. (2003). Adeno-associated virus terminal repeat (TR) mutant generates self-complementary vectors to overcome the rate-limiting step to transduction in vivo. *Gene Ther* **10**(26), 2112-8.
- McCarty, D. M., Monahan, P. E., and Samulski, R. J. (2001). Self-complementary recombinant adeno-associated virus (scAAV) vectors promote efficient transduction independently of DNA synthesis. *Gene Ther* **8**(16), 1248-54.
- McCarty, D. M., Pereira, D. J., Zolotukhin, I., Zhou, X., Ryan, J. H., and Muzyczka, N. (1994). Identification of linear DNA sequences that specifically bind the adeno-associated virus Rep protein. *J Virol* **68**(8), 4988-97.
- McLaughlin, S. K., Collis, P., Hermonat, P. L., and Muzyczka, N. (1988). Adeno-associated virus general transduction vectors: analysis of proviral structures. *J Virol* **62**(6), 1963-73.
- McPherson, R. A., Rosenthal, L. J., and Rose, J. A. (1985). Human cytomegalovirus completely helps adeno-associated virus replication. *Virology* **147**(1), 217-22.
- Melnick, J. L., Mayor, H. D., Smith, K. O., and Rapp, F. (1965). Association of 20-Millimicron Particles with Adenoviruses. *J Bacteriol* **90**(1), 271-4.
- Melo, L. G., Ghecchi, M., Pachori, A. S., Kong, D., Wang, K., Liu, X., Pratt, R. E., and Dzau, V. J. (2004). Endothelium-targeted gene and cell-based therapies for cardiovascular disease. *Arterioscler Thromb Vasc Biol* **24**(10), 1761-74.
- Melo, L. G., Pachori, A. S., Ghecchi, M., and Dzau, V. J. (2005). Genetic therapies for cardiovascular diseases. *Trends Mol Med* **11**(5), 240-50.
- Minato, S., Iwanaga, K., Kakemi, M., Yamashita, S., and Oku, N. (2003). Application of polyethyleneglycol (PEG)-modified liposomes for oral vaccine: effect of lipid dose on systemic and mucosal immunity. *J Control Release* **89**(2), 189-97.
- Minucci, S., Horn, V., Bhattacharyya, N., Russanova, V., Ogryzko, V. V., Gabriele, L., Howard, B. H., and Ozato, K. (1997). A histone deacetylase inhibitor potentiates retinoid receptor action in embryonal carcinoma cells. *Proc Natl Acad Sci U S A* **94**(21), 11295-300.
- Miyahara, A., Johnson, P. A., Elam, R. L., Dai, Y., Witztum, J. L., Verma, I. M., and Friedmann, T. (1992). Direct gene transfer to the liver with herpes simplex virus type 1 vectors: transient production of physiologically relevant levels of circulating factor IX. *New Biol* **4**(3), 238-46.
- Moore, K. A., and Lemischka, I. R. (2006). Stem cells and their niches. *Science* **311**(5769), 1880-5.
- Mori, S., Wang, L., Takeuchi, T., and Kanda, T. (2004). Two novel adeno-associated viruses from cynomolgus monkey: pseudotyping characterization of capsid protein. *Virology* **330**(2), 375-83.
- Morishita, K., Johnson, D. E., and Williams, L. T. (1995). A novel promoter for vascular endothelial growth factor receptor (flt-1) that confers endothelial-specific gene expression. *J Biol Chem* **270**(46), 27948-53.
- Morishita, R., Aoki, M., Hashiya, N., Makino, H., Yamasaki, K., Azuma, J., Sawa, Y., Matsuda, H., Kaneda, Y., and Ogihara, T. (2004). Safety evaluation of clinical gene therapy using hepatocyte growth factor to treat peripheral arterial disease. *Hypertension* **44**(2), 203-9.

- Moskalenko, M., Chen, L., van Roey, M., Donahue, B. A., Snyder, R. O., McArthur, J. G., and Patel, S. D. (2000). Epitope mapping of human anti-adenovirus-associated virus type 2 neutralizing antibodies: implications for gene therapy and virus structure. *J Virol* **74**(4), 1761-6.
- Moss, R. B., Rodman, D., Spencer, L. T., Aitken, M. L., Zeitlin, P. L., Waltz, D., Milla, C., Brody, A. S., Clancy, J. P., Ramsey, B., Hamblett, N., and Heald, A. E. (2004). Repeated adeno-associated virus serotype 2 aerosol-mediated cystic fibrosis transmembrane regulator gene transfer to the lungs of patients with cystic fibrosis: a multicenter, double-blind, placebo-controlled trial. *Chest* **125**(2), 509-21.
- Mukhopadhyay, D., and Riezman, H. (2007). Proteasome-independent functions of ubiquitin in endocytosis and signaling. *Science* **315**(5809), 201-5.
- Muller, O. J., Kaul, F., Weitzman, M. D., Pasqualini, R., Arap, W., Kleinschmidt, J. A., and Trepel, M. (2003). Random peptide libraries displayed on adeno-associated virus to select for targeted gene therapy vectors. *Nat Biotechnol* **21**(9), 1040-6.
- Nakai, H., Yant, S. R., Storm, T. A., Fuess, S., Meuse, L., and Kay, M. A. (2001). Extrachromosomal recombinant adeno-associated virus vector genomes are primarily responsible for stable liver transduction in vivo. *J Virol* **75**(15), 6969-76.
- Nathwani, A. C., Hanawa, H., Vandergriff, J., Kelly, P., Vanin, E. F., and Nienhuis, A. W. (2000). Efficient gene transfer into human cord blood CD34+ cells and the CD34+CD38- subset using highly purified recombinant adeno-associated viral vector preparations that are free of helper virus and wild-type AAV. *Gene Ther* **7**(3), 183-95.
- Ni, T. H., Zhou, X., McCarty, D. M., Zolotukhin, I., and Muzyczka, N. (1994). In vitro replication of adeno-associated virus DNA. *J Virol* **68**(2), 1128-38.
- Nicklin, S. A., Buening, H., Dishart, K. L., de Alwis, M., Girod, A., Hacker, U., Thrasher, A. J., Ali, R. R., Hallek, M., and Baker, A. H. (2001a). Efficient and selective AAV2-mediated gene transfer directed to human vascular endothelial cells. *Mol Ther* **4**(3), 174-81.
- Nicklin, S. A., Reynolds, P. N., Brosnan, M. J., White, S. J., Curiel, D. T., Dominiczak, A. F., and Baker, A. H. (2001b). Analysis of cell-specific promoters for viral gene therapy targeted at the vascular endothelium. *Hypertension* **38**(1), 65-70.
- Nicosia, R. F., Villaschi, S., and Smith, M. (1994). Isolation and characterization of vasoformative endothelial cells from the rat aorta. *In Vitro Cell Dev Biol Anim* **30A**(6), 394-9.
- Oh, H., Bradfute, S. B., Gallardo, T. D., Nakamura, T., Gaussin, V., Mishina, Y., Pocius, J., Michael, L. H., Behringer, R. R., Garry, D. J., Entman, M. L., and Schneider, M. D. (2003). Cardiac progenitor cells from adult myocardium: homing, differentiation, and fusion after infarction. *Proc Natl Acad Sci U S A* **100**(21), 12313-8.
- Oka, M., Yanagawa, Y., Asada, T., Yoneda, A., Hasezawa, S., Sato, T., and Nakagawa, H. (2004). Inhibition of proteasome by MG-132 treatment causes extra phragmoplast formation and cortical microtubule disorganization during M/G1 transition in synchronized tobacco cells. *Plant Cell Physiol* **45**(11), 1623-32.
- Olson, E. J., Haskell, S. R., Frank, R. K., Lehmkuhl, H. D., Hobbs, L. A., Warg, J. V., Landgraf, J. G., and Wunschmann, A. (2004). Isolation of an adenovirus

- and an adeno-associated virus from goat kids with enteritis. *J Vet Diagn Invest* **16**(5), 461-4.
- Omori, N., Maruyama, K., Jin, G., Li, F., Wang, S. J., Hamakawa, Y., Sato, K., Nagano, I., Shoji, M., and Abe, K. (2003). Targeting of post-ischemic cerebral endothelium in rat by liposomes bearing polyethylene glycol-coupled transferrin. *Neurol Res* **25**(3), 275-9.
- Onishi, A., Iwamoto, M., Akita, T., Mikawa, S., Takeda, K., Awata, T., Hanada, H., and Perry, A. C. (2000). Pig cloning by microinjection of fetal fibroblast nuclei. *Science* **289**(5482), 1188-90.
- Pacak, C. A., Mah, C. S., Thattaliyath, B. D., Conlon, T. J., Lewis, M. A., Cloutier, D. E., Zolotukhin, I., Tarantal, A. F., and Byrne, B. J. (2006). Recombinant adeno-associated virus serotype 9 leads to preferential cardiac transduction in vivo. *Circ Res* **99**(4), e3-9.
- Pajusola, K., Gruchala, M., Joch, H., Luscher, T. F., Yla-Herttuala, S., and Bueler, H. (2002). Cell-type-specific characteristics modulate the transduction efficiency of adeno-associated virus type 2 and restrain infection of endothelial cells. *J Virol* **76**(22), 11530-40.
- Palomeque, J., Chemaly, E. R., Colosi, P., Wellman, J. A., Zhou, S., Del Monte, F., and Hajjar, R. J. (2007). Efficiency of eight different AAV serotypes in transducing rat myocardium in vivo. *Gene Ther* **14**(13), 989-97.
- Papayannopoulou, T. (2003). Bone marrow homing: the players, the playfield, and their evolving roles. *Curr Opin Hematol* **10**(3), 214-9.
- Papayannopoulou, T., Priestley, G. V., Bonig, H., and Nakamoto, B. (2003). The role of G-protein signaling in hematopoietic stem/progenitor cell mobilization. *Blood* **101**(12), 4739-47.
- Parks, W. P., Melnick, J. L., Rongey, R., and Mayor, H. D. (1967). Physical assay and growth cycle studies of a defective adeno-satellite virus. *J Virol* **1**(1), 171-80.
- Paterna, J. C., Moccetti, T., Mura, A., Feldon, J., and Bueler, H. (2000). Influence of promoter and WHV post-transcriptional regulatory element on AAV-mediated transgene expression in the rat brain. *Gene Ther* **7**(15), 1304-11.
- Peichev, M., Naiyer, A. J., Pereira, D., Zhu, Z., Lane, W. J., Williams, M., Oz, M. C., Hicklin, D. J., Witte, L., Moore, M. A., and Rafii, S. (2000). Expression of VEGFR-2 and AC133 by circulating human CD34(+) cells identifies a population of functional endothelial precursors. *Blood* **95**(3), 952-8.
- Perabo, L., Buning, H., Kofler, D. M., Ried, M. U., Girod, A., Wendtner, C. M., Enssle, J., and Hallek, M. (2003). In vitro selection of viral vectors with modified tropism: the adeno-associated virus display. *Mol Ther* **8**(1), 151-7.
- Pereira, D. J., McCarty, D. M., and Muzyczka, N. (1997). The adeno-associated virus (AAV) Rep protein acts as both a repressor and an activator to regulate AAV transcription during a productive infection. *J Virol* **71**(2), 1079-88.
- Podsakoff, G., Wong, K. K., Jr., and Chatterjee, S. (1994). Efficient gene transfer into nondividing cells by adeno-associated virus-based vectors. *J Virol* **68**(9), 5656-66.
- Ponnazhagan, S., Mukherjee, P., Wang, X. S., Qing, K., Kube, D. M., Mah, C., Kurpad, C., Yoder, M. C., Srour, E. F., and Srivastava, A. (1997). Adeno-associated virus type 2-mediated transduction in primary human bone marrow-derived CD34+ hematopoietic progenitor cells: donor variation and correlation of transgene expression with cellular differentiation. *J Virol* **71**(11), 8262-7.

- Qing, K., Mah, C., Hansen, J., Zhou, S., Dwarki, V., and Srivastava, A. (1999). Human fibroblast growth factor receptor 1 is a co-receptor for infection by adeno-associated virus 2. *Nat Med* **5**(1), 71-7.
- Qiu, J., Nayak, R., Tullis, G. E., and Pintel, D. J. (2002). Characterization of the transcription profile of adeno-associated virus type 5 reveals a number of unique features compared to previously characterized adeno-associated viruses. *J Virol* **76**(24), 12435-47.
- Qiu, J., and Pintel, D. J. (2002). The adeno-associated virus type 2 Rep protein regulates RNA processing via interaction with the transcription template. *Mol Cell Biol* **22**(11), 3639-52.
- Raake, P. W., Hinkel, R., Muller, S., Delker, S., Kreuzpointner, R., Kupatt, C., Katus, H. A., Kleinschmidt, J. A., Boekstegers, P., and Muller, O. J. (2008). Cardio-specific long-term gene expression in a porcine model after selective pressure-regulated retroinfusion of adeno-associated viral (AAV) vectors. *Gene Ther* **15**(1), 12-7.
- Rabinowitz, J. E., Rolling, F., Li, C., Conrath, H., Xiao, W., Xiao, X., and Samulski, R. J. (2002). Cross-packaging of a single adeno-associated virus (AAV) type 2 vector genome into multiple AAV serotypes enables transduction with broad specificity. *J Virol* **76**(2), 791-801.
- Raper, S. E., Chirmule, N., Lee, F. S., Wivel, N. A., Bagg, A., Gao, G. P., Wilson, J. M., and Batshaw, M. L. (2003). Fatal systemic inflammatory response syndrome in a ornithine transcarbamylase deficient patient following adenoviral gene transfer. *Mol Genet Metab* **80**(1-2), 148-58.
- Redemann, B. E., Mendelson, E., and Carter, B. J. (1989). Adeno-associated virus rep protein synthesis during productive infection. *J Virol* **63**(2), 873-82.
- Reyes, M., Dudek, A., Jahagirdar, B., Koodie, L., Marker, P. H., and Verfaillie, C. M. (2002). Origin of endothelial progenitors in human postnatal bone marrow. *J Clin Invest* **109**(3), 337-46.
- Richardson, W. D., and Westphal, H. (1981). A cascade of adenovirus early functions is required for expression of adeno-associated virus. *Cell* **27**(1 Pt 2), 133-41.
- Rideg, K., Hirka, G., Prakash, K., Bushar, L. M., Nothias, J. Y., Weinmann, R., Andrews, P. W., and Gonczol, E. (1994). DNA-binding proteins that interact with the 19-base pair (CRE-like) element from the HCMV major immediate early promoter in differentiating human embryonal carcinoma cells. *Differentiation* **56**(1-2), 119-29.
- Rieger, R., Edenhofer, F., Lasmezas, C. I., and Weiss, S. (1997). The human 37-kDa laminin receptor precursor interacts with the prion protein in eukaryotic cells. *Nat Med* **3**(12), 1383-8.
- Rose, J. A., Maizel, J. V., Jr., Inman, J. K., and Shatkin, A. J. (1971). Structural proteins of adenovirus-associated viruses. *J Virol* **8**(5), 766-70.
- Rotondaro, L., Mele, A., and Rovera, G. (1996). Efficiency of different viral promoters in directing gene expression in mammalian cells: effect of 3'-untranslated sequences. *Gene* **168**(2), 195-8.
- Russell, D. W., Miller, A. D., and Alexander, I. E. (1994). Adeno-associated virus vectors preferentially transduce cells in S phase. *Proc Natl Acad Sci U S A* **91**(19), 8915-9.
- Rutledge, E. A., Halbert, C. L., and Russell, D. W. (1998). Infectious clones and vectors derived from adeno-associated virus (AAV) serotypes other than AAV type 2. *J Virol* **72**(1), 309-19.

- Sakoda, T., Kasahara, N., Kedes, L., and Ohyanagi, M. (2007). Lentiviral vector-mediated gene transfer to endothelial cells compared with adenoviral and retroviral vectors. *Prep Biochem Biotechnol* **37**(1), 1-11.
- Samulski, R. J., Chang, L. S., and Shenk, T. (1987). A recombinant plasmid from which an infectious adeno-associated virus genome can be excised in vitro and its use to study viral replication. *J Virol* **61**(10), 3096-101.
- Sanlioglu, S., Benson, P. K., Yang, J., Atkinson, E. M., Reynolds, T., and Engelhardt, J. F. (2000). Endocytosis and nuclear trafficking of adeno-associated virus type 2 are controlled by rac1 and phosphatidylinositol-3 kinase activation. *J Virol* **74**(19), 9184-96.
- Santat, L., Paz, H., Wong, C., Li, L., Macer, J., Forman, S., Wong, K. K., and Chatterjee, S. (2005). Recombinant AAV2 transduction of primitive human hematopoietic stem cells capable of serial engraftment in immune-deficient mice. *Proc Natl Acad Sci U S A* **102**(31), 11053-8.
- Saygili, E., Rana, O. R., Saygili, E., Reuter, H., Frank, K., Schwinger, R. H., Muller-Ehmsen, J., and Zobel, C. (2007). Losartan prevents stretch-induced electrical remodeling in cultured atrial neonatal myocytes. *Am J Physiol Heart Circ Physiol* **292**(6), H2898-905.
- Scaffidi, P., Misteli, T., and Bianchi, M. E. (2002). Release of chromatin protein HMGB1 by necrotic cells triggers inflammation. *Nature* **418**(6894), 191-5.
- Scallan, C. D., Jiang, H., Liu, T., Patarroyo-White, S., Sommer, J. M., Zhou, S., Couto, L. B., and Pierce, G. F. (2006). Human immunoglobulin inhibits liver transduction by AAV vectors at low AAV2 neutralizing titers in SCID mice. *Blood* **107**(5), 1810-7.
- Schachinger, V., Assmus, B., Britten, M. B., Honold, J., Lehmann, R., Teupe, C., Abolmaali, N. D., Vogl, T. J., Hofmann, W. K., Martin, H., Dimmeler, S., and Zeiher, A. M. (2004). Transplantation of progenitor cells and regeneration enhancement in acute myocardial infarction: final one-year results of the TOPCARE-AMI Trial. *J Am Coll Cardiol* **44**(8), 1690-9.
- Schachinger, V., Assmus, B., Honold, J., Lehmann, R., Hofmann, W. K., Martin, H., Dimmeler, S., and Zeiher, A. M. (2006a). Normalization of coronary blood flow in the infarct-related artery after intracoronary progenitor cell therapy: intracoronary Doppler substudy of the TOPCARE-AMI trial. *Clin Res Cardiol* **95**(1), 13-22.
- Schachinger, V., Erbs, S., Elsasser, A., Haberbosch, W., Hambrecht, R., Holschermann, H., Yu, J., Corti, R., Mathey, D. G., Hamm, C. W., Suselbeck, T., Assmus, B., Tonn, T., Dimmeler, S., and Zeiher, A. M. (2006b). Intracoronary bone marrow-derived progenitor cells in acute myocardial infarction. *N Engl J Med* **355**(12), 1210-21.
- Schachinger, V., Erbs, S., Elsasser, A., Haberbosch, W., Hambrecht, R., Holschermann, H., Yu, J., Corti, R., Mathey, D. G., Hamm, C. W., Suselbeck, T., Werner, N., Haase, J., Neuzner, J., Germing, A., Mark, B., Assmus, B., Tonn, T., Dimmeler, S., and Zeiher, A. M. (2006c). Improved clinical outcome after intracoronary administration of bone-marrow-derived progenitor cells in acute myocardial infarction: final 1-year results of the REPAIR-AMI trial. *Eur Heart J* **27**(23), 2775-83.
- Scherer, W. F., Syverton, J. T., and Gey, G. O. (1953). Studies on the propagation in vitro of poliomyelitis viruses. IV. Viral multiplication in a stable strain of human malignant epithelial cells (strain HeLa) derived from an epidermoid carcinoma of the cervix. *J Exp Med* **97**(5), 695-710.

- Schimmenti, S., Boesen, J., Claassen, E. A., Valerio, D., and Einerhand, M. P. (1998). Long-term genetic modification of rhesus monkey hematopoietic cells following transplantation of adenoassociated virus vector-transduced CD34+ cells. *Hum Gene Ther* **9**(18), 2727-34.
- Schlehofer, J. R., Ehrbar, M., and zur Hausen, H. (1986). Vaccinia virus, herpes simplex virus, and carcinogens induce DNA amplification in a human cell line and support replication of a helpervirus dependent parvovirus. *Virology* **152**(1), 110-7.
- Schmeisser, A., Garlichs, C. D., Zhang, H., Eskafi, S., Graffy, C., Ludwig, J., Strasser, R. H., and Daniel, W. G. (2001). Monocytes coexpress endothelial and macrophagocytic lineage markers and form cord-like structures in Matrigel under angiogenic conditions. *Cardiovasc Res* **49**(3), 671-80.
- Schmidt, M., Katano, H., Bossis, I., and Chiorini, J. A. (2004). Cloning and characterization of a bovine adeno-associated virus. *J Virol* **78**(12), 6509-16.
- Schmidt, M., Voutetakis, A., Afione, S., Zheng, C., and Chiorini, J. A. (2006). AAV12, isolated from Vervet Monkey, has unique tropism and biological as well as neutralization properties. *Mol. Ther.* **Vol. 13**(supplement 1), S288.
- Schmidt, M., Voutetakis, A., Afione, S., Zheng, C., Mandikian, D., and Chiorini, J. A. (2007). AAV12: A Novel AAV Serotype with Sialic Acid and HSPG Independent Transduction Activity. *J Virol*.
- Schmidt, M., Zickler, P., Hoffmann, G., Haas, S., Wissler, M., Muessig, A., Tisdale, J. F., Kuramoto, K., Andrews, R. G., Wu, T., Kiem, H. P., Dunbar, C. E., and von Kalle, C. (2002). Polyclonal long-term repopulating stem cell clones in a primate model. *Blood* **100**(8), 2737-43.
- Scott, L. M., Priestley, G. V., and Papayannopoulou, T. (2003). Deletion of alpha4 integrins from adult hematopoietic cells reveals roles in homeostasis, regeneration, and homing. *Mol Cell Biol* **23**(24), 9349-60.
- Seisenberger, G., Ried, M. U., Endress, T., Buning, H., Hallek, M., and Brauchle, C. (2001). Real-time single-molecule imaging of the infection pathway of an adeno-associated virus. *Science* **294**(5548), 1929-32.
- Shalaby, F., Rossant, J., Yamaguchi, T. P., Gertsenstein, M., Wu, X. F., Breitman, M. L., and Schuh, A. C. (1995). Failure of blood-island formation and vasculogenesis in Flk-1-deficient mice. *Nature* **376**(6535), 62-6.
- Shi, Q., Rafii, S., Wu, M. H., Wijelath, E. S., Yu, C., Ishida, A., Fujita, Y., Kothari, S., Mohle, R., Sauvage, L. R., Moore, M. A., Storb, R. F., and Hammond, W. P. (1998). Evidence for circulating bone marrow-derived endothelial cells. *Blood* **92**(2), 362-7.
- Shintani, S., Murohara, T., Ikeda, H., Ueno, T., Honma, T., Katoh, A., Sasaki, K., Shimada, T., Oike, Y., and Imaizumi, T. (2001). Mobilization of endothelial progenitor cells in patients with acute myocardial infarction. *Circulation* **103**(23), 2776-9.
- Sipo, I., Fechner, H., Pinkert, S., Suckau, L., Wang, X., Weger, S., and Poller, W. (2007). Differential internalization and nuclear uncoating of self-complementary adeno-associated virus pseudotype vectors as determinants of cardiac cell transduction. *Gene Ther* **14**(18), 1319-29.
- Soligo, D., Schiro, R., Luksch, R., Manara, G., Quirici, N., Parravicini, C., and Lambertenghi Deliliers, G. (1990). Expression of integrins in human bone marrow. *Br J Haematol* **76**(3), 323-32.
- Sonntag, F., Bleker, S., Leuchs, B., Fischer, R., and Kleinschmidt, J. A. (2006). Adeno-associated virus type 2 capsids with externalized VP1/VP2

- trafficking domains are generated prior to passage through the cytoplasm and are maintained until uncoating occurs in the nucleus. *J Virol* **80**(22), 11040-54.
- Springer, T. A. (1994). Traffic signals for lymphocyte recirculation and leukocyte emigration: the multistep paradigm. *Cell* **76**(2), 301-14.
- Srivastava, A., Lusby, E. W., and Berns, K. I. (1983). Nucleotide sequence and organization of the adeno-associated virus 2 genome. *J Virol* **45**(2), 555-64.
- Stocker, G., Drzeniek, Z., Just, U., Ostertag, W., Siebertz, B., Greiling, H., and Haubeck, H. D. (1996). Proteoglycan synthesis in human and murine haematopoietic progenitor cell lines: isolation and characterization of a heparan sulphate proteoglycan as a major proteoglycan from the human haematopoietic cell line TF-1. *Biochem J* **317** (Pt 1), 203-12.
- Su, H., Huang, Y., Takagawa, J., Barcena, A., Arakawa-Hoyt, J., Ye, J., Grossman, W., and Kan, Y. W. (2006). AAV serotype-1 mediates early onset of gene expression in mouse hearts and results in better therapeutic effect. *Gene Ther* **13**(21), 1495-502.
- Su, H., Yeghiazarians, Y., Lee, A., Huang, Y., Arakawa-Hoyt, J., Ye, J., Orcino, G., Grossman, W., and Kan, Y. W. (2008). AAV serotype 1 mediates more efficient gene transfer to pig myocardium than AAV serotype 2 and plasmid. *J Gene Med* **10**(1), 33-41.
- Summerford, C., Bartlett, J. S., and Samulski, R. J. (1999). AlphaVbeta5 integrin: a co-receptor for adeno-associated virus type 2 infection. *Nat Med* **5**(1), 78-82.
- Summerford, C., and Samulski, R. J. (1998). Membrane-associated heparan sulfate proteoglycan is a receptor for adeno-associated virus type 2 virions. *J Virol* **72**(2), 1438-45.
- Sutherland, D. R., Keating, A., Nayar, R., Anania, S., and Stewart, A. K. (1994). Sensitive detection and enumeration of CD34+ cells in peripheral and cord blood by flow cytometry. *Exp Hematol* **22**(10), 1003-10.
- Svensson, E. C., Marshall, D. J., Woodard, K., Lin, H., Jiang, F., Chu, L., and Leiden, J. M. (1999). Efficient and stable transduction of cardiomyocytes after intramyocardial injection or intracoronary perfusion with recombinant adeno-associated virus vectors. *Circulation* **99**(2), 201-5.
- Takahashi, T., Kalka, C., Masuda, H., Chen, D., Silver, M., Kearney, M., Magner, M., Isner, J. M., and Asahara, T. (1999). Ischemia- and cytokine-induced mobilization of bone marrow-derived endothelial progenitor cells for neovascularization. *Nat Med* **5**(4), 434-8.
- Theiss, H. D., Kofler, D. M., Buning, H., Aldenhoff, A. L., Kaess, B., Decker, T., Baumert, J., Hallek, M., and Wendtner, C. M. (2003). Enhancement of gene transfer with recombinant adeno-associated virus (rAAV) vectors into primary B-cell chronic lymphocytic leukemia cells by CpG-oligodeoxynucleotides. *Exp Hematol* **31**(12), 1223-9.
- Thum, T., Hoerber, S., Froese, S., Klink, I., Stichtenoth, D. O., Galuppo, P., Jakob, M., Tsikas, D., Anker, S. D., Poole-Wilson, P. A., Borlak, J., Ertl, G., and Bauersachs, J. (2007). Age-dependent impairment of endothelial progenitor cells is corrected by growth-hormone-mediated increase of insulin-like growth-factor-1. *Circ Res* **100**(3), 434-43.
- Timpe, J. M., Verrill, K. C., and Trempe, J. P. (2006). Effects of adeno-associated virus on adenovirus replication and gene expression during coinfection. *J Virol* **80**(16), 7807-15.

- Touma, S. E., Goldberg, J. S., Moench, P., Guo, X., Tickoo, S. K., Gudas, L. J., and Nanus, D. M. (2005). Retinoic acid and the histone deacetylase inhibitor trichostatin inhibit the proliferation of human renal cell carcinoma in a xenograft tumor model. *Clin Cancer Res* **11**(9), 3558-66.
- Tsui, T. Y., Wu, X., Lau, C. K., Ho, D. W., Xu, T., Siu, Y. T., and Fan, S. T. (2003). Prevention of chronic deterioration of heart allograft by recombinant adeno-associated virus-mediated heme oxygenase-1 gene transfer. *Circulation* **107**(20), 2623-9.
- Urbich, C., and Dimmeler, S. (2004). Endothelial progenitor cells: characterization and role in vascular biology. *Circ Res* **95**(4), 343-53.
- Urbich, C., Heeschen, C., Aicher, A., Dernbach, E., Zeiher, A. M., and Dimmeler, S. (2003). Relevance of monocytic features for neovascularization capacity of circulating endothelial progenitor cells. *Circulation* **108**(20), 2511-6.
- Vajkoczy, P., Blum, S., Lamparter, M., Mailhammer, R., Erber, R., Engelhardt, B., Vestweber, D., and Hatzopoulos, A. K. (2003). Multistep nature of microvascular recruitment of ex vivo-expanded embryonic endothelial progenitor cells during tumor angiogenesis. *J Exp Med* **197**(12), 1755-65.
- Vana, K., and Weiss, S. (2006). A trans-dominant negative 37kDa/67kDa laminin receptor mutant impairs PrP(Sc) propagation in scrapie-infected neuronal cells. *J Mol Biol* **358**(1), 57-66.
- Vana, K., Zuber, C., Nikles, D., and Weiss, S. (2007). Novel aspects of prions, their receptor molecules, and innovative approaches for TSE therapy. *Cell Mol Neurobiol* **27**(1), 107-28.
- Vandenbergh, L. H., and Wilson, J. M. (2007). AAV as An Immunogen. *Curr Gene Ther* **7**(5), 325-33.
- Vassalli, G., Fleury, S., Li, J., Goy, J. J., Kappenberger, L., and von Segesser, L. K. (2003). Gene transfer of cytoprotective and immunomodulatory molecules for prevention of cardiac allograft rejection. *Eur J Cardiothorac Surg* **24**(5), 794-806.
- Visnjic, D., Kalajzic, I., Gronowicz, G., Aguila, H. L., Clark, S. H., Lichtler, A. C., and Rowe, D. W. (2001). Conditional ablation of the osteoblast lineage in Col2.3deltatk transgenic mice. *J Bone Miner Res* **16**(12), 2222-31.
- Wade, E. J., Klucher, K. M., and Spector, D. H. (1992). An AP-1 binding site is the predominant cis-acting regulatory element in the 1.2-kilobase early RNA promoter of human cytomegalovirus. *J Virol* **66**(4), 2407-17.
- Wagner, J. A., Messner, A. H., Moran, M. L., Daifuku, R., Kouyama, K., Desch, J. K., Manley, S., Norbash, A. M., Conrad, C. K., Friborg, S., Reynolds, T., Guggino, W. B., Moss, R. B., Carter, B. J., Wine, J. J., Flotte, T. R., and Gardner, P. (1999). Safety and biological efficacy of an adeno-associated virus vector-cystic fibrosis transmembrane regulator (AAV-CFTR) in the cystic fibrosis maxillary sinus. *Laryngoscope* **109**(2 Pt 1), 266-74.
- Wagner, J. A., Reynolds, T., Moran, M. L., Moss, R. B., Wine, J. J., Flotte, T. R., and Gardner, P. (1998). Efficient and persistent gene transfer of AAV-CFTR in maxillary sinus. *Lancet* **351**(9117), 1702-3.
- Walter, D. H., Rittig, K., Bahlmann, F. H., Kirchmair, R., Silver, M., Murayama, T., Nishimura, H., Losordo, D. W., Asahara, T., and Isner, J. M. (2002). Statin therapy accelerates reendothelialization: a novel effect involving mobilization and incorporation of bone marrow-derived endothelial progenitor cells. *Circulation* **105**(25), 3017-24.
- Walters, R. W., Yi, S. M., Keshavjee, S., Brown, K. E., Welsh, M. J., Chiorini, J. A., and Zabner, J. (2001). Binding of adeno-associated virus type 5 to 2,3-

- linked sialic acid is required for gene transfer. *J Biol Chem* **276**(23), 20610-6.
- Wang, Z., Ma, H. I., Li, J., Sun, L., Zhang, J., and Xiao, X. (2003). Rapid and highly efficient transduction by double-stranded adeno-associated virus vectors in vitro and in vivo. *Gene Ther* **10**(26), 2105-11.
- Wang, Z., Zhu, T., Qiao, C., Zhou, L., Wang, B., Zhang, J., Chen, C., Li, J., and Xiao, X. (2005). Adeno-associated virus serotype 8 efficiently delivers genes to muscle and heart. *Nat Biotechnol* **23**(3), 321-8.
- Warrington, K. H., Jr., Gorbatyuk, O. S., Harrison, J. K., Opie, S. R., Zolotukhin, S., and Muzyczka, N. (2004). Adeno-associated virus type 2 VP2 capsid protein is nonessential and can tolerate large peptide insertions at its N terminus. *J Virol* **78**(12), 6595-609.
- Weitzman, M. D., Kyostio, S. R., Kotin, R. M., and Owens, R. A. (1994). Adeno-associated virus (AAV) Rep proteins mediate complex formation between AAV DNA and its integration site in human DNA. *Proc Natl Acad Sci U S A* **91**(13), 5808-12.
- White, S. J., Nicklin, S. A., Buning, H., Brosnan, M. J., Leike, K., Papadakis, E. D., Hallek, M., and Baker, A. H. (2004). Targeted gene delivery to vascular tissue in vivo by tropism-modified adeno-associated virus vectors. *Circulation* **109**(4), 513-9.
- Wijelath, E. S., Rahman, S., Murray, J., Patel, Y., Savidge, G., and Sobel, M. (2004). Fibronectin promotes VEGF-induced CD34 cell differentiation into endothelial cells. *J Vasc Surg* **39**(3), 655-60.
- Work, L. M., Buning, H., Hunt, E., Nicklin, S. A., Denby, L., Britton, N., Leike, K., Odenthal, M., Drebber, U., Hallek, M., and Baker, A. H. (2006). Vascular bed-targeted in vivo gene delivery using tropism-modified adeno-associated viruses. *Mol Ther* **13**(4), 683-93.
- Wu, A. M., Till, J. E., Siminovitch, L., and McCulloch, E. A. (1968). Cytological evidence for a relationship between normal hemotopoietic colony-forming cells and cells of the lymphoid system. *J Exp Med* **127**(3), 455-64.
- Wu, P., Xiao, W., Conlon, T., Hughes, J., Agbandje-McKenna, M., Ferkol, T., Flotte, T., and Muzyczka, N. (2000). Mutational analysis of the adeno-associated virus type 2 (AAV2) capsid gene and construction of AAV2 vectors with altered tropism. *J Virol* **74**(18), 8635-47.
- Wu, Z., Asokan, A., and Samulski, R. J. (2006). Adeno-associated Virus Serotypes: Vector Toolkit for Human Gene Therapy. *Mol Ther* **14**(3), 316-27.
- Wu, Z., Miller, E., Agbandje-McKenna, M., and Samulski, R. J. (2006). Alpha2,3 and alpha2,6 N-linked sialic acids facilitate efficient binding and transduction by adeno-associated virus types 1 and 6. *J Virol* **80**(18), 9093-103.
- Wysoczynski, M., Reza, R., Ratajczak, J., Kucia, M., Shirvaikar, N., Honczarenko, M., Mills, M., Wanzeck, J., Janowska-Wieczorek, A., and Ratajczak, M. Z. (2005). Incorporation of CXCR4 into membrane lipid rafts primes homing-related responses of hematopoietic stem/progenitor cells to an SDF-1 gradient. *Blood* **105**(1), 40-48.
- Xia, X., Zhang, Y., Zieth, C. R., and Zhang, S. C. (2007). Transgenes delivered by lentiviral vector are suppressed in human embryonic stem cells in a promoter-dependent manner. *Stem Cells Dev* **16**(1), 167-76.

- Xiao, W., Chirmule, N., Berta, S. C., McCullough, B., Gao, G., and Wilson, J. M. (1999). Gene therapy vectors based on adeno-associated virus type 1. *J Virol* **73**(5), 3994-4003.
- Xiao, W., Warrington, K. H., Jr., Hearing, P., Hughes, J., and Muzyczka, N. (2002). Adenovirus-facilitated nuclear translocation of adeno-associated virus type 2. *J Virol* **76**(22), 11505-17.
- Xiao, X., Li, J., and Samulski, R. J. (1996). Efficient long-term gene transfer into muscle tissue of immunocompetent mice by adeno-associated virus vector. *J Virol* **70**(11), 8098-108.
- Xiao, X., Li, J., and Samulski, R. J. (1998). Production of high-titer recombinant adeno-associated virus vectors in the absence of helper adenovirus. *J Virol* **72**(3), 2224-32.
- Xie, Q., Somasundaram, T., Bhatia, S., Bu, W., and Chapman, M. S. (2003). Structure determination of adeno-associated virus 2: three complete virus particles per asymmetric unit. *Acta Crystallogr D Biol Crystallogr* **59**(Pt 6), 959-70.
- Yakobson, B., Hrynko, T. A., Peak, M. J., and Winocour, E. (1989). Replication of adeno-associated virus in cells irradiated with UV light at 254 nm. *J Virol* **63**(3), 1023-30.
- Yakobson, B., Koch, T., and Winocour, E. (1987). Replication of adeno-associated virus in synchronized cells without the addition of a helper virus. *J Virol* **61**(4), 972-81.
- Yalkinoglu, A. O., Heilbronn, R., Burkle, A., Schlehofer, J. R., and zur Hausen, H. (1988). DNA amplification of adeno-associated virus as a response to cellular genotoxic stress. *Cancer Res* **48**(11), 3123-9.
- Yamaguchi, J., Kusano, K. F., Masuo, O., Kawamoto, A., Silver, M., Murasawa, S., Bosch-Marce, M., Masuda, H., Losordo, D. W., Isner, J. M., and Asahara, T. (2003). Stromal cell-derived factor-1 effects on ex vivo expanded endothelial progenitor cell recruitment for ischemic neovascularization. *Circulation* **107**(9), 1322-8.
- Yan, Z., Zak, R., Luxton, G. W., Ritchie, T. C., Bantel-Schaal, U., and Engelhardt, J. F. (2002). Ubiquitination of both adeno-associated virus type 2 and 5 capsid proteins affects the transduction efficiency of recombinant vectors. *J Virol* **76**(5), 2043-53.
- Yan, Z., Zak, R., Zhang, Y., Ding, W., Godwin, S., Munson, K., Peluso, R., and Engelhardt, J. F. (2004). Distinct classes of proteasome-modulating agents cooperatively augment recombinant adeno-associated virus type 2 and type 5-mediated transduction from the apical surfaces of human airway epithelia. *J Virol* **78**(6), 2863-74.
- You, H., Liu, Y., Prasad, C. K., Agrawal, N., Zhang, D., Bandyopadhyay, S., Liu, H., Kay, H. H., Mehta, J. L., and Hermonat, P. L. (2006). Multiple human papillomavirus genes affect the adeno-associated virus life cycle. *Virology* **344**(2), 532-40.
- Zabner, J., Seiler, M., Walters, R., Kotin, R. M., Fulgeras, W., Davidson, B. L., and Chiorini, J. A. (2000). Adeno-associated virus type 5 (AAV5) but not AAV2 binds to the apical surfaces of airway epithelia and facilitates gene transfer. *J Virol* **74**(8), 3852-8.
- Zabner, J., Wadsworth, S. C., Smith, A. E., and Welsh, M. J. (1996). Adenovirus-mediated generation of cAMP-stimulated Cl⁻ transport in cystic fibrosis airway epithelia in vitro: effect of promoter and administration method. *Gene Ther* **3**(5), 458-65.

- Zaiss, A. K., Liu, Q., Bowen, G. P., Wong, N. C., Bartlett, J. S., and Muruve, D. A. (2002). Differential activation of innate immune responses by adenovirus and adeno-associated virus vectors. *J Virol* **76**(9), 4580-90.
- Zhong, L., Li, W., Li, Y., Zhao, W., Wu, J., Li, B., Maina, N., Bischof, D., Qing, K., Weigel-Kelley, K. A., Zolotukhin, I., Warrington, K. H., Jr., Li, X., Slayton, W. B., Yoder, M. C., and Srivastava, A. (2006). Evaluation of primitive murine hematopoietic stem and progenitor cell transduction in vitro and in vivo by recombinant adeno-associated virus vector serotypes 1 through 5. *Hum Gene Ther* **17**(3), 321-33.
- Zhou, S. Z., Cooper, S., Kang, L. Y., Ruggieri, L., Heimfeld, S., Srivastava, A., and Broxmeyer, H. E. (1994). Adeno-associated virus 2-mediated high efficiency gene transfer into immature and mature subsets of hematopoietic progenitor cells in human umbilical cord blood. *J Exp Med* **179**(6), 1867-75.
- Zobel, C., Rana, O. R., Saygili, E., Bolck, B., Saygili, E., Diedrichs, H., Reuter, H., Frank, K., Muller-Ehmsen, J., Pfitzer, G., and Schwinger, R. H. (2007). Mechanisms of Ca²⁺-dependent calcineurin activation in mechanical stretch-induced hypertrophy. *Cardiology* **107**(4), 281-90.
- Zolotukhin, S., Byrne, B. J., Mason, E., Zolotukhin, I., Potter, M., Chesnut, K., Summerford, C., Samulski, R. J., and Muzyczka, N. (1999). Recombinant adeno-associated virus purification using novel methods improves infectious titer and yield. *Gene Ther* **6**(6), 973-85.
- Zuber, C., Knackmuss, S., Rey, C., Reusch, U., Rottgen, P., Frohlich, T., Arnold, G. J., Pace, C., Mitteregger, G., Kretzschmar, H. A., Little, M., and Weiss, S. (2008). Single chain Fv antibodies directed against the 37 kDa/67 kDa laminin receptor as therapeutic tools in prion diseases. *Mol Immunol* **45**(1), 144-51.
- Zuber, C., Ludewigs, H., and Weiss, S. (2007). Therapeutic approaches targeting the prion receptor LRP/LR. *Vet Microbiol* **123**(4), 387-93.
- Zuo, Z., Wang, C., Carpenter, D., Okada, Y., Nicolaidou, E., Toyoda, M., Trento, A., and Jordan, S. C. (2001). Prolongation of allograft survival with viral IL-10 transfection in a highly histoincompatible model of rat heart allograft rejection. *Transplantation* **71**(5), 686-91.

Danksagung

Herzlich bedanken möchte ich mich bei PD Dr. Hildegard Büning für die Möglichkeit in ihrer Arbeitsgruppe an interessanten Fragestellungen zu arbeiten. Ausserdem danke ich ihr für die sehr gute, direkte und intensive Betreuung während der gesamten Zeit.

Ich danke Prof. Dr. M. Hallek für die Möglichkeit meine Promotionsarbeit in der Medizinischen Klinik I des Universitätsklinikum zu Köln anzufertigen.

Prof. Dr. J. Brüning möchte ich für die Bereitschaft danken, meine Doktorarbeit extern zu betreuen und sie so zu ermöglichen.

Desweiteren gilt mein Dank Dr. M. Pesce, für die hervorragende Unterstützung und die Chance Neues zu Lernen während der drei Monate, die ich in seiner Arbeitsgruppe hospitieren durfte. Ebenso danke ich der gesamten Arbeitsgruppe, die mich herzlich empfing, mich stets unterstützte und mir Mailand näherbrachte.

L. Burdorf und seinen Kollegen möchte ich für die Durchführung der Tierexperimente danken. Desweiteren bedanke ich mich bei der gesamten DFG Forschergruppe Xenotransplantation für die gute Zusammenarbeit.

Ganz lieben Dank an alle früheren und aktuellen Mitglieder unserer Arbeitsgruppe für ihre Hilfsbereitschaft und gute Diskussionen genauso wie für die freundschaftliche Arbeitsatmosphäre und die Aufmunterungen, wenn es mit der Etablierung mal wieder schwieriger war als erwartet. Besonders danken möchte ich Stefanie Stahnke für ihre Hilfe bei der konfokalen Mikroskopie, Jorge Boucas für Rettung in Computerfragen und Hanna Janicki für die Versorgung mit „Nervennahrung“.

Vielen Dank an sämtliche Arbeitsgruppen im LFI, die stets hilfsbereit und freundlich waren und für ein sehr angenehmes Arbeitsumfeld sorgten.

Bei Prof. Dr. M. Odenthal bedanke ich mich für das Fertigen der Cryoschnitte im Pathologischen Institut.

Ich möchte mich bei Dr. B. Petersen, Dr. W. Kues, Dr. M. Seifert, Dr. B. Böck und N. Fein für interessante Gespräche und die Bereitstellung von Zellen bedanken.

Ganz herzlich danke ich meinen Freunden und meiner Familie, die mir während dieser Zeit zur Seite standen.

Erklärung

Ich versichere, dass ich die von mir vorgelegte Dissertation selbständig angefertigt, die benutzten Quellen und Hilfsmittel vollständig angegeben und die Stellen der Arbeit – einschließlich Tabellen, Karten und Abbildungen –, die anderen Werken im Wortlaut oder dem Sinn nach entnommen sind, in jedem Einzelfall als Entlehnung kenntlich gemacht habe; dass diese Dissertation noch keiner anderen Fakultät oder Universität zur Prüfung vorgelegen hat; dass sie – abgesehen von unten angegebenen Teilpublikationen – noch nicht veröffentlicht worden ist sowie, dass ich eine solche Veröffentlichung vor Abschluss des Promotionsverfahrens nicht vornehmen werde. Die Bestimmungen der Promotionsordnung sind mir bekannt. Die von mir vorgelegte Dissertation ist von Frau PD Dr. Hildegard Büning betreut worden.